Insulin regulated glucose transport in rat and 3T3-LI adipocytes

Palfreyman, Robin W.

Award date:
1994

Awarding institution:
University of Bath

Insulin regulated glucose transport in rat and 3T3-L1 adipocytes

submitted by Robin W. Palfreyman
for the degree of PhD
of the University of Bath
1994

ProQuest LLC
789 East Eisenhower Parkway
P.O. Box 1346
Ann Arbor, MI 48106-1346

Contents

Abstract

A photolabel displacement method was developed to resolve the separate kinetic properties of the glucose transporters GLUT1 and GLUT4 in 3T3-L1 adipocytes, which contain both transporter isoforms. The photolabel, 2-*N*-[4-(1-azi-2,2,2-trifluoroethyl)benzoyl]-1,3-bis-(D-mannos-4-yloxy)-2-propylamine, was displaced with 3-*O*-methyl-D-glucose. The half maximal displacement by 3-*O*-methyl-D-glucose occurred at 20 mM for GLUT1 and 7.0 mM for GLUT4. The calculated transport capacities (turnover number/K_m) were 0.36 x 10^4 $mM^{-1}\cdot min^{-1}$ for GLUT1 and 1.13 x 10^4 $mM^{-1}\cdot min^{-1}$ for GLUT4. The ≈ 3-fold higher transport capacity of GLUT4 at low glucose concentrations is mainly due to the higher K_m of GLUT1.

The potential role of phosphorylation in the insulin signalling pathway to the glucose transporter was investigated using the phosphatase inhibitor okadaic acid. This was found to increase both 3-*O*-methyl-D-glucose uptake and the level of cell surface GLUT4 photolabelling in unstimulated adipocytes. In insulin stimulated rat adipocytes okadaic acid reduced the transport rate and the level of cell surface transporter photolabelling. Okadaic acid appears to alter both the intrinsic activity and translocation of transporters. The tyrosine kinase inhibitor α-cyano-3,4-dihydroxythiocinnamide (453C89) was used to examine the role of tyrosine kinases in the insulin induced increase in glucose transport. The inhibitor appeared not to inhibit the insulin receptor tyrosine kinase but to inhibit 3-*O*-methyl-D-glucose uptake perhaps by reducing the intrinsic activity of GLUT4.

In adipocytes GLUT1 and GLUT4 have a different distribution between the cell surface and the intracellular pools. The subcellular distribution of GLUT4 was shown to be intrinsic to the protein since when it was expressed in insulin-insensitive fibroblasts it

adopted a distribution different to that of GLUT1. In order to determine which regions of GLUT4 are involved in its sorting and sequestration peptides corresponding to different regions of GLUT1 and GLUT4 were added to streptolysin-O permeabilized 3T3-L1 adipocytes. The addition of a peptide corresponding to the N terminus of GLUT4 increased the transport rate and the level of cell surface GLUT4 suggesting that the N terminus of GLUT4 may be involved in its sequestration from the plasma membrane.

The GTP-binding rab proteins are involved in the regulation of vesicular trafficking. Both rab4 and rab3d have been implicated in the trafficking of GLUT4 containing vesicles. Rab4 was detected in the supernatant of rat adipocytes using an anti-rab4 antiserum. The expression of Rab3d in CHO fibroblasts expressing GLUT4 appeared not to affect the subcellular distribution of GLUT4 but may have affected the distribution of GLUT1. The addition of the nonhydrolyzable GTP analogue, GTPγS, to streptolysin-O permeabilized 3T3-L1 adipocytes caused a small increase in basal 2-deoxy-D-glucose uptake but had little effect on the insulin stimulated transport rate. GTPγS appears to cause GLUT4 to accumulate at the cell surface, with most transporters inactive. Thus G-proteins may be involved in insulin signalling and glucose transporter translocation.

Acknowledgements

I am grateful to the Medical Research Council for the provision of financial support throughout this study.

Thanks are due to my supervisor, Dr. Geoffrey D. Holman, for all his advice and support throughout the project. A big thank you to all those who are or have been residents of "Transport House" and who have helped me in whatever way.

Finally, I am greatly indebted to my parents and grandparents for all their support, to Dr. Nicola Jordan for her encouragement and to the members of the Bath Christadelphian Ecclesia for sustaining me during my sojourn in this city.

"Happy is the man that findeth wisdom,
and the man that getteth understanding."

Proverbs 3:13

Abbreviations

ATB-BMPA	2-*N*-[4-(1-azi-2,2,2-trifluoroethyl)benzoyl]-1,3-bis-(D-mannos-4-yloxy)-2-propylamine	
B_{max}	Cell surface transporter abundance	
DMF	N,N-dimethylformamide	
DMSO	Dimethyl sulphoxide	
DMEM	Dulbecco's modification of Eagle's medium	
DMEM-FCS	Complete DMEM with 10 % foetal calf serum	(section 2.2.1)
DMEM-NCS	Complete DMEM with 10 % newborn calf serum	(section 2.2.1)
GLUT	Facilitative glucose transporter isoform	
GTPγS	Guanosine 5'-*O*-(3-thiotriphosphate)	
IAPS-forskolin	3-iodo-4-azidophenethylamido-7-*O*-succinyldeacetyl-forskolin	
IC buffer	Intracellular buffer	(section 2.3.6)
IIC buffer	Intracellular incubation buffer	(section 2.3.6)
IRS-1	Insulin receptor substrate-1	
K_d	Dissociation constant	
K_{en}	Endocytosis constant	
K_{ex}	Exocytosis constant	
KRH	Krebs-Ringer-HEPES buffer for 3T3-L1 adipocytes	(section 2.3.3)
KRM	Krebs-Ringer-MES buffer for 3T3-L1 adipocytes	(section 2.3.5)
LDM	Low density microsomes	
MAP kinase	Mitogen activated protein kinase	
PI3-kinase	Phosphatidylinositol 3'-kinase	
PM	Plasma membrane	
PP-1	Protein phosphatase-1	
PP-2A	Protein phosphatase-2A	
Rat KRH	Krebs-Ringer-HEPES buffer for rat adipocytes	(section 2.3.3)
SGLT1	Na^+/glucose cotransporter	
SLO	Streptolysin-*O*	
TBS	Tris buffered saline	(section 2.6.6)
TE buffer	Tris/EDTA buffer	(section 2.7.1)
TEMED	N,N,N',N'-tetramethylethylenediamine	
TES	Tris/EDTA/sucrose buffer	(section 2.6.1)
TK	Transporter transport capacity	
TKI	Tyrosine kinase inhibitor	

1.0 Introduction

1.1 The need for glucose transport

Glucose is a major source of energy for many mammalian cells and some, such as the brain, are virtually dependent on it. The blood of mammals delivers glucose to the cells at a concentration of 5 to 10 mM. Because cells possess an impermeant polar plasma membrane the hydrophilic sugar molecules are unable to diffuse into the cells unaided. To allow glucose entry, all cell surface membranes contain specific transporters that facilitate the energy independent diffusion of glucose across the membrane and into the cell. In addition to these facilitative glucose transporters certain mammalian cells, such as the epithelial cells that line the small intestine and the proximal tubule of the kidney, also possess an active glucose transporter, the Na^+/glucose cotransporter, SGLT1. This transports glucose against the concentration gradient, the energy being supplied by the Na^+/K^+ ATPase.

Different cells within the mammalian body have different requirements for glucose and play different roles in the maintenance of blood glucose homeostasis. While most cells simply require a minimum intake of glucose some, such as the brain, require a much higher rate of uptake. Other cell types, such as hepatocytes, muscle and adipocytes are involved in removing glucose from the blood while the liver also releases glucose. In order to provide the range of differing glucose transport capacities required, mammals possess a family of facilitative glucose transporters, designated GLUT1-7, whose kinetics are designed to meet the specific requirements of the cells in which they are found. One of the roles of glucose transporters is the regulation of the blood glucose concentration. After a meal the blood glucose level rises, stimulating the release of insulin which binds to receptors on the surface of insulin sensitive muscle and adipose cells increasing the rate of glucose uptake into these cells thus maintaining glucose homeostasis (Bell *et al.*, 1990; Baldwin, 1993; Birnbaum, 1993).

1.2 The facilitative glucose transporter family

Even before the isolation of a specific glucose transporter protein it was recognised that the sensitivity to inhibitors and the kinetics of glucose uptake varied in a tissue-specific manner (Baldwin, 1993). In 1977 Kasahara and Hinkle successfully purified the human erythrocyte glucose transporter from Triton X-100 solubilized cells using a sonication method that included a freeze-thaw step. The purified protein gave a broad band of Mr 55,000 on SDS-PAGE. It was stained by periodic acid-Schiff reagent, a glycoprotein stain. When the purified protein was reconstituted into liposomes it was found to catalyse D-glucose transport. This transport activity was inhibited by cytochalasin B and mercuric ions at the same concentration as that of erythrocyte membranes. Because the protein was glycosylated and antibodies against the purified protein were absorbed by inside-out erythrocyte vesicles they proposed that the protein spanned the membrane (Kasahara and Hinkle, 1977). The protein was later shown to have the same kinetic properties as the erythrocyte glucose transporter and to be inhibited by phloretin and diethylstilbestrol (Wheeler and Hinkle, 1981).

The protein was first sequenced by Mueckler *et al* (1985). A cDNA library was made from a human hepatoma cell line, HepG2. This was expressed using the phage expression vector λgt11 and screened with an antiserum against the purified erythrocyte glucose transporter. The largest positive plaque was sequenced and found to code for a polypeptide of 492 residues. A hydropathy plot of the amino acid sequence led to the proposal of a model of the transporter with 12 membrane spanning domains and with two intracellular termini.

Once one sequence was obtained other cDNA libraries were screened and to date six other glucose transporter gene sequences have been obtained. All have a very similar hydropathy plot and have ≈ 40 % amino acid sequence identity. They were designated GLUT1 to 7 by Fukumoto *et al.* (1989). The six transporter proteins are compared in Table 1.1, GLUT6 being a pseudogene.

Isoform designation (common name)	Size Mr	Size Amino acid	Major sites of expression	Chromosome location	K_m (mM)	Reference
GLUT1 (Erythrocyte, HepG2, Brain)	54,117	492	Erythrocyte, brain, kidney, colon, foetal tissue	1	17.6	Mueckler *et al.*, 1985 Gould *et al.*, 1991
GLUT2 (Liver)	57,000	524	Liver, pancreatic B-cell, kidney, small intestine	3	42.3	Fukumoto *et al.*, 1988 Gould *et al.*, 1991
GLUT3 (Brain)	53,933	496	Brain, placenta, kidney	12	10.6	Kayano *et al.*, 1988 Gould *et al.*, 1991
GLUT4 (adipocyte/muscle, Insulin regulatable)	54,797	509	Brown and white adipocytes, heart and skeletal muscle	17	1.8	Fukumoto *et al.*, 1989 Keller *et al.*, 1989
GLUT5 (Small intestine)	54,983	501	Small intestine	1	N.D.	Kayano *et al.*, 1990
GLUT7 (Hepatic microsomal)	53,000	528	Hepatocyte endoplasmic reticulum	N.D.	N.D.	Waddell *et al.*, 1992

Table 1.1 The facilitative glucose transporter family

The sizes and chromosomal locations given are those of the human glucose transporters except for those of the rat GLUT7. The K_m given is that of 3-O-methyl-D-glucose equilibrium exchange for the human (GLUT1-6) or rat (GLUT4) transporter expressed in *Xenopus* oocytes (Baldwin, 1993).

1.2.1 GLUT1

GLUT1 is perhaps the most ubiquitous of the facilitative glucose transporters. Both the protein and the mRNA have been identified in most tissues although the level of expression varies between tissues (Flier *et al.*, 1987a). GLUT1 is very abundant in endothelial and epithelial cells at the blood-tissue barrier (Takata et al., 1990) with a high concentration of transporters at the blood-nerve barrier (Froehner *et al.*, 1988). It is expressed in foetal tissue at much higher levels than occur in the adult tissue (Asano *et al.*, 1988). In humans, GLUT1 is most abundant in erythrocytes where it is the only glucose transporter. Here it accounts for over 5 % of the total membrane protein (Allard and Lienhard, 1985). GLUT1 occurs in insulin responsive tissues such as muscle and fat, tissues that also express GLUT4 at much higher levels (Gould and Holman, 1993). GLUT1 is expressed at high levels in transformed (Flier *et al.*, 1987b) and cultured cells (Flier *et al.*, 1987a) and this is increased by stimulation with growth factors (Hiraki *et al.*, 1988), by mitogens (Weber *et al.*, 1984) and by glucose starvation (Haspel *et al.*, 1986).

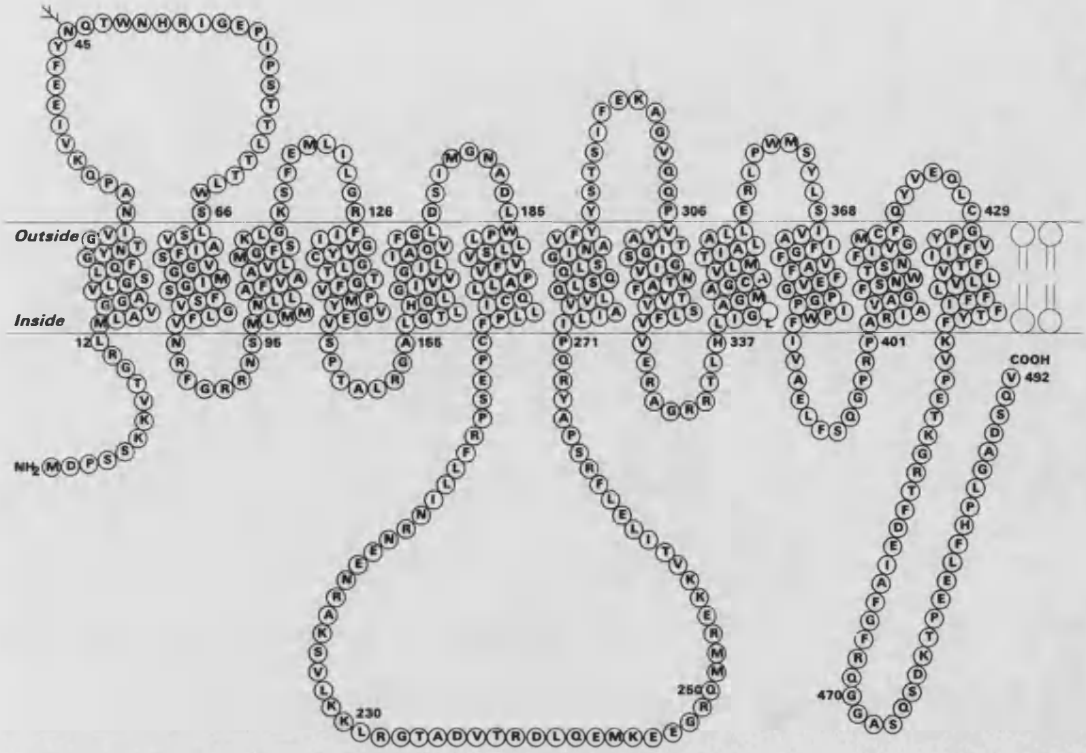

Figure 1.1 A model for the GLUT1 glucose transporter

The model shows the proposed membrane spanning domains based on hydropathy plots. The sequence given is that of the 3T3-L1 adipocyte GLUT1 (Kaestner *et al.*, 1989).

The GLUT1 transporter protein is 492 residues long in humans (Mueckler *et al.*, 1985), rats (Birnbaum *et al.*, 1986), mice (Kaestner *et al.*, 1989), pigs (Weiler-Guettler *et al.*, 1989) and rabbits (Asano *et al.*, 1988). On the basis of hydropathy plots and computer modelling GLUT1, in common with all the facilitative glucose transporters, is proposed to contain 12 membrane spanning α-helices as described in figure 1.1. The protein has been orientated and arranged in the membrane on the basis of a range of experiments. Ultraviolet circular dichroism analysis of GLUT1 indicated that it is composed of approximately 82 % α-helices, 10 % β-turns and 8 % random coil (Chin *et al*, 1987). Tryptic digestion cleaved residues 213-269, the loop between helices 6 and 7, and 457-492, the C terminus, from the cytoplasm face of human erythrocyte membranes (Cairns *et al*, 1987). A number of other potential cleavage sites on the smaller loops were not cleaved, presumably because the phospholipid polar head groups prevented trypsin gaining access to them. Anti-peptide antibodies against many

regions of the protein were able to confirm the predicted locations of the loops and termini (Davies *et al.*, 1990). With the exception of the loops between transmembrane helices 2 and 3 and 6 and 7 the loops are short and constrain the possible packing of the helices (Gould and Holman, 1993). The most likely arrangement is in two groups of six helices from the N- and C- terminal halves of the transporter, as shown in figure 1.2. In this model the glucose carrying channel is formed within the C-terminal half of the transporter by transmembrane helices 7, 8, 10 and 11. When the N- and C-terminal halves of GLUT1 were expressed separately neither bound ATB-BMPA or cytochalasin B. When both were expressed in the same cell the C-terminal half bound both labels, suggesting that both halves must pack together to obtain the correct ligand-binding conformation (Cope *et al.*, 1994).

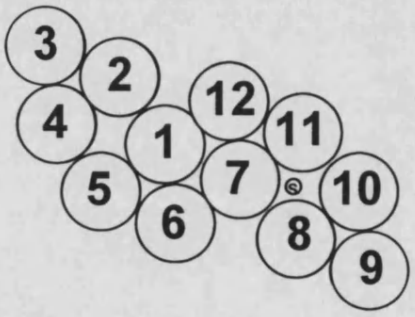

Figure 1.2 A proposed model for the arrangement of membrane helices
Helices are numbered from the N terminus. The small circle represents a sugar molecule in the proposed channel (Baldwin, 1993).

In addition to the 12 membrane spanning α-helices other physical features of GLUT1 include the intracellular N- and C-terminal regions and the large loop between transmembrane helices 1 and 2. This loop contains a potential glycosylation site. The C-terminal region of the facilitative glucose transporter family shows the greatest sequence diversity. This makes the C terminus a suitable region for raising antibodies against specific members of the facilitative glucose transporter family.

An alternative model of the glucose transporter was proposed by Fischbarg *et al.* (1993). Based on antibody studies and analysis of the hydrophobicity, amphiphilicity and turn propensity of GLUT1 they proposed a porin-like structure formed from a

16-stranded transmembrane antiparallel β-barrel. In this model the glucose carrying channel is located down the centre of the β-barrel. Both termini remain intracellular.

The possible involvement of various residues or regions in conformational changes and transport have been investigated by observing the effect of mutations on transport rates, ATB-BMPA binding to the exofacial site and the binding of cytochalasin B and forskolin at an intracellular site. A glycine/proline rich region, residues 382-387, in α-helix 10 of the 12 transmembrane α-helix model introduces a flexible region into the protein which allows a conformational change enabling helices 10 and 11 to either expose or close the external binding site (Hodgson *et al.*, 1992; Gould and Holman, 1993). The role of Pro^{385} in conformational flexibility was demonstrated by two substitutions. When this proline was substituted by glycine (P385G) then ATB-BMPA labelling was half that of the wild type transporter while 2-deoxy-D-glucose transport and cytochalasin B binding at the internal site was not reduced. When it was substituted by isoleucine (P385I) then both ATB-BMPA binding and glucose transport were greatly reduced and only binding at the internal binding site was unaffected, suggesting that this mutation prevents the transporter adopting an outward facing conformation (Tamori *et al.*, 1994). The substitution of Trp^{388} in helix 10 by leucine (W388L) decreased both IAPS-forskolin binding and transport activity (Katagiri *et al.*, 1993; Schürmann *et al.*, 1993). This suggests that Trp^{388} is also involved in the conformational change between the inside and outside-facing conformers (Katagiri *et al.*, 1993).

The C-terminal region has also been implicated in the conformational change. When the last 37 residues of GLUT1 were deleted both the transport rate and ATB-BMPA labelling were reduced but cytochalasin B binding was unaffected. This suggests that the C terminus may be involved in stabilising the outward facing conformation (Oka *et al.*, 1990). When only the last 12 residues of the C terminus of GLUT1 was deleted there was no effect on transport activity, labelling or protein stability suggesting that residues between the last 12 and 37 are important for transport activity (Lin *et al.*,

1992). Deleting the last 24 residues had no effect on labelling at either the inside or outside while deleting the last 25 residues reduced ATB-BMPA labelling. Thus deleting more than the last 24 residues appears to lock the transporter into a stable inward facing conformation (Mori *et al.*, 1994). Another mutation which significantly reduces ATB-BMPA labelling is Q282L. Gln^{282} occurs in transmembrane helix 7 and appears to be involved in the hydrogen bonding of glucose at the exofacial binding site (Hashiramoto *et al.*, 1992).

The opposite effect occurred with substitutions at Tyr^{292} and Tyr^{293} in transmembrane helix 7. These residues are believed to create a hydrophobic patch on the external face of the transporter, helping to isolate the bound glucose from the extracellular solution. The substitutions Y292I/F and Y293F were without effect but Y293I abolished cytochalasin B binding without affecting ATB-BMPA labelling. It was suggested that the substitution Y293I locks GLUT1 in an outward facing conformation and that Tyr^{293} is required to close the exofacial site (Mori *et al.*, 1994).

When Asp^{415} in transmembrane helix 11 was substituted by an asparagine (D415N) both the transport activity and cytochalasin B binding were greatly reduced. This residue was proposed as being near the inner glucose binding site and involved in the conformational change (Ishihara *et al.*, 1991). The substitution of Leu^{412} for a tryptophan (W412L) in helix 11 also reduced the intrinsic activity of GLUT1 but did not abolish cytochalasin B or IAPS forskolin binding on the inner face or affect ATB-BMPA binding to the extracellular site. This tryptophan residue must therefore be at or near the inner glucose binding site but it is not the cytochalasin B binding site (Katagiri *et al.*, 1991; Schürmann *et al.*, 1993).

GLUT1 is *N*-glycosylated at a single site on Asn^{45}. This was confirmed by mutational analysis. When the Asn was substituted for an Asp, Tyr or Gln (N45D, N45Y or N45Q) a single sharp band at 38 kDa was obtained on Western blots confirming that Asn^{45} is the only *N*-glycosylation site. These substitutions also reduced cytochalasin B

and ATB-BMPA labelling and raised the K_m for 2-deoxy-D-glucose uptake. This suggests that *N*-glycosylation may have a role in maintaining the correct structure of GLUT1 (Asano *et al.*, 1991). GLUT1 *N*-glycosylation also affects the distribution and stability of the transporter. Whereas most of the wild type GLUT1 expressed in CHO fibroblasts was expressed at the cell surface the glycosylation defective GLUT1 mutants were mostly intracellular. The half-life of GLUT1 with any of the three substitutions at Asn^{45} was about a third shorter than that of the wild type (Asano *et al.*, 1993).

1.2.2 GLUT2

Liver cells express only low levels of GLUT1 and the kinetics of liver glucose transport are very different to those of erythrocytes. The K_d for cytochalasin B binding to liver membranes is an order of magnitude higher than to erythrocytes. This led to the proposal that liver cells may possess a unique glucose transporter (Axelrod and Pilch, 1983). This assumption was proved to be correct with the sequencing of GLUT2 from a human and rat liver cDNA library. Fukumoto *et al.* (1988) sequenced the human GLUT2 and found it to be 524 residues long. The rat sequence, with 522 residues, was isolated by Thorens *et al.* (1988). There is about 55 % sequence identity between GLUT1 and GLUT2. Human GLUT2 is 32 residues longer than GLUT1 and has an additional 34 residues in the first extracellular loop making it twice the size of that in GLUT1. In addition very few of the last 28 residues in the C terminus of GLUT1 are the same in GLUT2 (Fukumoto *et al.*, 1988). Hydropathy plots suggest that GLUT2 adopts the same 12 membrane spanning α-helical secondary structure as GLUT1. GLUT2 is expressed in the liver, intestine, kidney and pancreatic islet β-cells.

When expressed in *Xenopus* oocytes human GLUT2 was found to have a K_m of 42 mM for 3-*O*-methyl-D-glucose under conditions of equilibrium exchange. This is more than twice that of GLUT1 and much higher than the concentration of glucose in the blood (Gould *et al.*, 1991). The K_m for glucose has been reported as 66 mM making GLUT2

a high capacity high K_m glucose transporter (Elliott and Craik, 1983). GLUT2, unlike GLUT1, can transport fructose with a K_m of 66 mM (Gould *et al.*, 1991; Gould and Holman, 1993). Unlike GLUT1 and GLUT4, liver membrane GLUT2 does not exhibit glucose inhibitable binding of cytochalasin B or forskolin (Hellwig and Joost, 1991).

Two properties of the liver glucose transport system enable rapid transport in and out of hepatocytes without transport becoming rate limiting. Because GLUT2 is a high capacity high K_m transporter it is able to respond to changes in the glucose concentration in a linear manner. Secondly the high concentration of GLUT2 in the liver ensures a high V_{max}. In the pancreatic β–cells GLUT2 is part of the glucose sensing mechanism, allowing the rapid equilibration of glucose across the plasma membrane. The β–cell glucose sensor is believed to be a high K_m glucokinase. The kinetics of GLUT2 therefore allow the glucokinase to respond linearly to the blood glucose concentration (Matschinsky, 1990).

In the small intestine and kidney GLUT2 is localised at the basolateral membrane of the epithelial cells. Glucose is actively transported across the apical membrane and concentrated in the cell by SGLT1. The accumulated glucose is then released into the blood via the high-capacity GLUT2 (Thorens *et al.*, 1990).

1.2.3 GLUT3

GLUT3, the third member of the facilitative glucose transporter family to be sequenced, was isolated from a human foetal skeletal muscle cDNA library by Kayano *et al.* (1988). GLUT3 is 496 residues long, only 4 residues longer than GLUT1. It has about 64 % sequence homology with GLUT1. In rodents GLUT3 mRNA can only be detected in the brain (Yano *et al.*, 1991). In humans GLUT3 mRNA can be detected in the placenta, liver, heart, kidney and brain. The protein, however, can only be detected at high levels in the brain and other neural tissue (Shepherd *et al.*, 1992).

When expressed in *Xenopus* oocytes the K_m of GLUT3 for 3-*O*-methyl-D-glucose under equilibrium exchange conditions is 10 mM, nearly half that of GLUT1 (Gould *et al.*, 1991). The brain is a tissue with a high demand for glucose. The combination of GLUT1 and GLUT3 in the brain ensures that it receives a constant plentiful supply. The low K_m of GLUT3 ensures glucose uptake by neurones even when the concentration of glucose in the blood is low (Asano *et al.*, 1992a).

1.2.4 GLUT4

The discovery of GLUT1-3 lead to the idea that a unique transporter might be involved in the insulin stimulated glucose transport rate in adipose and muscle tissue. Indeed a monoclonal antibody which only detected a 45 kDa doublet in muscle and adipose tissue had already been used to immunoprecipitate a rat adipocyte protein that could be labelled with cytochalasin B in a glucose displaceable manner and whose plasma membrane concentration increased with insulin (James et al, 1988). The search for the insulin sensitive glucose transporter led to the simultaneous isolation of the GLUT4 sequence from human (Fukumoto *et al.*, 1989), rat (Charron *et al*, 1989; James *et al.*, 1989a and Birnbaum 1989) and mouse (Kaestner *et al.*, 1989) cDNA libraries. The major sites of GLUT4 expression are the heart, skeletal muscle and adipose tissue. Glucose uptake in these tissues is the most sensitive to insulin.

GLUT4 is 509 amino acid long, 17 residues more than GLUT1 except in the mouse, including 3T3-L1 adipocytes, where GLUT4 is 510 amino acids long (Kaestner *et al.*, 1989). Most of the additional residues are located at the N terminus. GLUT4 has an approximately 65 % sequence identity with the GLUT1 amino acid sequence. Many of these differences occur in the two termini and the loops between helices 1 and 2 and 6 and 7. The hydropathy plots of GLUT1 and GLUT4 are almost superimposible and both have a putative glycosylation site on the first loop. The sequence and proposed secondary structure of the mouse GLUT4 are shown in figure 1.3.

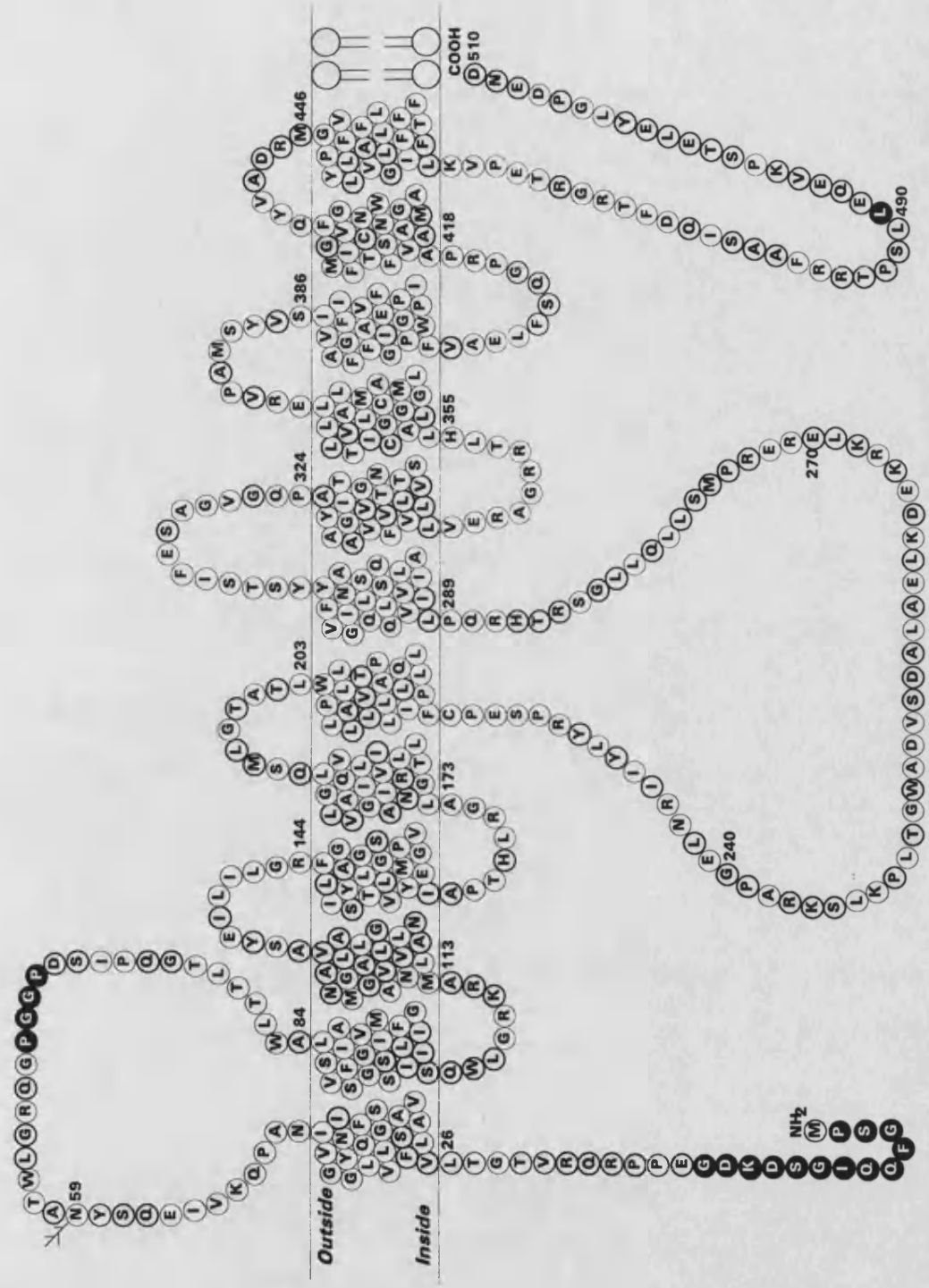

Figure 1.3. A model for the GLUT4 glucose transporter

The model shows the proposed membrane spanning domains based on hydropathy plots. The sequence given is that of the 3T3-L1 adipocyte GLUT4 (Kaestner *et al.*, 1989).

○ Amino acids identical with those of GLUT1. ○ Amino acids that differ from GLUT1. ● Amino acids unique to GLUT4.

When expressed in *Xenopus* oocytes the K_m of rat GLUT4 is 1.8 mM for 3-O-methyl-D-glucose compared to a K_m of 21 mM for the human GLUT1 under conditions of equilibrium exchange (Keller *et al.*, 1989). Under the same conditions the K_m for rat GLUT1 and GLUT4 were 26 mM and 4.3 mM respectively (Nishimura *et al.*, 1993). The low K_m of GLUT4 ensures that the transporter will be operating near its V_{max} and so will be able to efficiently remove glucose from the blood. The rate of uptake is governed by the concentration of GLUT4 at the cell surface. The primary mechanism for the insulin stimulated increase in transport is the translocation mechanism, see section 1.4.1. In addition, the intrinsic activity of the transporter in basal adipocytes appears to be about 2-fold lower than in the insulin stimulated cells. This suggests than insulin may also regulate the intrinsic activity of the transporter (Clark *et al.*, 1991).

1.2.5 GLUT5

GLUT5 was isolated from a human small intestine cDNA library with a GLUT1 cDNA probe (Kayano *et al.*, 1990). The gene codes for a 501 amino acid protein. This transporter has a 41.7 % sequence identity with GLUT1. In the human, GLUT5 mRNA expression was detected in the intestine with lower expression levels in the kidney, skeletal muscle and adipose tissues. In the intestine GLUT5 is localised to the brush border membrane of mature enterocytes (Davidson *et al.*, 1992) where glucose is transported by the Na^+/glucose cotransporter, SGLT1.

When expressed in *Xenopus* oocytes GLUT5 was found to transport 2-deoxy-D-glucose very poorly. Instead GLUT5 was found to transport fructose with a K_m of 6 mM. Unlike the fructose transport mediated by GLUT2, GLUT5 fructose transport is insensitive to cytochalasin B (Burant *et al.*, 1992). GLUT5 mRNA and protein was subsequently detected in human testis and spermatozoa. This enables spermatozoa to utilise the fructose in seminal fluid. The distribution and kinetics of GLUT5 are consistent with it being a fructose transporter (Burant *et al.*, 1992).

1.2.6 GLUT6

The GLUT6 cDNA clone was isolated from a human jejunum cDNA library. Within a 3400 base pair sequence of the GLUT6 cDNA is a 1495 base pair region which has 79.6 % identity with GLUT3. However, because the sequence contains multiple nonsense codons and frame shifts it cannot encode a functional transporter protein. The GLUT6 pseudogene has been detected in all the tissues tested, both tumour and normal, with varying levels of expression (Kayano *et al.*, 1990).

1.2.7 GLUT7

The latest member of the facilitative glucose transporter family is GLUT7. This was obtained by screening a rat liver cDNA library using an antibody which bound to T_3 of the glucose-6-phosphatase system (Waddell *et al.*, 1991). Sequence analysis found that it encodes a protein of 528 amino acids with 68 % sequence identity to GLUT2 (Waddell *et al.*, 1992). GLUT7 is 6 amino acids longer than GLUT2 and the additional residues are located at the C terminus. The 6 amino acids, KKMKND, contain a consensus motif (KK–K–––) which retains transmembrane proteins in the endoplasmic reticulum. The intracellular location of the transporter was confirmed by the transient expression of GLUT7 in COS-7 fibroblasts. Using a microsomal 3-O-methyl-D-glucose uptake assay and immunocytochemical localisation the protein was observed in the endoplasmic reticulum but not the plasma membrane. Transport across the plasma membrane of hepatocytes is facilitated by GLUT2. GLUT7 is required in the endoplasmic reticulum because the liver, unlike other tissues, in addition to absorbing glucose also releases it into the blood. The liver produces glucose by glycogenolysis and gluconeogenesis. The last step of both is catalysed by glucose-6-phosphatase which is located within the endoplasmic reticulum lumen. GLUT7 is required to allow the newly synthesised glucose to cross the endoplasmic reticulum membrane into the cytoplasm and leave the cell via GLUT2 (Waddell *et al.*, 1992).

1.3 The kinetics of glucose transport

Because of the ready availability of GLUT1 in human erythrocytes, where it is the only transporter isoform, the kinetics of GLUT1 have been widely studied. GLUT1 facilitated transport in the erythrocyte is a purely passive process. Widdas recognised that simple diffusion was insufficient to explain the transfer of glucose across the sheep placenta. Instead he proposed a carrier model. He characterised the transport mechanism as simple hyperbolic Michaelis-Menten kinetics (Widdas, 1952). From this was developed the asymmetric alternating conformation model of glucose transport (Geck, 1971) shown in figure 1.4.

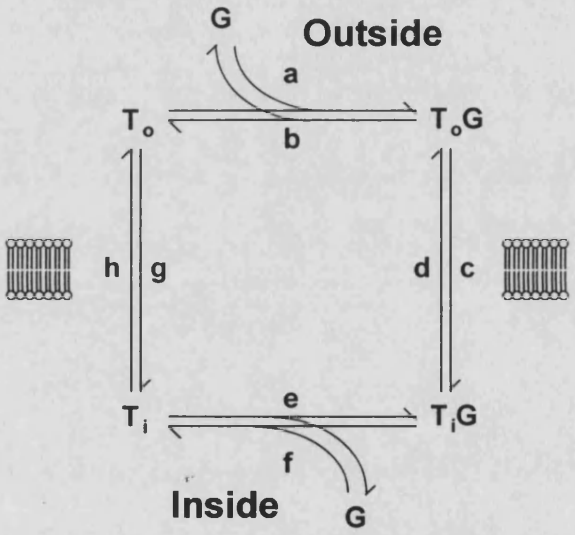

Figure 1.4. The alternating conformation model of glucose transport

T_o is the outward facing and T_i the inward facing conformation of the glucose transporter. b/a and e/f are the dissociation constants for the binding of the sugar (G). c, d, g and h are the reorientation rate constants (Baldwin, 1993).

For the single site model the sugar binding site can be inward facing (T_i) or outward facing (T_o) and free (T_x) or bound (T_xG) but the four states are mutually exclusive. The conformational change involved in reorienting the substrate binding site from an outward to an inward facing site can occur in the presence or absence of bound glucose. This conformational change could be the result of the movement predicted to occur around the flexible glycine/proline rich region of helix 10 (as discussed in section

1.2.1). This model is not consistent with all the available kinetic data so other models have been proposed such as the simultaneous site model of Carruthers (1986). Such inconsistencies could, however, simply be due to technical difficulties in measuring transport. Most of the recent evidence points towards the simple alternating conformation model (Baldwin, 1993). Positive evidence for this model was provided by Lowe and Walmsley (1987). They demonstrated a single half-turnover of the glucose carrier. Transporters were recruited to the outward facing conformation either by pre-equilibrating erythrocytes with maltose, which cannot be transported, or by pre-warming the cells to 38 °C. The simultaneous addition of glucose and dilution of the maltose or cooling to 0 °C respectively resulted in a burst of glucose uptake consistent with that predicted by the alternating conformation model.

While the kinetics of GLUT1 is passive, simple, Michaelis-Menten kinetics, the K_m and V_{max} values that are measured depend on the conditions under which they are measured, equilibrium exchange, zero-*trans*, infinite *cis*, etc. (Baldwin 1993). There is also a difference between the kinetics of zero-*trans* efflux and zero-*trans* influx. This asymmetry was demonstrated by Lowe and Walmsley (1986) who found that the affinity for glucose is about 2.5 fold higher for the outward facing than the inward facing binding site at physiological temperatures. Unlike GLUT1, GLUT2 and GLUT4 do not exhibit asymmetric transport, the others are unknown (Gould and Holman, 1993). Carruthers and Helgerson (1986) have shown that GLUT1 binds ATP. They have suggested that GLUT1 transport is intrinsically symmetrical, the asymmetry being regulated by the binding of cytosolic factors such as ATP.

GLUT1 transport shows *trans*-acceleration whereby, for example, the presence of unlabelled sugar on one side of the membrane stimulates the uptake of labelled sugar on the other side of the membrane. The phenomenon of *trans*-acceleration is due to the rate constants for the reorientation of the loaded site, (c, d) being higher than those for the empty site (g, h) (Lowe and Walmsley, 1986). Thus transport occurs faster under equilibrium exchange conditions than under net flux conditions as during

net flux it is necessary for the transporter to undergo the slower unbound conformational change. Both NMR studies (Wang et *al.*, 1986) and low temperature kinetics have revealed that the rate of binding and dissociation at both sites are higher than the turnover of the transporter. Thus the limiting step in transport is transporter reorientation rather than glucose binding. The asymmetry of transport is due to two factors. One is the higher proportion of inward facing conformations which increases with lower temperatures. The second is the 2.5-fold higher affinity for glucose at the outward facing conformation relative to the inward facing conformation. At physiological temperatures, where the distribution of the two conformations is fairly equal, the latter of these factors is the more important (Lowe and Walmsley, 1986).

The thermodynamic basis for the asymmetry of GLUT1 is believed to lie in the hydration state of the transporter. The binding of glucose excludes water from the binding site and the glucose molecule. New hydrogen bonds are then formed between glucose and the binding site. This stabilises the binding site and lowers the reorientation energy barrier. This makes the reorientation of the loaded transporter more favourable than that of the unloaded transporter. It is believed that the changes in hydrogen bonding result in a reorientation of the helices around the channel causing the closing of the hydrophobic cleft at the external binding site. This is now the inner binding site and the bound glucose is now exposed to the cytosol. A decrease in enthalpy for the inward facing conformation is thought to be due to an increased level of hydration. Transporter conformations are also believed to be stabilised by lipid interactions. Under physiological conditions the kinetics of GLUT1 allow rapid equilibration of glucose across the membrane in either direction (Walmsley, 1988).

The kinetic properties of GLUT4 have been studied in rat adipocytes where GLUT4 is the predominant transporter isoform (Taylor and Holman, 1981). Unlike GLUT1, GLUT4 exhibits symmetrical 3-*O*-methyl-D-glucose transport. Insulin stimulation does not alter either the internal or external affinity constants of the transporter system. Insulin increases adipocyte transport by increasing V_{max} without altering the K_m.

1.4 The regulation of glucose transport and transporter translocation

1.4.1 Insulin stimulated glucose uptake and translocation in adipocytes

It has been recognised since the mid 1950's that insulin acts to facilitate the transfer of extracellular glucose into the cell (Levine and Goldstein, 1955). In kinetic experiments with frog muscle, insulin increased the V_{max} of 3-*O*-methyl-D-glucose penetration without appreciably altering the K_m (Narahara and Özand, 1963). Such kinetic experiments were unable to ascertain whether the increase in V_{max} was the result of an increase in the intrinsic activity of the transporters or an increase in the number of sites participating in sugar transport as postulated by Narahara and Özand (1963). This question was answered following the discovery that cytochalasin B, a metabolite of *Helminthosporum dermatoideum*, is a specific hexose transport inhibitor (Mizel and Wilson, 1972). Wardzala *et al.* (1978) used the ability of cytochalasin B to bind to the transport system to quantify the number of glucose transporter systems in the plasma membrane of rat adipocytes. They found that insulin stimulation increased the number of cytochalasin B binding sites four-fold without changing the cytochalasin B binding characteristics. This increase, they proposed, was due to the activation of identical but basally inactive glucose transport systems. This could have been due to an uncovering of latent transporters or the recruitment of transporters from an intracellular pool. In 1980 Cushman and Wardzala and Suzuki and Kono independently published results which supported the idea that insulin induces the translocation of transporters from an intracellular pool to the plasma membrane. Cushman and Wardzala (1980) detected glucose displaceable cytochalasin B binding sites at the plasma membrane and in a microsomal fraction. In basal adipocytes most of the labelling was associated with the microsomal fraction but insulin stimulation caused a rise in the number of plasma membrane sites and a reciprocal decrease in the microsomal fraction sites. Suzuki and Kono (1980) showed the same translocation effect on transport activity. They fractionated rat adipocytes on a sucrose density gradient and separated two peaks of activity. One peak was associated with the plasma membrane marker 5'-nucleotidase

while the other was associated with a Golgi marker. The two peaks were incorporated into liposomes. Under basal conditions most of the transport activity was associated with the Golgi marker pool. Insulin caused an increase in the transport activity of the plasma membrane peak and a corresponding decrease in the activity of the Golgi marker peak. The K_m of both peaks was about 10-15 mM. Both groups suggested that insulin caused the translocation of transport activity or systems to the plasma membrane from an intracellular microsomal pool.

Translocation was found to be a reversible process with a time course very similar to that for the reversal of insulin stimulated hexose uptake (Karnieli *et al.*, 1981). Both a D-glucose-inhibitable cytochalasin B binding assay and a 3-*O*-methyl-D-glucose transport assay were used to demonstrate that the insulin stimulated decrease in the concentration of glucose transporter systems in the intracellular pool and their increase at the plasma membrane both had a half time of 2.5 min. When insulin was removed and insulin stimulation reversed, the transporter systems were redistributed away from the plasma membrane with a half time of 9 min. There was a similar half time for the decrease in 3-*O*-methyl-D-glucose transport following the removal of insulin. During insulin stimulation, however, there was a 1.5 min lag between the arrival of cytochalasin B binding sites at the plasma membrane and the increase in the transport rate (Karnieli *et al.*, 1981).

Translocation is an energy dependent process. Metabolic inhibitors that lower the cellular ATP levels, such as 10 mM sodium azide, 2 mM potassium cyanide and 1 mM 2,4-dinitrophenol, also inhibit the translocation of transporters to and from the low density microsomes (Ezaki and Kono, 1982). Translocation is also a temperature sensitive process. Low temperatures of, for example, 10 °C induce the slow translocation of transporters to the cell surface but they also slow the rate of insulin stimulated translocation (Ezaki and Kono, 1982).

The intracellular pool of transporters was characterised by Cushman's group (Simpson *et al.* 1983). They characterised the subcellular fractions of rat adipocytes and identified a specialised species of low density microsomes which contained the transporters. These specialised microsomes were associated with but were distinct from the Golgi markers. In basal adipocytes 90 % of the glucose transporters were associated with the intracellular pool while insulin stimulation resulted in 50 % of the transporters being found at the plasma membrane. They also found that in whole cells insulin increased the turnover number of the transporters in the plasma membrane in addition to their concentration.

The development of the membrane impermeant photoaffinity label 2-*N*-[4-(1-azi-2,2,2-trifluoroethyl)benzoyl]-1,3-bis-(D-mannos-4-yloxy)-2-propylamine (ATB-BMPA) (see section 1.4.3) enabled the adipocyte cell surface transporters to be quantified. Holman's group used ATB-BMPA to photolabel GLUT1 and GLUT4 at the surface of basal and insulin stimulated rat adipocytes (Holman *et al.*, 1990). They were able to demonstrate that the 20-30-fold increase in 3-*O*-methyl-D-glucose uptake is associated with a 15-20-fold increase in surface GLUT4 and an ≈ 5-fold increase in surface GLUT1. Using ATB-BMPA to determine the rates of the appearance and disappearance of transporters at the surface of rat adipocytes they found that both GLUT1 and GLUT4 appeared at the cell surface with a $t_{½}$ of ≈ 2.3 min. The insulin stimulated transport rate increased with a $t_{½}$ of 3.2 min but with a lag of 47 s. The lag, they suggested, may represent the time required for the ≈ 2-fold increase in the intrinsic activity of the transporters or may be the result of labelling transporters at the cell surface which are occluded from participating in transport. Following the removal of insulin the $t_{½}$ for the disappearance of transporters from the cell surface was ≈ 12 min, consistent with the $t_{½}$ of 9-11 min for the decrease in the transport rate at 37 °C (Clark *et al.*, 1991). They were also able to confirm that incubating basal rat adipocytes at the low temperature of 18 °C raises both the transport rate and the levels of transporters at the cell surface by ≈ 3-fold. They also observed that at 18 °C

following the removal of insulin stimulation there was no significant decrease in the transport rate or the cell surface transporter levels, suggesting that transporter internalisation is a more temperature sensitive process than transporter recruitment.

ATB-BMPA was also used to follow the trafficking of transporters in 3T3-L1 adipocytes (Yang *et al.*, 1992a). In these cells, as in the rat adipocytes, there is a lag in the insulin stimulated increase in the transport rate of 3T3-L1 adipocytes incubated at 27 °C. At this temperature they measured a $t_{½}$ of 5.4 min for the appearance of GLUT4 at the cell surface and 5.7 min for the appearance of GLUT1. The $t_{½}$ for the increase in the transport rate was 8.6 min. When insulin stimulated adipocytes were treated with phenylarsine oxide (PAO), an inhibitor of receptor and fluid-phase endocytosis, the decrease in the transport rate corresponded with the decrease in cell surface GLUT4. The level of GLUT1 in the plasma membrane, however, remained high. They suggested that PAO may inhibit the exocytosis of transporters. The transport activity of the cell surface GLUT1 appears to be reduced by the presence of PAO, perhaps because of an inability of the transporter to dissociate from the trafficking proteins (Yang *et al.*, 1992a). These trafficking proteins have been shown to include clathrin (Robinson *et al.*, 1992).

The accessibility of transporters at the plasma membrane to glucose and ATB-BMPA was investigated in rat adipocytes by Cushman's group. Compared to insulin stimulation alone, insulin plus adenosine increased both the accessibility of GLUT4 to ATB-BMPA and the rate of transport without affecting the level of immunodetectable surface GLUT4. Isoprenaline had the opposite effect, reducing the insulin stimulated transport rate and the accessibility of the transporter to ATB-BMPA without causing GLUT4 to be lost from the plasma membrane. These results suggested that the transporter exists in the plasma membrane in two distinct states one of which is functional while the other is inaccessible and so non-functional (Vannucci *et al.* (1992).

Cushman's group then used ATB-BMPA to track the recycling of GLUT4 between the cell surface and intracellular pools in rat adipocytes. After the insulin stimulated plasma membrane pool of GLUT4 had been photolabelled, the insulin stimulation was either maintained or reversed by the addition of collagenase. The trafficking of the labelled transporters was followed and the distribution was compared with the total level of immunodetectable transporters in both pools. Following collagenase treatment the half times were similar for the decrease in the level of photolabelled and immunodetectable GLUT4 in the plasma membrane and for the decrease in the transport activity. When the collagenase treated adipocytes were restimulated with insulin then a proportion of both the labelled and non labelled transporters were recycled from the low density microsomal intracellular pool to the plasma membrane. Under conditions of continued incubation with insulin, while there was no alteration in the transport rate or in level of immunodetectable GLUT4 at the plasma membrane, there was a drop in the level of cell surface photolabelled GLUT4 as a result of internalisation. This effect is the result of all the transporters being continuously recycled so that the original cell surface pool of labelled transporters and the intracellular pool of unlabelled transporters eventually become mixed with the labelled transporters being distributed between the two pools (Satoh *et al.*, 1993). Kinetic analysis of the translocation of the labelled transporters shows that insulin stimulates exocytosis rather than inhibiting endocytosis. The endocytosis rate constant k_{en} was not significant different whether the cells were stimulated with insulin or the insulin stimulation was reversed. Insulin did, however, increase the exocytosis rate constant, k_{ex}, by $\approx$ 10-fold (Satoh *et al.*, 1993). Increases in cell surface GLUT4 are immunodetectable before they can be photolabelled and both of these increases occur before the transport rate increases. This, they suggested, may be the result of an intermediate step between the transporters in the occluded vesicles and the fully active transporters. Transporters in these partially occluded vesicles are immunodetectable and can be photolabelled but can not participate in transport (Satoh *et al.*, 1993).

They also suggested that insulin might act at the docking and fusion steps of translocation. The current model of transporter translocation is given in figure 1.5.

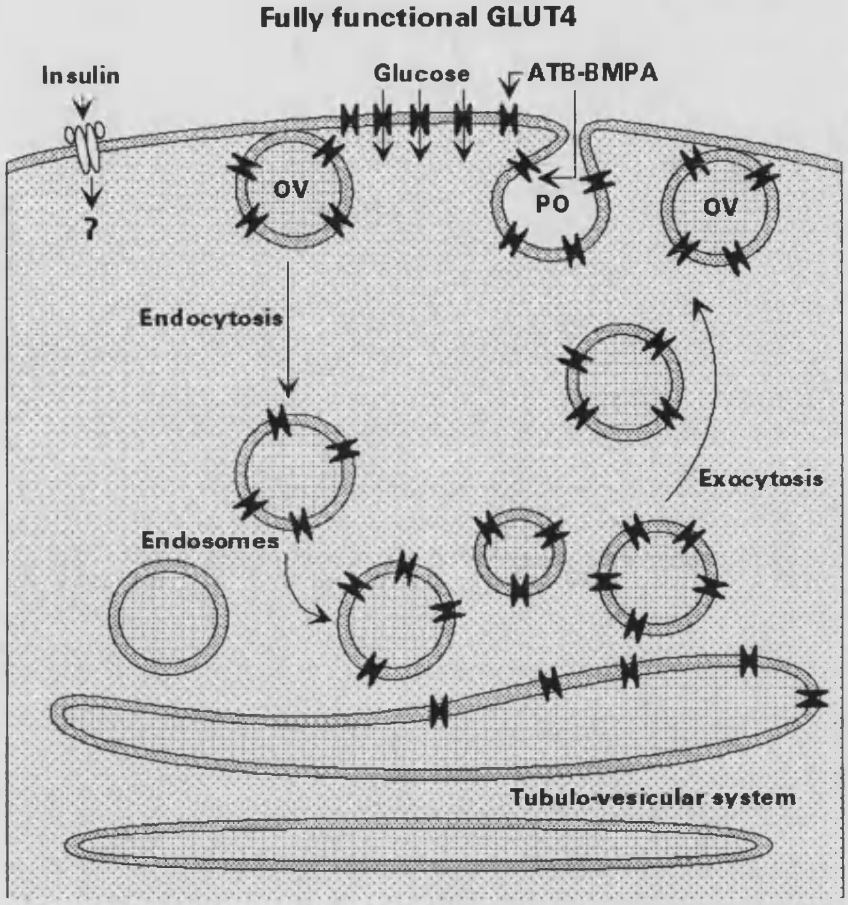

Figure 1.5 Model of the insulin regulated translocation of glucose transporter to and from an intracellular pool

GLUT4 is continuously recycled between the cell surface and tubulo-vesicular structures in both the presence and absence of insulin. In basal adipocytes most of the GLUT4 is located in the tubulo-vesicular structure. Insulin stimulation increases the rate of exocytosis resulting in an increase in cell surface GLUT4. Occluded and partially occluded vesicles form as vesicles fuse with the membrane.
OV: occluded vesicle. PO: Partially occluded vesicle. M: GLUT4. (From Gould and Holman, 1993)

The insulin stimulated steady state recycling of both GLUT4 and GLUT1 in 3T3-L1 adipocytes were kinetically analysed by Yang and Holman (1993). They were able to confirm that both GLUT1 and GLUT4 are continuously recycled between the cell surface and the low density microsome membrane fraction in both basal and insulin stimulated adipocytes. In basal adipocytes the GLUT4 exocytosis rate is low. Insulin

stimulation decreases the endocytosis rates of both isoforms by ≈ 30 % but increases the exocytosis rate for GLUT1 and GLUT4 by 3- and 9-fold respectively.

When ultrathin cryosections of 3T3-L1 adipocytes were analysed by immunocytochemistry a large proportion of the glucose transporter (probably GLUT1) population was detected in the *trans*-Golgi reticulum and in cytoplasmic vesicles. Insulin stimulation caused a decrease in the population of GLUT1 in the tubulovesicular structure but did not affect the level of transporter labelling in the cytoplasmic vesicles (Blok *et al.*, 1988). The vesicles involved in transporter translocation in 3T3-L1 adipocytes were isolated by immunoadsorption and were further characterised by Brown *et al.* (1988). They found that transporters constituted 3 % of the 50 nm vesicles which equates to about 8 transporters per vesicle. Insulin stimulation did not alter the degree of vesicle protein phosphorylation.

1.4.2 Separate sorting of GLUT4 and GLUT1

The plasma membrane of basal rat adipocytes contains low levels of both GLUT1 and GLUT4 but GLUT4 is twice as abundant as GLUT1. Following insulin stimulation the level of GLUT4 at the cell surface increases by 15–20-fold while GLUT1 increases by only 5-fold (Holman *et al.*, 1990). In 3T3-L1 adipocytes where GLUT1 is the predominant isoform GLUT1 is most abundant at the cell surface in basal cells. Here insulin causes a 17-fold increase in GLUT4 and a 6.5-fold increase in GLUT1 (Calderhead *et al.*, 1990). Thus in both rat and 3T3-L1 adipocytes GLUT1 and GLUT4 have a unique distribution between the cell surface and the intracellular pool with a higher proportion of GLUT1 at the surface of basal adipocytes while insulin stimulation has a different effect on the translocation of the two transporter isoforms.

In basal adipocytes the majority of both the GLUT4 and GLUT1 transporters reside in the low density microsomes within the cell. Zorzano *et al.* (1989) reported the

presence of at least two transporter containing vesicle populations in rat adipocytes, one recognised by an anti-GLUT4 antibody and the other recognised by an anti-GLUT1 antibody. The transporter containing vesicles in 3T3-L1 adipocytes were characterised by Calderhead *et al.* (1990). The vesicles were found to have an average diameter of 72 nm. When they immunoadsorbed vesicles with anti-GLUT1 antibodies they precipitated 95 % of the GLUT4 while immunoadsorption with anti-GLUT4 antibodies precipitated 85 % of the GLUT1. A later study on 3T3-L1 adipocytes found further evidence for the differential sorting of GLUT4 and GLUT1 with the proportion of total GLUT1 at surface of basal cells being 1:2 while it was 1:30 for GLUT4. Using an anti-GLUT4 antibody they were able to immunoisolate vesicles which contained 90 % of the GLUT4 but only 30 % of the GLUT1 (Piper *et al.*, 1991). Double labelling immunocytochemical experiments also showed distinct compartments enriched with one, but not the other, transporter isoform. Differences between these two 3T3-L1 adipocyte studies may be due to different homogenisation techniques but both show that sorting is less rigorous in 3T3-L1 adipocytes where there are much higher levels of GLUT1 than in rat adipocytes.

The differential localisation of GLUT4 and GLUT1 in rat and 3T3-L1 adipocytes between the plasma membrane and microsomes and the two vesicle populations requires some mechanism whereby the two isoforms can be distinguished and differentially sorted. The GLUT4 protein itself is an obvious candidate for such a mechanism. The sorting of transporters is isoform specific rather than dependent on the cell type. GLUT1 and GLUT4 have been expressed in a number of different insulin insensitive cell types. 3T3-L1 fibroblasts and HepG2 hepatoma cells were transfected with GLUT1 and GLUT4 by Haney *et al.* (1991). In 3T3-L1 fibroblasts GLUT1 was concentrated in the plasma membrane and increased the transport rate. GLUT4 transfection did not increase transport even following treatment with insulin and the protein was concentrated in the *trans*-Golgi reticulum. A similar isoform specific distribution with GLUT1 at the plasma membrane and GLUT4 in intracellular stores

was seen in the HepG2 cells (Haney *et al.*, 1991), NIH-3T3 fibroblasts (Hudson *et al.*, 1992), CHO fibroblasts (Shibasaki *et al.*, 1992), COS-7 fibroblasts (Schürmann *et al.*, 1992b) and *Xenopus* oocytes (Thomas *et al.*, 1993). When GLUT4 was expressed in the neuroendocrine cell line PC12 it was specifically sorted to the specialised secretory compartment of the cells (Hudson *et al.*, 1993). These results all showed that the targeting of GLUT4 must be intrinsic to the transporter protein itself.

The major regions of sequence deviation between GLUT4 and GLUT1 occur in the cytoplasmic portions of the transporters and three such regions have been implicated as containing specific targeting information. The first region to be implicated in the sorting of GLUT4 was the N-terminal domain. Piper *et al.* (1992) found that either deleting the first eight amino acids from the N terminus or the mutation at Phe^5, F5A, both resulted in the accumulation of GLUT4 in the plasma membrane when the mutants were transiently expressed in CHO fibroblasts. These mutations also abolished the colocalization of GLUT4 with the clathrin lattices (Piper *et al.*, 1993a). Other substitutions around Phe^5 had a similar but smaller effect on cell surface expression. When the N terminus of GLUT1 was replaced with that of GLUT4 the mutant adopted a GLUT4-like distribution. The opposite effect was seen when the N terminus of GLUT4 was replaced with that of GLUT1 (Piper *et al.*, 1992). When the C terminus of the H1 subunit of the asialoglycoprotein receptor was replaced with the N terminus of GLUT4 the mutant protein was sequestered into an intracellular compartment similar to that of GLUT4 while the wild type protein was localised at the cell surface. The sequence within the N-terminal domain of GLUT4 that is responsible for this targeting has been identified as a phenylalanine based motif, PSGFQQI, residues 2 to 8 (Piper *et al.*, 1993a). This internalisation motif occurs in other internalised proteins such as the mannose-6-phosphate/IGF-II receptor (Jadot *et al.*, 1992) and surface glycoproteins (Ktistakis *et al.*, 1990). The main features of the motif are an aromatic residue and a bulky hydrophobic residue with two amino acids between them. The aromatic residue can be a tyrosine or a phenylalanine but the latter is less

efficient which would allow GLUT4 to accumulate in the plasma membrane to the required extent. At the same time Asano *et al.* (1992b) stably transfected CHO fibroblasts with mutant transporters containing different segments of GLUT1 and GLUT4. They identified two domains in a region containing transmembrane helices 7 and the N-terminal half of the loop between helix 7 and 8 rather than the N– or C–terminal domains.

More recently the C-terminal domain has been shown to be involved in the localisation of the glucose transporters. Verhey *et al.* (1993) made chimeric transporters and expressed them in NIH 3T3 and PC12 cells. They found that the N-terminal half of GLUT4 and the last 30 amino acids of the C-terminal tail were responsible for the differential targeting of GLUT1 and GLUT4. Of these two regions, however, the C-terminal domain was found to be the more important region. The C-terminal domain was also identified as being responsible for the targeting of GLUT4 by Czech *et al.* (1993). They made GLUT1/GLUT4 chimeras and expressed them in COS-7 and CHO fibroblasts. They also found that the last 30 amino acids of GLUT4 could promote the intracellular sequestration of GLUT1. Within this region they identified two leucines, Leu^{489} and Leu^{490} in GLUT4. This dileucine motif is important for the targeting of proteins such as the mannose-6-phosphate/IGF-II receptor (Johnson and Kornfeld, 1992) to the endocytic pathway. It has been suggested that the C- and N-terminal targeting sequences of GLUT4 may play different roles in the intracellular sequestration, the N-terminus involved in clathrin coated pit mediated internalisation and the C-terminus retaining it within the intracellular pool (Garippa *et al.*, 1994).

1.4.3 ATB-BMPA, the exofacial glucose transporter photolabel

2-*N*-[4-(1-azi-2,2,2-trifluoroethyl)benzoyl]-1,3-bis-(D-mannos-4-yloxy)-2-propylamine, ATB-BMPA, was developed as a specific cell surface glucose transporter label. It is based on a bis-D-mannose with the two mannose joined at the C4 position by a 2-

propylamine bridge. The bis-D-mannose makes the compound sufficiently hydrophilic to be soluble in physiological buffers and membrane impermeant. Thus it is unable to label intracellular transporters (Clark and Holman, 1990). The outward facing binding site will not accept glucose analogues with a bulky substitution at the C1 position but is unaffected by substitutions at the C4 position. At the inward facing binding site the situation is reversed (Barnett *et al.*, 1975). Thus the 2-propylamine substitution at the C4 position does not prevent binding at the outward facing site but does prevent the label being transported or binding to the inner binding site. The bulky photolabile 4-(1-azi-2,2,2-trifluoroethyl)-benzoic acid group is coupled to the 2-propylamine bridge where it does not interfere with the binding of mannose to the outer binding site. Irradiating the diazirine portion of ATB-BMPA with 300 nm ultra violet light generates a carbene which binds irreversibly to the glucose transporter at helix 8 (Baldwin, 1993) and adds to its specificity (Clark and Holman, 1990). ATB-BMPA it is a powerful tool for labelling and quantifying cell surface transporters without the need for subcellular fractionation and the inherent danger of contamination by intracellular transporters.

The affinity constant of ATB-BMPA is approximately equal for all transporter isoforms so far investigated. In 3T3-L1 adipocytes the K_d of GLUT1 and GLUT4 for ATB-BMPA is ≈ 150 μM (Palfreyman *et al.*, 1992) and 250 μM for GLUT2 in liver plasma membranes (Jordan and Holman, 1992).

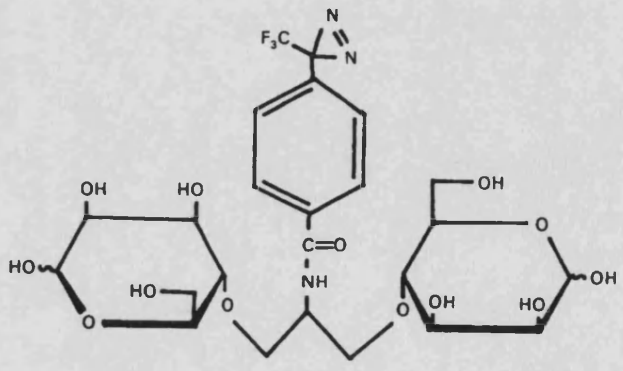

Figure 1.6 The structure of ATB-BMPA (Clark and Holman, 1990)

1.5 Insulin and the insulin receptor

1.5.1 Insulin secretion and its effects

The effect of insulin on metabolism and cell growth have been well characterised and the sequence and 3-D structure of the insulin protein itself have been known since the early fifties yet the molecular basis for the actions of insulin at the cellular level are proving more elusive. Insulin is synthesised by the β-cells of the Islets of Langerhans and is the only hormone that can effectively decrease the blood sugar concentration. After a meal the blood glucose concentration rises. This is detected directly within the β-cells, the kinetics of GLUT2 allowing the intracellular glucose concentration to change in tandem to the blood glucose concentration (as described in section 1.2.2.). The β-cells glucokinase is activated by glucose and phosphorylates glucose with a higher K_m than hexokinase, (Matschinsky, 1990). Thus glucose-6-phosphate, ADP and H^+ are produced within β-cells at a rate proportional and specific to the blood glucose level. Glucose phosphorylation is believed to be important as inhibitors of glucose phosphorylation also inhibit glucose induced insulin secretion (Hedeskov, 1980). The exact mechanism linking glucokinase to insulin secretion is unclear but an increase in ATP inducing an influx of Ca^{2+} appears to be involved (Prentki and Matschinsky, 1987).

Once secreted insulin has a range of physiological effects on insulin sensitive cells. Some effects occur instantly while others take minutes or hours (Denton, 1986). Insulin affects both cell metabolism and cell growth (Rosen, 1987). Effects requiring longer exposures to insulin, such as those on cell growth and transformation, are probably the result of changes in gene expression. For example in 3T3-L1 adipocytes chronic exposure to insulin results in an increased level of expression of GLUT1 mRNA and protein (Tordjman *et al.*, 1989). Insulin induced changes in cell metabolism generally require a shorter exposure to the hormone (Denton, 1986). Many of these events are the result of increases and decreases in the phosphorylation of particular proteins. These metabolic changes are anabolic in nature, and result in a reduction in

the level of blood glucose. In muscle, insulin induces the translocation of GLUT4 to the plasma membrane, decreases the phosphorylation of glycogen synthase which increases glycogen synthesis and increases amino acid uptake and general protein synthesis. In the liver glycogen, fatty acid, cholesterol and general protein synthesis are increased while gluconeogenesis, fatty acid oxidation and ketogenesis are decreased. In adipocytes insulin increases glucose uptake by raising the concentration of GLUT4 in the plasma membrane. Fatty acid synthesis is increased by activating pyruvate dehydrogenase by dephosphorylation and acetyl CoA carboxylase by phosphorylation. Triglyceride synthesis is probably increased by the activation of glycerol phosphate acyl transferase. Glycogen synthesis and general protein synthesis are increased as well as more specific changes in protein synthesis such as GLUT1. Insulin also decreases the activity of triglyceride lipase in adipocytes by the dephosphorylation of the enzyme.

1.5.2 Structure of the insulin receptor

While it is known that insulin increases glucose uptake in adipocytes by increasing the translocation of GLUT4 to the plasma membrane and so raising the V_{max}, the precise signalling mechanism is unknown. Insulin is believed to produce all its effect by binding to the insulin receptor rather than by entering the cell itself.

The cells of the major insulin responsive tissues, the liver, muscle and adipose tissues, contain between 20,000 to 100,000 insulin receptors per cell although insulin only needs to bind to 1,000 to 2,000 receptors to produce a maximal insulin effect (Denton, 1986). The insulin receptor is a heterotetrameric glycoprotein with the structure β-α-α-β. The complex is held together by disulphide bonds. It has an apparent mass of 350-400 kDa. The molecular weight of the α-subunit is 95 kDa while that of the β-subunit is 135 kDa. The receptor is synthesised as a precursor which is cleaved to give the α- and β-subunit. The human insulin receptor cDNA was independently cloned by two groups (Ullrich *et al.*, 1985, Ebina *et al.*, 1985). There

are two isoforms of the receptor which differ with the presence or absence of a 12 amino acid sequence near the C-terminus of the α-subunit. Ullrich *et al.* (1985) sequenced the 1370 amino acid precursor while Ebina *et al.* (1985) sequenced the longer 1382 amino acid precursor which contains the additional mini-exon. The nomenclature used here is that of Ebina *et al.* (1985). The distribution of the two isoforms is both specific and distinct but the physiological significance of this is unclear (Goldstein and Dudley, 1990).

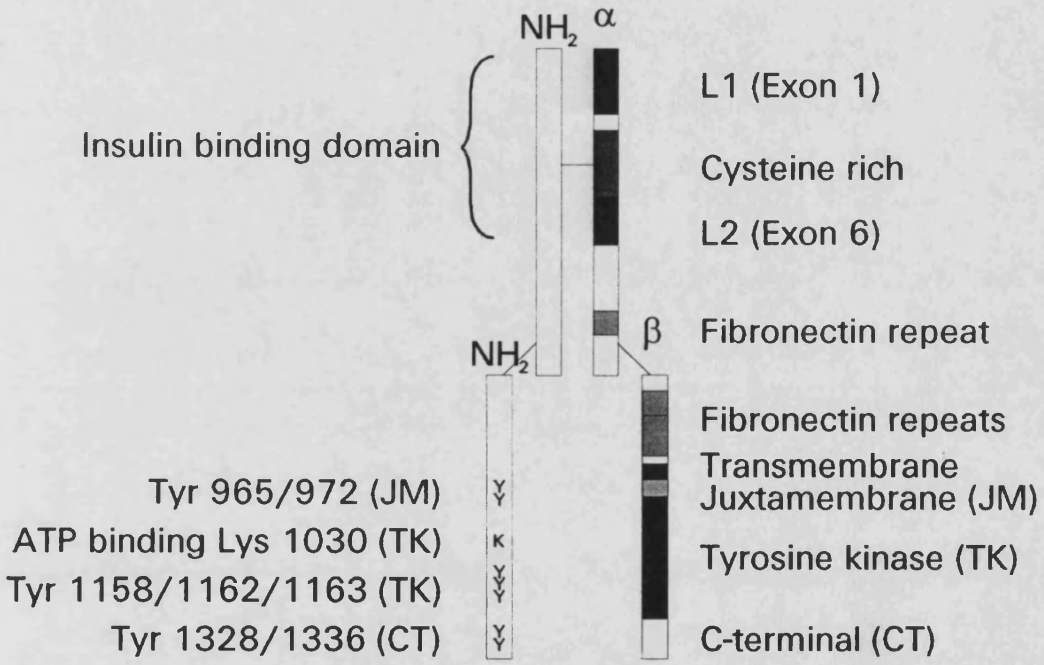

Figure 1.7 A model of the insulin receptor

The two insulin receptor α-subunits are joined to one another and the two β-subunits by disulphide bonds. The relative positions of the receptor domains are shown on the right and the autophosphorylation and other functional sites are shown on the left (from White and Kahn, 1994).

The 719 or 731 amino acids of the insulin receptor α-subunit are entirely extracellular and bind insulin. Insulin binds between the L1 domain of one α-subunit and the L2 domain of the other (Schumacher *et al.*, 1993). The insulin-like growth factor I binds to the cysteine rich domains (Schumacher *et al.*, 1991). The 620 amino acids of the β-subunit spans the plasma membrane. It has two globular domains, one extracellular

and the other intracellular. They are linked by the 23 uncharged membrane spanning amino acids of the transmembrane domain. The receptor is a member of the tyrosine kinase family of receptors that includes the epidermal growth receptor and the platelet derived growth factor receptor and oncogenic proteins such as v-*erb-B*. The insulin-like growth factor 1 receptor and the insulin receptor are similar both having the same heterotetrameric structure (Ullrich and Schlessinger, 1990). The tyrosine kinase domain is the most similar region among this family of tyrosine kinase receptors.

1.5.3 The activation of the insulin receptor

The binding of insulin to the α-subunit of the insulin receptor is believed to cause a conformational change in the receptor which is transmitted to the intracellular domain thus allowing the tyrosine kinase to be active. It has been demonstrated in several ways that the role of the extracellular domain of the receptor is to inhibit kinase activity in the absence of insulin rather than to activate the kinase in its presence. Trypsin treatment of the insulin receptor cleaves the α-subunit at Arg^{576} - Arg^{577}. This results in the loss of the insulin binding site and the separation of the receptor into two heterodimers. The tyrosine kinase of this truncated receptor was constitutively activated (Shoelson *et al.*, 1988). A similar effect was seen when mouse L cells were transfected with a recombinant membrane-anchored insulin receptor kinase which has only 15 extracellular residues. This too possessed insulin independent tyrosine kinase activity and enhanced 2-deoxy-D-glucose uptake (Lebwohl *et al.*, 1991).

The role of the transmembrane domain in the activation of the receptor has been investigated by a number of groups but with contradictory results. While most groups consider this region to play an essentially passive role others disagree. The role of the transmembrane region in the activation of the receptor by insulin therefore remains unclear (Tavaré and Siddle, 1993). An intact juxtamembrane region is essential for the activity of the receptor. This region contains two XPXY motifs which may adopt a β-

turn and be involved in insulin stimulated, coated pit mediated, receptor endocytosis (Backer *et al.*, 1992b). Replacing the two tyrosines with alanines did not affect insulin binding or receptor autophosphorylation but did reduce receptor internalisation by 70 %. Essential to the correct activity of the insulin receptor is the ATP binding residue, Lys^{1030} (McClain *et al.*, 1987). The mutation K1030A prevented insulin activation of the tyrosine kinase, blocked insulin stimulation of glucose transport and glycogen synthase activity and inhibited receptor internalisation.

Crucial to the activity of the insulin receptor is the tyrosine kinase and its autophosphorylation. Three phosphorylation sites have been identified in the insulin receptor β-subunit; the juxtamembrane region, the tyrosine kinase domain and the C-terminal region. Within the juxtamembrane region tyrosine residues 965 and 972 (Kohanski, 1993b) are slowly phosphorylated in the absence of insulin and this is favoured by a low ATP concentration (Kohanski, 1993a). Tyrosine residues 1158, 1162 and 1163 within the kinase domain are phosphorylated in response to insulin (Tavaré and Denton, 1988). Unlike the juxtamembrane site these tyrosines are rapidly phosphorylated in response to insulin (Kohanski, 1993a). The insulin receptor is symmetrical and possesses two binding sites but it only binds one insulin molecule with high affinity and only one site need be occupied to fully stimulate receptor autophosphorylation (Shoelson *et al.*, 1993). Once insulin has bound, the activated insulin receptor tyrosine kinase of one β-subunit *trans*-autophosphorylates the other β-subunit of the receptor. This has been demonstrated using hybrid receptors of kinase defective and insulin/IGF-1 binding domains (Treadway *et al.*, 1991) and by the use of covalently bound insulin (Lee *et al.*, 1993). Autophosphorylation has a range of physiological responses including increases in glycogen and DNA synthesis (Wilden *et al.*, 1992a) and glucose transport. A comparison of the concentration-response curves for insulin stimulation of the tyrosine kinase and glucose uptake found that only 4 % and 14 % of the maximal kinase activity was required for half maximal and maximal insulin stimulation of glucose uptake respectively (Klein *et al.*, 1991). Replacement of

any of the three tyrosine kinase domain tyrosines with phenylalanine reduced insulin stimulated autophosphorylation by over 50 %. Double replacements reduced it by 60-70 % while the triple substitution decreased it over 80 % (Wilden *et al.*, 1992b). These mutations also decreased IRS-1 tyrosine phosphorylation and insulin stimulated receptor internalisation (Wilden *et al.*, 1992a). Mutation of Y1162F or Y1162/63F, in addition to reducing autophosphorylation, also reduced or almost completely blocked insulin stimulated glucose transport (Ellis *et al.*, 1986). The mutation of these two tyrosines did not affect the long term insulin stimulated increase in GLUT1 mRNA and protein levels (Desbois *et al.*, 1992). These contrasting results indicate a divergence of pathways at the level of the insulin receptor itself.

The third site of autophosphorylation in the C-terminal region of the receptor is at residues Y1328 and Y1334 (Tornqvist *et al.*, 1987). When a mutant human insulin receptor lacking the last 43 amino acids (hIRΔCT43) was expressed in rat-1 fibroblasts it was found to inhibit insulin stimulated glucose transport without affecting autophosphorylation or mitogenic effects (Maegawa *et al.*, 1988). Others have reported that this deletion mutation has no effect but this could be related to the cells used for expression (Tavaré and Siddle, 1993). The C-terminal region also contains the Ser/Thr phosphorylation sites Thr^{1348} and $Ser^{1305/6}$ (Chin *et al.*, 1993). The serines are phosphorylated by the insulin sensitive serine kinase, a kinase which is closely associated with and copurifies with the insulin receptor (Lewis *et al.*, 1990). This phosphorylation does not inhibit the receptor tyrosine kinase but it can inhibit insulin stimulated responses (Chin *et al.*, 1993).

1.6 Potential second messenger systems

1.6.1 The insulin receptor substrate-1 and phosphatidylinositol 3'-kinase

Insulin induced autophosphorylation of the insulin receptor β-subunit increases the activity of the insulin receptor tyrosine kinase toward other substrates. White *et al.* (1985) identified two proteins whose tyrosine phosphorylation was increased by insulin stimulation. One of these, pp95, was the insulin receptor β-subunit. This remained phosphorylated throughout the hour long insulin stimulation. The second was the specific substrate pp185 which, like pp95, was maximally phosphorylated within 30 s. However, unlike pp95 this protein was dephosphorylated during the one hour insulin stimulation. pp185, the major insulin stimulated tyrosine phosphorylated protein, was purified, partially sequenced, (Rothenberg *et al.*, 1991) cloned and called IRS-1 (insulin receptor substrate-1) (Sun *et al.*, 1991). IRS-1 contains 21 potential phosphorylation sites six of which have the motif YMXM while a further three are YXXM. Synthetic peptides containing these motifs are phosphorylated by the purified insulin receptor, supporting the idea that they are insulin receptor tyrosine kinase phosphorylation sites in IRS-1 (Shoelson *et al.*, 1992). When phosphorylated, these motifs are thought to act as docking sites for proteins possessing SH2/3 domains, the large number of sites allowing it to act as a multisite docking protein, see figure 1.8.

Once phosphorylated IRS-1 forms a stable complex with the p85 subunit of phosphatidylinositol 3'-kinase (PI3-kinase) with the SH2 domains of p85 associating with the phosphorylated YXXM motifs. This association activates the PI3-kinase p110 subunit which phosphorylates phosphatidylinositols (PI) at D3 producing PI(3)P, $PI(3,4)P_2$ and $PI(3,4,5)P_3$ (Backer *et al.*, 1992a). Most PI3-kinase activity is associated with intracellular membranes, the IRS-1/PI3-kinase complex being localised in a very low density membrane fraction which is not enriched in either GLUT4 or insulin receptors in rat adipocytes (Kelly *et al.*, 1993). A link between PI3-kinase and insulin stimulated glucose transport was made by comparing the effect of okadaic acid on

transport and PI3-kinase activity. Although okadaic acid stimulates basal transport it inhibits insulin stimulated glucose uptake in adipocytes and muscle and inhibits the association of phosphorylated IRS-1 with PI3-kinase as detected by immunoprecipitation with antiphosphotyrosine antibodies. Okadaic acid, however, does not inhibit the activity of the insulin receptor tyrosine kinase. Okadaic acid did not block insulin stimulated aminoisobutyric acid uptake in muscle so IRS-1 and PI3-kinase are not required for all the effects of insulin (Jullien *et al.*, 1993). Wortmannin, believed to be a specific PI3-kinase inhibitor, supports this link. Wortmannin inhibits both PI3-kinase activity and insulin stimulated glucose uptake (Clarke *et al.*, 1994).

1.6.2 Serine and threonine phosphorylation second messengers

1.6.2.1 GLUT4 phosphorylation

GLUT4 phosphorylation was first detected by James *et al.* (1989b). When rat adipocytes were treated with either isoproterenol, dibutyryl-cAMP or 8-bromo-cAMP GLUT4 phosphorylation was stimulated 2-fold. The phosphorylation site was identified as Ser^{488} using ^{32}P labelling and CNBr cleavage (Lawrence *et al.*, 1990a). This site has also been confirmed by Piper *et al.* (1993b) who substituted Ser^{488} for Ala (S488A) and abolished GLUT4 phosphorylation.

There are two possible regulatory roles for transporter phosphorylation. One is the regulation of translocation and the other is the regulation of intrinsic transporter activity. Lawrence *et al.* (1990a, b) were unable to report an insulin induced change in GLUT4 phosphorylation but they suggested that phosphorylation may promote transporter internalisation. Reusch *et al.* (1993) were able to demonstrate a decrease in GLUT4 phosphorylation in the presence of insulin. They, however, did not find evidence that GLUT4 phosphorylation affected transporter translocation. They treated rat adipocytes with parathyroid hormone which increased GLUT4

phosphorylation but did not alter the translocation of the transporter to the plasma membrane. Phosphorylation of rat adipocyte GLUT4 did reduce the intrinsic activity of GLUT4 in both intact adipocytes and reconstituted vesicles. In plasma membrane vesicles GLUT4 phosphorylation resulted in a 35 % reduction in intrinsic activity. They were unable to confirm that phosphorylation itself rather than a conformational change was responsible for the change in activity.

1.6.2.2 Protein phosphatases and okadaic acid

Okadaic acid is produced by dinoflagellates and concentrated in the marine sponges *Halichondria okadaii* and *Halichondria melanodocia*. It was first identified as the cause of diarrhetic seafood poisoning (reviewed in Cohen *et al.*, 1990). Okadaic acid was found to be a potent inhibitor of the two major serine/threonine phosphatases PP1 and 2A (Bialojan and Takai *et al.*, 1988) Purified PP1 is inhibited by okadaic acid with an IC_{50} of 20 nM while for PP2A it is only 0.2 nM. In intact cells the maximal inhibitory effects of okadaic acid are obtained at a concentration of 1 μM (Haystead *et al.*, 1989). The effects of okadaic acid on hexose transport in rat adipocytes were first described by Haystead *et al.* (1989) who showed that okadaic acid stimulates 2-deoxy-D-glucose uptake in a manner similar to that of insulin but with a 5 min lag. The effect of okadaic acid on GLUT4 in rat adipocytes was further investigated by Lawrence *et al.* (1990b). They found that in adipocytes fully stimulated with okadaic acid (1 μM for 20 min) the rate of uptake of 2-deoxy-D-glucose was only half of that for insulin. Furthermore when the cells were stimulated with both insulin and okadaic acid the rate was less than for insulin alone. They also looked at the effect of okadaic acid on the distribution of GLUT4. They found that okadaic acid alone stimulated the translocation of GLUT4 by only ≈ 40 % of that with insulin. With insulin and okadaic acid together the stimulation was only ≈ 70 % of that for insulin alone. They found that okadaic acid but not insulin increased the level of GLUT4 phosphorylation. From

this they concluded that okadaic acid stimulates transport as a result of the translocation of GLUT4 to the plasma membrane by causing the phosphorylation of proteins that regulate vesicle movement perhaps including proteins within the GLUT4 containing vesicles. A similar study was carried out by Corvera *et al.* (1991). They too looked at the effect of okadaic acid on insulin stimulated glucose uptake in rat adipocytes. They found that okadaic acid caused a small increase in transport and the level of cell surface transporters but blocked insulin stimulated transporter translocation. They also found a discrepancy between plasma membrane levels of GLUT4 and the rate of 3-O-methyl-D-glucose uptake. This led them to suggest that okadaic acid may cause a 10-20 % decrease in the intrinsic activity of GLUT4.

Okadaic acid causes the phosphorylation and activation of a number of proteins including the myelin basic protein kinase (Haystead *et al.*, 1990), cAMP phosphodiesterase (Shibata *et al.*, 1991) and the Na^+/H^+ antiport (Bianchini *et al.*, 1991). Although okadaic acid does not alter the insulin induced autophosphorylation of the insulin receptor it does inhibit the insulin induced tyrosine phosphorylation of IRS-1 (Jullien *et al.*, 1993). This lack of IRS-1 tyrosine phosphorylation prevents IRS-1 associating with and activating PI3-kinase. Okadaic acid alone had no effect on anti-phosphotyrosine immunoprecipitable PI3-kinase activity. They suggested that okadaic acid may inhibit insulin induced IRS-1 tyrosine phosphorylation by causing the phosphorylation of either the insulin receptor or IRS-1 so impairing their binding.

Other links have been made between the insulin receptor and protein phosphatases. The insulin receptor can phosphorylate the catalytic subunit of PP-2A on Tyr^{307}. This deactivates the phosphatase. Phosphorylation is enhanced by the presence of okadaic acid. It was therefore suggested that the transient deactivation of PP-2A may allow insulin to activate kinase cascades including ribosomal protein S6 kinases and mitogen-activated protein kinases (Chen *et al.*, 1992). Insulin appears to have the opposite effect on PP-1. The activity of PP-1 was studied in rat-1 fibroblasts expressing either the human insulin receptor (hIR) or a mutant receptor lacking the last 43 amino acids

(hIRΔCT43). When insulin binds to the mutant receptor autophosphorylation occurs normally but metabolic effects, including the stimulation of glucose transport, are blocked. In cells expressing hIR, insulin caused a 25-30 % increase in the activity of PP-1 toward phosphorylase a. In cells expressing hIRΔCT43 insulin did not activated PP-1. This suggests that PP-1 may interact with the C terminus of the insulin receptor and that PP-1 my be involved in the metabolic actions of insulin (Begum *et al.*, 1993b).

1.6.2.3 Protein kinase C

Protein kinase C is activated by a number of hormones and growth factors including insulin. So far ten isoforms in three subfamilies have been identified. Ca^{2+} phosphatidylserine, free fatty acids and diacylglycerol (DAG) are required for the activation of the classical protein kinase C group. The new protein kinase C group and the atypical protein kinase C group have less requirements for activation (Nishizuka, 1992). The concentration of diacylglycerol within a cell can be increased by hydrolysis of phosphatidylinositol (PI) or phosphatidylcholine (PC) by phospholipase C or by *de novo* synthesis of DAG by glycerol-3-phosphate acyl transferase. Insulin has been shown to increase DAG levels in adipocytes both by PC hydrolysis and *de novo* synthesis (Farese *et al.*, 1985). PI hydrolysis is pertussis toxin sensitive while PC hydrolysis is pertussis toxin insensitive (Hoffman *et al.*, 1991; Luttrell *et al.*, 1988).

Tumour promoting phorbol esters (Shoyab and Todaro, 1980) such as phorbol 12-myristate 13 acetate (PMA) can activate protein kinase C in addition to DAG (Nishizuka, 1988). PMA increases the basal glucose transport rate by 2-fold (Kirsch *et al.*, 1985) to ≈ 3-fold in rat adipocytes (Holman *et al.*, 1990) and by ≈ 2-fold in 3T3-L1 adipocytes (Gibbs *et al.*, 1991), several fold less than insulin. The stimulatory effect of PMA is not additive with that of maximal stimulating concentrations of insulin (Gibbs *et al.*, 1986). At submaximal insulin concentrations, however, PMA does have an additive effect on the insulin stimulation of transport (Gibbs *et al.*, 1991).

In addition to stimulating protein kinase C, PMA also down-regulates the enzyme. Incubating 3T3-L1 fibroblasts with PMA for 16 h results in the loss of immunodetectable protein kinase C and the kinase activity (Blackshear *et al.*, 1985). In 3T3-L1 adipocytes this down-regulation, while inhibiting PMA stimulated transport, had no effect on insulin stimulated transport (Gibbs *et al.*, 1991).

PMA also affects the translocation of GLUT1 and 4 in adipocytes. In rat adipocytes PMA stimulates the translocation of GLUT1 by 100 % and GLUT4 by 18 % of the maximal insulin stimulated level (Holman *et al.*, 1990). In 3T3-L1 adipocytes GLUT1 increases by only 40 % and GLUT4 by 10 % of the insulin stimulated level (Gibbs *et al.*, 1991). Since the translocation of GLUT4 to the plasma membrane is the major mechanism for the insulin stimulated increase in transport, the small stimulatory effect of PMA can be explained by its small increase in cell surface GLUT4. In addition to overnight exposure to PMA, PMA stimulated transport in 3T3-L1 fibroblasts can be inhibited by the selective protein kinase C inhibitor Roche 31-8220. This inhibitor, however, has no effect on the insulin stimulated transport rate (Merrall *et al.*, 1993).

Taken together these results indicate that in adipocytes while PMA does cause a small stimulation in glucose transport insulin and PMA work through different mechanisms. However such experiments, especially those involving the down regulation of protein kinase C by PMA, do not preclude all the protein kinase C subspecies from a role in the action of insulin. Yano *et al.* (1993) reported that staurosporine (SSP), a protein kinase C inhibitor to which certain protein kinase C isoforms are particularly sensitive, inhibits insulin stimulated glucose transport and transporter translocation. While their results do indicate a potential role for protein kinase C in the insulin stimulated glucose transport pathway they did not rule out the effect of SSP being due to the inhibition of other protein kinases such as the insulin receptor tyrosine kinase. The different subspecies of protein kinase C also have different sensitivities toward PMA induced down-regulation (Huang *et al.*, 1989). A possible candidate for an insulin activated protein kinase C is the ubiquitous atypical ζ subspecies. Protein kinase C ζ is not

translocated or down-regulated by phorbol esters or diacylglycerol derivatives (Ways *et al.*, 1992) and is calcium and DAG insensitive (Nishizuka, 1992). Instead this kinase is activated by phosphatidylinositol 3,4,5 triphosphate (Nakanishi *et al.*, 1993). Thus insulin could activate this enzyme via IRS-1 activation of PI3-kinase (see 1.6.1). While the substrate for protein kinase C ζ is unknown it is involved in insulin induced maturation of *Xenopus* oocytes and mitogenic signalling (Berra *et al.*, 1993).

1.6.2.4 Ca^{2+} as a second messenger for insulin

Ca^{2+} is unlikely to be a second messenger for insulin in the stimulation of glucose transport as insulin does not increase cytosolic free calcium levels in adipocytes (Blackmore and Augert, 1989). Indeed at high intracellular concentrations Ca^{2+} has an inhibitory effect on insulin action. High levels of cytosolic free calcium significantly inhibit the dephosphorylation of the insulin receptor (Begum *et al.*, 1991) and induce the phosphorylation of inhibitor-1. Inhibitor-1, when activated by phosphorylation inhibits the phosphoserine phosphatases and may therefore block some of the actions of insulin (Begum *et al.*, 1992). While a high intracellular $[Ca^{2+}]$ does not inhibit the insulin stimulated translocation of transporters to the plasma membrane it does inhibit 2-deoxy-D-glucose uptake and increases GLUT4 phosphorylation (Reusch *et al.*, 1991). Thus high $[Ca^{2+}]_i$ as a result of the inhibition of the phosphatase PP-1, causes the phosphorylation of GLUT4 and lowers its intrinsic activity (Begum *et al.*, 1993a).

1.6.2.5 The role of cAMP

The effect of cAMP on glucose transport was first recognised by Joost *et al.* (1986) who found that when the β-adrenergic agonist isoproterenol was added to rat adipocytes in the presence of adenosine deaminase, while there was no effect on transporter translocation the insulin stimulated transport rate V_{max} decreased by 60 %.

Since incubating rat adipocytes with isoproterenol or with the cAMP analogues dibutyryl-cAMP or 8-bromo-cAMP at 5 mM increases GLUT4 phosphorylation 2-fold it was suggested that GLUT4 is phosphorylated by a cAMP dependent protein kinase (James *et al.*, 1989b). GLUT4 can also be phosphorylated by incubating rat adipocyte microsomes with the catalytic subunit of cAMP dependent protein kinase. The phosphorylation of GLUT4 at Ser^{488} was proposed as a mechanism for β-adrenergic agonist inhibition of insulin stimulated glucose transport (Lawrence *et al.*, 1990a).

In contrast to this Clancy and Czech (1990) found that a 4 h incubation with either cholera toxin or dibutyryl cAMP caused the translocation of transporters to the plasma membrane and an increase in the rate of hexose uptake in 3T3-L1 adipocytes. A 12 h incubation increased the total cellular levels of GLUT1 but with little change in GLUT4. Since the increase in the level of cell surface transporters could not fully explain the increase in hexose transport they suggested that prolonged exposure to cholera toxin increases the intrinsic activity of the transporters. The effect of cAMP on GLUT1 and GLUT4 expression in 3T3-L1 adipocytes was studied using 8-bromo-cAMP. After a 16 h incubation with 8-bromo-cAMP GLUT4 decreased by 70 % while GLUT1 increased 3-fold as a result of mRNA stabilisation and transient transcriptional activation of GLUT1 and repression of the GLUT4 transcription rate (Kaestner *et al.*, 1991). The stimulatory effects of cAMP were also reported using dibutyryl-cAMP with rat adipocytes. At low concentrations (10 μM) it stimulated transport by causing the translocation of GLUT4 to the plasma membrane. At higher concentrations (1 mM), GLUT4 translocation was further increased but the transport rate decreased as a result of a decrease in intrinsic activity (Kelada *et al.*, 1992).

The inhibitory effect of cAMP on transport was further investigated in CHO cells transfected with transporters (Piper *et al.*, 1993b). While dibutyryl cAMP had no effect on either the concentration or distribution of transporters it did inhibit GLUT4 but not GLUT1 mediated 2-deoxy-D-glucose transport. The role of cAMP-dependent protein kinase was investigated using 8-bromo-cAMP, which activates the kinase, and

8-bromo-AMP, which does not. The former had no effect but the latter inhibited transport suggesting that the kinase is not involved in the inhibitory effects of cAMP. Nishimura *et al.* (1991) were also unable to find a link between the cAMP-dependent protein kinase, GLUT4 phosphorylation and the cAMP inhibition of glucose transport.

The role of GLUT4 phosphorylation at Ser^{488} was also investigated by Piper *et al.* (1993b). The substitution of an Ala, while preventing phosphorylation, did not inhibit transport or prevent dibutyryl-cAMP inhibition of transport. Furthermore the deletion of the last 29 residues from the C terminus prevented the dibutyryl cAMP inhibition of transport. These results suggest that the inhibitory effect of dibutyryl cAMP is the result of direct nucleotide binding to the transporter at a site within the C terminus.

1.6.2.6 The role of other kinases in insulin stimulated glucose transport

While the complete pathway for the mediation of insulin stimulation is unknown a number of potential insulin cascade components have been identified as being activated in the presence of insulin. These include raf-1 (Blackshear *et al.*, 1990), the mitogen activated protein (MAP) kinases $pp42^{mapk}$ and $pp44^{mapk}$ (Ray and Sturgill, 1987) and the ribosomal S6 protein kinases $pp90^{rsk}$ and $pp70^{s6k}$ (Fingar *et al.*, 1993) (see figure 1.8).

The role of the MAP kinases in insulin stimulated glucose transport was investigated using the myosin light chain kinase inhibitor, ML-9. ML-9 inhibits insulin stimulated transport and GLUT4 translocation in 3T3-L1 adipocytes but does not prevent the phosphorylation of $pp42^{mapk}$ or $pp44^{mapk}$ although it inhibits their activity. ML-9 also inhibits the ribosomal S6 protein kinases. While this does suggests that insulin stimulates glucose transport by activating the MAP kinases ML-9 may not be specific and may inhibit other kinases (Inoue *et al.*, 1993).

The role of $pp70^{s6k}$ in insulin stimulated glucose transport in 3T3-L1 adipocytes was investigated using rapamycin, a specific $pp70^{s6k}$ inhibitor. While rapamycin did inhibit

insulin activation of $pp70^{s6k}$ it had no effect on the stimulation of transport or GLUT4 translocation. Thus $pp70^{s6k}$ is not involved in the insulin stimulation of glucose transport (Fingar *et al.*, 1993). Both $pp90^{rsk}$ and $pp44^{mapk}$ are rapidly activated by insulin although the activation of these kinases alone is insufficient to activate glucose transport. This suggests that while there is a linear pathway from ras to the MAP kinases, each mediator is likely to act as a branch point (Fingar and Birnbaum, 1994a). It has been suggested that the activation of the MAP kinases is not sufficient in itself to bring about the translocation of GLUT4 in 3T3-L1 adipocytes. Epidermal growth factor (EGF), platelet-derived growth factor (PDGF) and insulin were all shown to activate the MAP kinases, as detected by a change in electrophoretic mobility. However, while insulin also induced a 13-fold increase in cell surface GLUT4, EGF and PDGF only induced a 2-fold rise in cell surface GLUT1 (Gould *et al.*, 1994).

The activation of raf-1 has also been shown to be insufficient to induce the translocation of GLUT4. Activated raf-1 was expressed in 3T3-L1 adipocytes. The basal transport rate in these cells was 40-fold higher than the parental basal transport rate. Insulin increased this higher basal rate by a further 1.2-fold. When the distribution of GLUT1 and 4 were examined then the presence of the activated raf-1 was found to greatly increase both surface and total levels of GLUT1. In contrast, activated raf-1 had no effect on either the surface or total levels of GLUT4 in the basal 3T3-L1 adipocytes. GLUT4 was still translocated to the cell surface in the presence of insulin, however (Fingar and Birnbaum, 1994b). These results suggests that GLUT1 and GLUT4 may be regulated by divergent signalling pathways in 3T3-L1 adipocytes.

A kinase known to be involved in the insulin stimulation of glucose transport in adipocytes is the insulin receptor tyrosine kinase, see section 1.4.3. The role of tyrosine kinases have been investigated in a range of systems with specific kinase inhibitors such as genistein, a tyrosine kinase inhibitor which competes with ATP (Akiyama *et al.*, 1987), and erbstatin and a range of compounds termed tryphostins, which compete with the kinase substrate, (Yaish *et al.*, 1988).

When genistein was added to rat adipocytes it was found to inhibit insulin stimulated glucose oxidation and other responses without inhibiting insulin receptor autophosphorylation (Alber *et al.*, 1992). While genistein inhibits the insulin stimulated increase in glucose transport it does not inhibit insulin stimulated translocation. Genistein does, however, decrease the C-terminal immunocytochemical labelling of plasma membrane GLUT4. It was therefore concluded that genistein, rather than inhibiting the insulin receptor tyrosine kinase, lowers the intrinsic activity of GLUT4 by causing a conformational change at the C terminus (Smith *et al.*, 1993).

Tyrosine kinases have now been shown to have an effect on a range of kinase-independent systems. For example, genistein was found to be an uncoupler of oxidative phosphorylation in mitochondria while both genistein and erbstatin inhibited H^+-lactate co-transport in erythrocytes (Young *et al.*, 1993).

1.6.3 G-proteins and guanine nucleotides in insulin signalling

1.6.3.1 G-proteins

G-proteins can be divided into two groups but all share the common feature of being activated by the binding of GTP and inactivated by the hydrolysis of GTP to GDP (Bourne *et al.*, 1991). Thus the activity of G-proteins can be probed using nonhydrolyzable GTP analogues. One group, the classical heterotrimeric G-protein, is made up of one GTP binding and hydrolysing α-subunit, one β- and one γ-subunit. These are mainly involved in the transduction of signals from G-protein coupled receptors. When activated by the binding of GTP the α-subunit dissociates from the βγ-subunits (Birnbaumer, 1990). While most of the classical G-protein signalling occurs via the α-subunit the βγ subunits are also active. The βγ subunits can activate the ras dependent MAP kinase pathway (Crespo *et al.*, 1994). The second group of G-

proteins is the small G-proteins. These small G-proteins make up the *ras* family and are thought to be involved in trafficking within cells and secretion (Hall, 1990).

The potential role of some of the heterotrimeric G-proteins in insulin stimulation in rat adipocytes was investigated using the bacterial toxins cholera toxin and pertussis toxin. Cholera toxin, which inhibits G_s, was found to have only a small effect on glucose transport. Pertussis toxin, which acts on G_i and G_o, was found to affect glucose transport by decreasing the binding affinity of insulin and by decreasing the efficiency of the signalling process (Ciaraldi and Maisel, 1989). A similar effect was obtained by Honnor *et al.* (1992) who also found that neither toxin had an inhibitory effect at supramaximal concentrations of insulin. These results indicate a possible role for heterotrimeric G-proteins in insulin stimulated glucose transport in rat adipocytes, possibly by directly interacting with the transporter in the plasma membrane and modifying its intrinsic activity. Recently a direct effect of insulin on the $G_i\alpha$ subunit of a heterotrimeric G-protein was detected using an antiserum to the C terminus. Staining in the plasma membrane with this antiserum was much stronger in insulin stimulated cells than basal rat adipocytes suggesting that insulin causes a conformational change within the $G_i\alpha$ G-protein subunit (Record *et al.*, 1993).

The subcellular distribution of G-proteins was analysed in rat adipocytes. The 40-50 kDa α-subunits of the heterotrimeric G-proteins were detected almost entirely in the plasma membrane although specific $G_i\alpha_1$ and $G_i\alpha_2$ antibodies also detected a 100 kDa band in the low density microsomes. Insulin does not affect the distribution of these G-proteins. Small G-proteins were detected in the low density microsomes but they were more abundant in the plasma membrane. A different subset of G-proteins was found in each fraction. Small G-proteins were detected in vesicles immunoprecipitated with a specific GLUT4 antibody. Such an association could allow G-proteins to regulate the exocytosis of the GLUT4 containing vesicles (Cormont *et al.*, 1991).

The presence and distribution of both the α-subunit of the heterotrimeric G-proteins and the small *ras*-family G-proteins was investigated in 3T3-L1 cells before and after differentiation to adipocytes. Differentiation was found to decrease the α_i, α_o and the 47 kDa α_s G-protein subunits by 10-50 %. The 43 kDa α_s however, increased three fold. These G-protein were all found to have a plasma membrane location. A similar pattern of expression during differentiation was seen with the small G-proteins. Ha-*ras* decreased by 50 % while rab-1 and other rab isoforms increased by 100 % and 70 % respectively following differentiation. The rab G-proteins were detected in both the plasma membrane and the low density microsomes. Ha-*ras* and K-*ras* were not detected in the low density microsomes at all. While insulin caused the translocation of GLUT4 to the plasma membrane there was no detectable change in the distribution of the G-proteins studied following insulin stimulation (Huppertz *et al.*, 1993).

Ras is part of the insulin activated MAP kinase pathway. Ras-GTP activates raf, the first kinase of the MAP kinase pathway, by localising raf at the plasma membrane (Leevers *et al.*, 1994). Ras itself is activated by Sos, a guanine nucleotide exchange protein which exchanges GDP for GTP (Baltensperger *et al.*, 1993). Sos is active when it is bound to the SH3 domain of the adapter molecule GRB2 which in turn is bound to a tyrosine phosphorylated IRS-1 via the SH2 domain (Skolnik *et al.*, 1993). The mechanism whereby Sos may be activated by binding to GRB2 is unclear but it may be the result of a conformational change in Sos, the phosphorylation of Sos or simply by bringing it into association with the plasma membrane bound ras. Insulin stimulation causes a rapid increase in the level of active GTP bound ras. The MAP kinases activated by ras can also be activated by okadaic acid to a similar level as insulin (Porras *et al.*, 1992). When N-ras^{61k}, an activated mutant, was overexpressed in 3T3-L1 adipocytes the transport rate was found to be similar to the insulin stimulated rate in non transfected adipocytes. The ras induced transport rate was not additive with that of insulin. N-ras^{61k} was also found to cause the translocation of most of the

GLUT1 and all the GLUT4 to the cell surface (Kozma *et al.*, 1993). Thus ras appears to be part of the insulin signalling pathway for the stimulation of glucose transport.

Several rab proteins have been detected in adipocytes including rab3d. Rab 3d mRNA is present in 3T3-L1 fibroblasts and it increases during adipocyte differentiation (Baldini *et al.*, 1992). Rab 3d shares a high sequence identity with Rab 3a which is localised to synaptic vesicles in the brain and is involved in exocytosis (Mollard *et al.*, 1990). In rat adipocytes the highest levels of rab3d were detected in the high density microsomes. The distribution of rab3d is unaffected by insulin and was not detected in vesicles immunoprecipitated with a GLUT4 antibody (Guerre-Millo *et al.*, 1993).

Several other rab proteins have been detected in rat adipocytes. Rab3b and rab3c are cytosolic and rab4 and rab8 are membrane associated. Only the distribution of rab4 is affected by insulin stimulation. In basal adipocytes most of the rab4 is found in the low density microsomal fraction as is GLUT4. In insulin stimulated adipocytes rab4 is present at the plasma membrane and in the cytosol. Rab4 can also be detected in vesicles immunopurified with an antibody to GLUT4. In addition to insulin rab4 recycling can be stimulated by okadaic acid. This suggests that a phosphorylation event is required to activate rab4 (Cormont *et al.*, 1993). Rab4 is therefore a good candidate for regulating the translocation of GLUT4 to the plasma membrane.

Inactive GDP bound rab proteins can be detected in the cytoplasm associated with the GDP dissociation inhibitor (GDI). The GDI delivers the rab to the donor membrane (Araki, *et al.*, 1990) where the rab-GDI interacts with the GDI-dissociation factor which releases the rab. Rab is prenylated at the C terminus and this localises the protein at the membrane. The membrane bound rab then interacts with the guanine nucleotide exchange protein (GEF) which exchanges GDP for GTP (Ullrich *et al.*, 1994; Soldati *et al.*, 1994). The GTP bound rab is then incorporated into the vesicles. At the acceptor membrane the GTP is hydrolysed and the GDP bound rab is released from the membrane by binding to GDI (Araki *et al.*, 1990).

The precise mechanism of vesicle trafficking, targeting and membrane fusion is unclear. Both the vesicle and acceptor membranes contain a SNARE (SNAP receptor). The vesicle SNARE (v-SNARE) and target membrane SNARE (t-SNARE) interact in the presence of a 20S particle which contains *N*-ethylmaleimide-sensitive fusion protein (NSF) and soluble NSF attachment proteins (SNAPs) (Söllner *et al.*, 1993). The interactions of these components may require the association of GTP bound rab with the v-SNARE (Bennett and Scheller, 1993). A VAMP-like (vesicle associated membrane protein) v-SNARE has been identified in adipocytes. This protein is found in the vesicles which transport GLUT4 to the plasma membrane (Cain *et al.*, 1992).

1.6.3.2 GTPγS

The nonhydrolyzable GTP analogue GTPγS, like GTP, will activate G-proteins (Gilman, 1987). In CHO fibroblasts GTPγS inhibits transport through the Golgi stack by blocking vesicle attachment and fusion at the acceptor Golgi membrane. This suggested that G-proteins may be involved in Golgi transport (Melançon *et al.*, 1987).

The effect of GTPγS upon insulin stimulated glucose transport in adipocytes was first investigated by Baldini *et al.* (1991). They first demonstrated that insulin still stimulates GLUT4 translocation in α-toxin permeabilized rat adipocytes. They then tested a number of GTP analogues. The nonhydrolyzable analogues guanosine 5'-*O*-(3-thiotriphosphate) (GTPγS), guanylyl imidodiphosphate (GMPPNP) or guanylyl β,γ-methylenediphosphate (GMPPCP) all caused a 3-6 fold increase in the GLUT4 content of the plasma membrane of basal rat adipocytes. GTP itself and adenosine 5'-β,γ-imino)triphosphate had no effect on transport. From these experiments they were unable to determine whether GTPγS affects exocytosis or inhibits endocytosis. A similar study was carried out in streptolysin-O permeabilized 3T3-L1 adipocytes by Robinson *et al.* (1992). They found that in the presence of ATP insulin, GTPγS or insulin plus GTPγS the level of cell surface GLUT4 was similar to that of insulin

stimulated intact cells. In the absence of ATP the level of cell surface GLUT4 in the presence of GTPγS or insulin was lower. The removal of ATP from unstimulated cells increased the level of GLUT4 at the cell surface. GTPγS and insulin together overcame the ATP dependency. They suggested that ATP is required for a phosphorylation/ dephosphorylation event which excludes GLUT4 from the plasma membrane.

The effect of GTPγS on 3-*O*-methyl-D-glucose uptake was measured in electropermeabilized rat adipocytes. 1.0 mM GTPγS stimulated transport as much as insulin. 0.3 mM but not 1.0 mM GTPγS enhanced insulin stimulation. NaF and mastoparan, both of which activate G-proteins, stimulated transport (Suzuki *et al.*, 1992). GTPγS also has an inhibitory effect on hexose transport (Schürmann *et al.*, 1989). When the transport activity from insulin stimulated rat adipocyte membrane fractions was reconstituted into vesicles GTPγS and GTP inhibited glucose transport by 50 %. They had no inhibitory effect in membrane fractions from basal cells and ATPγS and AMP were without effect. The inhibitory effect of GTPγS was lost when the transporters were partially purified from G-proteins on a sucrose gradient (Schürmann *et al.*, 1992a). GTP binds directly to the C terminus of GLUT4 where it might act as a gate for GLUT4 (Studelska *et al.*, 1993). The uptake of 2-deoxy-D-glucose in oocytes expressing GLUT1 is inhibited by the injection of GTPγS or GppNHp, indicating a decrease in the intrinsic activity of GLUT1 in oocytes by these GTP analogues (Wellner *et al.*, 1993). The microinjection of GTPγS into oocytes expressing GLUT4 had no effect on the transport rate however the transport rate was unaffected by insulin and very little GLUT4 was expressed at the plasma membrane (Thomas *et al.*, 1993).

The addition of GTPγS to 3T3-L1 adipocytes enhances MAP kinase and $pp90^{rsk}$ activity to a similar level as insulin although the effects are not additive. Both kinases are part of the ras activated protein kinase cascade (Klarlund *et al.*, 1993).

GTPγS will regulate the function of the insulin receptor in adipocytes. GTPγS inhibits the binding of insulin to isolated receptors and inhibits autophosphorylation without

competing with ATP (Davis and McDonald, 1990). Insulin was found to selectively stimulate the binding of GTPγS to a 40 kDa plasma membrane protein. This in turn inhibited both the binding of insulin to the insulin receptor and the insulin stimulation of the receptor kinase. This suggests that there may be a link between insulin signalling and a 40 kDa G-protein (Kellerer *et al.*, 1991). Two G-protein binding motifs have been identified within the insulin receptor. A peptide representing one of these, $GPBP_{1147\text{-}1168}$, (notation of Ebina *et al.*, 1985) from a sequence within the tyrosine kinase domain which contains the three tyrosine phosphorylation sites, was found to bind to a 67 kDa G-protein from human placenta, and stimulate the binding of GTPγS to the G-protein. It is therefore possible that the insulin receptor might specifically associate with and activate G-proteins (Jo *et al.*, 1993).

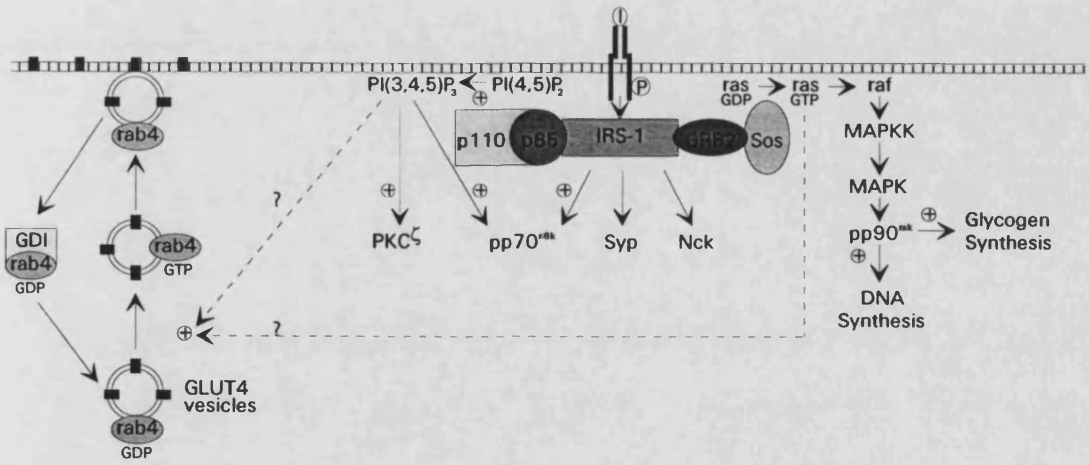

Figure 1.8 Schematic representation of the insulin signalling pathways from IRS-1 and the stimulation of GLUT4 translocation

Insulin receptor autophosphorylation occurs in the presence of insulin. The insulin receptor tyrosine kinase then phosphorylates the IRS-1 (insulin receptor substrate-1) at the SH2 and SH3 binding domains. GRB2 links IRS-1 to Sos, the guanine nucleotide exchange factor, which activates ras triggering the serine cascade including MAPKK (MAP kinase kinase) and MAPK (MAP kinase). The p110 subunit of PI3-kinase is activated by the association of p85 with IRS-1. Soluble rab is recycled from the cell surface to the microsomal pool of transporter vesicles in association with GDI (guanine dissociation inhibitor). See text for details (from Cormont *et al.*, 1993 and White and Kahn, 1994).

1.7 Cultured cell lines

1.7.1 3T3-L1 fibroblasts and adipocytes

3T3-L1 fibroblasts were cloned from a mouse embryo fibroblast line by Green and Kehinde (1974). The cells can be maintained as fibroblasts while in the growing state but on reaching confluence they spontaneously differentiated into adipocytes containing triglyceride droplets (Green and Meuth, 1974). The differentiation can be accelerated using dexamethasone, isobutylmethylxanthine and insulin (Frost and Lane, 1985). Associated with differentiation is a change in the pattern of gene expression with changes in over 300 proteins and many changes at the level of mRNA (Sadowski *et al.*, 1992). These changes include the expression of a new transporter gene, GLUT4 (de Herreros *et al.*, 1989). Thus while 3T3-L1 fibroblasts express only GLUT1 adipocytes express both GLUT1 and GLUT4. The 3T3-L1 transporters were sequenced by Kaestner *et al.* (1989).

3T3-L1 fibroblasts bind and respond to insulin but the number and affinity of the binding sites and the response to insulin increases during differentiation to adipocytes (Rubin *et al.*, 1978). Insulin stimulates glucose uptake by 15- to 20-fold in adipocytes (Frost and Lane, 1985). The increase in transport is associated with transporter translocation from the *trans*-Golgi reticulum to the plasma membrane (Blok *et al.*, 1988; Calderhead and Lienhard, 1988). Quantitative immunoblotting detected 950,000 copies of GLUT1 and 280,000 copies of GLUT4 per adipocyte and found that insulin causes a 6-fold increase in surface GLUT1 and a 17-fold increase in surface GLUT4 so that there equal levels of both transporter isoforms at the surface of insulin stimulated adipocytes (Calderhead *et al.*, 1990). ATB-BMPA labelling of the total transporter pool detects equal levels of both GLUT1 and GLUT4 (Yang *et al.*, 1992b).

The total number of transporters per 3T3-L1 adipocyte can be moderated by a number of factors including chronic insulin stimulation. Chronic insulin treatment, 24 h with 500 nM insulin, stimulates transport but results in a different pattern of

transporter expression and translocation compared with acute insulin stimulation. Chronic insulin stimulation causes a 3- to 4-fold rise in surface and total levels of GLUT1 (Tordjman *et al.*, 1989; Kozka *et al.*, 1991) but halves the level of surface GLUT4 (Kozka *et al.*, 1991). The differential effects of insulin on GLUT1 and 4 were studied by Sargeant and Pâquet (1993). Without insulin stimulation the half-lives of GLUT1 and GLUT4 are 19 h and 50 h respectively. Insulin at 100 nM lowers the half-life of both isoforms to 15.5 h while the average half-life of all proteins remains at 55 h. A 24 h insulin treatment resulted in a 3.5- and 2-fold rise in GLUT1 and GLUT4 synthesis respectively. After 72 h the rate of GLUT1 synthesis was 2.5-fold higher while that of GLUT4 was the same as control levels and the level of GLUT1 mRNA was 4.5-fold higher while GLUT4 mRNA was 50 % lower. Thus the levels of GLUT1 and GLUT4 appear to be regulated independently.

Glucose also regulates transport rates in 3T3-L1 adipocytes. Glucose deprivation increases 2-deoxy-D-glucose transport 5-fold in a protein synthesis dependent manner (van Putten *et al.*, 1985). During 72 h glucose starvation GLUT1 mRNA increased 2.4-fold the protein increased 7-fold. Starvation caused a 10-fold decrease in the level of GLUT4 mRNA but the protein level remained the same. Glucose starvation increases the cell surface levels of both GLUT1 and GLUT4 (Tordjman *et al.*, 1990).

1.7.2 COS-7 and CHO fibroblasts

COS-7 fibroblasts were derived from CV-1, an established cell line derived from African green monkey kidney cells. The COS-7 fibroblasts were created by transforming the CV-1 cells with origin defective SV40. These cells support the replication of DNA with the SV40 origin and can be used for transient protein expression (Gluzman, 1981). CHO cells were derived from the ovary of an adult Chinese hamster (Puck *et al.*, 1958). They can be used for the study of gene expression and can be stably transfected.

1.8 Aims

The aim of the work described in this thesis was to investigate the mechanism whereby insulin stimulates glucose transport. Several aspects of this were investigated including transport kinetics and the insulin signalling mechanism.

Insulin induces a 20-fold increase in the transport rate but only a 5-6-fold increase in the level of transporters at the surface of 3T3-L1 adipocytes. This is associated with an increase in the ratio of GLUT4 to GLUT1 at the cell surface, suggesting that GLUT1 and GLUT4 make different contributions to the rate of uptake. Experiments were therefore devised to determine their separate contributions to the transport rate.

The signalling pathway whereby insulin increases the glucose transport rate in adipocytes is, as yet, unclear. It has been suggested, however, that phosphorylation events are involved. This idea was tested by treating adipocytes with okadaic acid, which inhibits protein phosphatases, thus increasing serine/threonine phosphorylation, and tyrosine kinase inhibitors which decrease tyrosine phosphorylation.

GLUT4, the insulin regulatable glucose transporter, adopts a different subcellular distribution to that of GLUT1. In order to investigate whether the distribution of GLUT4 is intrinsic to the transporter or is conferred on it by the insulin sensitivity of the cell in which it is expressed, GLUT4 was transfected into insulin insensitive fibroblasts. The regions of GLUT4 involved in its unique distribution were analysed by adding peptides corresponding to different regions of GLUT1 and GLUT4 to permeabilized 3T3-L1 adipocytes and observing their effects on the transport rate.

Rab proteins, small G-proteins, are believed to regulate transporter translocation. This idea was studied by looking for rab4 in 3T3-L1 adipocytes and by observing what effect transfected rab3d had on the distribution of GLUT4. GTPγS was also added to permeabilized 3T3-L1 adipocytes to investigate the involvement of G-proteins in the insulin signalling pathway and GLUT4 translocation.

2.0 Methods

2.1 Materials

Standard laboratory reagents were obtained from Fisons Plc. (Loughborough, UK), BDH Laboratory Supplies (Poole, Dorset, UK), Sigma Chemical Co. (Poole, Dorset, UK) and Aldrich Chemical Co. Ltd. (Gillingham, Dorset, UK). Radiochemicals were obtained from Amersham International plc (Aylesbury, UK). Monocomponent porcine insulin was donated by Dr. Ronald Chance, Eli Lilly Corporation. The sources of other specific chemicals are given as appropriate.

2.2 Cell culture

2.2.1 Media and buffers

DMEM-NCS/FCS:

Dulbecco's modification of Eagle's medium (87 % v/v) (Flow Laboratories, Irvine, UK)

supplemented with: Penicillin (100 IU/ml)/Streptomycin (100 µg/ml)
Glutamine (2 mM)
Newborn Calf Serum (-NCS) 10 % (v/v)

or Foetal Calf Serum(-FCS) 10 % (v/v) (Gibco, BRL, Paisley, UK)

Serum was heat treated at 56 °C for 30 min before freezing in 50 ml aliquots.

Phosphate Buffered Saline (PBS):

Dulbecco 'A' Phosphate buffered saline, pH 7.3, autoclaved (Oxoid, Unipath Ltd, UK).

Trypsin/EDTA:

Trypsin/EDTA (Gibco BRL):

Trypsin 0.05 % (w/v)
EDTA 0.02 % (w/v)

diluted 10-fold in PBS or Modified Puck's Saline A (Gibco BRL).

2.2.2 Storage of 3T3-L1 fibroblast stocks

3T3-L1 fibroblasts were obtained from the American Type Culture Collection and the number of cells expanded. In order to store the fibroblasts, 0.5 x 10^6 cells in 0.5 ml DMEM-NCS were mixed with 50 % glycerol on ice and then slowly cooled above liquid nitrogen for 24 h before immersing into liquid nitrogen for storage.

Frozen 3T3-L1 fibroblasts in 50 % glycerol were removed from liquid nitrogen, rapidly thawed at 37 °C, added to warm DMEM-NCS and the cells spun down at 1500 rpm for 3 min. The medium was poured off and the cells were resuspended in 2 ml of DMEM-NCS using a 21 g needle and syringe. The cells were added to 40 ml DMEM-NCS in a 175 cm^2 flask (Nunc, InterMed, Denmark) and grown in a 10 % CO_2, 37 °C incubator. Cell numbers were allowed to expand toward confluence before being harvested while still subconfluent.

2.2.3 Harvesting a flask

While the cells in a flask were still subconfluent they were washed twice with 10 ml of 37 °C PBS. Cells were loosened by a 1 min incubation with 4 ml of 37 °C trypsin/EDTA per 175 cm^2 flask. The flask was knocked to detach the cells. 20 ml of 37 °C DMEM-NCS medium was added to the flask and then transferred, with the cells, to a 30 ml universal tube. The cells were pelleted by centrifuging the tubes at 1500 rpm for 3 min in a bench top centrifuge. The cell pellet was resuspended in 2 ml of DMEM-NCS with a 21 g needle and syringe. Cells were counted by mixing 50 µl of suspended cells with 50 µl 0.1 % (w/v) trypan blue stain and counting them with a haemocytometer. Cells were plated out in 35 mm dishes (Nunc, InterMed, Denmark) at a density of 0.05 x 10^6 cells in 2 ml of DMEM-NCS per dish or equivalent and between 0.1 to 0.2 x 10^6 cells in 40 ml in a 175 cm^2 flask. Cells were passaged up to ten times before being discarded.

2.2.4 3T3-L1 adipocyte differentiation and culture

3T3-L1 fibroblasts were grown to confluence in a 37 °C, 10 % CO_2 incubator replacing the DMEM-NCS every 3 days. Three days after the cells had reached confluence they were differentiated using the method developed by Frost and Lane (1985). The DMEM-NCS was replaced with DMEM-FCS containing 0.25 µM dexametasome, 0.5 mM 3-isobutyl-1-methylxanthine and 0.2 µM insulin. After 2 days this was replaced with DMEM-FCS and 0.2 µM insulin for a further 2 days. Thereafter medium was replaced with 2 ml DMEM-FCS alone every 2 days. Cells were fully differentiated and used for experiments 9 to 13 after the initiation of differentiation.

2.2.5 COS-7 fibroblast culture

COS-7 fibroblasts, provided by Dr. A. Wolstenholme (University of Bath), were stored in liquid nitrogen and defrosted as for 3T3-L1 fibroblasts. COS-7 fibroblasts were maintained in a 175 cm^2 flask with 40 ml DMEM-FCS in a 37 °C, 5 % CO_2 incubator. Cells harvested using the 3T3-L1 method were seeded at a density of 2 x 10^6 cells per 90 mm dish in 10 ml DMEM-FCS and grown at 37 °C in 5 % CO_2 (Gluzman, 1981).

2.2.6 CHO fibroblast culture

CHO fibroblasts, provided by Dr M. Hashiramoto (Kobe University, Japan), were stored in liquid nitrogen and defrosted as for 3T3-L1 fibroblasts. Cells were seeded in a 175 cm^2 flask at a density of 0.1 x 10^6 cells in 40 ml HAMS-F12-FCS (87 % (v/v) HAMS-F12, 10 % (v/v) FCS, 100 IU/ml penicillin, 100 mg/ml streptomycin, 2 mM L-glutamine) in a 37 °C, 5 % CO_2 incubator. Cells harvested as for 3T3-L1 fibroblasts, were seeded at a density of 0.05 x 10^6 cells per 35 mm dish in 2 ml HAMS-F12-FCS and grown at 37 °C in 5 % CO_2 (Asano *et al.*, 1989).

2.3 Preparation of cells for experiments

2.3.1 Preparation of isolated rat adipocytes

Male Wistar rats weighing 180-200 g were fed ad libitum. They were stunned and then killed by cervical dislocation. The epididymal pads were removed and washed in 1.0 % (w/v) albumin in rat KRH buffer (140 mM NaCl, 4.7 mM KCl, 2.5 mM CaCl, 1.25 mM $MgSO_4$, 2.5 mM NaH_2PO_4, 10 mM HEPES, pH 7.4). Before use bovine serum albumin fraction V was dialysed overnight and sequentially filtered under pressure using Whatman filters 41 and 42 and Millipore AAWP 0.8 µm pore size. The pH was adjusted to pH 7.6 and the albumin, at a concentration of 10 % (w/v), was stored at -20 °C. After washing the two fat pads were transferred to a 20 ml tube containing 3.5 ml digestion buffer (3.5 % (w/v) albumin in rat KRH, pH 7.6, supplemented with 1.0 mg/ml collagenase (Worthington, Freehold, USA.) and 0.1 mg/ml glucose) and cut into small pieces with 70 vigorous scissors strokes. The fat pads were incubated in a 37 °C shaking water bath until the connective tissue was digested and the adipocytes freed. The adipocytes were then filtered through nylon gauze to remove undigested cellular material. The cells were washed three times with 1 % albumin in rat KRH, allowing the cells to float to the surface between washes and changing the tubes to remove free lipid. The cytocrit was adjusted to 40 % in 1 % albumin in rat KRH (Taylor and Holman, 1981).

2.3.2 Reversal of insulin stimulation in rat adipocytes

Rat adipocytes at a cytocrit of 40 % were insulin stimulated with 10 nM insulin. This stimulation was reversed by treating the adipocytes with 2.5 mg/ml collagenase at 37 °C (Kono *et al.*, 1981).

2.3.3 Preparation of 3T3-L1 adipocytes

Prior to use 3T3-L1 adipocytes were washed twice with 2 ml PBS at 37 °C and incubated for 2 h in a 10 % CO_2, 37 °C, incubator in serum-free DMEM supplemented with 2 mM L-glutamine, 100 IU/ml penicillin and 100 mg/ml streptomycin. They were then washed three times with 2 ml Krebs-Ringer-HEPES (KRH) buffer (136 mM NaCl, 4.7 mM KCl, 1.25 mM $CaCl_2$, 1.25 mM $MgSO_4$, 10 mM HEPES, pH 7.4).

2.3.4 Chronic insulin stimulation of 3T3-L1 adipocytes

Where chronically insulin stimulated 3T3-L1 adipocytes were used then 24 h before required, 500 nM insulin was added to the normal DMEM-FCS medium. The 500 nM insulin was maintained throughout the further incubations (Kozka *et al.*, 1991).

2.3.5 Reversal of insulin stimulation in 3T3-L1 adipocytes

3T3-L1 adipocytes were stimulated with 100 nM insulin. The stimulation was reversed by washing the cells twice with KRM (136 mM NaCl, 4.7 mM KCl, 1.25 mM $CaCl_2$, 1.25 mM $MgSO_4$, 10 mM MES, 25 mM glucose, pH 6.0) at 37 °C followed by incubation with the KRM at 37 °C. Before assaying transport the cells were washed with KRH and incubated for 5 min in KRH (Yang *et al.*, 1992a).

2.3.6 Permeabilizing 3T3-L1 adipocytes

3T3-L1 adipocytes were washed three times with intracellular (IC) buffer (140 mM potassium glutamate, 5 mM EGTA, 5 mM $MgCl_2$, 5 mM NaCl, 20 mM HEPES, pH 7.2) and then incubated with 0.8 IU/ml streptolysin-*O* for 5 min at 37 °C. The dishes were then again washed three times with IC buffer. The cells were then incubated in

incubation intracellular (IIC) buffer, (IC buffer with 1 mg/ml BSA, 10 mM ATP and 3 mM sodium pyruvate, pH 7.2) with appropriate additions (Robinson *et al.*, 1992).

The effectiveness of the streptolysin-O in permeabilizing the 3T3-L1 adipocytes was confirmed by permeabilizing in the presence of 1 μg/ml propidium iodide. When examined by fluorescence microscopy only the permeabilized cells fluoresce. Fluorescence was compared in cells incubated with propidium iodide in the presence and absence of streptolysin-O. Stock propidium iodide, 50 μg/ml in 0.1 % (w/v) trisodium citrate dihydrate, was stored in a lightproof container at 4 °C where it is stable for at least 3 months (Ockleford *et al.*, 1981).

Streptolysin-O was prepared in double distilled water at a concentration of 20 IU/ml, quickly frozen and stored at -70 °C. The streptolysin-O was removed and defrosted just before it was required.

2.4 Transport assays

2.4.1 Assaying transport in rat adipocytes

Rat adipocytes with a cytocrit of 40 % were incubated as required in 1 % albumin in rat KRH at 37 °C. Typically basal, unstimulated, cells were left without any additions for 30 min while insulin stimulated cells were treated with 10 nM insulin for 30 min. To assay the rate of 3-O-methyl-D-glucose uptake, a 50 μl sample of cells was taken and added to 10 μl of label cocktail for an appropriate length of time, ideally allowing the fractional filling to be about a half. Typically basal cells were incubated with the label for 120 s and insulin stimulated cells for 3 s. The cocktail, in rat KRH, gave a final concentration of 50 μM 3-O-methyl-D-glucose with 0.3 μCi 3-O-methyl-D-[U-^{14}C]glucose. After the required time uptake was stopped with 3 ml rat KRH containing phloretin at a concentration of 0.1 mg/ml dissolved in ethanol. Silicone oil was layered on the KRH and the cells were spun at 3,000 rpm for 45 s in a MSE Centra R bench

top centrifuge which causes the cells to float up through the oil. The cells were scooped off the surface, put in a scintillation vial with 9 ml of Optiphase Safe scintillation fluid and the ^{14}C c.p.m. in the vial counted. Generally each condition was assayed in triplicate. In order to calculate the fractional filling the capacity of the cells was measured by incubated them with the labelled sugar for 9 min, sufficient time for the labelled sugar in the extracellular medium to equilibrate in the intracellular water space, and the ^{14}C c.p.m. counted (∞). To obtain the level of non-specific, background binding of the sugar the stopping buffer was added to the cells before adding the sugar cocktail and the ^{14}C c.p.m. counted (bg) (Taylor and Holman, 1981).

Uptake is assumed to be first order, v=k[S], where k is the first order rate constant (Carruthers, 1990). The uptake rate constant was calculated from the ^{14}C c.p.m. using fractional filling (Rees and Holman, 1981):

$$\text{Rate constant} = \frac{-\ln(1-f)}{\text{time (s)}} \quad \text{where f (fractional filling)} = \frac{(^{14}\text{C c.p.m.} - \text{bg c.p.m.})}{(\infty \text{ c.p.m.} - \text{bg c.p.m.})}.$$

2.4.2 Assaying transport in 3T3-L1 adipocytes

2.4.2.1 Basic assay for 3-O-methyl-D-glucose uptake

To each 35 mm dish of prepared 3T3-L1 adipocytes was added 400 µl of KRH containing any additions. The dish was placed in a 37 °C incubator for the appropriate length of time. The typical insulin stimulation was 100 nM for 30 min. Basal cells were left without additions for the same length of time. The uptake of 3-O-methyl-D-glucose was assayed by the addition of 100 µl of sugar cocktail in KRH to give a final concentration of 50 µM 3-O-methyl-D-glucose with 0.3 µCi/dish 3-O-methyl-D-[U-^{14}C]glucose. After a suitable length of time transport was stopped by the addition of 3 ml of stopping buffer, KRH containing phloretin at 0.1 mg/ml (dissolved in ethanol). The dishes of cells were then washed four times with stopping buffer to remove non-transported labelled sugar. Insulin stimulated uptake was assayed over 10 s while basal

uptake was assayed over 90 s. The infinity uptake was calculated after 15 min, sufficient time for the labelled sugar in the extracellular medium to equilibrate in the intracellular water space, and the ^{14}C c.p.m. counted (∞). The background non-specific labelling was determined by adding the sugar cocktail after the 3 ml stopping buffer and the ^{14}C c.p.m. counted (bg). The cells were removed from the dishes by dissolving them in 1 ml of 0.1 M NaOH. This was added to a scintillation vial with 9 ml Optiphase Safe scintillation fluid and the radioactivity counted in a scintillation counter. Transport for each condition was generally carried out in triplicate (duplicate background). Uptake was assumed to be first order (Carruthers, 1990) and the rate constant calculated from the ^{14}C c.p.m. using the equation (Rees and Holman, 1981):

$$\text{Rate constant} = \frac{-\ln(1-f)}{\text{time (s)}} \quad \text{where f (fractional filling)} = \frac{(^{14}\text{C c.p.m.} - \text{bg c.p.m.})}{(\infty \text{ c.p.m.} - \text{bg c.p.m.})}.$$

2.4.2.2 Basic assay for 2-deoxy-D-glucose uptake

3T3-L1 adipocytes in 35 mm dishes were prepared and incubated in 950 µl KRH. The cells were stimulated as described in section 2.4.2.1. Transport was assayed over 5 min following the addition of 50 µl label in KRH to give a final concentration of 50 µM 2-deoxy-D-glucose and 0.3 µCi/dish 2-deoxy-D-[2,6-^{3}H]glucose. After the 5 min the cells were rapidly washed 4 times with 3 ml KRH. Cells were dissolved and the radioactivity counted. The background count was determined by adding the sugar cocktail in the presence of 50 µM cytochalasin B (Kozka *et al.*, 1991). The rate of uptake was assumed to be linear over 5 min (Olefsky, 1978) and was determined as the pmol taken up in 5 min per 35 mm dish.

2.4.2.3 Assaying transport in permeabilized 3T3-L1 adipocytes

Permeabilized 3T3-L1 adipocytes in 35 mm dishes (section 2.3.6) were stimulated in 380 µl IIC buffer. The typical insulin stimulation was 100 nM for 30 min and basal for 30 min. Transport was assayed over 5 min by the addition of 20 µl of sugar cocktail to give a final concentration of 50 µM 2-deoxy-D-glucose with 0.12 µCi/dish 2-deoxy-D-[2,6-^{3}H]glucose and 50 µM sucrose with 0.024 µCi/dish [U-^{14}]sucrose. Uptake was stopped by rapidly aspirating the buffer followed by one rapid wash with 3 ml IC buffer. The cells were dissolved in 1 ml 0.1 M NaOH and added to a scintillation vial with 9 ml Optiphase Safe scintillation fluid. A dual counting protocol was used to count ^{3}H dpm in a narrow window (0.0-12.0 keV) and ^{14}C (12.0-156 keV). Specific 2-deoxy-D-glucose uptake was calculated using the following equation, with ^{14}C counts being used to calculate the non-specific uptake of ^{3}H counts:

$$\text{Specific } ^{3}\text{H 2-deoxy-D-glucose counts} = {}^{3}\text{H counts} \times \left({}^{14}\text{C counts} - \left(\frac{^{3}\text{H S.A.}}{^{14}\text{C S.A.}}\right)\right).$$

The specific ^{3}H counts were used to calculate the pmol of uptake in 5 min per 35 mm dish. Uptake was assumed to be linear over the 5 min assay (Olefsky, 1978).

2.4.2.4 Alternative transport assay in permeabilized 3T3-L1 adipocytes

Permeabilized 3T3-L1 adipocytes in 35 mm dishes (section 2.3.6) were stimulated in 380 µl IIC buffer as described above. Transport was assayed over 5 min by the addition of the sugar cocktail to give a final concentration of 50 µM 2-deoxy-D-glucose and 0.12 µCi/dish 2-deoxy-D-[2,6-^{3}H]glucose. After 5 min uptake was stopped with 2 ml boiling water. The cells were scraped from the plate and the cell suspension added to a DE81 Whatman filter under suction. This was washed three times with 2 ml cold double distilled water. The filter paper was added to a vial with Optiphase Safe scintillation fluid and the radioactivity associated with the phosphorylated 2-deoxy-D-[2,6-^{3}H]glucose bound to the membrane counted (adapted from Rist *et al.*, 1990).

2.5 ATB-BMPA photolabelling of glucose transporters

2.5.1 Preparation of ATB-[2-^{3}H]BMPA

2-*N*-[4-(1-azi-2,2,2-trifluoroethyl)benzoyl]-1,3-bis-(D-mannos-4-yloxy)-2-propylamine (ATB-BMPA) at a specific activity of ≈ 10 Ci/mmol was prepared in phosphate buffer as previously described (Clark and Holman, 1990).

2.5.2 Photolabelling rat adipocytes

Rat adipocytes in KRH were stimulated as required. To 1 ml of 40 % cytocrit room temperature cells in a 35 mm dish without a lid was added 250 µCi ATB-[2-^{3}H]BMPA in the dark. They were irradiated with 300 nm UV light from RPR-3000 lamps in a Rayonet Photochemical reactor RPR-100 for 1 min. Following irradiation the cells were washed 3 times with 1 % albumin in rat KRH at room temperature to remove unbound label. After the first and second wash the cells were spun up to 1,000 rpm and up to 1,500 rpm for the third wash in a MSE Centra bench top centrifuge. Cells were solubilized in 1.2 ml of solubilization buffer (5 mM phosphate buffer pH 7.2, 2 % (w/v) Thesit ($C_{12}E_9$) (Boehringer, Mannheim), 1 µg/ml antipain, aprotinin, leupeptin, pepstatin A) for 20 min after an initial vortex. This was spun at 20,000 g_{max} for 20 min in a TLA-100 rotor and the supernatant between the fat and cell debris pellet was removed with a needle and syringe for immunoprecipitation (Holman et *al.*, 1990).

2.5.3 Photolabelling 3T3-L1 adipocytes

3T3-L1 adipocytes in 35 mm dishes in KRH were stimulated as required. The incubation medium was replaced with 230 µl of KRH at room temperature. In the dark 100 µCi of ATB-[2-^{3}H]BMPA in 20 µl was added. The dishes without the lids were irradiated with 300 nm UV light from a Rayonet Photochemical reactor for

1 min. Immediately after photolabelling dishes were washed four times with 3 ml of phloretin stopping buffer (phloretin, 10 mg/100 ml in KRH). Cells were solubilized and scraped off the dish in 1.2 ml of solubilization buffer (5 mM phosphate buffer pH 7.2, 2 % (w/v) Thesit ($C_{12}E_9$), 1 µg/ml antipain, aprotinin, leupeptin, pepstatin A) and spun at 20,000 rpm, 20,000 g_{max} in a Beckman TLA-100 rotor for 20 min. The supernatant could then be used for immunoprecipitation.

2.6 Processing of cell samples

2.6.1 Subcellular fractionation of 3T3-L1 adipocytes and fibroblasts

Unlabelled 3T3-L1 adipocytes or 3T3-L1 adipocytes after ATB-BMPA labelling but before solubilization were washed with 0 °C TES (10 mM Tris, 5 mM EDTA, 250 mM sucrose, pH 7.2), scraped from the plate in 3 ml TES and homogenised by 15 hand or machine strokes in a 50 ml Potter tissue grinder. The homogenate was spun for 15 min at 12,500 g_{max} (15,000 rpm in TLA-100 rotor in a Beckman ultracentrifuge) to obtain a crude plasma membrane pellet. This supernatant was then spun for 9 min at 16,000 g_{max} (17,000 rpm) to obtain the high density microsome pellet and the supernatant spun for 17 min at 554,400 g_{max} (100,000 rpm) to obtain the low density microsome pellet. The crude plasma membrane pellet was purified by resuspending it in TES and spinning it for 20 min at 104,000 g_{max} (35,000 rpm, TLS-55 rotor) on a 38 % sucrose cushion (1.12 M sucrose, 10 mM Tris, 5 mM EDTA). The two layers and the plasma membrane at the interface was poured off into a separate tube and spun for 9 min at 76,000 g_{max} (37,000 rpm, TLA-100 rotor). The plasma membrane pellet was resuspended in TES and spun for 9 min at 37,000 g_{max} (adapted from Weiland *et al.*, 1990). A diagrammatic representation of the subcellular fractionation procedure is given in figure 2.1. All the pellets were resuspended in phosphate buffer for protein estimation. The protein could be solubilized in 2 % Thesit and used for immunoprecipitation or in sample buffer and run on a thin gel for Western blotting.

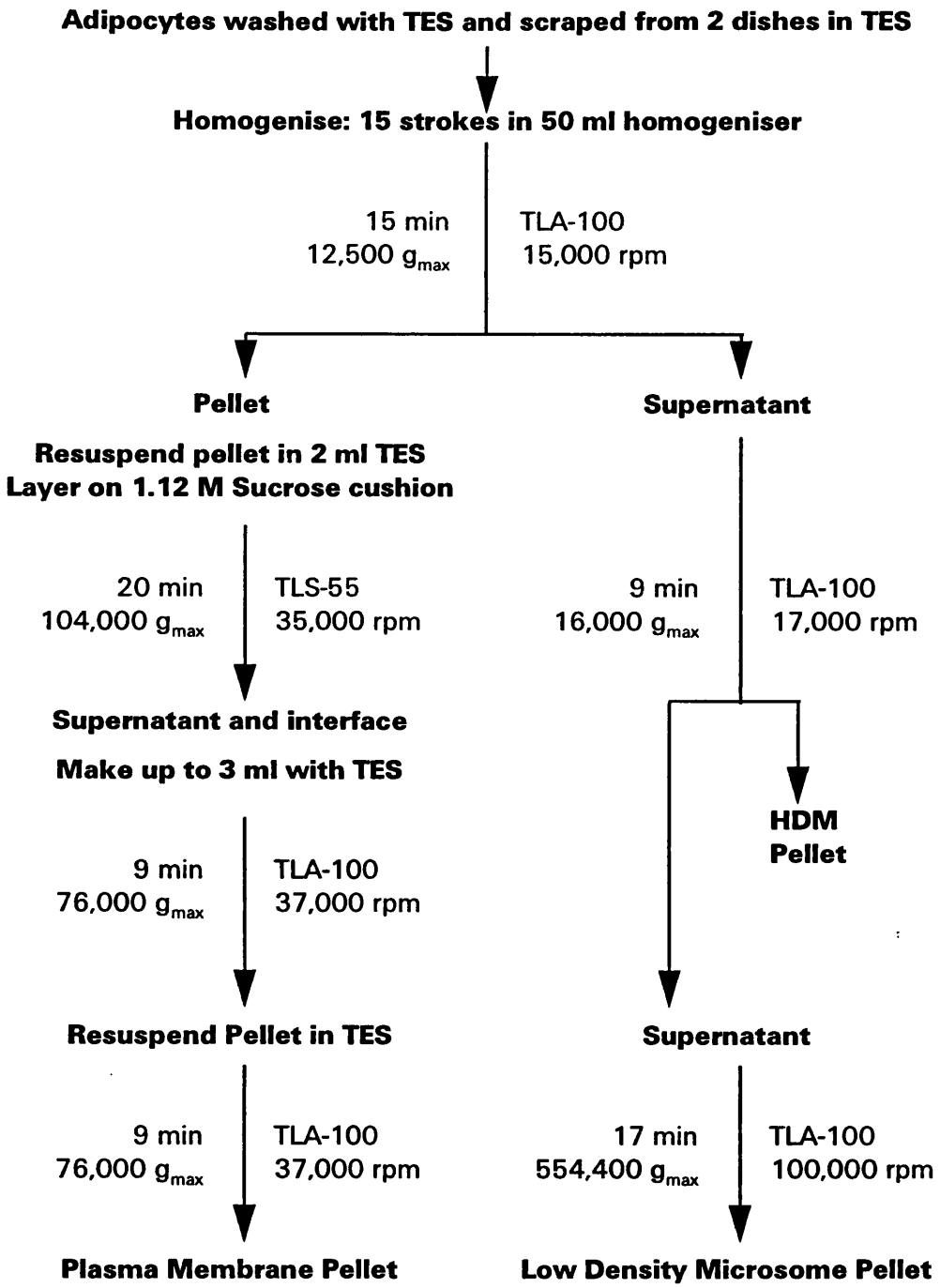

Figure 2.1 The subcellular fractionation of 3T3-L1 adipocytes

Centrifugation times and speeds are optimised for fractionation with a Beckman bench top ultracentrifuge. See text for details.

2.6.2 Chloroform/methanol protein precipitation

To a sample containing protein (in ≈ 1300 µl TES) was added an equal volume (1300 µl) of methanol. This was mixed before the addition of 300 µl of chloroform and a further mixing. After spinning at 9,000 g for 2 min in a bench top centrifuge the upper phase was aspirated off taking care to leave the protein at the interface. A further 600 µl of methanol was added and mixed. A second 2 min 9,000 g spin gave a protein pellet. The supernatant was aspirated and the pellet dried with N_2 gas (Wessel and Flügge, 1984). The protein can be solubilized for further use.

2.6.3 Immunoprecipitation of GLUT1 and GLUT4

Protein A-sepharose, 5 mg per sample for GLUT4 and 7 mg per sample for GLUT1 was swollen by rotating it with phosphate buffer (5 mM phosphate buffer, pH 7.2) at 4 °C. This was washed twice with phosphate buffer. To the protein A-sepharose was added 60 µl of anti-GLUT4 antiserum and 100 µl of anti-GLUT1 antiserum per sample. The total volume was made up to 1.3 ml with phosphate buffer and rotated at 4 °C for a minimum of 2 h to bind the antibody to the protein A. After washing three times with phosphate buffer the solubilized adipocyte supernatant in solubilization buffer was added to the protein A-sepharose anti-GLUT1 or 4. These were rotated at 4 °C for 2 h. The protein A-sepharose was washed three times with 1 % washing buffer (1 % (w/v) Thesit ($C_{12}E_9$), 5 mM phosphate buffer pH 7.2, 1 µg/ml antipain, aprotinin, leupeptin, pepstatin A) and once with 0.1 % washing buffer (0.1 % (w/v) Thesit ($C_{12}E_9$), 5 mM phosphate buffer pH 7.2, 1 µg/ml antipain, aprotinin, leupeptin, pepstatin A). The immunoprecipitated GLUT1 or GLUT4 was released by the addition of sample buffer (6 M urea, 10 % (w/v) SDS, 0.05 % (w/v) 5-bromophenol blue, 10 % 2-mercaptoethanol) to the protein A-sepharose. This could then be loaded onto a 3 mm thick SDS-PAGE gel (section 2.6.4).

2.6.4 SDS-polyacrylamide gel electrophoresis

Resolving gel buffer, pH 8.8

Tris	1.5 M
SDS	0.4 % (w/v)

Stacking gel buffer, pH 6.8:

Tris	0.5 M
SDS	0.4 % (w/v)

Acrylamide stock:

Acrylamide	30 % (w/v)
N'$_5$ N' methylene bis acrylamide	2.5 % (w/v)
Sucrose	30 % (w/v)

Gel (for 3 x 120 mm resolving gel):	10 % Resolving	12 % Resolving	Stacking
Gel buffer (resolving/stacking)	25 ml	25 ml	3.75 ml
Acrylamide stock	25 ml	30 ml	2.0 ml
ddH_2O	17 ml	12 ml	9.75 ml
Ammonium Persulphate (100 mg/ml)	500 µl	500 µl	100 µl
TEMED	40 µl	40 µl	20 µl

Electrophoresis running buffer, pH 8.3:

Tris	25 mM
SDS	1 % (w/v)
Glycine	192 mM

SDS-Polyacrylamide gel electrophoresis (SDS-PAGE) was used to separate proteins (Laemmli, 1970). Protein samples were solubilized in sample buffer (6 M urea, 10 % (w/v) SDS, 0.05 % (w/v) 5-bromophenol blue, 10 % (v/v) mercaptoethanol) for 15 min before spinning out unsolubilized protein and sepharose beads from an immunoprecipitation. This was then loaded into wells in the stacking gel of a 10 % acrylamide SDS-polyacrylamide gel. The molecular weight markers, also in sample buffer, were carbonic anhydrase, 26 kDa, ovalbumin, 45 kDa, bovine plasma albumin, 66 kDa, phosphorylase B, 97.4 kDa, β-galactosidase, 116 kDa and myosin 205 kDa. Prestained markers (carbonic anhydrase and β-galactosidase) were frequently added to the samples. Thick gels (3 mm) were run at a constant current of 25 mA per gel overnight or 50 mA during the day. Thin gels (1.5 mm) required half the current.

2.6.5 Counting ATB-[2-^{3}H]BMPA labelled transporters

Once the proteins had been separated by SDS-PAGE the gel was shaken for 2 h in destain (30 % (v/v) acetic acid, 10 % (v/v) methanol, 60 % (v/v) dH_2O) containing a small amount of Coomassie blue (≈ 0.005 % w/v). The gel was cut into lanes and the lanes cut into 6.5 mm slices. The slices were placed in vials and dried in an 80 °C oven. The dry slices were dissolved in 0.5 ml of 2 % (v/v) NH_4OH in 30 % (w/w) H_2O_2 in the oven. When dissolved 9 ml of Optiphase Safe scintillation fluid was added and the radioactivity counted (Clark and Holman, 1990).

2.6.6 Western blotting and ^{125}I immunoblotting

Proteins separated on a thin, 1.5 mm, gel by SDS-PAGE were transferred to the nitrocellulose membrane using the semi-dry method with a Pharmacia LKB Multiphor II blotter. The filter paper, nitrocellulose, gel and dialysis membrane were soaked in continuous transfer buffer (48 mM Tris, 39 mM glycine, 20 % (v/v) methanol, 0.0375 % (w/v) SDS, pH 8.8). A current of 0.8 mA/cm^2 of the transunit was applied for 1-1.5 h. The transferred proteins on the nitrocellulose were stained with 0.1 % (w/v) Ponceau S stain in 3 % (w/v) trichloroacetic acid in ddH_2O.

All detection, washing and incubation steps were carried out by shaking at room temperature. The membrane was blocked for 2 h with 3 % (w/v) BSA in TBS-T (10 mM Tris, 0.9 % (w/v) NaCl, pH 7.4, 0.1 % (v/v) Tween 20). The primary antibody, diluted 1:100-500 in 3 % (w/v) BSA in TBS-T, was shaken with the membrane for 2 h. The membrane was then subjected to six 5 min washes with TBS-T. It was then incubated with affinity purified ^{125}I-labelled Protein A at 0.1 µCi/ml in TBS-T. The membrane was again washed six times with TBS-T for 5 min, air dried, wrapped in cling film and exposed to x-ray film at -70 °C. The protein bands could be cut out and counted on a gamma counter or the film analysed by densitometry.

2.7 Transfection of fibroblasts with GLUT4

2.7.1 Maxi-prep of pRC-CMV-hGLUT4

To a bijou containing 10 ng of the plasmid DNA was added 100 µl of competent *E. coli*. They were left on ice for 10 min and then heat shocked for 1 min in a 42 °C water bath. 1 ml of LB medium (1 % tryptone, 0.5 % yeast extract, 0.5 % NaCl) was added and the cell incubated at 37 °C for 1 h. Aliquots of cells were then plated out onto LB plates (LB medium containing 1.5 % agar) containing 5 µg/ml ampicillin and incubated overnight at 37 °C. One colony (transformed cells) was taken and added to 2 l of LB medium containing 5 µg/ml ampicillin and left shaking overnight at 37 °C.

The *E. coli* were collected in a Sorvall GSA rotor at 6,000 rpm (6,000 x g) for 10 min at 4 °C. The pellet was resuspended in 1 volume of GTE (50 mM glucose, 25 mM Tris pH 8.0, 10 mM EDTA) with a pipette and left on ice for 20 min for cell lysis to occur. This was transferred to a 50 ml Sorvall tube with two volumes of NaOH/SDS (0.2 M NaOH, 1 % (w/v) SDS) and incubated on ice for 10 min. A 1.25 volume of 3 M sodium acetate, pH 4.6 was added and left on ice for a further 20 min. The solution was centrifuged in a SS-34 rotor at 15,000 rpm (27,000 x g) for 15 min at 4 °C.

The supernatant was transferred to a fresh tube and extraction carried out twice with an equal volume of phenol (pH 8.0)/chloroform/IAA (24:1) and then once with chloroform/IAA. Two volumes of ice cold ethanol were then added, followed by incubation at 4 °C for at least 30 min. This was then centrifuged at 15,000 rpm for 15 min and the pellet washed with 70 % ethanol. After the pellet had been air dried it was resuspended in 9 ml of TE buffer (10 mM Tris, 1 mM EDTA, pH 8.0). To this was added 9 g caesium chloride and 0.6 ml of 10 mg/ml ethidium bromide. This was then placed in a Quickseal tube and spun for 40 h (> 24 h) in a Ti70 rotor at 56,000 rpm at 20 °C in a Beckman ultracentrifuge. An alternative method was to add to the supernatant 10.17 g CsCl per 10 ml of supernatant and 125 µl of 10 mg/ml ethidium bromide before phenol/chloroform/IAA extraction. This could then be centrifuged.

The lower, plasmid, band was removed with a 21 g needle. The syringe was then filled with a CsCl saturated 1-butanol solution and shaken. This was repeated four times to remove all signs of pink from the DNA. The DNA solution was then dialysed in TE buffer for 24 h to remove the CsCl. The DNA was then precipitated out by adding to the solution a 1/10 volume of 3 M sodium acetate and 2 volumes of room temperature ethanol. After 10 min to allow precipitation, the DNA was spun down in a SS-34 rotor at 10,000 rpm (12,000 x g) for 15 min. The dried pellet was resuspended in 1 ml sterile dd$H_2$0 in a sterile lidded tube.

2.7.2 Determination of DNA purity

To 1 ml TE buffer was added 10 µl of the DNA solution in a matched quartz cell, TE being in the other cell. This was scanned from 320 to 240 nm in a scanning spectrophotometer. The absorbance ratio at 260/280 nm indicates the purity of the DNA from protein, a value of 2 is pure DNA. One A_{260} unit = 50 µg/ml of ds DNA.

2.7.3 Restriction digest mapping of pRC-CMV-hGLUT4

To 0.2 µg DNA was added 2 µl 10 x One Phor All buffer and 17 µl H_2O, 0.5 µl HindIII and 0.5 µl XbaI This was left to digest for 1 h at 37 °C.

1 g agarose was dissolved in 100 ml TBE buffer (89.0 mM Tris, 89.0 mM boric acid, 2.0 mM EDTA (4 ml per l of 0.5 M EDTA, pH 8.0)), 0.5 mg ethidium bromide was added and the gel cast. The gel was put in TBE running buffer. The restriction digest was loaded onto the gel with 2 µl 10 x loading dye (30 % (w/v) glycerol, 0.25 % (w/v) bromophenol blue, 0.25 % (w/v) xylene cyanole FF). Uncut plasmid and the lambda Pst size marker were also loaded. A voltage of 100 - 150 V was applied across the gel. The gel was viewed under UV light and a Polaroid photograph taken.

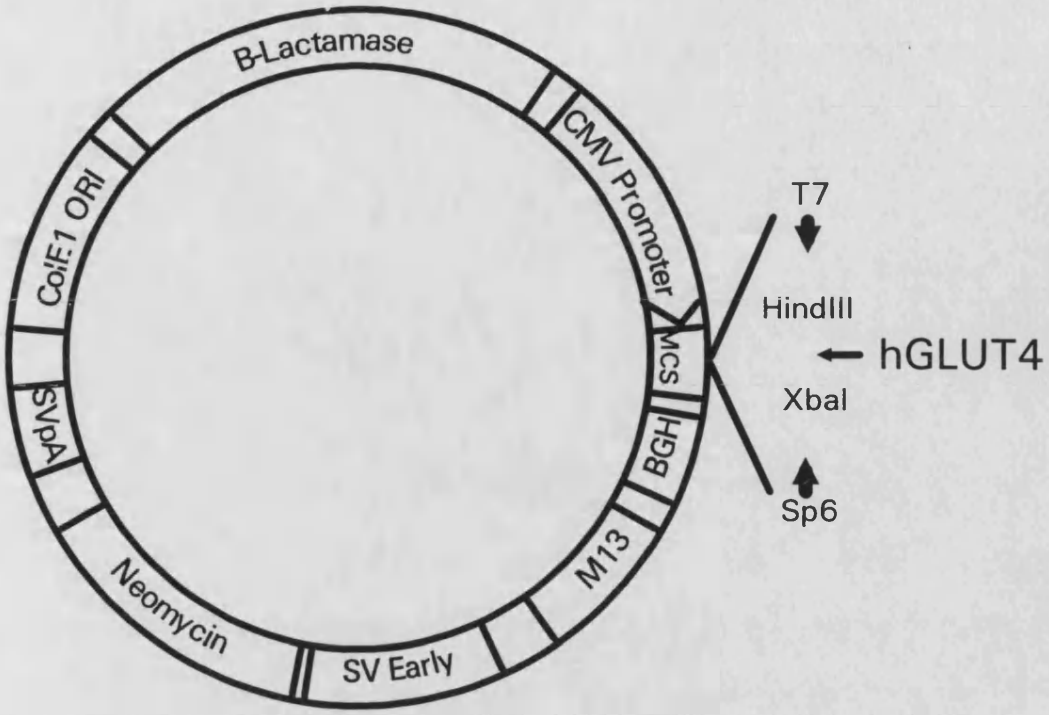

Figure 2.2. Map of the plasmid pRC-CMV-hGLUT4

The total length of the plasmid before the addition of the hGLUT4 cDNA is 5452 bp. The CMV promoter spans bases 209-864. T7 begins at base 865, the polylinker spans bases 891-995 and the Sp6 promoter begins at 1019. The BGH poly A signals spans bases 1020-1251, the M13 origin spans 1260-1793, the SV40 promoter spans 1800-2125, the neomycin gene spans 2131-2925 and the SV40 3' and poly A span bases 2928-3138. The pUC 19 backbone, origin and beta lactamase gene begin at base 3236. The hGLUT4 cDNA was spliced into the plasmid at the HindIII and Xbal sites within the polylinker. In the hGLUT4 cDNA the HindIII site is 29-33 bases upstream of the start codon and the Xbal 351 bases beyond the end.

2.7.4 Transfection of 3T3-L1 fibroblasts with pRC-CMV-hGLUT4

The 3T3-L1 fibroblasts were transfected by the calcium phosphate precipitation method (Kingston, 1992). A 85 cm^2 flask of confluent 3T3-L1 fibroblasts was split 1:15 into 90 mm dishes (section 2.2.3) 24 h before transfecting. The medium was replaced with 9 ml DMEM-FCS 2-4 h before transfection. Between 10-50 mg of the plasmid DNA was sterilised by ethanol precipitated in 1 ml of cold 95 % ethanol and 1/20 volume of 3 M sodium acetate, pH 5.2. The DNA precipitate was spun down by

a high speed spin in a MSE microcentrifuge. When dry it was resuspended in 450 µl sterile ddH_2O. To this was added 50 µl of filter sterilised 2.5 M calcium chloride solution. This was slowly added dropwise to 500 µl of 2x HEPES buffered saline, HBS (280 mM NaCl, 50 mM HEPES, 1.7 mM Na_2HPO_4, pH 7.05-7.12) while bubbling air through the 2 x HBS with a mechanical pipettor. This was vortexed and allowed to stand for 20 min for the precipitate to form. It was then added to the 3T3-L1 fibroblast medium and mixed. The dishes were incubated for up to 16 h in a 37 °C, 5 % CO_2 incubator. The cells were then washed twice with warm PBS, fresh DMEM-FCS was added and the cells were grown for 3-5 days as normal in a 10 % CO_2 incubator before being used as required.

2.7.5 Transfection of COS-7 fibroblasts with pRC-CMV-hGLUT4

90 mm dishes were seeded with COS-7 fibroblasts at a cell density of 2 x 10^6 cells per dish. The cells were allowed to grow for 24 h in DMEM-FCS at 37 °C in a 5 % CO_2 incubator. The dishes were then washed twice with 10 ml PBS and once with 10 ml TBS-D (25 mM Tris, 138 mM NaCl, 2.6 mM KCl, 0.1 % (w/v) glucose, pH 7.4). The cells were incubated with 1.5 ml TBS-D containing 7.5 µg plasmid DNA and 1.5 mg DEAE-Dextran per dish. After 1 h the cells were washed once with TBS-D and once with PBS. They were incubated with 10 % DMSO in PBS for 1 min, washed once with PBS and then grown for 72 h in DMEM-FCS at 37 °C in a 5 % CO_2 incubator. COS-7 fibroblasts were also transfected in 35 mm dishes with the incubation volumes scaled down (adapted from Schürmann *et al.*, 1992b).

2.8 Purification of the GLUT4 C-terminal peptide

The previously synthesised C-terminal GLUT4 peptide was stored at -20 °C on the resin on which it was synthesised. To 300 mg of GLUT4 resin was added a solution of 90 % (v/v) trifluoroacetic acid, 5 % (v/v) thioanisole, 3 % (v/v) ethanedithiol and 2 % (v/v) anisole. This was left for 2-2.5 h to cleave the peptide from the resin. This was then washed three times with petroleum ether, the supernatant being discarded. It was then washed a further three times with diethyl ether, discarding the supernatant. The remaining residue was the crude peptide. The peptide was then reduced with 20 mg dithioerythritol in 15 ml 5 % acetonitrile, pH 8.3, overnight. The peptide was purified by HPLC on an acetonitrile gradient, collecting the appropriate GLUT4 C-terminal peptide peak. The collected peak was freeze dried and stored at -20 °C.

2.9 Antibody production

The free cysteine groups of the GLUT4 C-terminal and rab4 peptides were tested for by the Ellman's test. A sample of the peptide dissolved in phosphate buffer was diluted in 0.1 M phosphate buffer (0.1 M Na_2HPO_4, pH 8.0). To this was added Ellman's reagent, 5,5'-dithio-bis(2-nitrobenzoic acid), or 2-nitro-5-thiocyanobenzoic acid at a final concentration of 0.36 mg/ml. The number of free cysteines was determined by comparing the absorbance at 412 nm against a standard cysteine curve.

8 mg Keyhole Limpet haemocyanin (KLH) was dissolved in 0.5 ml 10 mM phosphate buffer, pH 7.2. 1.4 mg 3-maleimidobenzoic acid N-hydroxysuccinimide ester (MBS) dissolved in dry DMF was slowly added, stirred for 30 min and passed down a Sephadex G-25 column equilibrated with 50 mM phosphate buffer, pH 6.0. Fractions were collected, measured at 280 nm and turbid fractions pooled. 9.5 mg of peptide in 2 ml 10 mM phosphate buffer, pH 7.2, was added to the KLH-MBS and stirred for 3 h, to couple the peptide to the KLH-MBS. This was stored at -20 °C (Liu *et al.*, 1979).

Peptide	Amino acids	No. of residues	Sequence	Source
GLUT1 C-terminal peptide	480-492	14	C E E L F H P L G A D S Q V Cys Glu Glu Leu Phe His Pro Leu Gly Ala Asp Ser Gln Val	A. E. Clark
GLUT2 loop peptide	47-60	15	C G V P L D D R R A T I N Y D Cys Gly Val Pro Leu Asp Asp Arg Arg Ala Thr Ile Asn Tyr Asp	N. J. Jordan
GLUT4 C-terminal peptide	497-509	15	C G S T E L E Y L G P D E N D Cys Gly Ser Thr Glu Leu Glu Tyr Leu Gly Pro Asp Glu Asn Asp	Crude peptide: I. J. Kozka
GLUT4 N-terminal peptide	2-17	16	P S G F Q Q I G S E D G E P P Q Pro Ser Gly Phe Gln Gln Ile Gly Ser Glu Asp Gly Glu Pro Pro Gln	A. E. Clark
Rab3a peptide	52-67	16	V S T V G I D F K V K T I Y R N Val Ser Thr Val Gly Ile Asp Phe Lys Val Lys Thr Ile Tyr Arg Asn	J. F. Clarke
Rab4 peptide	122-132	14	K K D L D A D R E V T G G C Lys Lys Asp Leu Asp Ala Asp Arg Glu Val Thr Gly Gly Cys	A. E. Clark

Table 2.1 The sequence and source of peptides used for antibody production and transport assays

In order to inoculate sandy half-lop-eared rabbits ≈ 250 µg peptide-KLH conjugate was diluted to 500 µl in PBS and diluted with an equal volume of either complete Freund's (by rapid mixing just before injection) or Imject Alum (Pierce, Rockford, USA) (added dropwise into the PBS and stirred for 30 min before injection). This was injected into four subcutaneous sites. This was repeated one month later with either incomplete Freund's or Imject Alum. Thereafter the rabbits were boosted with the conjugate in Imject Alum every month and a 35 ml bleed was taken. The blood was allowed to clot and the serum was removed and stored at -70 °C until required when it was defrosted, divided into small aliquots and frozen at -20 °C until required.

2.10 ELISA determination of antibody levels in serum

To multiwell microplate ELISA wells were added 100 µl 50 mM $NaHCO_3$, pH 9.6, containing 20 ng/well GLUT4 or rab4 peptide or 1 µg/well of protein depleted erythrocyte membrane for GLUT1. This was left at 4 °C for 16 h to coat the plates. The wells were emptied and blocked with three 10 min washes of blocking buffer (PBS with 1 % casein and 0.05 % Tween 20). The antiserum was then serially diluted in duplicate from 1/200 to 1/25,600 in blocking buffer. This was added to the wells for 2 h at 37 °C. The wells were then washed with three 10 min blocking buffer washes. The second antibody, goat anti rabbit IgG peroxidase, was diluted 1:5000 in blocking buffer and added to the wells for 2 h at 37 °C. This was then washed with four 5 min washes of washing buffer (PBS with 0.05 % Tween 20). To each well was then added 100 µl of substrate (10 ml 0.1 M sodium acetate, 0.1 ml tetramethylbenzidine diluted 10 mg/ml in DMSO and 1.5 µl H_2O_2 (30 % v/v)). After 30 min at room temperature 100 µl of 2 M H_2SO_4 was added to each well and the colour read at 450 nm, filters 3 and 8 on the Titertek plate reader. The new serum absorbance was compared against that of a previously measured serum (from Kenna *et al.*, 1985).

2.11 Protein assays

2.11.1 BioRad protein assay

The BioRad protein assay is a Coomassie Brilliant Blue G-250 binding assay originally developed by Bradford (1976). The protein sample was diluted in phosphate buffer to a suitable concentration to fit on the standard curve. The protein standard, bovine serum albumin, was diluted in phosphate buffer to give a concentration range between 0 and 3.0 µg in a final volume of 155 µl in a microplate well. To both sample and standard was added 5 µl of 0.1 M NaOH and 40 µl BioRad reagent. After mixing the absorbance at 595 nm was read on a Titertek microplate reader using filters 6 and 7.

2.11.2 Micro BCA protein assay

The BCA protein assay reagent, bicichoninic acid (BCA), chelates Cu^{+} forming a colour complex in the presence of protein. To a microplate well was added 5 µl of sample diluted in phosphate buffer. To each well was added a range of 0 to 10 µg/well of the standard protein, BSA, in 0.1 M NaOH. All volumes were made up to 10 µl with 0.1 M NaOH. To each well was added 200 µl of BCA reagent (sodium carbonate, sodium bicarbonate, and sodium tartrate in 0.2 M NaOH (MA), 4 % BCA in water (MB), 4 % cupric sulphate pentahydrate in water (MC) MA:MB:MC 50:48:2 (Pierce, Rockford, USA)). After a 30 min incubation at 37 °C the absorbance was read at 562 nm on a Titertek plate reader using filters 6 and 3.

2.12 Statistical analysis

During the statistical analysis of experimental data each individual sample of a replicate was treated as an individual experiment. Where necessary statistical significance was determined using the t-test.

3.0 Results

3.1 Kinetic analysis of GLUT1 and GLUT4 in 3T3-L1 adipocytes

When 3T3-L1 adipocytes are acutely stimulated with 100 nM insulin both the rate of glucose uptake and the concentration of glucose transporters in the plasma membrane increase. This was demonstrated by assaying the uptake of 3-*O*-methyl-D-glucose and by purifying plasma membrane with ATB-BMPA photolabelled glucose transporters. Figure 3.1 shows that 100 nM insulin stimulated transport by 19-fold while the concentration of transporters in the plasma membrane only increased by 5.6-fold.

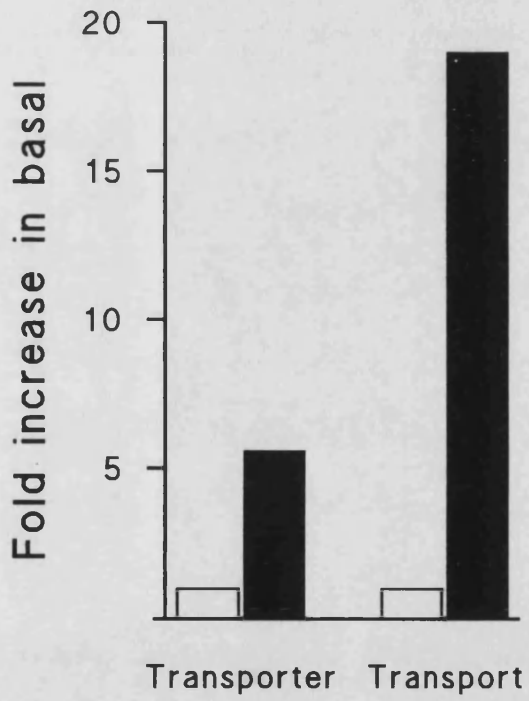

Figure 3.1. Effect of acute insulin stimulation on ATB-BMPA photolabelling and transport

3T3-L1 adipocytes in 35 mm dishes were incubated at 37 °C in KRH for 30 min in the absence (□) or presence of 100 nM insulin (■). The 3-*O*-methyl-D-glucose transport was assayed as described in section 2.4.2.1. The transport values are the average of seven experiments.

The increase in the concentration of cell surface transporters was assayed by photolabelling two dishes per condition with ATB-[2-^{3}H]BMPA at 50 μCi/dish. After washing the dishes 6 times with 3 ml KRH containing phloretin at 10 mg/ml the cells were scraped from the dishes and homogenised in 1 ml TES with 10 strokes of a tight fitting homogeniser. The homogenate was spun at 16,000 g_{max}, 17,000 rpm for 20 min. The pellet was washed twice with TES, resuspended in 0.5 ml TES and applied to a discontinuous Ficoll gradient (0.15 g/ml TES). This was spun at 34,000 g_{max}, 20,000 rpm for 70 min. The plasma membrane at the interface was collected with a needle and syringe, diluted with TES and spun down at 34,000 rpm for 20 min. The pellet was dissolved in sample buffer, run on SDS-PAGE, the gel was processed and counted as described in section 2.6.

The effect of insulin on the translocation of GLUT1 and GLUT4 in 3T3-L1 adipocytes is shown in figure 3.2. Basal and insulin stimulated cells were photolabelled with ATB-BMPA and solubilized. GLUT1 and GLUT4 were sequentially immunoprecipitated with protein A-sepharose linked specific anti-C-terminal peptide antiserum. This has the advantage over the purified plasma membrane of reducing non-specific labelling on the gel and enables the separate changes in GLUT1 and GLUT4 to be resolved.

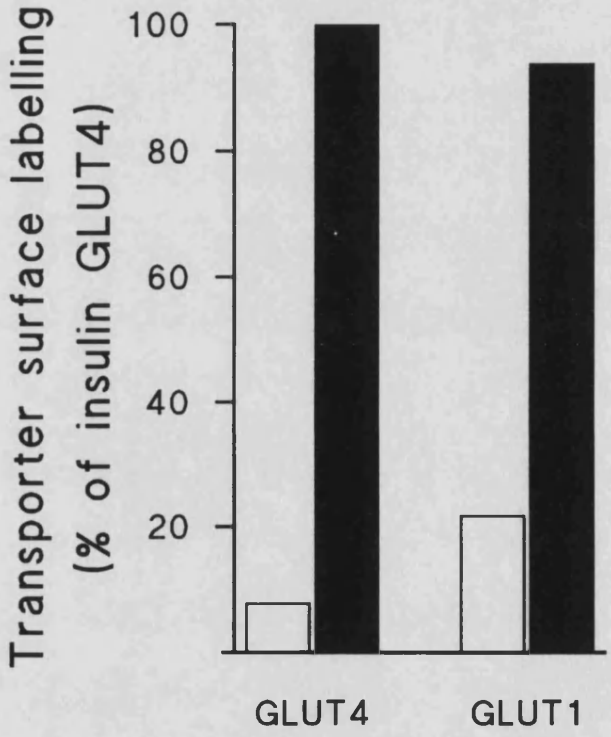

Figure 3.2. Comparison of the relative levels of GLUT1 and GLUT4 at the surface of basal and insulin stimulated 3T3-L1 adipocytes

3T3-L1 adipocytes in 35 mm dishes were incubated at 37 °C for 20 min in KRH in the absence (□) or presence of 100 nM insulin (■). Adipocytes were photolabelled with 150 μCi ATB-[2-^{3}H]BMPA per dish and transporters immunoprecipitated as in sections 2.5-6. A representative experiment is shown.

Figure 3.2 shows that the insulin stimulated 20-fold increase in transport is associated with a 13-fold increase in GLUT4 and a 4.3-fold increase in GLUT1 at the plasma membrane. This suggests that the two transporter isoforms make an unequal

contribution towards the transport rate. The activity of the two isoforms have been investigated separately in, for example, *Xenopus* oocytes where the two transporters do indeed possess different kinetic properties. The presence of two isoforms within the same cell means that the kinetics may not be linear, making it difficult to determine their separate contributions. This problem was overcome by examining the kinetics under conditions with different proportions of GLUT1 and GLUT4 at the cell surface. Figure 3.2 shows that the proportion of cell surface GLUT4 to GLUT1 is different in basal and insulin stimulated 3T3-L1 adipocytes. A similar proportion of both transporters are at the surface of insulin stimulated cells. In basal cells there is nearly 3-fold more GLUT1 than GLUT4 but the low level of transporters at the surface of basal adipocytes increases the possibility of errors. Therefore chronically insulin stimulated 3T3-L1 adipocytes were used. Chronic insulin treatment, 500 nM insulin for 24 h, halves the level of cell surface GLUT4 while increasing the level of GLUT1 by about 3.5-fold relative to acute insulin stimulation. The GLUT4 B_{max}, determined from ATB-BMPA binding, was 0.17±0.03 μM in acutely insulin stimulated adipocytes and 0.099±0.017 μM following chronic stimulation. The GLUT1 B_{max} was 0.19±0.03 μM for acute and 0.7±0.07 μM for chronic insulin stimulation (Palfreyman et *al.*, 1992).

The K_m and V_{max} for transport in acute and chronically insulin stimulated 3T3-L1 adipocytes were calculated from the results shown in figure 3.3. Uptake of 3-*O*-methyl-D-[U-^{12}C]glucose was determined over the range of 0 to 40 mM 3-*O*-methyl-D-glucose. The adipocytes were equilibrated with the appropriate concentration of unlabelled 3-*O*-methyl-D-glucose before the addition of the labelled sugar to ensure that transport was measured under conditions of equilibrium exchange. The data in figure 3.3 were plotted as concentration against rate (s) over cell volume (v) (s/v). The cell volume was calculated by dividing the uptake of 3-*O*-methyl-D-glucose at infinity per dish by the specific activity per μl. A cell volume of 2.81±0.43 μl·dish^{-1} (SEM) was calculated from six experiments. A line fitted to the points of the reciprocal plot of figure 3.3 appeared to be curvilinear, indicating a different contribution by GLUT1 and

GLUT4 across the concentration range. Fitting the data to the Michaelis-Menten equation gave a K_m of 12.3±1.3 mM and a V_{max} of 0.52±0.04 mM·s^{-1} for 3-*O*-methyl-D-glucose in acute insulin treated 3T3-L1 adipocytes. In chronically insulin treated cells the K_m for 3-*O*-methyl-D-glucose was 23.0±9.1 mM and the V_{max} was 1.24±0.40 mM·s^{-1} (SEM). K_m and V_{max} were calculated by least-squares regression, as described by Cleland (1979), using the equation $1/v = K_m/(1+[S]\cdot V_{max})$. The same experiment was carried out in basal 3T3-L1 adipocytes, figure 3.4, where the K_m for 3-*O*-methyl-D-glucose was 11.5±1.7 mM and the V_{max} was 0.028±0.003 mM·s^{-1} (SEM).

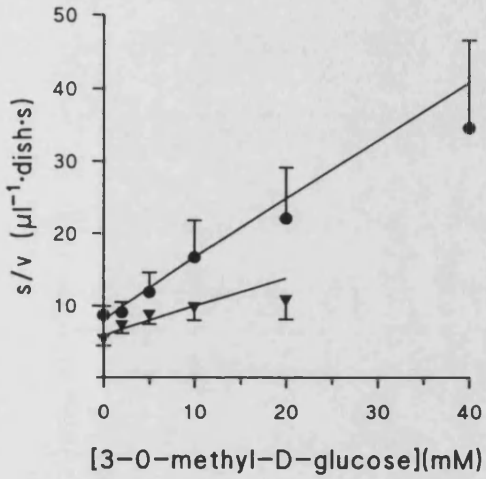

Figure 3.3. Equilibrium exchange uptake of 3-*O*-methyl-D-glucose in stimulated 3T3-L1 adipocytes

3T3-L1 adipocytes in 35 mm dishes were treated acutely with 100 nM insulin for 30 min (●) or chronically with 500 nM insulin for 24 h (▼).

Following the equilibration of 3-*O*-methyl-D-glucose, uptake was assayed as described in section 2.4.2.1. Values are the average of four triplicate experiments (n=12). The rate in s was converted to s/v (µl^{-1}.dish.s) by dividing by the equilibrium intracellular volume of 2.81 µl/dish. Errors are S.E.M. The lines were calculated using the combined data in line 5 of table 3.1

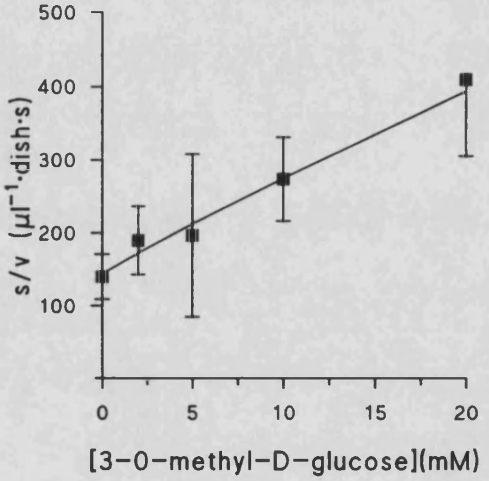

Figure 3.4. Equilibrium exchange uptake of 3-*O*-methyl-D-glucose in basal 3T3-L1 adipocytes

The uptake of 3-*O*-methyl-D-glucose was determined in basal 3T3-L1 adipocytes in 35 mm dishes (■) after 30 min equilibration.

Following the equilibration of 3-*O*-methyl-D-glucose, uptake was assayed as described in section 2.4.2.1. Values are the average of two triplicate experiments (n=6). The rate in s was converted to s/v (µl^{-1}.dish.s) by dividing by the equilibrium intracellular volume of 2.81 µl/dish. Errors are S.E.M. The line was calculated using the data in line 6 of table 3.1

In order to determine the separate affinities of GLUT1 and GLUT4 toward 3-*O*-methyl-D-glucose, acute and chronically insulin treated 3T3-L1 adipocytes were photolabelled in the presence of a range of 3-*O*-methyl-D-glucose concentrations. The photolabelled GLUT1 and GLUT4 were separately immunoprecipitated and subjected to SDS-PAGE. The gel was sliced and counted. Figure 3.5. shows a typical gel profile.

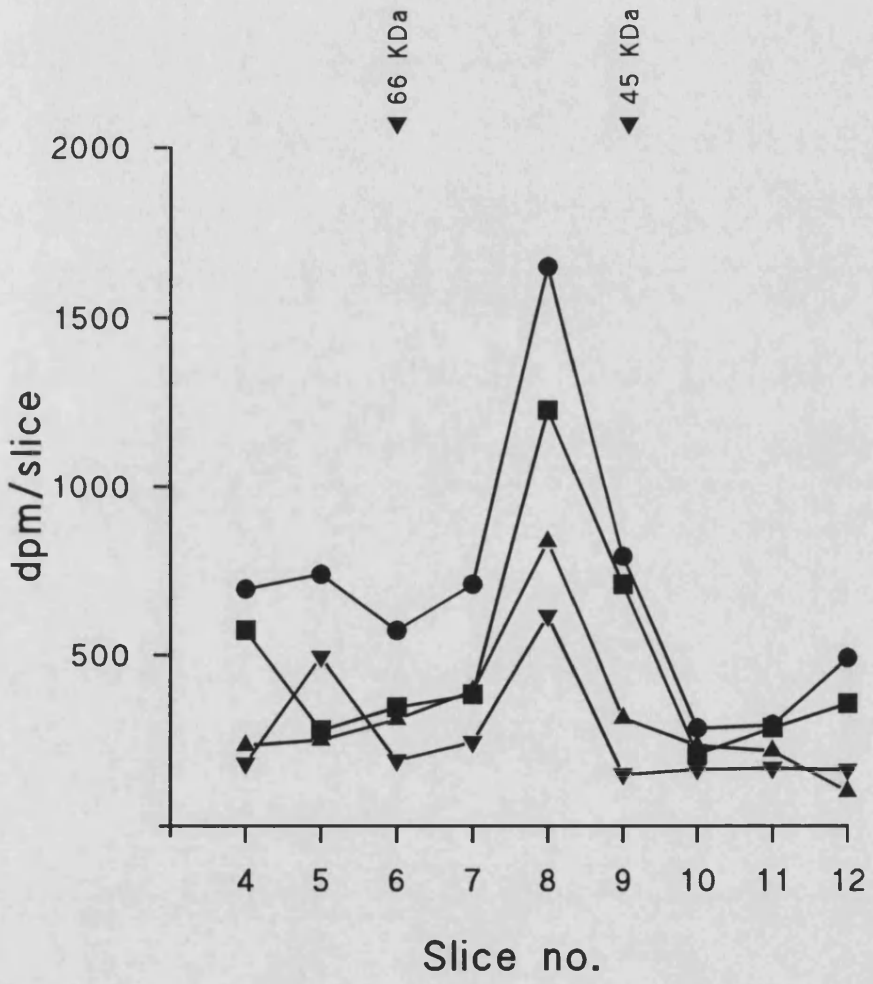

Figure 3.5. An example of ATB-[2-^{3}H]BMPA displacement from GLUT4 by 3-O-methyl-D-glucose in acutely insulin stimulated 3T3-L1 adipocytes

3T3-L1 adipocytes in 35 mm dishes were acutely stimulated with 100 nM insulin for 30 min and then photolabelled with 100 μCi ATB-BMPA in the presence of 0 mM (●), 2 mM (■), 10 mM (▲) or 40 mM (▼) 3-*O*-methyl-D-glucose. Photolabelling, immunoprecipitation and SDS-PAGE are described in sections 2.5 and 2.6. The gel profiles for 5 mM and 20 mM are omitted for clarity.

The radioactivity associated each transporter peak was converted to the ratio A_0/A by dividing the ATB-BMPA peak area in the absence of 3-*O*-methyl-D-glucose (A_0) by the peak area in the presence of 3-*O*-methyl-D-glucose (A). This ratio was plotted against the 3-*O*-methyl-D-glucose concentration used to displace the photolabel in figure 3.6. Since K_m, K_i and K_s were all assumed to be the same (Devés and Krupka, 1984) the data in figure 3.6 were used to calculate K_m values for 3-*O*-methyl-D-glucose displacement of ATB-BMPA using the equation $A_0/A = 1 + S/K_m$ and non-linear regression analysis with relative error weighting. In the acutely insulin treated cells the K_m was 7.2±2.0 mM for GLUT4 and 23.4±7.6 mM for GLUT1. In the chronically treated cells the K_m was 6.85±1.5 mM for GLUT4 and 16.4±2.9 mM for GLUT1.

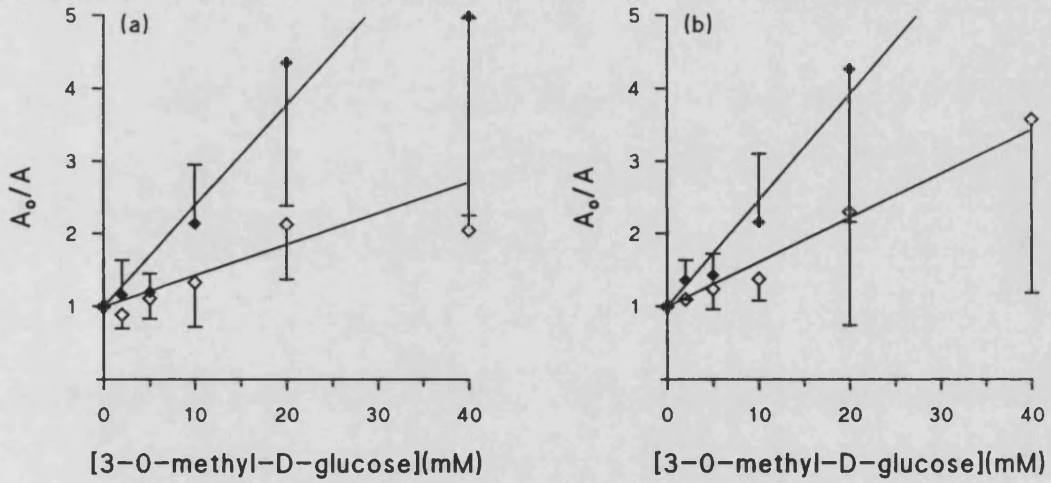

Figure 3.6. Determination of K_m for 3-*O*-methyl-D-glucose displacement of ATB-BMPA from GLUT4 and GLUT1 in acute and chronically insulin stimulated 3T3-L1 adipocytes

3T3-L1 adipocytes in 35 mm dishes were either acutely treated with 100 nM insulin for 30 min (a) or chronically treated with 500 nM insulin for 24 h (b). The dishes were photolabelled with 100 µCi of ATB-BMPA in the presence of the concentration of 3-*O*-methyl-D-glucose indicated. GLUT4 (◆) and GLUT1 (◇) were then immunoprecipitated, subjected to SDS-PAGE, and counted as described in sections 2.5 and 2.6. The radioactivity peak in the presence of 3-*O*-methyl-D-glucose (A) is shown relative to the value in the absence of 3-*O*-methyl-D-glucose (A_0). Results are the means of three experiments for (a) and two for (b). Errors are the $SD_{(n-1)}$.

The TK value, the turnover number/K_m, of GLUT1 and GLUT4 can be calculated from the transport and photolabelling data using the following equation where the transporter concentration is the B_{max} value given in table 3.1:

$$v = \frac{TK1 \cdot S \cdot [GLUT1]}{(1 + S/K_{m1})} + \frac{TK4 \cdot S \cdot [GLUT4]}{(1 + S/K_{m4})}$$

Since $A_0/A = 1 + S/K_m$, the fraction of unoccupied sites can be calculated with the ATB-BMPA displacement data or the K_m values from figure 3.3. The TK values were calculated using least square regression of the following equation:

$$v/S = TK1 \cdot x1 + TK4 \cdot x4$$

where x1 and x4, the concentration of unoccupied sites, are equal to the B_{max} multiplied by either A/A_0 or $1/(1 + S/K_m)$, the reciprocal fraction of unoccupied sites. The calculated TK values and the constants used to calculated them are given in table 3.1. The table also gives a calculated TK for GLUT1 and GLUT4 in basal 3T3-L1 adipocytes. This uses the combined acute and chronic K_m values. The basal B_{max} was determined using a tracer concentration of ATB-BMPA.

Stimulation data	Method used	B_{max1}	B_{max4}	K_{m1}	K_{m4}	TK1 x 10^{-3} ($mM^{-1} \cdot min^{-1}$)	TK4 x 10^{-3} ($mM^{-1} \cdot min^{-1}$)
Acute insulin	A/A_0	0.19 µM	0.17 µM	-	-	4.90±2.03	7.92±2.86
Chronic insulin	A/A_0	0.70 µM	0.099 µM	-	-	3.82±2.20	8.60±18.4
Combined acute and chronic	A/A_0	0.19 µM 0.70 µM	0.17 µM 0.099 µM	-	-	3.71±0.31	9.50±1.26
Combined acute and chronic	$1/(1+S/K_m)$ $1/(1+S/K_m)$	0.19 µM 0.70 µM	0.17 µM 0.099 µM	23.4 mM 16.4 mM	7.2 mM 6.85 mM	3.73±0.26	10.92±1.11
Combined acute and chronic	$1/(1+S/K_m)$	0.19 µM 0.70 µM	0.17 µM 0.099 µM	19.9 mM	7.0 mM	3.58±0.24	11.34±1.06
Basal	$1/(1+S/K_m)$	0.055 µM	0.015 µM	19.9 mM	7.0 mM	1.20±0.36	5.73±2.02

Table 3.1. Calculation of GLUT1 and GLUT4 TK values for 3-O-methyl-D-glucose in 3T3-L1 adipocytes Errors are the S.E.M.

3.2 Okadaic acid treatment and insulin stimulation of adipocytes

The effect of okadaic acid on the uptake of 2-deoxy-D-glucose in rat adipocytes was investigated by Haystead *et al.* (1989) and by Lawrence *et al.* (1990b) who found that the 1 μM okadaic acid stimulated transport rate was half that following insulin treatment. To determine the effect of okadaic acid on the uptake of 3-*O*-methyl-D-glucose, firstly rat adipocytes were treated with okadaic acid for different lengths of time to find the optimum time for okadaic acid stimulation, figure 3.7. Rat adipocytes with a 40 % cytocrit were stimulated with 10 nM insulin for 30 min or with 1 μM okadaic acid for 5, 10, 15 or 30 min. Uptake was measured over 3 s for both okadaic acid and insulin treatment. While insulin treatment stimulated transport by 19.1-fold, a 15 min incubation with okadaic acid increased the basal transport rate 7.7-fold, about 40 % of the insulin response.

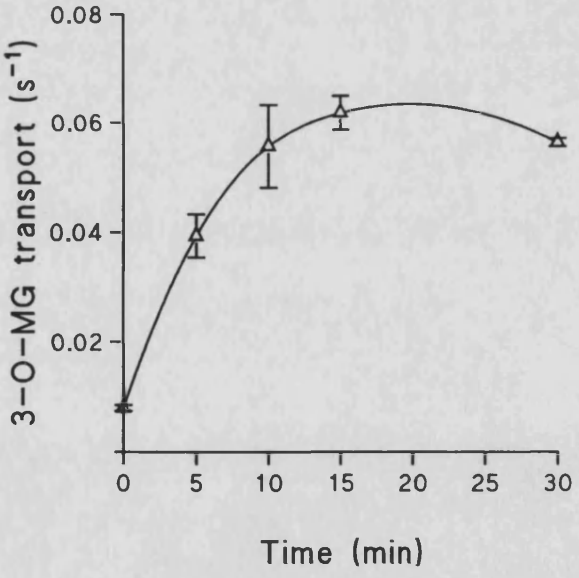

Figure 3.7. Determining the optimum time for the stimulation of rat adipocyte uptake of 3-*O*-methyl-D-glucose with 1.0 μM okadaic acid

Rat adipocytes were treated with 1.0 μM okadaic acid for the specified length of time before removing a sample to assay the rate of 3-*O*-methyl-D-glucose uptake. The methods used for preparing rat adipocytes and assaying 3-*O*-methyl-D-glucose uptake are described in sections 2.3.1 and 2.4.1 respectively. Values are the means of a single triplicate experiment. Errors are the S.E.M. The transport rate at 0 min is equivalent to basal transport. Acute insulin (10 nM) stimulation was 19-fold.

Figure 3.7 shows that the maximum transport rate in the presence of 1 μM okadaic acid was achieved after about 10 min and longer incubation times gave about the same rate. An incubation time of 20 min was used to find the optimum concentration for okadaic acid stimulation. Three experiments in triplicate were used to generate the concentration curve over the range of 0.05 to 5 μM shown in figure 3.8. The optimum okadaic acid concentration was found to be between 0.2 and 1.0 μM. The okadaic acid stimulated transport rate at this concentration was only about 40 % of the insulin stimulated rate. Thus a maximum increase in 3-*O*-methyl-D-glucose uptake with ≈ 0.5 μM okadaic acid for 20 min was in agreement with the 1 μM okadaic acid for 20 min used by Lawrence *et al.* (1990b) for stimulating 2-deoxy-D-glucose transport.

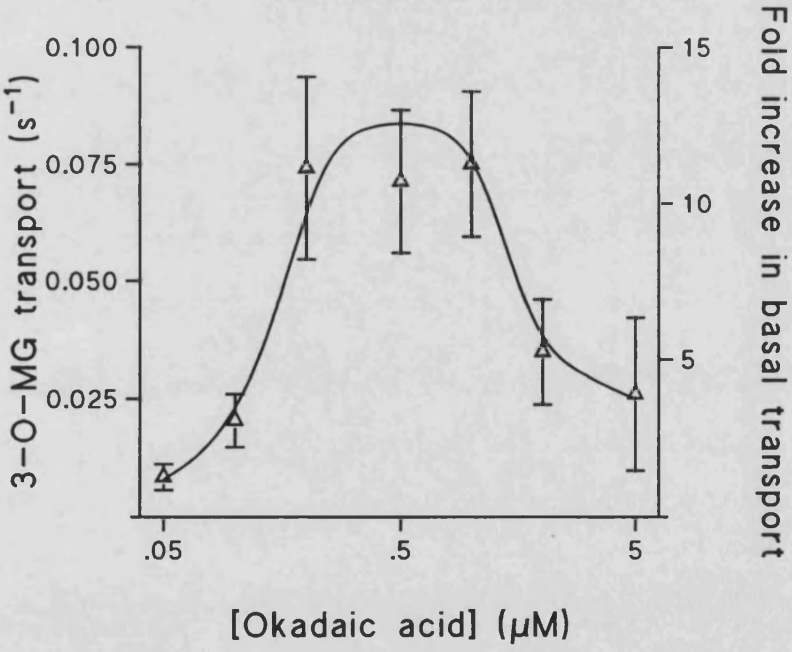

Figure 3.8. Determining the optimum concentration of okadaic acid for the stimulation of rat adipocyte uptake of 3-O-methyl-D-glucose

Rat adipocytes were stimulated with the specified okadaic acid concentration for 20 min before assaying 3-O-methyl-D-glucose uptake. The methods for preparing rat adipocytes and assaying 3-O-methyl-D-glucose transport are described in sections 2.3.1 and 2.4.1 respectively. Values are the means of one (0.05 and 0.1 μM), two (2.0 and 5.0 μM) or three (0.2, 0.5 and 1.0 μM) experiments carried out in triplicate. Errors are the S.E.M.

The fold increase in the transport rate following acute insulin (10 nM) treatment was 30.0 ± 7.3.

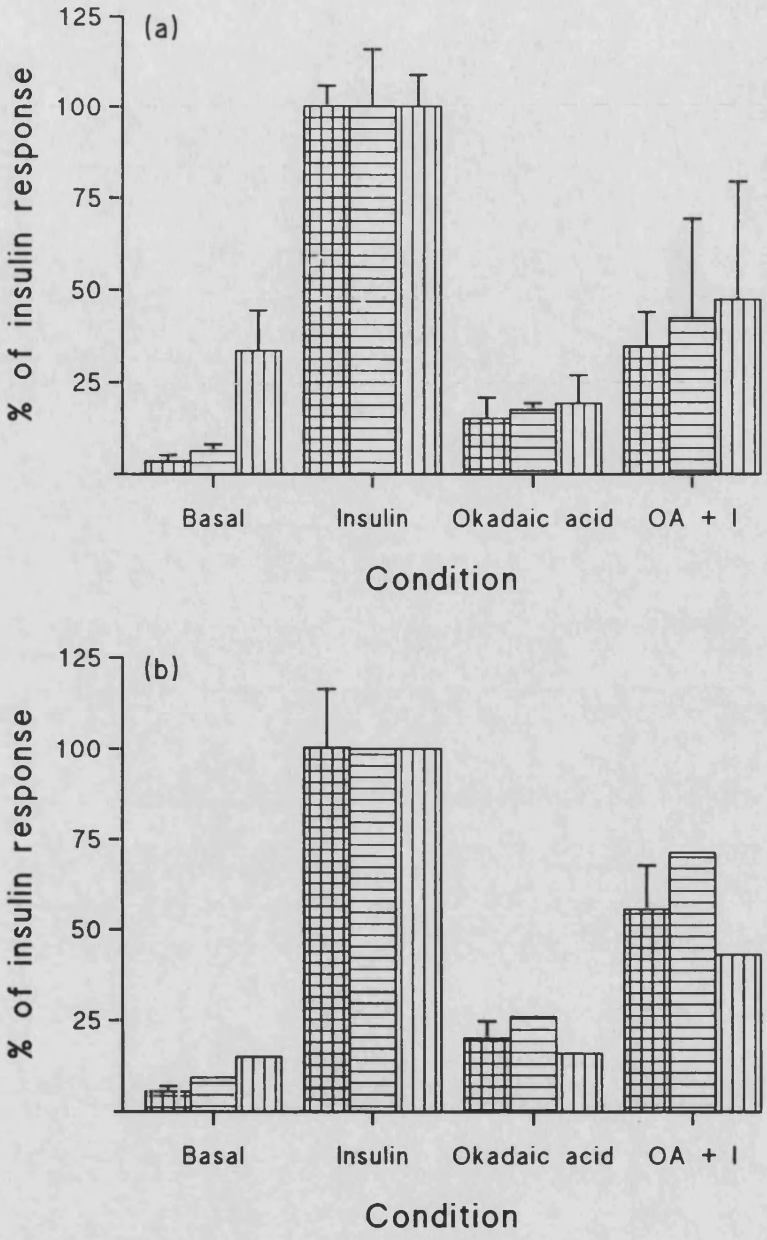

Figure 3.9. The effect of 5.0 μM (a) and 1.0 μM (b) okadaic acid on basal and insulin stimulated transport and transporter distribution in rat adipocytes

Rat adipocytes were incubated for 20 min with no additions (basal), with 10 nM insulin, with okadaic acid or with 10 nM insulin and okadaic acid (OA+I) before removing 1 ml of cells for photolabelling and using the remainder to assay 3-*O*-methyl-D-glucose uptake. The concentration of okadaic acid used was 5.0 μM in (a) and 1.0 μM in (b). The preparation of rat adipocytes, photolabelling and the assaying of 3-*O*-methyl-D-glucose uptake are described in section 2.0.

Data are the means of two (a) or one (b) experiments. Results are expressed relative to the mean insulin value. Transport results (▦) are the means of five (a) or three (b) values. GLUT4 (▤) and GLUT1 (▥) photolabelling are the means of two (a) or one (b) values. Errors are the $SD_{(n-1)}$.

Figure 3.8 suggests that higher concentrations of okadaic acid, such as 5.0 μM, stimulate transport less than 1.0 μM. Rat adipocytes were therefore stimulated with either 10 nM insulin, 5.0 μM okadaic acid or both for 20 min. 3-*O*-methyl-D-glucose uptake was then assayed and cell surface transporters were photolabelled with ATB-BMPA. The results are shown in figure 3.9.

Figure 3.9a shows that 5.0 μM okadaic acid caused a 4.5-fold increase in the basal rate of 3-*O*-methyl-D-glucose uptake, similar to that of figure 3.8. Okadaic acid also caused a 2.9-fold rise in the level of GLUT4 in the plasma membrane. Its effect on GLUT1, however, was to decrease it to only 65% of the basal value. If in rat adipocytes the transport capacity of GLUT4 is ≈ 3-fold higher than that of GLUT1 as it is in 3T3-L1 adipocytes (Palfreyman *et al.* 1992; section 3.1) then the increase in GLUT4 is sufficient to counter the decrease in GLUT1 and still cause a rise in 3-*O*-methyl-D-glucose uptake. A comparison of the transport rates and transporter levels in okadaic acid and insulin treated cells, however, does suggest that the intrinsic activity of the transporters in the okadaic acid treated cells is about 80 % of that in the insulin treated cells. When rat adipocytes were incubated with 5.0 μM okadaic acid and 10 nM insulin then again the transport rate increased but only to 35 % of the insulin stimulated rate. This depression of the insulin stimulated transport rate was reflected in the surface levels of GLUT1 and GLUT4. GLUT1 was 48 % and GLUT4 was 42 % of the insulin stimulated level. Thus the effect of 5.0 μM okadaic acid in rat adipocytes is to increase the transport rate by causing the translocation of GLUT4 and by increasing the intrinsic activity of the basal transporter but not by as much as insulin.

A similar experiment with 1.0 μM okadaic acid is shown in figure 3.9b. At this concentration the rate of 3-*O*-methyl-D-glucose uptake rose 4-fold and the GLUT4 surface levels rose 2.5-fold while GLUT1 levels remained the same, rather than decreasing it as with 5.0 μM okadaic acid. 1.0 μM okadaic acid reduced insulin stimulated transport but to a lesser extent than 5.0 μM, reflected in the smaller decrease in the GLUT1 and GLUT4 surface levels.

An alternative way to study the effect of okadaic acid was to add it to the rat adipocytes as the insulin stimulated increase in transport was being reversed, figure 3.10. Rat adipocytes were stimulated for 30 min with 10 nM insulin. The stimulation was reversed by the addition of 0.25 mg/ml collagenase. Insulin stimulation was also reversed in the presence of 0.5 μM okadaic acid. Collagenase alone fully reversed the insulin stimulation and after about 30 min the rate had returned to the basal transport rate. The addition of okadaic acid, however, prevented transport returning to the basal rate. Instead after 30 min the rate had dropped to 50 % of the insulin stimulated rate. This is slightly higher than the 40 % of the insulin stimulated rate for 0.5 μM okadaic acid alone for 20 min in figure 3.8. This difference could be the result of the much longer incubation time. The half-time for the reversal in the presence or absence of okadaic acid appeared to be about 10 min.

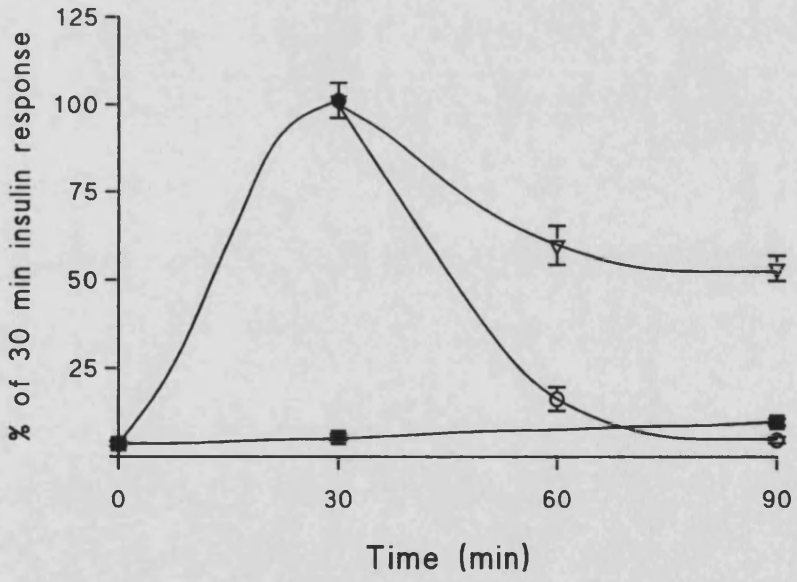

Figure 3.10. The effect of 0.5 μM okadaic acid on the reversal of insulin stimulation of rat adipocytes

Rat adipocytes were prepared and transport assayed as described in sections 2.3 and 3.4. Cells were left unstimulated (■), or stimulated acutely with 10 nM insulin (●). After 30 min the insulin stimulation was reversed by treating the insulin stimulated adipocytes with 0.25 mg/ml collagenase alone (○) or with 0.25 μM/ml collagenase and 0.5 μM okadaic acid (▽).

Values are the means of five experiments carried out in triplicate. Errors are the S.E.M.

Okadaic acid had a similar effect in 3T3-L1 adipocytes as it had in rat adipocytes. Figure 3.11 shows the effect of different concentrations of okadaic acid on basal and insulin stimulated transport rates. As in rat adipocytes, treating 3T3-L1 adipocytes with 0.5 or 1.0 μM okadaic acid increased in transport rate which appeared to plateau at ≈ 38 % of the insulin stimulated rate. There was no significant difference between the level of stimulation with 0.5 or 1.0 μM okadaic acid. With 0.05 μM okadaic acid the transport rate was higher than the basal rate but it was not significantly higher.

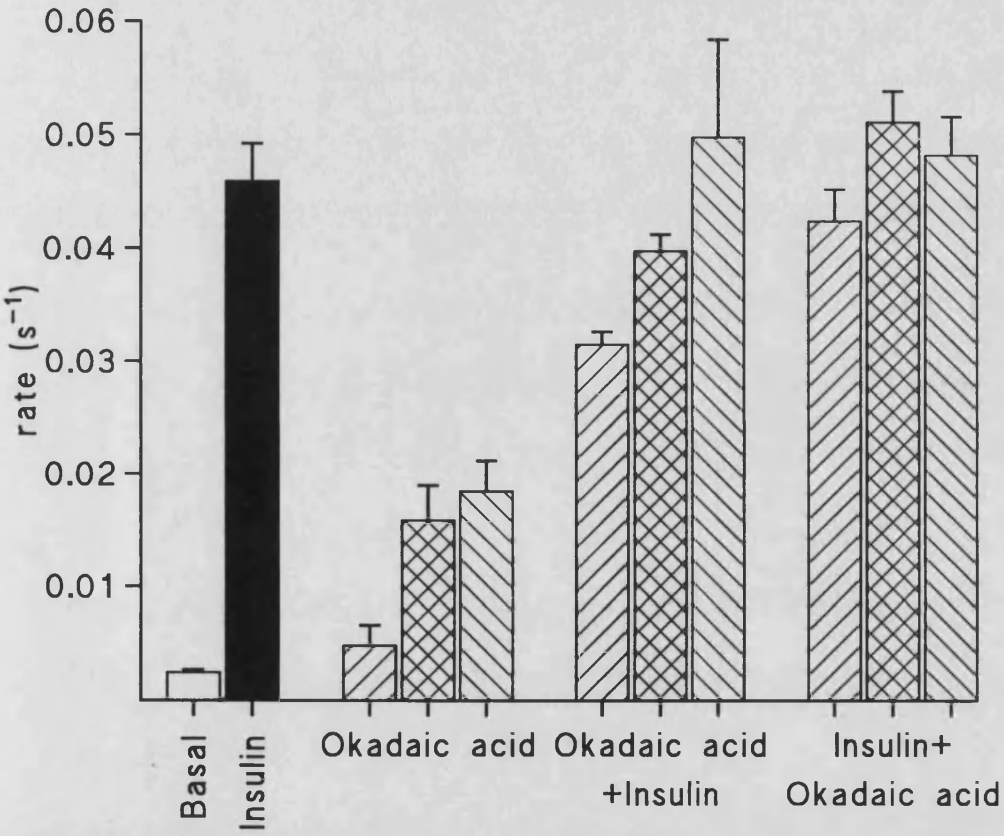

Figure 3.11. The effect of okadaic acid on the stimulation of transport in 3T3-L1 adipocytes

3T3-L1 adipocytes in 35 mm dishes were untreated, basal, (□), acutely stimulated with 100 nM insulin, (■) or stimulated with okadaic acid at 0.05 μM (▨), 0.5 μM (▩) or 1.0 μM (▧). Cells stimulated with okadaic acid were either stimulated with okadaic acid alone for 30 min (OA), stimulated with okadaic acid for 15 min and okadaic acid plus insulin for a further 15 min (OA+I) or stimulated with insulin for 15 min and then okadaic acid plus insulin for a further 15 min (I+OA). The preparation of cells and assaying of transport in 3T3-L1 adipocytes are described in sections 2.3.3 and 2.4.2.1.

Values are the means of one (0.05 and 1.0 μM) or two (rest) triplicate experiments. Errors are S.E.M.

The effect of okadaic acid on the insulin stimulated transport rate is also shown in figure 3.11. Either insulin was added to okadaic acid treated 3T3-L1 adipocytes or okadaic acid was added to insulin treated cells. Under these conditions okadaic acid had no significant effect on the insulin stimulated transport rate except when insulin was added to adipocytes previously stimulated with 0.05 μM okadaic acid. Since 0.05 μM alone caused only a small increase in transport this lower rate might be due to incomplete insulin stimulation after 15 min rather than inhibition by okadaic acid.

The effect of 5.0 μM okadaic acid on the level of transporters in the plasma membrane of 3T3-L1 adipocytes is shown in figure 3.12. Okadaic acid caused a 3.9-fold rise in GLUT4 and a 1.9-fold rise in GLUT1. Unlike its effect in rat adipocytes okadaic acid only depressed the insulin stimulated increase in cell surface transporters by a small amount. This agrees with figure 3.11 where okadaic acid had very little effect on the insulin stimulated transport rate. In 3T3-L1 adipocytes 5.0 μM okadaic acid increased the basal level of cell surface GLUT1 but okadaic acid reduced it in rat adipocytes.

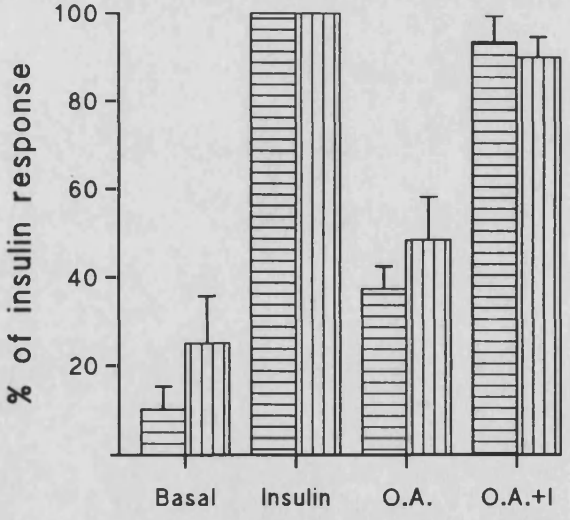

Figure 3.12. The effect of 5.0 μM okadaic acid on the levels of GLUT4 and GLUT1 at the plasma membrane of 3T3-L1 adipocytes

3T3-L1 adipocytes in 35 mm dishes were either untreated, basal, or treated for 20 min with 100 nM insulin, 5.0 μM okadaic acid (O.A.), or 5.0 μM okadaic acid plus 100 nM insulin (O.A.+I). They were photolabelled with 150 μCi of ATB-BMPA per dish and processed as described in section 2.0. GLUT4 (▤) and GLUT1 (▥) are expressed relative to the peak area of insulin for that isoform.

Values are the means of two experiments. Errors are the $SD_{(n-1)}$.

The effect of okadaic acid on the reversal of insulin stimulated transport in 3T3-L1 adipocytes is shown in figure 3.13a. Again the addition of 1.0 μM okadaic acid to fully insulin stimulated adipocytes caused only a slight depression in the insulin stimulated transport rate to 96 % of the rate at 30 min and 84 % of the 60 min insulin treatment rate. When okadaic acid was added with KRM to insulin stimulated cells the rate after 30 min was about 5-fold higher than the rate following reversal in the absence of okadaic acid and about 2.5-fold higher than the rate with okadaic acid alone.

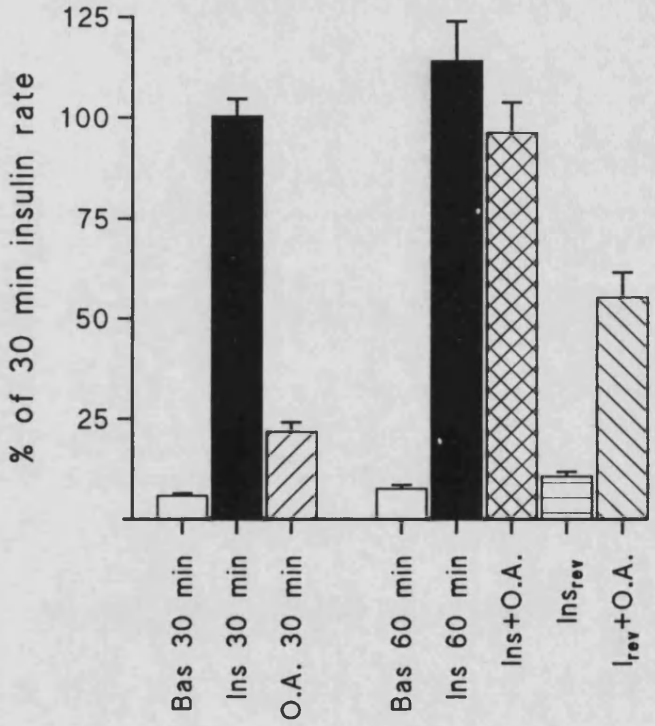

Figure 3.13a. The reversal of transport in 3T3-L1 adipocytes in the presence of 1.0 μM okadaic acid

The preparation of 3T3-L1 adipocytes in 35 mm dishes and the 3-*O*-methyl-D-glucose uptake assay is described in section 2.0. Basal cells (□) were untreated for either 30 min or 60 min before assaying transport. Cells treated with 1.0 μM okadaic acid (▨) were stimulated for 30 min before assaying transport. All other dishes of 3T3-L1 adipocytes were stimulated with 100 nM insulin for 30 min. Dishes treated with insulin alone (■) were stimulated for either 30 min or 60 min. Dishes treated with both 1.0 μM okadaic acid and 100 nM insulin (▩) were first stimulated with insulin for 30 min and then treated with both insulin and okadaic acid for a further 30 min. Insulin stimulation was reversed (▤) by incubating the cells with KRM (pH 6.0) for 30 min. Insulin stimulation was also reversed with KRM in the presence of 1.0 μM okadaic acid (▧).

Values are the means of three (n=9) or two (n=6) experiments for basal 60 min. Errors are the S.E.M.

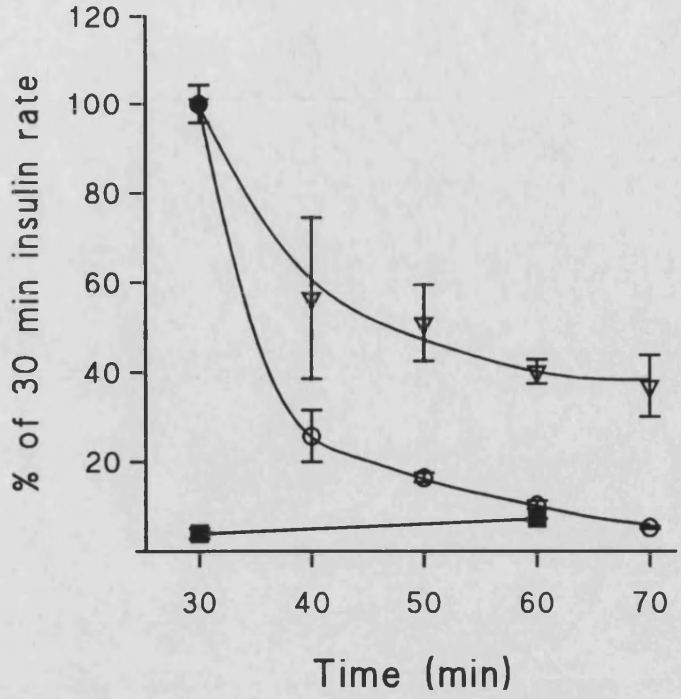

Figure 3.13b. A time course for the reversal of insulin stimulated transport in 3T3-L1 adipocytes in the presence of 1.0 μM okadaic acid

3T3-L1 adipocytes in 35 mm dishes were left untreated, basal, (■) for either 30 min or 60 min before assaying 3-*O*-methyl-D-glucose uptake. All other dishes were stimulated with 100 nM insulin for 30 min when the transport was assayed (●). The insulin stimulated increase in transport was reversed by incubating the cells in KRM at pH 6.0 (○). Insulin stimulation was also reversed with KRM in the presence of 1.0 μM okadaic acid (▽). The preparation of the 3T3-L1 adipocytes, the reversal of insulin stimulation and the assaying of 3-*O*-methyl-D-glucose uptake are described in section 2.0.

Each point is the mean of the duplicate from a single experiment. Errors are the $SD_{(n-1)}$.

In order to see if okadaic acid affected the rate of change in the transport rate following the reversal of insulin stimulation a time course with more time points was undertaken. The time course for the reversal of insulin stimulated transport in the presence or absence of okadaic acid is shown in figure 3.13b. Okadaic acid altered the half-time for the change to a new transport rate. The $t_{½}$ for the decrease in the transport rate in the absence of okadaic acid was ≈ 4.4 min. When the insulin stimulation was reversed in the presence of okadaic acid the $t_{½}$ was ≈ 6.6 min. The half-times were calculated using the equation $t_{1/2} = \ln 2/(K_{ex} + K_{en})$ where K_{ex} and K_{en} were calculated from % at surface = $(K_{ex} + K_{en}\exp(-t(K_{ex} + K_{en}))/(K_{ex} + K_{en})$.

The effect of okadaic acid on the recycling of GLUT4 was also investigated. 3T3-L1 adipocytes were stimulated with insulin for 30 min and then photolabelled. The insulin stimulation was then either maintained for a further 30 min with 100 nM insulin or was reversed with KRM in either the absence or presence of 1.0 μM okadaic acid. The photolabelled transporters were thus allowed to recycle between the cell surface and the intracellular pool under these three different conditions. The cells were then homogenised and subjected to subcellular fractionation. The photolabelled GLUT4 was immunoprecipitated from the purified plasma membrane fraction, run on SDS-PAGE and the transporter peak counted (section 2.6).

The levels of photolabelled GLUT4 in the purified plasma membrane after recycling were compared. There was about 10 % more GLUT4 at the surface of the cells treated with KRM and okadaic acid than in the cells treated with insulin. In the 3T3-L1 adipocytes treated with KRM alone there was approximately 25 % less GLUT4 at the cell surface compared with the level in the presence of insulin. Thus okadaic acid appears to reduce the rate of endocytosis and so increase the level of GLUT4 remaining at the cell surface. The result of this experiment should, however, be treated with caution as the level of GLUT4 in the plasma membrane of the cells treated with KRM alone was higher than expected. This could be due to incomplete reversal, perhaps following cell damage during the UV irradiation. Alternatively it could be the result of contamination of the plasma membrane fraction by photolabelled transporters from the low density microsomes. However, the experiment does show a higher level of GLUT4 in the plasma membrane of photolabelled cells treated with both okadaic acid and KRM compared with the cells treated with either insulin or KRM alone.

3.3 The effect of tyrosine kinase inhibitors on transporters in adipocytes

A set of 10 tyrosine kinase inhibitors (TKI) were provided by Wellcome. The structure and IC_{50} of the inhibitors for the epidermal growth factor receptor tyrosine kinase are given in table 3.2. A starting concentration of 0.68 μM was initially used to test the effect of the inhibitors on the insulin stimulation of glucose transport. This concentration was chosen by doubling the average IC_{50} of all 10 inhibitors for the EGFRK. The rat adipocytes were incubated with each TKI for 30 min before stimulating the cells with insulin plus the TKI for a further 30 min. This was also repeated at the higher concentration of 500 μM. The results are shown in figure 3.14.

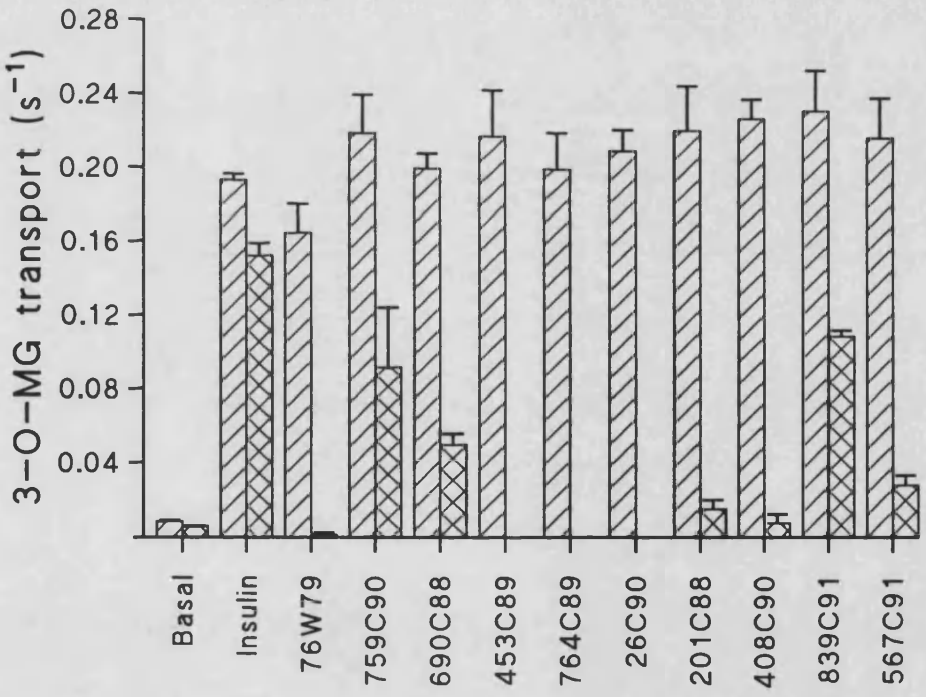

Figure 3.14. The effect of 0.68 μM and 500 μM tyrosine kinase inhibitors on the insulin stimulated rate of 3-O-methyl-D-glucose uptake

Rat adipocytes were prepared and transport assayed as described in sections 2.3.1 and 2.4.1. Cells were incubated with the indicated tyrosine kinase inhibitor (TKI) at either 0.68 μM (▨) or 500 μM (▩) for 30 min before stimulating with 10 nM insulin in the presence of the TKI for a further 30 min. All TKI were tested at both concentrations. At 0.5 mM 453C89, 764C89 and 26C90 the TKI inhibited transport rate was less than the basal rate. Results marked basal and insulin were not treated with TKI.

Values are the means of a single experiment carried out in triplicate. Errors are the S.E.M.

Wellcome Number	Chemical Name (Generic name)	Structure	IC_{50} EGFRK	Reference
76W79	4',5,7-trihydroxy-isoflavone (Genistein)	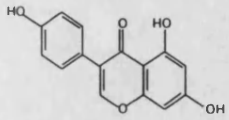	22.0 μM	Akiyama et *al.*, (1987)
759C90	Methyl 2,5-dihydroxy-cinnamate	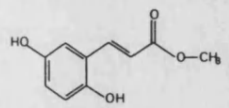	0.77 μM	Umezawa et *al.*, (1990)
690C88	α-cyano-4-hydroxy-3,5-diisopropyl-cinnamide (ST 271)	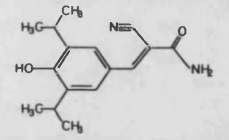	1.1 μM	Shiraishi et *al.*, (1989)
453C89	α-cyano-3,4-dihydroxythio-cinnamide (RG 50864)	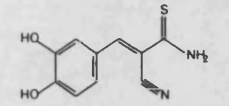	0.85 μM	Yaish et *al.*, (1988)
764C89	α-cyano-3-ethoxy-4-hydroxy-5-phenylthiomethyl-cinnamide (ST 638)	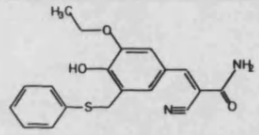	1.0 μM	Shiraishi et *al.*, (1989)
26C90	2-(3,4,5-trihydr-oxybenzylidene) malononitrile	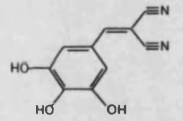	1.0 μM	Gazit et *al.*, (1989)
201C88	N-[2-(2,5-dihydroxyphenyl) ethenyl]formamide (Erbststin)	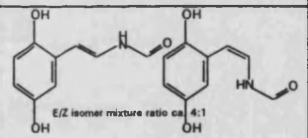	3.3 μM	Isshiki et *al.*, (1987)
408C90	2-amino-4-(4-hydroxyphenyl)-1,3-butadiene-1,13-tricarbonitrile	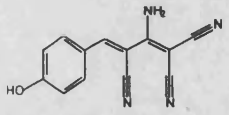	125 nM	Gazit et *al.*, (1989)
839C90	5-(2,5-dihydroxy-benzylamino)-2-hydroxybenzoic acid hemihydrate	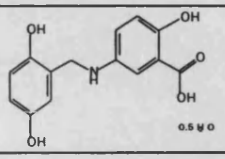	43.0 nM	Onoda et *al.*, (1989)
567C91	RG13022	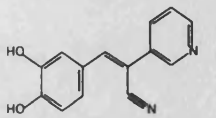	4.0 μM	Yoneda et *al.*, (1991)

Table 3.2 The structure of the tyrosine kinase inhibitors and their potency as epidermal growth factor tyrosine kinase (EGFRK) inhibitors

Figure 3.14 shows that that at the lower concentration of 0.68 μM the inhibitors had no significant effect on the insulin stimulated transport rate. At 500 μM all the inhibitors inhibited transport to some extent with several lowering the transport rate below the basal rate. As a result of these experiments inhibitor 453C89, α-cyano-3,4-dihydroxythiocinnamide was chosen for further experiments.

A more detailed study was carried out with 453C89 to determine the effect of different concentrations of the inhibitor on insulin stimulated transport as shown in figure 3.15. As seen in the previous figure the lowest concentration of 50 μM caused a slight but not significant rise in the rate of transport while increasing concentrations progressively increased the degree of inhibition until at the highest concentration, 500 μM, the transport rate was less than the basal transport rate.

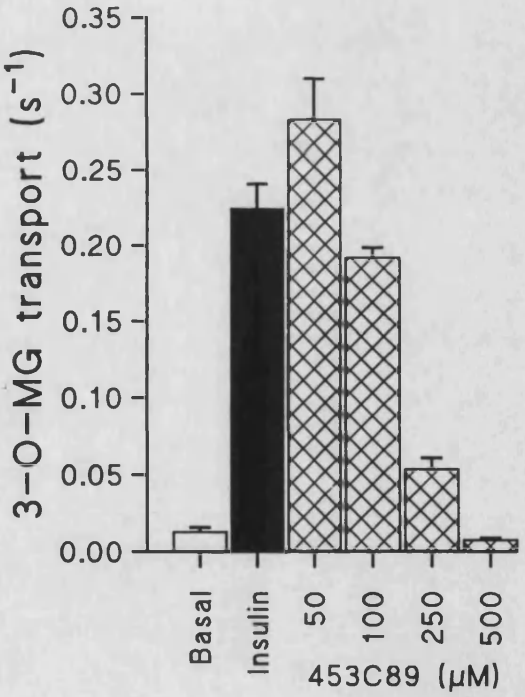

Figure 3.15. The effect of the tyrosine kinase inhibitor 453C89 on insulin stimulated 3-*O*-methyl-D-glucose uptake in rat adipocytes

Rat adipocytes were prepared and 3-*O*-methyl-D-glucose transport assayed as described in sections 2.3.1 and 2.4.1. Cells were incubated for 30 min with the indicated concentration of the tyrosine kinase inhibitor 453C89 (⊠) before stimulating them with 10 nM insulin for a further 30 min in the presence of 453C89. Basal (□) and insulin treated cells (■) were not incubated with TKI 453C89.

Data are the means of a single experiment carried out in triplicate. Errors are the S.E.M.

In the previous experiments the inhibitor was added to the adipocytes before they were stimulated with insulin. Figure 3.16 shows the effect of treating insulin stimulated rat adipocytes with 500 μM 453C89 for up to 30 min before assaying 3-*O*-methyl-D-glucose uptake. The data shows that a long incubation period was not required to completely inhibit transport. Inhibition by 500 μM 453C89 occurred within one minute. Such a rapid drop in the transport rate is unlikely to be due an effect on translocation but the inhibitor could be competing with 3-*O*-methyl-D-glucose at its binding site or it could be causing a decrease in the activity of the transporter.

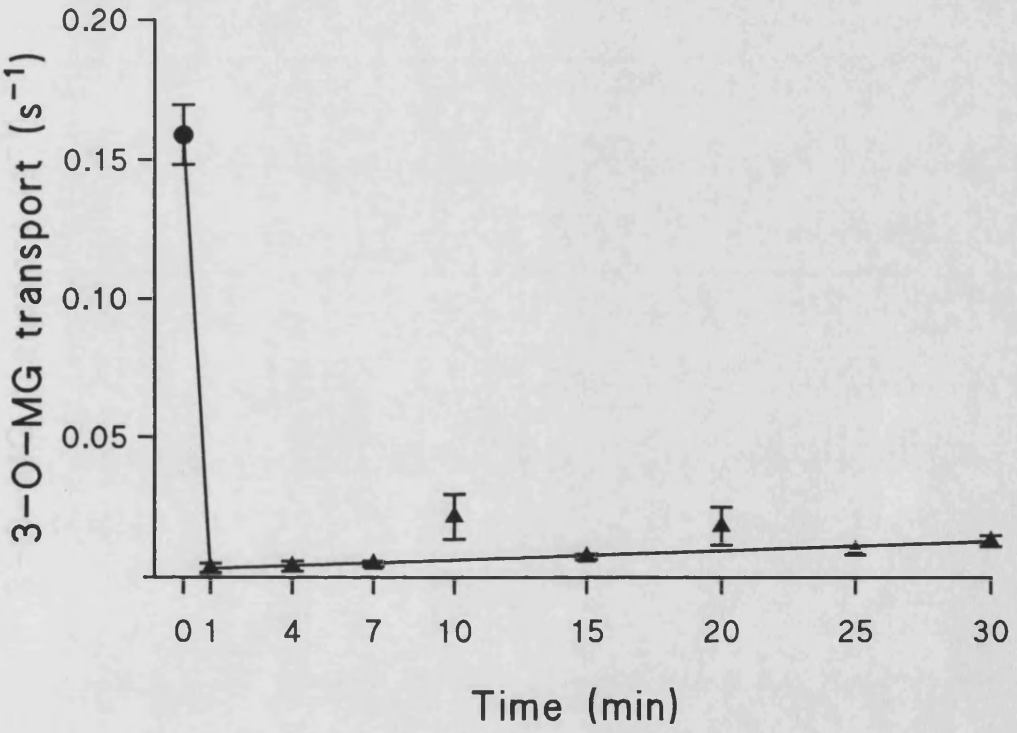

Figure 3.16. The inhibitory effect of 500 μM tyrosine kinase inhibitor 453C89 on insulin stimulated 3-*O*-methyl-D-glucose uptake

Rat adipocytes were prepared and 3-*O*-methyl-D-glucose transport assayed as described in sections 2.3.1 and 2.4.1. Cells were stimulated with 10 nM insulin for 40 min. After assaying the insulin stimulated transport rate at 0 min (●) tyrosine kinase inhibitor 453C89 was added at a final concentration of 500 μM and transport was assayed at the indicated times (▲).

Values are the means of triplicates from two independent experiments. Errors are the S.E.M.

The effect of the tyrosine kinase inhibitor 453C89 on insulin stimulated glucose transport in 3T3-L1 adipocytes was also investigated. Figure 3.17 shows a concentration curve for the inhibition of insulin stimulated transport following a 30 min incubation with 453C89. As in rat adipocytes the lowest concentration, 5 μM, appeared to further increase the insulin stimulated rise in transport. The insulin stimulated transport rate in the presence of 500 μM 453C89 was a little higher than the basal transport rate. The degree of inhibition by 500 μM 453C89 in 3T3-L1 adipocytes was less than it was in rat adipocytes where the TKI inhibited insulin stimulated rate was less than the basal transport rate.

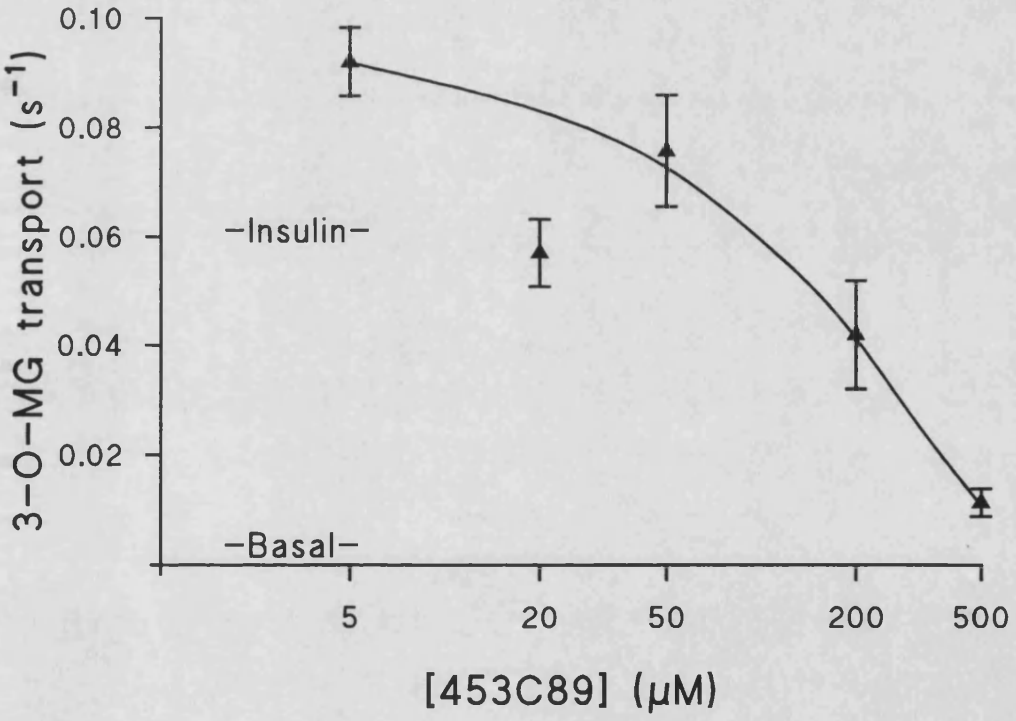

Figure 3.17. The effect of the tyrosine kinase inhibitor 453C89 on insulin stimulated 3-*O*-methyl-D-glucose uptake in 3T3-L1 adipocytes

3T3-L1 adipocytes were prepared and transport was assayed as described in sections 2.3.3 and 2.4.2.1. Cells were incubated with the tyrosine kinase inhibitor 453C89 for 30 min. They were then treated with 100 mM insulin and 453C89 for a further 30 min before assaying 3-O-methyl-D-glucose uptake. The mean basal and insulin stimulated transport rates are also shown.

Values are the means of triplicates from a single experiment. Errors are the S.E.M.

The results shown in figure 3.18 support the idea that at high concentrations 453C89 inhibits transport rather than having a rapid effect on translocation. When 500 μM 453C89 was added to the insulin stimulated 3T3-L1 adipocytes in the sugar cocktail used to assay 3-*O*-methyl-D-glucose transport then the insulin stimulated transport rate was halved although the rate was still double that for adipocytes incubated with the inhibitor before the transport assay. 500 μM 453C89 was also added to adipocytes at 18 °C one minute before the 3-*O*-methyl-D-glucose transport assay, sufficient time to inhibit transport in figure 3.16. 453C89 still inhibited insulin stimulated transport at 18 °C. This suggests that the inhibitor was not inducing a rapid endocytosis of cell surface transporters as the internalisation of cell surface glucose transporters in rat adipocytes is temperature sensitive and is inhibited by 18 °C (Clark *et al.*, 1991).

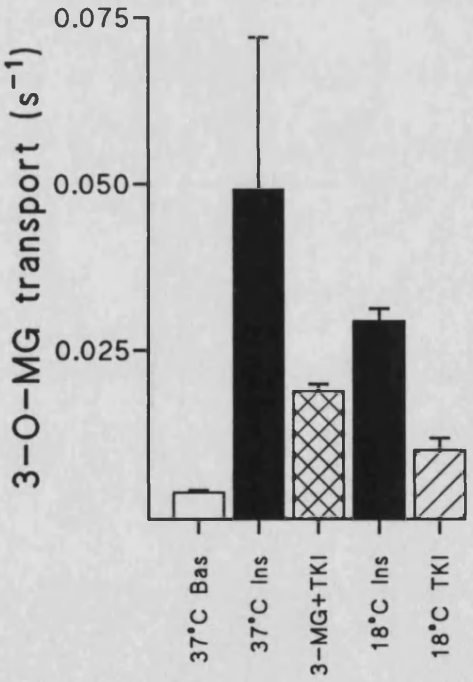

Figure 3.18. The effect of 500 μM tyrosine kinase inhibitor, 453C89 on insulin stimulated 3-*O*-methyl-D-glucose uptake in 3T3-L1 adipocytes

The preparation of 3T3-L1 adipocytes and assaying of 3-*O*-methyl-D-glucose are described in sections 2.3.3 and 2.4.2.1. Basal cells (□) were untreated for 30 min (n=5). Insulin stimulated cells were treated with 100 nM for 30 min before assaying transport at either 37 °C (n=5) or 18 °C (n=6) (■). 0.5 mM TKI 453C89 was added to insulin stimulated cells with the labelled 3-*O*-methyl-D-glucose (▩) (n=6) or was added to insulin stimulated cells at 18 °C 1 min before transport was assayed (▨) (n=3).

Values are the means of triplicates or duplicates from one or two experiments. Errors are the S.E.M.

Figure 3.19 shows the result of treating 3T3-L1 adipocytes with 5 μM 453C89. This was done to try to inhibit the tyrosine kinases with a low concentration of 453C89 for an extended length of time rather than a high concentration for a short time. 3T3-L1 adipocytes were treated with 5 μM 453C89 for between 1 to 50 hours with the inhibitor added to the cell culture medium as required. Although following treatment with the inhibitor there was a small drop in the transport rate it did not continue to decrease during the course of the experiment and the mean of all the values always lay within the S.E.M. of the individual points Thus prolonged incubation with 5 μM 453C89 had no significant effect on the rate of 3-*O*-methyl-D-glucose transport.

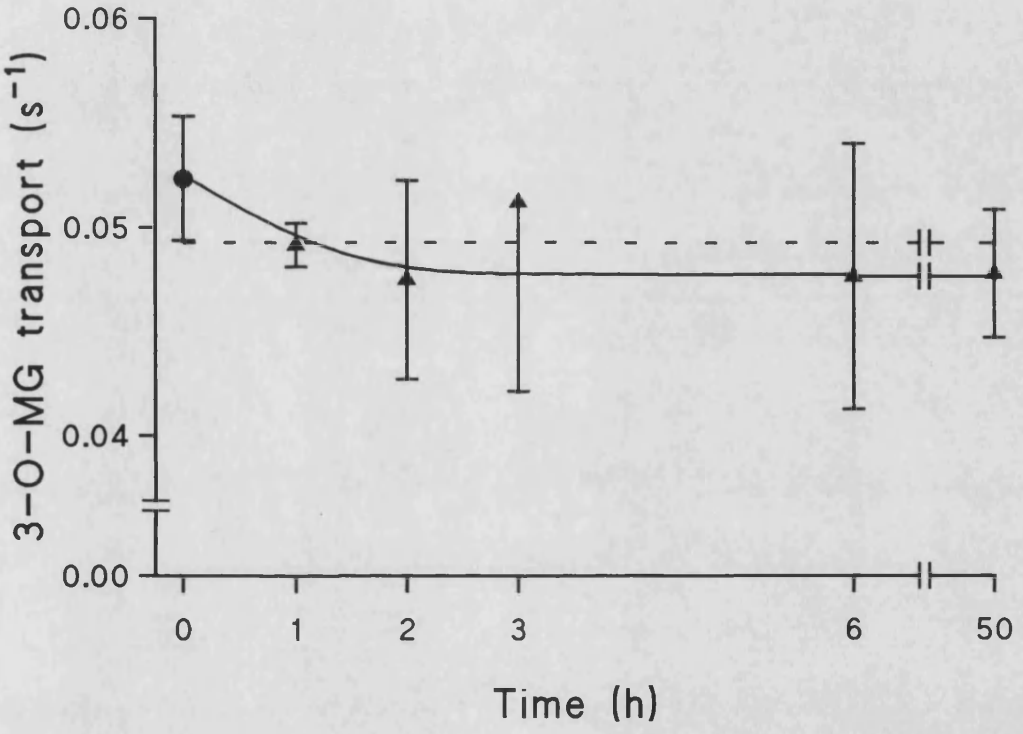

Figure 3.19. The effect of prolonged incubation with 5.0 μM tyrosine kinase inhibitor 453C89 on insulin stimulated 3-*O*-methyl-D-glucose uptake in 3T3-L1 adipocytes

The preparation of 3T3-L1 adipocytes and assaying of 3-*O*-methyl-D-glucose are described in sections 2.3.3 and 2.4.2.1. The 3T3-L1 adipocytes were treated with 5 μM 453C89 for the required time before treating then with 100 nM insulin and 453C89 for 30 min and then assaying 3-*O*-methyl-D-glucose uptake (▲). For the longer incubation times 453C89 was first added to the DMEM-FCS medium. The dashed line is the mean of all the values. At 0 h cells were only treated with insulin (●).

Values are the means of triplicates from a single experiment. Errors are the S.E.M.

3.4 The targeting of transfected GLUT4 in fibroblasts

The plasmid pRC-CMV-hGLUT4 was provided by Dr Mitsuru Hashiramoto and Dr Yoshikazu Tamori, (Kobe University, Japan). The human GLUT4 cDNA was originally provided by Dr G. I. Bell. The GLUT4 cDNA was approximately 1900 bp long of which 1530 bp were coding region. It was spliced into the plasmid at the HindIII and XbaI sites. The plasmid map is shown in figure 2.2.

A large quantity of plasmid DNA was prepared using the maxi-prep method described in section 2.7.1. To confirm that the correct plasmid had been purified it was restriction digest mapped using HindIII and XbaI (section 2.7.3) which cut at the sites used to splice the cDNA into the plasmid. The restriction digest map is shown in figure 3.20. Two bands were obtained, one ≈ 5000 kb and one ≈ 1900 kb as expected.

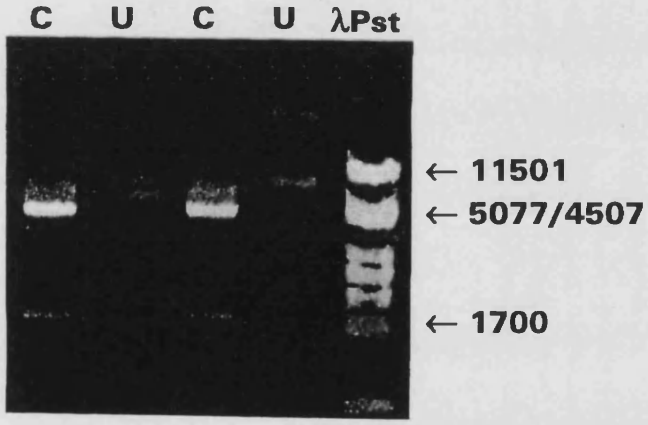

Figure 3.20. The restriction mapping of pRC-CMV-hGLUT4

0.2 µg of plasmid DNA was digested with both HindIII and XbaI in one Phor all buffer at 37 °C for 1 h. This was loaded onto an agarose gel (C) next to uncut plasmid (U) with λ Pst as a size marker. After electrophoresis the gel was viewed under UV light and photographed with Polaroid film, section 2.7.3.

The plasmid was first expressed in 3T3-L1 fibroblasts following transfection by the calcium phosphate method, section 2.7.4. When Western blots of the solubilized whole cells were immunoblotted with the anti-GLUT4 antiserum then only a weak band was detected in cells transfected with pRC-CMV-hGLUT4, figure 3.21. As the level of GLUT4 expression in 3T3-L1 fibroblasts was low the plasmid was transfected into COS-7 fibroblasts, figure 3.22.

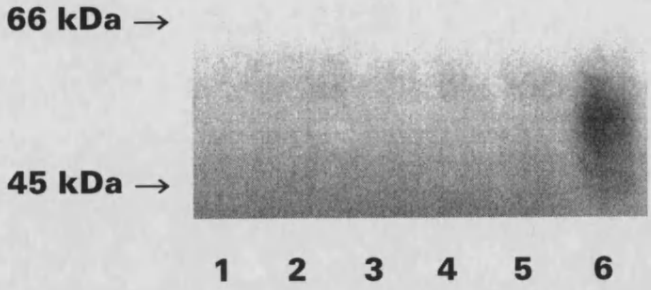

Figure 3.21. The immunoblotting of GLUT4 in 3T3-L1 fibroblasts transfected with pRC-CMV-hGLUT4

3T3-L1 fibroblasts were transfected with pRC-CMV-hGLUT4 by the calcium phosphate method, section 2.7.4. The fibroblasts were scraped from the dishes in 150 µl SDS-PAGE sample buffer and a third of a dish, 50 µl of solubilized cells, per lane was loaded onto a thin 10 % SDS-PAGE gel. The nitrocellulose was probed with 1:100 anti-GLUT4 antiserum and 0.1 µCi/ml ^{125}I-protein A, section 2.6.

Lane 1: nontransfected 3T3-L1 fibroblasts, lane 2: 3T3-L1 fibroblasts incubated with calcium phosphate in the absence of plasmid, lane 3: fibroblasts transfected with maxi prep pRC-CMV-hGLUT4, lanes 4 and 5: fibroblasts transfected with original pRC-CMV-hGLUT4, lane 6: 3T3-L1 adipocytes.

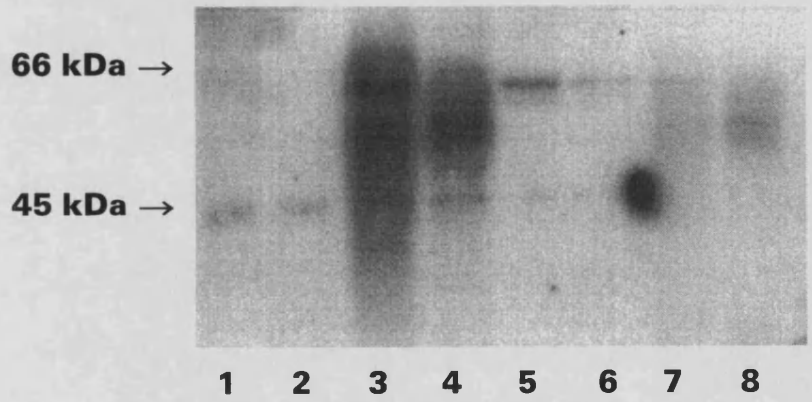

Figure 3.22. The immunoblotting of GLUT4 in COS-7 fibroblasts transfected with pRC-CMV-hGLUT4

COS-7 fibroblasts in 90 mm dishes were transfected with pRC-CMV-hGLUT4 using the DEAE-dextran method of section 2.7.5. The plasma membrane and low density microsomal fractions were purified as described in section 2.6.1. Approximately 20 µg protein was loaded per lane of a 10% thin gel. The nitrocellulose was probed with 1:200 anti-GLUT4 antiserum and 0.1 µCi/ml ^{125}I protein A, section 2.6.

Lanes 1 to 4 contain purified plasma membrane while lanes 5 to 8 contain low density microsomes. Lanes 1 and 5 are from nontransfected COS-7 fibroblasts. Lanes 2 and 6 are from COS-7 fibroblasts incubated with DEAE-dextran in the absence of plasmid. Lanes 3 and 7 are from COS-7 fibroblasts transfected with pRC-CMV-hGLUT4. Lanes 4 and 8 are from 3T3-L1 adipocytes.

Higher levels of GLUT4 were expressed when pRC-CMV-hGLUT4 was transfected into COS-7 fibroblasts using the DEAE-dextran method, section 2.7.5. Figure 3.22 shows the result of immunoblotting the plasma membrane and low density microsomal fractions from transfected and nontransfected COS-7 fibroblasts and 3T3-L1 adipocytes. GLUT4 was only detected in COS-7 fibroblasts transfected with pRC-CMV-hGLUT4 (lanes 3 and 7) where it was detected in both the plasma membrane and the low density microsomes. These bands, when compared with those of the 3T3-L1 adipocytes (lanes 4 and 8), were much broader and less dense. Volume densitometry measurements of the plasma membrane and low density microsome bands indicated a 9.8-fold higher level of GLUT4 in the plasma membrane in the COS-7 cells and 6.8-fold higher in the 3T3-L1 adipocytes.

Since ATB-BMPA was to be used to calculate what proportion of the GLUT4 expressed in COS-7 fibroblasts was at the cell surface it was necessary to characterise COS-7 fibroblast photolabelling. Figure 3.23 shows the gel profile of immunoprecipitated photolabelled GLUT1 and GLUT4 in both transfected and nontransfected COS-7 cells (solid symbols). To confirm that the immunoprecipitated peak was photolabelled transporter the cells were also photolabelled in the presence of 200 mM glucose to displace ATB-BMPA and prevent it labelling the transporter (open symbols). The GLUT4 glucose displaceable transporter peak was only seen in the COS-7 fibroblasts transfected with pRC-CMV-hGLUT4. A GLUT1 glucose displaceable peak was seen in both the transfected and nontransfected fibroblasts.

The subcellular distribution of GLUT4 expressed in COS-7 fibroblasts transfected with pRC-CMV-hGLUT4 was calculated by photolabelling the transporters in the presence or absence of 2.5 μg/ml digitonin. Digitonin permeabilizes the cells enabling the total transporter pool, both surface and intracellular, to be labelled (Yang *et al.*, 1992b). The proportion of the total transporter pool at the cell surface was calculated by comparing the labelling level in the presence and absence of digitonin. Figure 3.24 shows the result of three experiments.

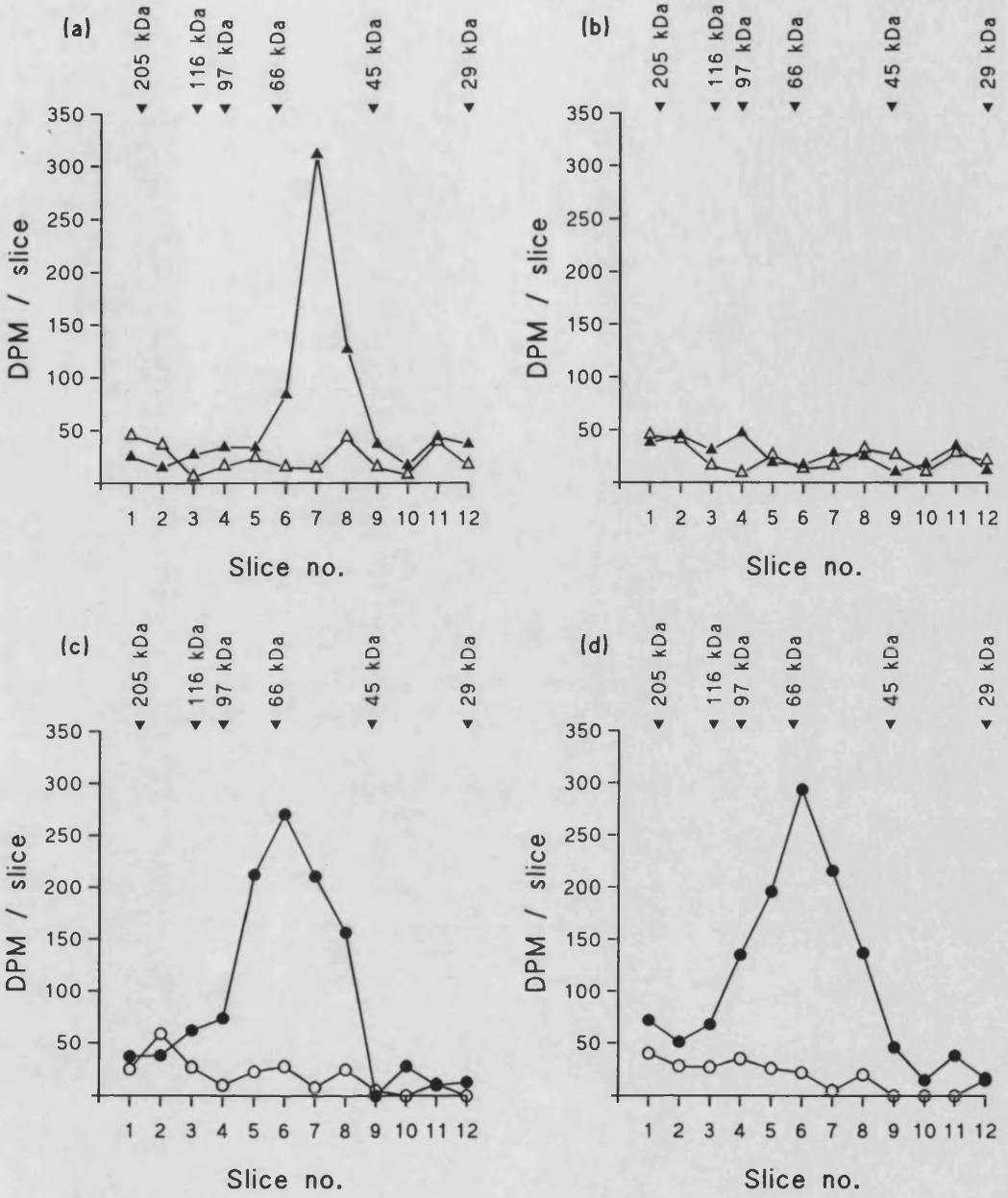

Figure 3.23. The photolabelling of COS-7 fibroblasts transfected with pRC-CMV-hGLUT4 in the presence and absence of glucose

COS-7 fibroblasts in 35 mm dishes were transfected with pRC-CMV-hGLUT4 using the DEAE-dextran method, section 2.7.5. Two dishes per condition were photolabelled with 100 µCi per dish in the presence (Δ,O) or absence (▲,●) of 200 mM glucose. Solubilized fibroblasts were immunoprecipitated with GLUT4 (▲,Δ) and GLUT1 (●,O) antiserum, subjected to SDS-PAGE and the slices counted as described in section 2.6.

Figures 3.23a and c are from pRC-CMV-hGLUT4 transfected COS-7 fibroblasts while b and d are from untransfected fibroblasts.

Figure 3.24 shows that the proportion of GLUT1 at the cell surface is similar in both nontransfected and pRC-CMV-hGLUT4 transfected COS-7 fibroblasts, 56 % in the nontransfected and 62.5 % in the transfected cells. The proportion of GLUT4 at the surface of the transfected COS-7 cells was ≈ 140 %. Such a percentage is not possible.

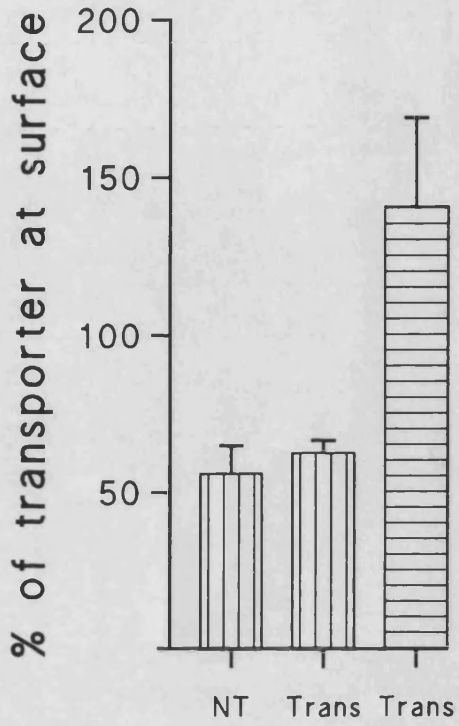

Figure 3.24. The percentage of total photolabelled transporter at the cell surface of COS-7 fibroblasts transfected with pRC-CMV-hGLUT4

COS-7 fibroblasts in 35 mm dishes were transfected with pRC-CMV-hGLUT4 using the DEAE-dextran method, section 2.7.5. Two dishes per condition were photolabelled with 100 µCi per dish in either the absence (surface) or presence (total) of 2.5 µg/ml digitonin. GLUT1 (▥) and GLUT4 (▤) were immunoprecipitated from solubilized cells and run on SDS-PAGE, section 2.6. The percentage of total transporters at the cell surface transporter was calculated by dividing the surface peak area by the total peak area. Percentages are given for GLUT1 in nontransfected fibroblasts (NT) and for GLUT1 and GLUT4 in COS-7 fibroblasts transfected with the pRC-CMV-hGLUT4 plasmid (Trans).
Values are the means of three experiments. Errors are the S.E.M.

As an alternative to transient transfection in COS-7 fibroblasts a CHO fibroblast line stably transfected with GLUT4, provided by Dr M. Hashiramoto (Kobe University, Japan), was used. As with the COS-7 cells the CHO cells were photolabelled in the presence and absence of glucose to confirm the suitability of ATB-BMPA, figure 3.25.

As expected a GLUT4 glucose displaceable peak was obtained in the GLUT4 transfected cell line (a) but not in the wild type cells (b). A GLUT1 glucose displaceable peak was detected in both GLUT4 transfected cell lines (c) and the wild type (d) but the peak was much larger in the wild type cells.

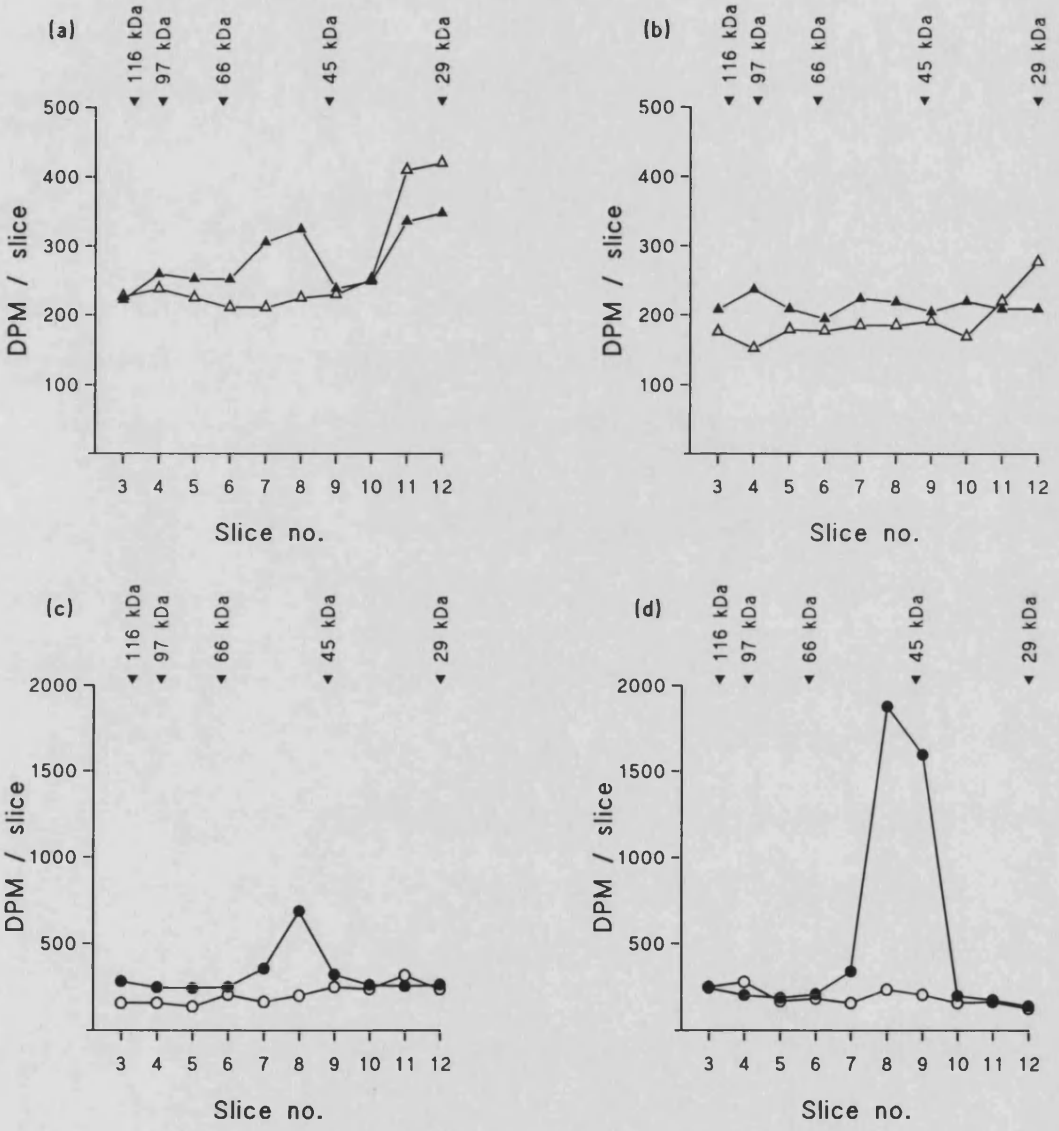

Figure 3.25. The photolabelling of CHO fibroblasts stably transfected with GLUT4 in the presence and absence of glucose

35 mm dishes were seeded with 0.05 x 10^6 CHO fibroblasts and allowed to reach confluence in 4 days. Two dishes per condition were photolabelled with 100 µCi per dish in the absence (▲,●) or presence (△,○) of 200 mM glucose. GLUT4 (▲,△) and GLUT1 (●,○) were immunoprecipitated from solubilized cells, run on SDS-PAGE and counted as described in section 2.6.

Figures 3.33a and c are from CHO fibroblasts stably transfected with GLUT4, b and d are from nontransfected CHO fibroblasts.

The proportion of GLUT1 and 4 at the surface of the CHO fibroblasts was determined by photolabelling in the presence or absence of digitonin as for the COS-7 cells. A protein assay found that the digitonin permeabilized cells had only 85 % of the protein of the untreated cells. Although the protein lost might be soluble protein in the light of the anomalous result in the COS-7 fibroblasts the transporter peaks were adjusted to account for this protein loss. Figure 3.26 shows that the proportion of GLUT1 at the cells surface was lower in the CHO fibroblasts than in the COS-7 cells. In the wild type CHO fibroblasts 38 % of the GLUT1 was at the cell surface while only 33 % was at the surface of the cells expressing GLUT4. There was also a difference in the absolute amounts of GLUT1 in the two cells lines. As figure 3.25 shows, there was over 4 times more GLUT1 in the nontransfected CHO cells than the cells expressing GLUT4. The percentage of GLUT4 at the cell surface of the transfected CHO fibroblasts was much higher than for GLUT1. About two thirds of the GLUT4 was at the cell surface.

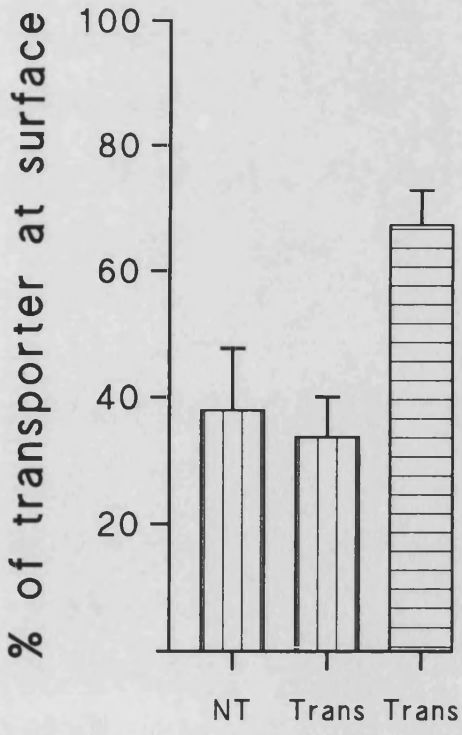

Figure 3.26. The percentage of total photolabelled transporter at the surface of CHO fibroblasts stably transfected with GLUT4

35 mm dishes were seeded with 0.05 x 10^6 CHO fibroblasts and allowed to reach confluence in 4 days. Two dishes per condition were photolabelled with 100 µCi per dish in either the absence (surface) or presence (total) of 2.5 µg/ml digitonin. GLUT1 (□) and GLUT4 (▤) were immunoprecipitated from solubilized cells, run on SDS-PAGE and counted as described in section 2.6. The percentage of the transporters at the cell surface was calculated by dividing the surface counts by the total counts. Percentages are for GLUT1 in wild type fibroblasts (NT) and for GLUT1 and GLUT4 in CHO fibroblasts stably transfected with GLUT4 (Trans). Values are the means of five experiments. Errors are the S.E.M.

3.5 Glucose transporter peptides and the targeting of GLUT4

Peptides corresponding to different regions of the glucose transporters were introduced into permeabilized 3T3-L1 adipocytes. To ensure that the cells were effectively permeabilized by a 5 min treatment with 0.8 IU/ml streptolysin-O (SLO) at 37 °C (Robinson *et al.*, 1992) 1 µg/ml propidium iodide was added with the SLO. The cells were then washed and photographed with either phase or fluorescence microscopy as shown in figure 3.27. Fluorescent nuclei were only seen where the cells were treated with SLO. Most of the SLO treated cells were fluorescent. Thus the concentration and incubation time was sufficient to permeabilize 3T3-L1 adipocytes.

In order to observe the effect of the peptides on the permeabilized cells it was necessary to develop a transport assay. The problem that had to be overcome was the leakage of labelled sugar from the cells during washing. Two different 2-deoxy-D-glucose assays were tested, figure 3.28. In intact 3T3-L1 adipocytes, following the addition of the labelled sugar to the dish, the medium was either (a) rapidly removed, the cells washed four times, dissolved and counted or (b) uptake was stopped with boiling water which lyses the cells and the cell lysate was passed through a DE81 filter which binds phosphorylated 2-deoxy-D-glucose. The filter was washed to remove non-phosphorylated, nontransported 2-deoxy-D-glucose and the filter counted. Both methods gave a similar level of insulin stimulation. Both methods were tested in SLO permeabilized 3T3-L1 adipocytes but with the following differences. In the non filter method (c) permeabilized cells were incubated with 2-deoxy-D-[2,4-^{3}H]glucose and [U-^{14}C]sucrose. This was rapidly removed and the cells washed once. The sucrose, which cannot be transported, was used to differentiate between specifically and non-specifically transported 2-deoxy-D-glucose while the single rapid wash prevented the loss of transported sugar. In permeabilized 3T3-L1 adipocytes the filter assay was ineffective (d) as the presence of cytochalasin B, which blocks transport, did not prevent 2-deoxy-D-glucose phosphorylation. Thus phosphorylation cannot be used to distinguish between specifically and non-specifically transported 2-deoxy-D-glucose.

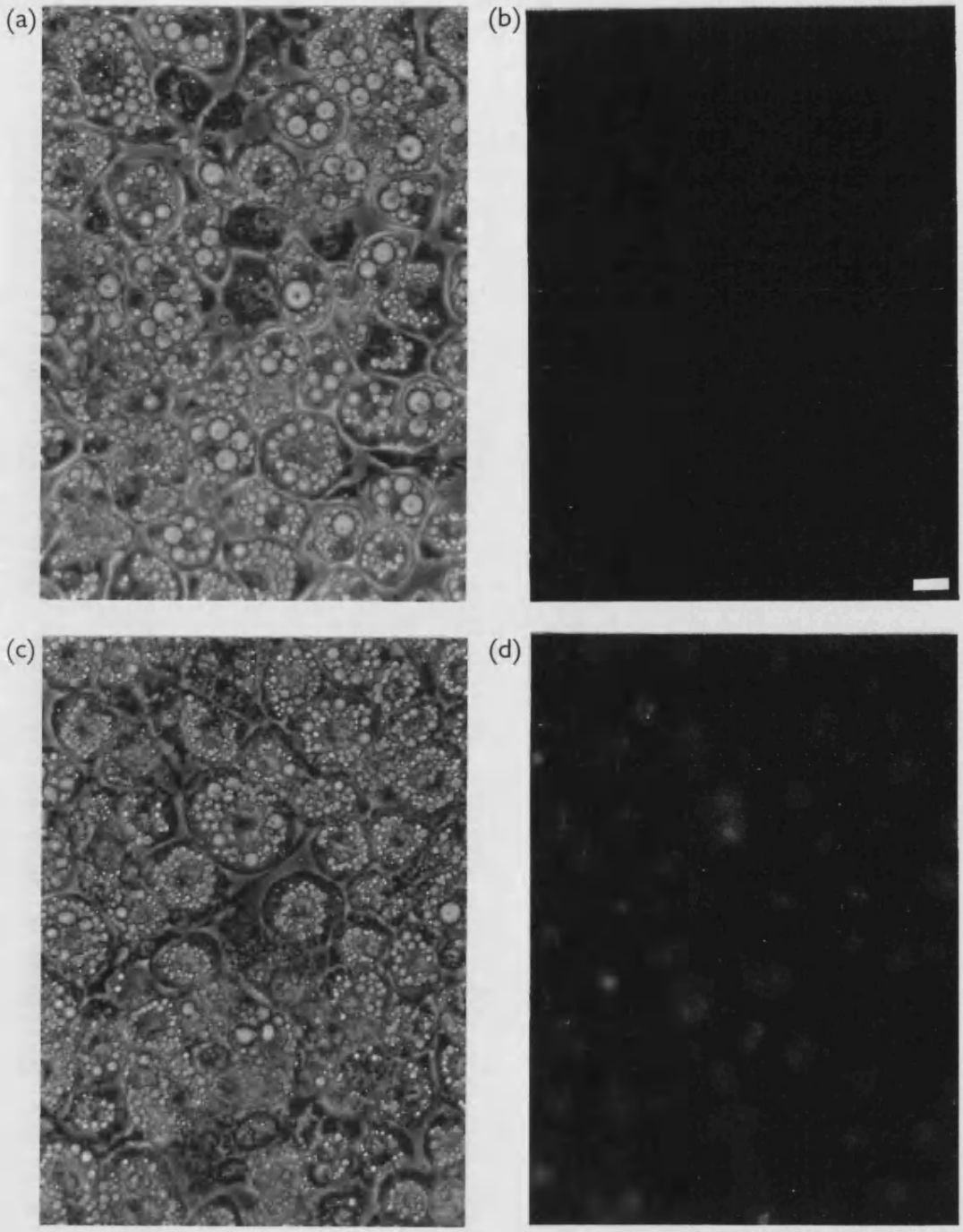

Figure 3.27. Testing the efficacy of streptolysin-O permeabilization of 3T3-L1 adipocytes with propidium iodide

The preparation of 3T3-L1 adipocytes is described in section 2.3.3. The cells were washed twice with IC buffer, pH 7.2, and incubated in IC buffer for 5 min at 37 °C with 1 μg/ml propidium iodide in the absence (a and b) or presence of 0.8 IU/ml streptolysin-O (c and d). The cells were then washed 3 times with PBS and observed and photographed at x400 magnification with a Nikon microscope with either phase (a and c) or fluorescence microscopy (b and d). Permeabilized 3T3-L1 adipocytes have red fluorescent nuclei. The bar represents 2.5 μm.

The transport assay method shown in figure 3.28 (c) gave an acceptable insulin stimulated increase in the transport rate of nearly 4-fold. Using sucrose to calculate the background was more successful than trying to reduce it with more washes as this reduced the insulin stimulation (results not shown).

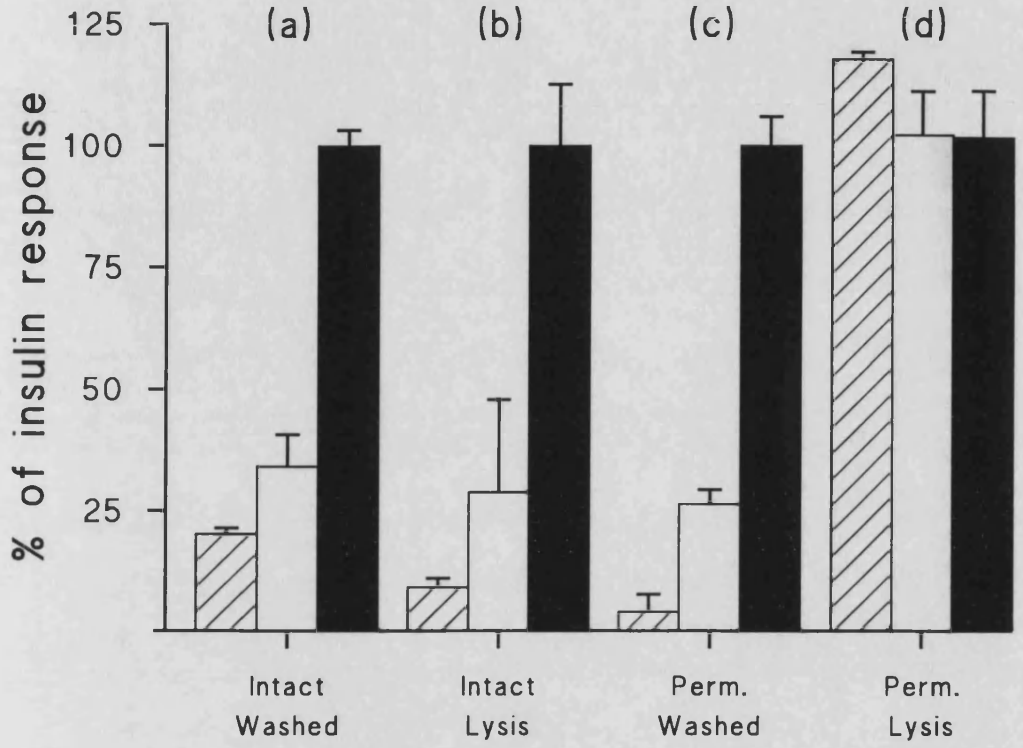

Figure 3.28. The development of a 2-deoxy-D-[2,4-^{3}H]glucose transport assay for use in streptolysin-*O* permeabilized 3T3-L1 adipocytes

3T3-L1 adipocytes in 35 mm dishes were prepared and permeabilized as required (section 2.3.3 and 6). Transport was assayed in untreated, basal, cells (□), in basal cells treated with 50 μM cytochalasin B five minutes before the assay (▨) or in cells stimulated with 100 nM insulin for 30 min (■).

In the washed transport assay (a) 50 μM, 0.12 μCi/dish, 2-deoxy-D-glucose was added for 5 min before 4 rapid washes with KRH (section 2.4.2.2). In the lysis transport assay (b and d) after 5 min with the labelled 2-deoxy-D-glucose uptake was stopped with 2 ml boiling double distilled water containing 200 μM sodium orthovanadate. The water and scraped cells were put through a DE81 filter which was washed 3 times with ice cold double distilled water and then counted (section 2.4.2.4). In the 2-deoxy-D-glucose uptake assay in permeabilized adipocytes both labelled and unlabelled 2-deoxy-D-glucose (^{3}H) and sucrose (^{14}C) were added at a ratio of 5:1. Following the 5 min incubation the cells were washed once with 3 ml IC buffer (section 2.4.2.3). The ^{3}H dpm were adjusted with the ^{14}C counts. With the exception of (c) the values shown are percentages of the insulin stimulated crude dpm counts.

Values are the means of single triplicate (a, c) or duplicate (b, d) experiments. Errors are $SD_{(n-1)}$.

To determine which regions of GLUT4 are involved in translocation several peptides corresponding to the terminal regions of GLUT4 and GLUT1 were added to permeabilized 3T3-L1 adipocytes. The GLUT2 loop peptide was used as a control. Figure 3.29 shows the effect of adding the peptides to basal adipocytes. The GLUT2 loop peptide caused a slight decrease in the transport rate and this was considered a non-specific peptide effect. The GLUT4 C-terminal peptide caused a slight rise in the transport rate but this was not significantly different from the basal rate. The GLUT4 N-terminal peptide did cause a significant, 1.7-fold, increase in the basal transport rate.

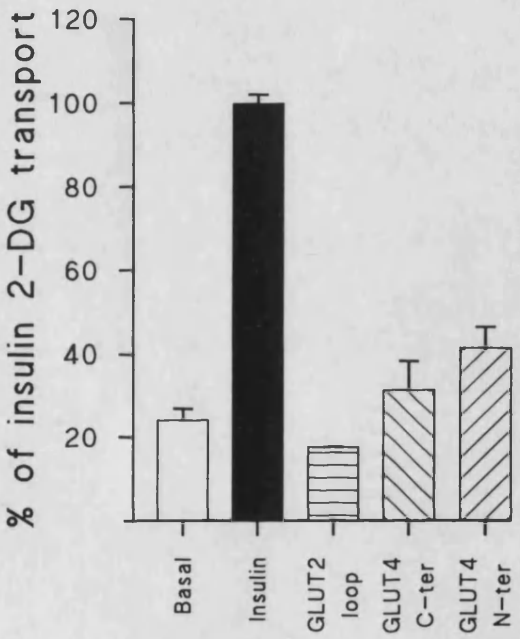

Figure 3.29. The effect of glucose transporter peptides on basal rate of 2-deoxy-D-glucose uptake in streptolysin-O permeabilized 3T3-L1 adipocytes

3T3-L1 adipocytes grown in 35 mm dishes were prepared, permeabilized and 2-deoxy-D-glucose uptake assayed as described in sections 2.3.3, 2.3.6 and 2.4.2.3 respectively. After permeabilization the adipocytes were incubated in IIC buffer at 37 °C for 30 min with no addition, basal (□), with 100 nM insulin, (■), ≈ 100 μM GLUT2 loop peptide (▤), 100 μM GLUT4 C-terminal peptide (▧) or 100 μM GLUT4 N-terminal peptide, (▨) before assaying transport. Peptide sequences are given in table 2.1. Values are the means of 9 (□, ■, n=19), 5 (▨, n=12), 3 (▧, n=9) or 1 (▤, n=2) experiments carried out in duplicate or triplicate. Errors are the S.E.M. The transport rate in the cells treated with the GLUT4 N-terminal peptide was significantly different ($p<0.01$) from the basal transport rate.

The effect of the two GLUT4 terminal peptides on the insulin stimulated transport rate in permeabilized 3T3-L1 adipocytes is shown in figure 3.30. The GLUT4 C-terminal peptide caused a slight, but not significant, decrease in the insulin stimulated transport rate. The GLUT4 N-terminal peptide caused a significant increase in the transport rate of 1.13-fold in the insulin stimulated transport rate. Thus the GLUT4 N-terminal peptide increases both the basal and insulin stimulated transport rates.

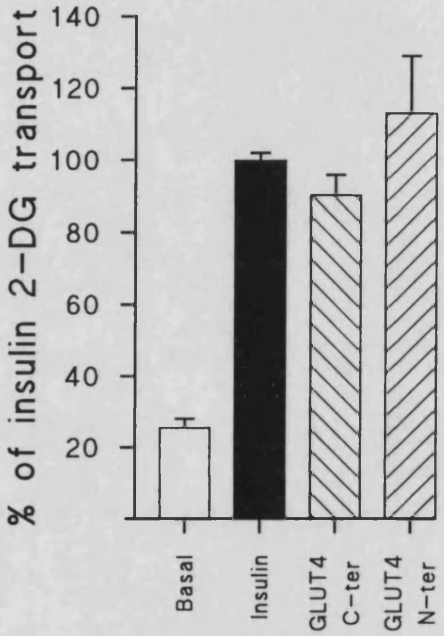

Figure 3.30. The effect of GLUT4 terminal peptides on insulin stimulated uptake of 2-deoxy-D-glucose in streptolysin-O permeabilized 3T3-L1 adipocytes

3T3-L1 adipocytes grown in 35 mm dishes were prepared, permeabilized and 2-deoxy-D-glucose uptake assayed as described in sections 2.3.3, 2.3.6 and 2.4.2.3 respectively. After permeabilization the adipocytes were incubated for 30 min in IIC buffer at 37 °C with no addition, basal (□), with 100 nM insulin, (■), 100 nM insulin and 100 μM GLUT4 C-terminal peptide (▨), or 100 nM insulin and 100 μM GLUT4 N-terminal peptide, (▨) before assaying transport. Peptide sequences are in table 2.1.

Values are the means of 9 (□, ■, n=19), 6 (▨, n=14) or 3 (▨, n=9) experiments carried out in duplicate or triplicate. Errors are the S.E.M. The transport rate with the GLUT4 N-terminal peptide was significantly different ($p<0.01$) from the insulin stimulated rate.

The effect of incubating the 3T3-L1 adipocytes with the peptides for 15 min before treating them with insulin for a further 30 min is shown figure 3.31. Each of the four peptides increased the insulin stimulated transport rate. This included an increase in the presence of the GLUT2 loop peptide. The transport rate in the presence of the other three peptides was higher than the GLUT2 loop peptide rate but only the rate in the presence of the GLUT4 N-terminal peptide was significantly higher than that with the GLUT2 loop peptide, 1.3-fold higher than the rate for insulin alone.

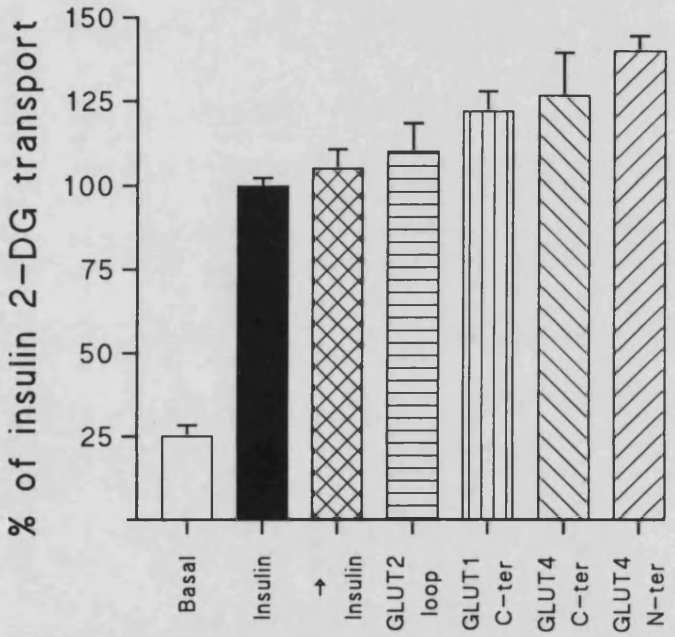

Figure 3.31. The effect of incubating streptolysin-O permeabilized 3T3-L1 adipocytes with glucose transporter peptides on the insulin stimulated uptake of 2-deoxy-D-glucose

3T3-L1 adipocytes grown in 35 mm dishes were prepared, permeabilized and 2-deoxy-D-glucose uptake assayed as described in sections 2.3.3, 2.3.6 and 2.4.2.3 respectively. After permeabilization some dishes were treated without (□) or with 100 nM insulin, (■) for 30 min in IIC buffer at 37 °C. The remaining dishes were preincubated for 15 min with 100 μM GLUT4 C-terminal peptide (▨), 100 μM GLUT4 N-terminal peptide (▨), 100 μM GLUT1 C-terminal peptide (▥), ≈ 100 μM GLUT2 loop peptide (▤), or no peptide (▩) before a further 30 min incubation with both the peptide and 100 nM insulin before assaying transport. Peptide sequences are given in table 2.1.

Values are the means of 9 (□, ■ n=18), 6 (▨ n=14), 5 (▨ n=12, ▩ n=10, ▤ n=10) or 3 (▥, n=6) experiments carried out in duplicate or triplicate. Errors are the S.E.M. The mean rate with the GLUT4 N-terminal peptide (▨) was significantly different ($p<0.001$) from that of the insulin stimulated rate after 15 min (▩) and from the rate with the GLUT2 loop peptide and insulin ($p<0.01$) (▤).

The effect of the GLUT4 N-terminal peptide on the insulin stimulated translocation of transporters was investigated by photolabelling 3T3-L1 adipocytes after a 30 min treatment with both the peptide and insulin, figure 3.32. The plasma membrane from these cells was purified before the transporters were immunoprecipitated. When peak areas were compared the addition of the GLUT4 N-terminal peptide increased the levels of both GLUT1 and GLUT4 in the plasma membrane above those for insulin alone, the increase in GLUT4 being 1.4-fold higher. Because of the greater error in the GLUT1 values, only the increase in the plasma membrane GLUT4 was significant.

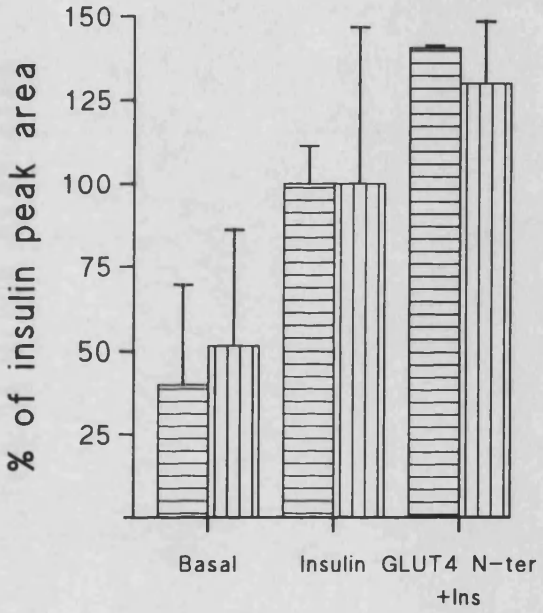

Figure 3.32. The effect of 100 μM GLUT4 N-terminal peptide on surface GLUT1 and GLUT4 in streptolysin-O permeabilized 3T3-L1 adipocytes

3T3-L1 adipocytes grown in 35 mm dishes were prepared and permeabilized as described in sections 2.3.3 and 2.3.6. After permeabilization 2 dishes of adipocytes per condition were incubated at 37 °C for 30 min in IIC buffer with no addition, basal, with 100 nM insulin or with 100 μM GLUT4 N-terminal peptide and 100 nM insulin, (GLUT4 N-ter+Ins). The cells were photolabelled with 300 μCi ATB-BMPA per dish, washed with IC buffer and TES and then subcellular fractionated to obtain purified plasma membrane for immunoprecipitating and counting cell surface GLUT4 and GLUT1 as described in section 2.6. The level of GLUT4 (▤) and GLUT1 (▥) are expressed relative to that for insulin.

Values are the mean of 2 independent experiments. Errors are the $SD_{(n-1)}$.

To see if the GLUT4 N-terminal peptide was blocking endocytosis or stimulating exocytosis the peptide was added to 3T3-L1 adipocytes that had been stimulated with insulin before being permeabilized with streptolysin-O. The effect of the peptide on the transport rate is shown in figure 3.33. 40 min after treating the permeabilized cells with the peptide the transport rate was higher than the rate for insulin alone.

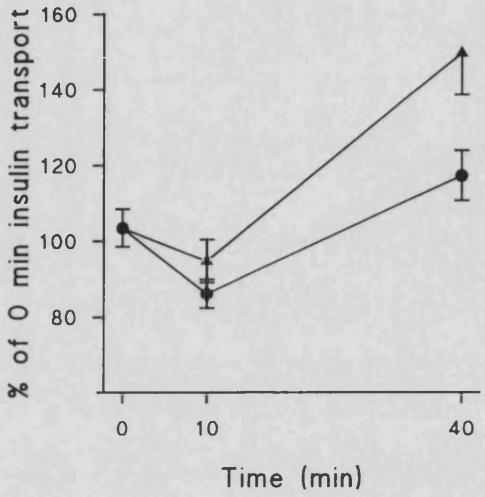

Figure 3.33. The effect of 100 μM GLUT4 N-terminal peptide and insulin on 2-deoxy-D-glucose uptake in insulin stimulated streptolysin-O permeabilized 3T3-L1 adipocytes

3T3-L1 adipocytes grown in 35 mm dishes were prepared as described in section 2.3.3. After washing with KRH the dishes they were treated with 100 nM insulin at 37 °C for 30 min. The cells were then permeabilized with 0.8 I.U./ml streptolysin-O as described in section 2.3.6. Insulin stimulation was then maintained in the absence (●) or presence of 100 μM GLUT4 N-terminal peptide (▲). The uptake of 2-deoxy-D-glucose (section 2.4.2.3) was assayed at the indicated times.

Values are the means of 2 independent experiments carried out in duplicate. Errors are the S.E.M. The difference between the 2 values at 40 min has a significance of $p<0.05$.

The experiment shown in figure 3.33 was repeated but the level of transporters in the plasma membrane was followed instead. Unlike in the transport assay the addition of the peptide had no effect of the cell surface levels of GLUT4 or GLUT1 when compared with insulin alone. After 40 min with insulin alone about 75 % of the labelled transporter remained at the cell surface instead of the expected 50 %. This suggests that either the cells may have been damaged by the UV irradiation or that the plasma membrane fraction was contaminated with labelled intracellular transporters.

Figure 3.34 shows a preliminary experiment to see if the GLUT4 N-terminal peptide prevents the departure of GLUT4 from the low density microsomal fraction. Basal 3T3-L1 adipocytes, with most of the GLUT4 in the low density microsomes (LDM), were permeabilized and photolabelled. They were then treated with either insulin or insulin and the GLUT4 N-terminal peptide. The level of labelled transporters remaining in the LDM was assayed. Figure 3.34 shows that the peptide does not appear to prevent GLUT4 leaving the LDM with ≈ 50 % of the transporters remaining in this fraction under both conditions, as expected for insulin stimulation. This results should be treated with caution, however, as the GLUT4 peak was associated with a high level of non-specific, background, labelling and this is a preliminary experiment.

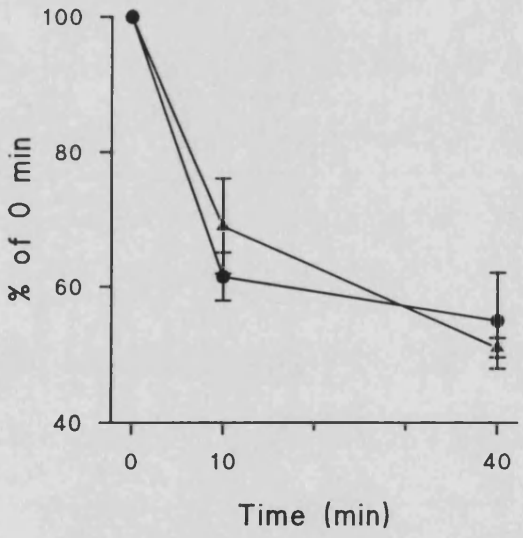

Figure 3.34. The effect of 100 μM GLUT4 N-terminal peptide and insulin on the level of GLUT4 in the low density microsomes of streptolysin-O permeabilized 3T3-L1 adipocytes

3T3-L1 adipocytes grown in 35 mm dishes were prepared and permeabilized as described in sections 2.3.3 and 2.3.6. Immediately after being permeabilized the cells were photolabelled with 300 μCi per dish for 1 min with a 1:1 ratio of 300 and 350 nm UV light. The unbound label was washed off and dishes of cells for 0 min were taken. The rest of the dishes of cells were stimulated with either 100 nM insulin (●) or 100 nM insulin and 100 μM GLUT4 N-terminal peptide (▲). At 0, 10 and 40 min cells were homogenised, the low density membrane purified, and GLUT4 immunoprecipitated and counted. The values are the mean of two counts from a single experiment. Errors are the $SD_{(n-1)}$.

3.6 Rab proteins and insulin stimulated transport in adipocytes

The ras-like GTP-binding protein rab4 has been shown to control the function or formation of endosomes involved in recycling by overexpressing the protein in CHO fibroblasts (van der Sluijs et al., 1992).

A peptide whose sequence (see table 2.1) was from a hydrophilic region in the middle of rab4 was used to produce antibodies against rab4. The rabbit serum was tested with a peptide ELISA to ensure that anti peptide antibody was being produced and that the maximum titre was obtained. The result of such an ELISA is shown in figure 3.35.

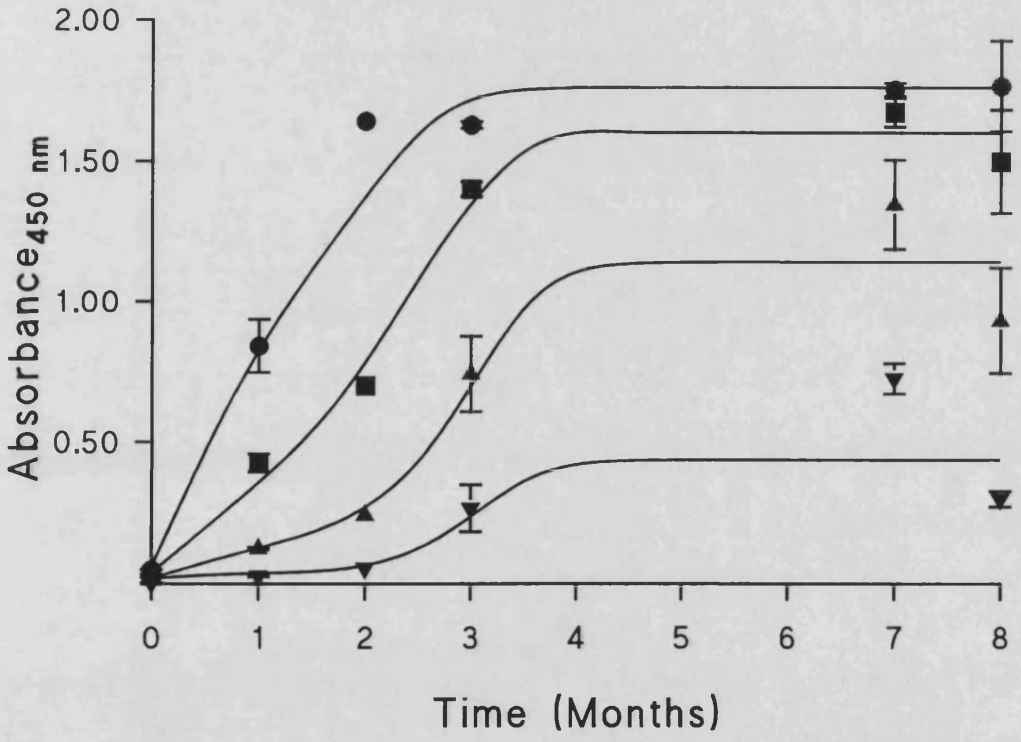

Figure 3.35. The production of antibodies against a rab4 peptide

The rab4 peptide coupled to KLH via MBS in Imject Alum was injected at four subcutaneous sites in a sandy half lop rabbit, as described in section 2.9. Anti-rab4 peptide IgG was detected with an ELISA (section 2.10) coated with rab4 peptide. Serum was diluted 1:100 (●),1:400 (■),1:1600 (▲) or 1:6400 (▼). The values are the mean of two counts from a single count. Errors are the $SD_{(n-1)}$.

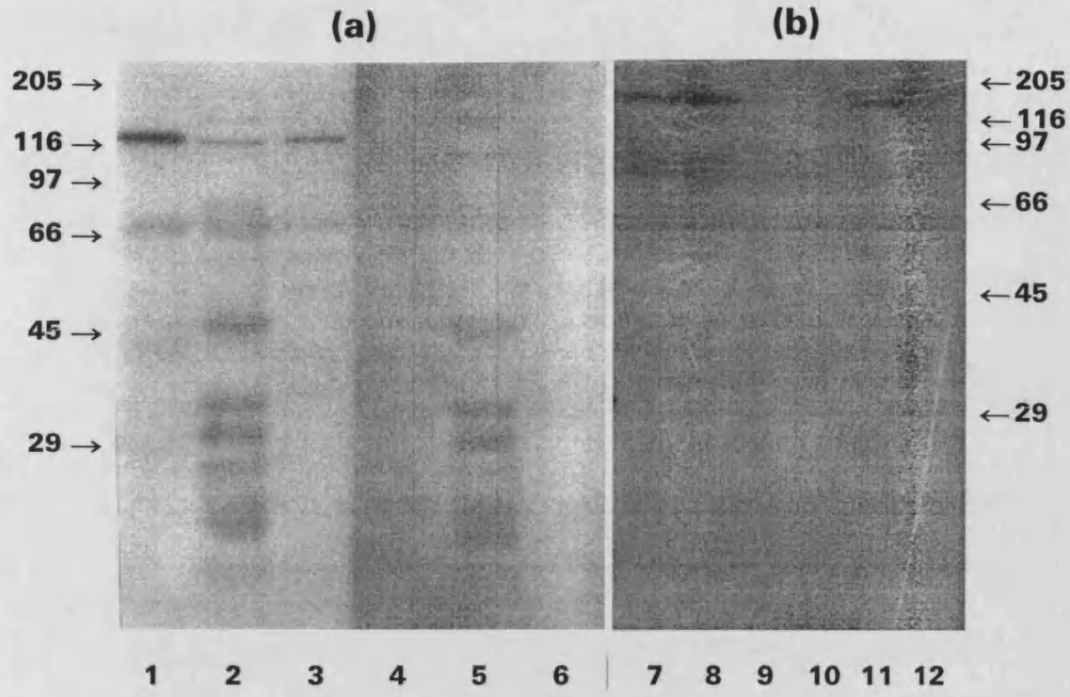

Figure 3.36. Immunoblotting of 3T3-L1 and rat adipocytes with anti-rab4 antiserum

Adipocytes were subcellular fractionated and Western blotted as described in section 2.6.

(a) (lanes 1-6) is of 3T3-L1 adipocyte plasma membrane, low density microsome (LDM) and whole cell fractions run on a 10 % acrylamide gel and probed with 1:100 anti-rab4 antiserum (lanes 1-3) or preimmune (PIM) serum (lanes 4-6) and 0.1 μCi/ml ^{125}I-protein A.

(b) (lanes 7-12) is of plasma membrane (PM) and low density microsome (LDM) fractions of basal and insulin stimulated 3T3-L1 and rat adipocytes run on a 12 % acrylamide gel and probed with 1:500 anti-rab4 antiserum, with a high (0.2 M) salt wash and 0.1 μCi/ml ^{125}I-protein A.

Lane 1: 3T3-L1 plasma membrane (160 μg) rab4
Lane 2: 3T3-L1 LDM (380μg) rab4
Lane 3: 3T3-L1 whole cells (105 μg) rab4
Lane 4: 3T3-L1 plasma membrane (160 μg) PIM
Lane 5: 3T3-L1 LDM (380μg) PIM
Lane 6: 3T3-L1 whole cells (105 μg) PIM
Lane 7: 3T3-L1 insulin PM (66 μg) rab4
Lane 8: 3T3-L1 basal PM (66 μg) rab4
Lane 9: 3T3-L1 insulin LDM (33 μg) rab4
Lane 10: 3T3-L1 basal LDM (33 μg) rab4
Lane 11: Rat insulin PM rab4
Lane 12: Rat insulin LDM rab4

Western blots of rat and 3T3-L1 adipocytes were probed with the anti-rab4 antiserum. Figure 3.36 shows immunoblots of whole and subcellular fractionated 3T3-L1 rat adipocytes. The samples from 3T3-L1 adipocytes in figure 3.31a were probed with preimmune serum and antiserum against rab4 and GLUT4. GLUT 4 was detected in all samples (results not shown).

The 3T3-L1 adipocyte proteins in lanes 1-3 of figure 3.36a were immunoblotted with the anti-rab4 antiserum were compared with their respective lanes 4-6 immunoblotted with the preimmune serum. There were no specific bands in any of the three lanes immunoblotted with anti-rab4 antiserum at the expected size of ≈ 24 kDa. No low molecular weight proteins were detected in any of the lanes in figure 3.36b. However, a unique band with an apparent mass of ≈ 150 kDa was found. This band was detected in all the fractions immunoblotted with the anti-rab4 antiserum, from both 3T3-L1 and rat adipocytes, but not in those blotted with the preimmune serum. This band appears to be stronger in the plasma membrane than in the low density microsomes fraction.

Figure 3.37 shows the result of a similar subcellular fractionation of rat adipocytes but with the addition of the high density microsomes and the chloroform/methanol precipitated proteins remaining in the final supernatant after the removal of the low density microsomes. Again the ≈ 150 kDa band was strongly detected in plasma membrane and weakly in LDM. It was not detected in either the high density microsomes or the supernatant. When all the blots were compared there was found to be no consistent difference in the intensities of the band in the basal and insulin simulated adipocytes. An additional band was also detected in the supernatant fraction of the blot shown in figure 3.37. This had a low molecular weight of under 29 kDa.

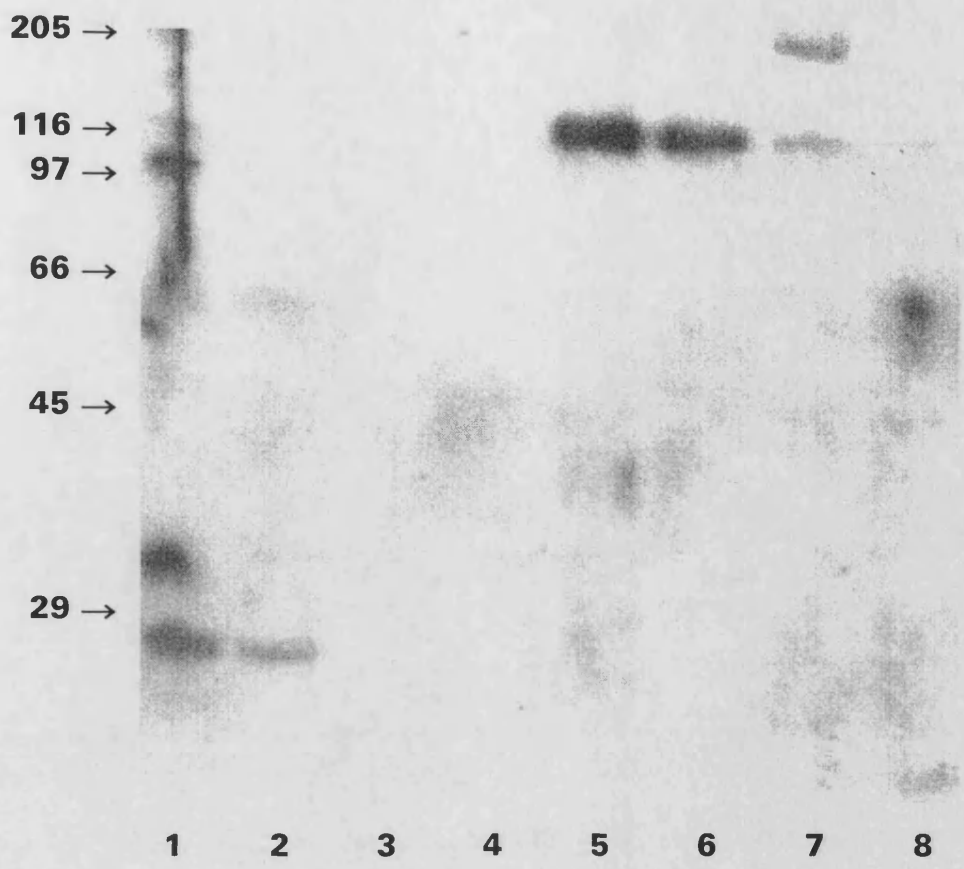

Figure 3.37. Immunoblotting of subcellular fractionated rat adipocytes with anti-rab4 antiserum

Rat adipocytes were either untreated or were treated with 10 nM insulin for 30 min, section 2.3.1. The adipocytes were then subcellular fractionated as described in section 2.6.1 but with the following alterations. The adipocytes were homogenised in TES (containing 150 µM sodium orthovanadate, 1 µg/ml protease inhibitors and a trace of PMSF) with 10 machine strokes. This homogenate was first spun at 1000 rpm in an IEC Centra-3R for 1 min to remove cell debris and fat. The supernatant was spun at 18,000 rpm (18,000 x g_{max}) for 20 min to obtain the crude plasma membrane pellet. The high density microsome pellet was obtained by a 9 min spin at 30,000 rpm (50,000 x g_{max}). The protein left in the supernatant after removing the LDM was precipitated by the chloroform/methanol method, section 2.6.2. An equal volume of each fraction was loaded onto a 10 % gel. The nitrocellulose was probed with a 1:200 diluted anti-rab4 antiserum and 0.1 µCi/ml ^{125}I-protein A.

Lane 1: Insulin stimulated rat adipocyte	supernatant
Lane 2: Basal rat adipocyte	supernatant
Lane 3: Insulin stimulated rat adipocyte	high density microsomes
Lane 4: Basal rat adipocyte	high density microsomes
Lane 5: Insulin stimulated rat adipocyte	plasma membrane
Lane 6: Basal rat adipocyte	plasma membrane
Lane 7: Insulin stimulated rat adipocyte	low density microsomes
Lane 8: Basal rat adipocyte	low density microsomes

Rab3d has been detected in adipocytes and its mRNA level increases during 3T3-L1 adipocyte differentiation (Baldini *et al.*, 1992). A rab3d effector domain peptide, residues 52-67, (see table 2.1) was used to test for the involvement of this small G-protein on insulin stimulated transport. Figure 3.38 shows the effect of the peptide on basal and insulin stimulated transport rates in streptolysin-*O* permeabilized 3T3-L1 adipocytes. The addition of the peptide to basal cells caused only a small rise in the rate of transport. When the peptide was added to insulin stimulated adipocytes there was a small decrease in the transport rate to ≈ 90 % of the rate for insulin alone. These effects are not significant, suggesting that the peptide has no effect on transport.

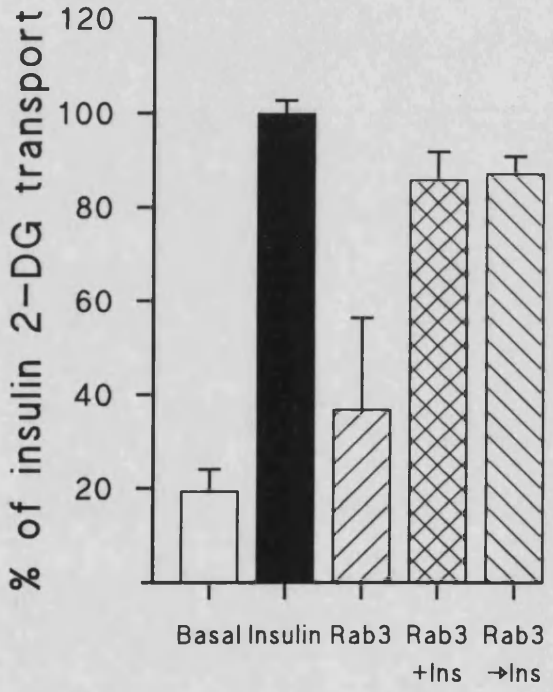

Figure 3.38 The effect of the rab3d effector domain protein on 2-deoxy-D-glucose uptake in streptolysin-*O* permeabilized 3T3-L1 adipocytes

3T3-L1 adipocytes grown in 35 mm dishes were prepared, permeabilized and 2-deoxy-D-glucose uptake assayed as described in sections 2.3.3, 2.3.6 and 2.4.2.3 respectively. After permeabilization the adipocytes were incubated for 30 min in IIC buffer at 37 °C with no addition, basal (□), with 100 nM insulin (■), with 100 μM rab3d peptide (▨), with 100 μM rab3d peptide and 100 nM insulin (▩) or 100 μM rab3d peptide and 100 nM insulin after an additional 15 min pretreatment with the peptide (▧) before assaying transport. The sequence of the peptide is given in table 2.1.

Values are the means of one or two experiments (□, ■, ▨ n=5; ▩ n=3; ▧ n=2). Errors are S.E.M.

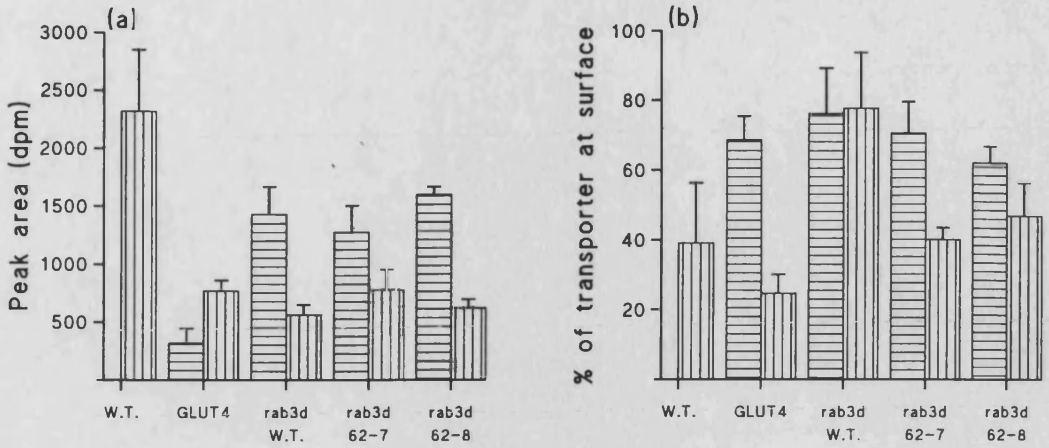

Figure 3.39. The effect of stably transfected rab3d on the distribution of stably transfected GLUT4 in CHO fibroblasts

35 mm dishes were seeded with 0.05 x 10^6 CHO fibroblasts and allowed to reach confluence in 4 days. Two dishes per condition were photolabelled with 100 µCi per dish in either the absence (surface) or presence (total) of 2.5 µg/ml digitonin. GLUT1 (▥) and GLUT4 (▤) were immunoprecipitated from solubilized cells and the gel counted as described in section 2.6. (a) The average peak area of the total transporter photolabelling. (b) The percentage of cell surface transporter was calculated by dividing the surface peak area by the total peak area. Values are given for GLUT1 in wild type fibroblasts and for GLUT1 and GLUT4 in the transfected CHO fibroblasts. W.T.: wild type CHO fibroblasts; GLUT4: CHO transfected with GLUT4; Rab3d W.T.: CHO transfected with GLUT4 and rab3d; Rab3d 62-7: CHO transfected with GLUT4 and Rab3d with a deletion between residues 62 and 67; Rab3d 67-8: CHO transfected with GLUT4 and Rab3d with a deletion between residues 62 and 68.
Values are the means of three experiments. Errors are the S.E.M.

The effect of rab3d on transporter translocation was investigated in CHO fibroblasts transfected with both rab3d and GLUT4, provided by Dr M. Hashiramoto (Kobe University, Japan). Figure 3.39 shows that neither the wild type or the mutant rab3d lacking an effector domain had a significant effect on the distribution of GLUT4 with ≈ 70 % at the cell surface. The transfected rab3d had a greater effect on the distribution of GLUT1. In the CHO cells cotransfected with both GLUT4 and the wild type rab3d there was a significant increase in the proportion of the GLUT1 at the cell surface to ≈ 75 %. The level of GLUT1 at the surface of cells expressing the deletion mutant rab3d was ≈ 40 %. This percentage is higher than that in cells expressing GLUT4 alone but is similar to level of GLUT1 at the surface of the nontransfected CHO fibroblasts.

3.7 The effect of GTPγS on glucose transport in 3T3-L1 adipocytes

GTPγS, because it cannot be hydrolysed, will constitutively activate G-proteins when it is exchanged for GDP. The effect of GTPγS on insulin stimulated glucose transport was therefore tested in streptolysin-*O* permeabilized 3T3-L1 adipocytes. Figure 3.40 shows the effect of GTPγS on the basal transport rate.

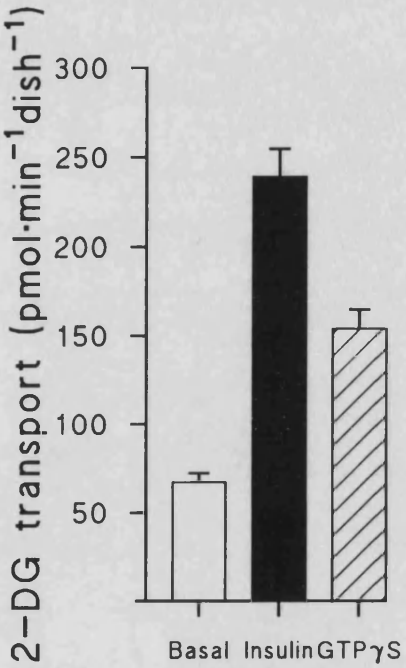

Figure 3.40. The effect of 0.2 mM GTPγS on 2-deoxy-D-glucose uptake in streptolysin-*O* permeabilized 3T3-L1 adipocytes.

3T3-L1 adipocytes grown on 35 mm dishes were prepared, permeabilized and 2-deoxy-D-glucose uptake assayed as described in section 2.3 and 2.4.2.3. After permeabilization the adipocytes were incubated for 30 min in IIC buffer at 37 °C with no addition, basal (□), with 100 nM insulin, (■) or with 0.2 mM GTPγS (▨) before assaying 2-deoxy-D-glucose.

Values are the means of 6 experiments generally carried out in duplicate (n=13). Errors are the S.E.M.

Insulin caused a 3.6-fold increase in the rate of 2-deoxy-D-glucose uptake. GTPγS also caused a rise in the rate of uptake of 2-deoxy-D-glucose but it was only about two thirds of the insulin stimulated rate, a 2.3-fold rise over basal. To get a clearer idea of how GTPγS stimulates transport in streptolysin-*O* permeabilized 3T3-L1 adipocytes the cells were stimulated and then photolabelled with ATB-BMPA, figure 3.41.

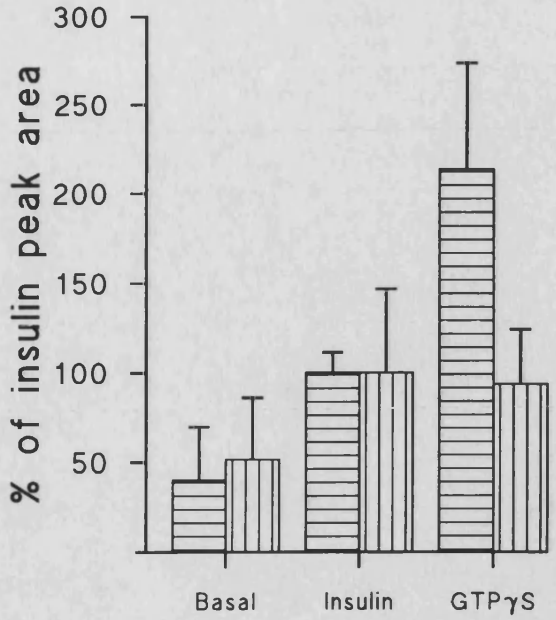

Figure 3.41. The effect of 0.2 mM GTPγS on the level of GLUT4 and GLUT1 at the surface of streptolysin-O permeabilized 3T3-L1 adipocytes

3T3-L1 adipocytes grown in 35 mm dishes were prepared and permeabilized as described in sections 2.3.3 and 2.3.6. After permeabilization 2 dishes of adipocytes per condition were incubated at 37 °C for 30 min in IIC buffer with no addition, basal, with 100 nM insulin or with 0.2 mM GTPγS. The cells were photolabelled with 300 µCi ATB-BMPA per dish, washed with IC buffer and TES and then subcellular fractionated to obtain purified plasma membrane for the immunoprecipitation and counting of GLUT4 and GLUT1 as described in section 2.6. The peak area for GLUT4 (▤) and GLUT1 (▨) are expressed relative to that for insulin.

Values are the means of 2 independent experiments. Errors are the $SD_{(n-1)}$.

Figure 3.41 shows the level GLUT1 and GLUT4 in purified plasma membrane. Insulin caused a 2.5-fold increase in GLUT4 and a 1.7-fold rise in GLUT1. Using the TK values of table 3.1 this would result in a 2-fold rise in the transport rate. The proposed 2-fold increase in intrinsic activity following insulin stimulation would give the transport rate shown in figure 3.40. GTPγS caused a 5.2-fold in GLUT4, twice that of insulin and a 1.7-fold rise in GLUT1, the same as for insulin. The over 200 % increase in cell surface level GLUT4 relative to the insulin stimulated level suggests that most of the total cellular GLUT4 was purified with the plasma membrane. The increase in the level of cell surface transporters is more than is required for the transport rate shown in figure 3.40. suggesting that not all the transporters may be as active as with insulin.

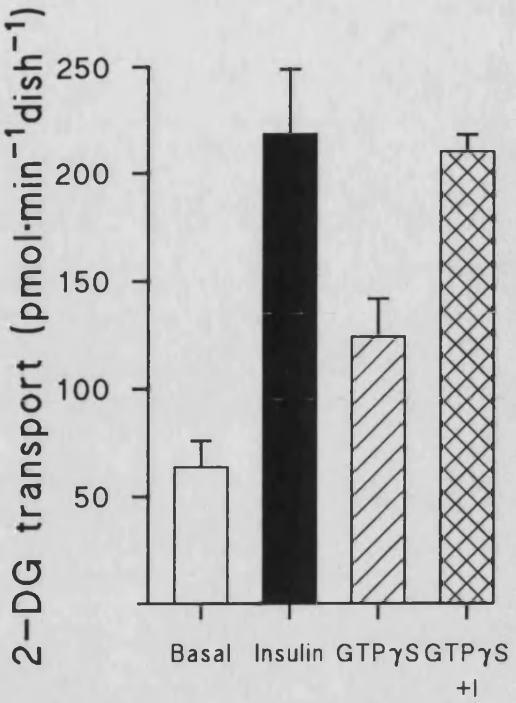

Figure 3.42. The effect of 0.2 mM GTPγS on insulin stimulated 2-deoxy-D-glucose uptake in streptolysin-O permeabilized 3T3-L1 adipocytes

3T3-L1 adipocytes grown on 35 mm dishes were prepared, permeabilized and 2-deoxy-D-glucose uptake assayed as described in section 2.3 and 2.4.2.3. After permeabilization the adipocytes were incubated for 30 min in IIC buffer at 37 °C with no addition, basal (□), with 100 nM insulin, (■), with 0.2 mM GTPγS (▨) or with 0.2 mM GTPγS and 100 nM insulin (▩) before assaying transport.
Values are the means of 2 experiments (n=5). Errors are the S.E.M.

The effect of GTPγS on basal transport and insulin stimulated transport is shown in figure 3.42. While both insulin and GTPγS separately stimulated transport when 3T3-L1 adipocytes were treated with insulin and GTPγS the effect of the two was not additive and the transport rate was no more than insulin alone. Indeed there was a slight drop in the rate of insulin stimulated transport in the presence of GTPγS. A similarly small effect was seen when insulin was added to cells that had been incubated GTPγS first (results not shown).

These results show that while both GTPγS and insulin stimulate glucose transport their effects are not additive. The effect of GTPγS appears to cause the translocation of GLUT4 to the cell surface but the level of cell surface transporters is more than is required for the GTPγS stimulated transport rate.

4.0 Discussion

4.1 Kinetic analysis of GLUT1 and GLUT4 in 3T3-L1 adipocytes

Insulin stimulation causes the rate of glucose uptake to increase about 20-fold in the highly insulin responsive cell line, 3T3-L1 adipocytes. The major mechanism whereby insulin achieves this stimulation is the translocation of transporters from an intracellular pool to the cell surface. However, translocation, as assessed by subcellular fractionation, results in only a 5-6-fold increase in the concentration of transporters at the cell surface. Thus this increase on its own is not sufficient to explain the increase in the transport rate. 3T3-L1 adipocytes possess two transporter isoforms, GLUT1 and GLUT4. Insulin, as well as increasing the total number of cell surface transporters also alters the ratio of the two isoforms there. Under basal conditions the ratio of GLUT1 to GLUT4 at the cell surface is 5:1 while insulin stimulation increases the proportion of GLUT4 to give a ratio of 1:1. This suggests that GLUT1 and GLUT4 may be making different contributions toward the transport rate.

Because the transport rate is contributed to by two different transporter isoforms the kinetic parameters for the individual isoform cannot be calculated directly from transport data as the kinetics of transport are a combination of two K_m and two V_{max} values. In order analyse the separate contributions of the two transporter isoforms, therefore, the separate affinities of GLUT1 and GLUT4 were determined for 3-O-methyl-D-glucose. This was achieved by measuring the displacement of the photolabel ATB-BMPA by a range of 3-O-methyl-D-glucose concentrations. This was used to calculate the specificity or transport constant, TK, for GLUT1 and GLUT4. TK incorporates both the K_m and V_{max} of the transporter as the TK is equal to the turnover number divided by the K_m and the turnover number is equal to the V_{max} divided by the concentration of transporters. The TK can therefore be defined thus:

$$TK = \frac{(V_{max}/K_m)}{[\text{GLUT1 or 4}]} \qquad \text{(equation 4.1).}$$

The TK value can therefore be used to determine the transport capacity of the

transporter isoforms at low substrate concentrations, the capacity being governed by both the turnover of the transporter and its affinity for the substrate.

As there are two transporter isoforms involved in the uptake of sugar by the 3T3-L1 adipocytes the rate of uptake is defined by the sum of two Michaelis-Menten equations:

$$v = \frac{V_{max.1} \cdot S/K_{m1}}{(1+S/K_{m1})} + \frac{V_{max.4} \cdot S/K_{m4}}{(1+S/K_{m4})} \qquad \text{(equation 4.2).}$$

Using equation 4.1, TK can be substituted into equation 4.2 in place of V_{max}:

$$v = \frac{TK1 \cdot S \cdot [GLUT1]}{(1+S/K_{m1})} + \frac{TK4 \cdot S \cdot [GLUT4]}{(1+S/K_{m4})} \qquad \text{(equation 4.3).}$$

Since $A_0/A = (1+S/K_m)$ the reciprocal of the fraction of the unoccupied sites in equation 4.3, $1/(1+S/K_m)$, can be determined from the displacement of ATB-BMPA by 3-*O*-methyl-D-glucose by dividing the radioactivity associated with transporters photolabelled with ATB-BMPA in the presence of 3-*O*-methyl-D-glucose (A) by the radioactivity associated with transporters in the absence of 3-*O*-methyl-D-glucose (A_0). This equation can also be used to calculate the K_m of GLUT1 and of GLUT4. These ratios (A_0/A) are given in figure 3.6. The values used for the concentration of either GLUT1 or 4 are taken from Palfreyman et *al.* (1992) and are the B_{max} values given in table 3.1. The transport rate (v) from figure 3.3 at a particular concentration of 3-*O*-methyl-D-glucose (S) can be used to calculate the TK values for GLUT1 and GLUT4 using least square regression of the equation:

$$v/S = TK1 \cdot x1 + TK4 \cdot x4 \qquad \text{(equation 4.4)}$$

where x1 and x4, the concentration of unoccupied sites, are equal to the B_{max} multiplied by either A/A_0 or $1/(1+S/K_m)$, the reciprocal fraction of unoccupied sites. By using the K_m values previously calculated from figure 3.6 the error in calculating the TK values is reduced. The use of acute and chronically insulin stimulated adipocytes, which have different concentrations of surface GLUT1 and GLUT4, aids the analysis.

The results of the analysis, given in table 3.1, show that the TK values of GLUT1 and GLUT4 are similar in both acute and chronically insulin stimulated 3T3-L1 adipocytes. Therefore the best estimate is given when these two sets of data are combined. This

gives TK1 as 3.6 x 10^{-3} $mM^{-1}\cdot min^{-1}$ and TK4 as 11.3 x 10^{-3} $mM^{-1}\cdot min^{-1}$. Thus the transport capacity of GLUT4 is ≈ 3-fold higher than that of GLUT1. When the average K_m are used to calculate the turnover number (K_{m1} = 19.9 mM and K_{m4} = 7.0 mM) then the turnover number is 7.2 x 10^4 min^{-1} for GLUT1 and 7.9 x 10^4 min^{-1} for GLUT4. Since these are very similar the difference in the transport capacity is due to the low affinity of GLUT1 for 3-O-methyl-D-glucose. Thus at low sugar concentrations more of the uptake occurs via GLUT4 than via GLUT1 due to the lower K_m of GLUT4.

In the basal 3T3-L1 adipocytes the TK values and turnover numbers for both GLUT1 and GLUT4 were ≈ 2-fold lower than the equivalent value in the insulin stimulated adipocytes. These values are less reliable than those in the insulin stimulated adipocytes as the low concentration of transporters and transport rate makes accurate measurement difficult. However, while not too much emphasis should be placed on this ≈ 2-fold difference in the activity of GLUT1 and GLUT4 in basal and insulin stimulated 3T3-L1 adipocytes it does suggest that, in addition to affecting transporter translocation, insulin also increases the intrinsic activity of the transporters. This insulin induced 1.5-2-fold increase in transporter activity has been reported by others, for example by Holman *et al.* (1990) in rat adipocytes.

During the analysis of the transport capacities of GLUT1 and GLUT4 several assumptions have been made. It was assumed that both GLUT1 and GLUT4 bind ATB-BMPA with equal efficiency even though their affinity for glucose is different. The K_d for both transporters for ATB-BMPA has been shown to be ≈ 150 μM (Palfreyman *et al.*, 1992). This is similar to the affinity of liver membrane GLUT2 toward ATB-BMPA where the K_d was reported to be ≈ 200 μM (Jordan and Holman, 1992). If the affinities of GLUT1 and GLUT4 were different then this would have the effect of increasing the TK and so the turnover number of one transporter isoform relative to the other one. Another factor associated with labelling is the efficiency of both labelling and immunoprecipitation. If a significant proportion of the cell surface transporters were either not photolabelled or immunoprecipitated then this would

result in an over estimation of the transporter turnover numbers. If one isoform was immunoprecipitated more efficiently than the other then this would have the same effect as if the two isoforms had different affinities for ATB-BMPA. In fact after immunoprecipitation there is less than 20 % of the radioactivity running in the same region as the transporters on SDS-PAGE still remaining in the solubilized cell supernatant (Palfreyman *et al.*, 1992). This percentage is similar to that for rat adipocytes (Holman *et al.*, 1990). A further problem in using ATB-BMPA to determine the concentrations of transporters at the cell surface is that ATB-BMPA may be able to photolabel transporters that are present at the plasma membrane but which are not yet involved in transport. These transporters were described by Satoh *et al.* (1993) as being in partially occluded vesicles. They used this state to explain the lag between the insulin stimulated increase in cell surface ATB-BMPA labelling and the increase in the transport rate. If transporters in such vesicles were included in the concentration of cell surface transporters then this would lead to an under estimation of the turnover numbers.

The K_m and turnover number of GLUT1 alone for 3-O-methyl-D-glucose have been relatively easy to measure because it is abundantly available in human erythrocytes where it is the only isoform. Here measurements made at 20 °C generally give a K_m of $\approx$ 25 mM and a turnover of 2.0 to 4.0 x 10^4 min^{-1} (Carruthers, 1990). Holman *et al.* (1981), for example, calculated a K_m of 20.0 mM and a turnover of 4.3 x 10^4 min^{-1}. These parameters have also been calculated in *Xenopus* oocytes expressing GLUT1. Keller *et al.* (1989) measured a K_m of 21 mM and a turnover of 13.2 x 10^4 min^{-1} for human GLUT1 at 22 °C. Gould *et al.*, at 18 °C, measured a K_m of 20 mM and a turnover of 1 x 10^4 min^{-1} for rat GLUT1 (Gould *et al.*, 1989) and a K_m of 17.6 mM for human GLUT1 (Gould *et al.*, 1991). More recently Nishmura *et al.* (1993) have measured the kinetics of rat GLUT1 at 20 °C and obtained a K_m of 26.2 mM and a turnover of 2.7 x 10^4 min^{-1} at 20 °C. Thus the K_m of 20 mM and turnover number of

7.2×10^4 min^{-1} measured here for the mouse transporter in 3T3-L1 adipocytes are similar to the findings of others.

The measurement of the kinetics of GLUT4 transport activity is less easy as there are no cells expressing exclusively GLUT4. In insulin stimulated adipocytes, where GLUT4 is by far the predominant species, the average K_m for 3-O-methyl-D-glucose is $\approx$ 5 mM (Birnbaum, 1992) at 37 °C. Taylor and Holman (1981) calculated a K_m of 4.5 mM while Simpson *et al.* (1983) calculated a turnover of 5.6×10^4 min^{-1} for rat adipocytes. In *Xenopus* oocytes at 22 °C Nishmura *et al.* (1993) calculated a K_m of 4.3 mM and a turnover of 1.7×10^4 min^{-1} for rat GLUT4 at 22 °C. These values are a little lower than the turnover number of 7.9×10^4 min^{-1} and K_m of $\approx$ 7 mM calculated here. Such a difference could be due in part to a low efficiency of photolabelling and immunoprecipitation.

All the measurements of the K_m of GLUT1 for 3-O-methyl-D-glucose agree on a value around 20 mM. The range of calculated turnover number for GLUT1 is greater. While the value obtained by Nishmura *et al.* (1993) in *Xenopus* oocytes is within the range for erythrocytes the value for GLUT1 in 3T3-L1 adipocytes is higher but within the same order of magnitude. The calculated values for K_m GLUT4 are also fairly comparable and are several fold lower than the K_m for GLUT1. All the GLUT4 turnover numbers are of the same order of magnitude although the turnover for GLUT4 in *Xenopus* oocytes (Nishmura *et al.*, 1993) is lower than that for GLUT4 in either rat or 3T3-L1 adipocytes. Despite the difference in the absolute GLUT1 and GLUT4 turnover numbers in the 3T3-L1 adipocytes and the oocytes of Nishmura the turnover numbers for GLUT1 and GLUT4 are similar in both studies. Thus both studies, where the K_m and the turnover number for GLUT4 and GLUT1 have been calculated at the same time, show that at high concentrations of 3-O-methyl-D-glucose the activity of both transporters would be the same and the greater activity of GLUT4 at lower concentrations is due to its lower K_m.

The difference in the absolute values between these two studies highlights the inherent dangers in measuring kinetic parameters in either system. There are several factors which could potentially affect the calculation of kinetic parameters in *Xenopus* oocytes. The transport measurements in both human erythrocytes and *Xenopus* oocytes were made at around 20 °C rather than at the more physiological temperature of 37 °C. This may cause a decrease in the turnover number and so result in a lower TK, which would explain the slightly lower turnover numbers that were calculated in *Xenopus* oocytes. Substitutions at Asn^{45}, the *N*-glycosylation site, have been shown to reduce the affinity of GLUT1 for glucose (Asano *et al.*, 1991). Since *Xenopus* oocytes are not mammalian cells they may be unable to correctly *N*-glycosylate the transporters which may affect the transport rate. The activity of GLUT1 and GLUT4 appears to be lower in basal than in insulin stimulated adipocytes. As oocytes are insulin insensitive it is not possible to tell which of these two states in adipocytes is comparable to the activity measured in the oocytes. One further difference is that the oocytes were transfected with rat transporters while 3T3-L1 are a mouse cell line.

In summary, these experiments have shown that ATB-BMPA and 3T3-L1 adipocytes can be used to estimate the separate kinetic activities of both GLUT1 and GLUT4 in an insulin sensitive cell line which expresses both transporter isoforms. The results have shown that the turnover numbers of GLUT1 and GLUT4 for 3-*O*-methyl-D-glucose are similar and that the difference in activity of the two isoforms at low sugar concentrations is due to their different K_m values. Thus the result of insulin stimulation is to increase the transport rate by increasing the total amount of transporter at the cell surface and to increase the proportion of surface GLUT4. A further effect of acute insulin stimulation appears to be to increase the intrinsic activity of the transporters relative to that in the basal adipocytes. Chronic insulin stimulation does not appear to further alter the activity of the transporters but instead, as with rat adipocytes (Kozka *et al.*, 1993), chronic insulin stimulation depresses the levels of GLUT4 reaching the cell surface while increasing the surface and total levels of GLUT1.

4.2 Okadaic acid and insulin stimulation in adipocytes

Okadaic acid is an inhibitor of the serine/threonine protein phosphatases PP1 and PP2A. It has been used to investigate the mechanism whereby insulin stimulates glucose transport. When okadaic acid is added to cells it causes an increase in the level of phosphorylated proteins by inhibiting their dephosphorylation (Cohen *et al.*, 1990). Okadaic acid has previously been shown to increase the basal rate of glucose transport and to decrease the insulin stimulated rate with a similar effect on the concentration of cell surface transporters (Lawrence *et al.*, 1990b). This led to the suggestion that a serine/threonine phosphorylation event may be involved in the insulin induced increase in the transport rate. These observations were made using 2-deoxy-D-glucose uptake assays and Western blotting in rat adipocytes.

In this study the effect of okadaic acid on hexose transport in both rat and 3T3-L1 adipocytes was assayed with a 3-O-methyl-D-glucose transport assay. The use of this sugar analogue to assay transport activity allows any effect of okadaic acid on the phosphorylation of 2-deoxy-D-glucose to be discounted. The level of GLUT1 and GLUT4 at the cell surface was determined by photolabelling, a more accurate and easily quantifiable method for determining the effects of okadaic acid on the level of cell surface transporters than Western blotting.

In basal rat adipocytes the optimum okadaic acid concentration for the stimulation of 3-O-methyl-D-glucose uptake was found to be between 0.2 to 1.0 μM. This is within the okadaic acid concentration range of 0.05 to 1.0 μM which Haystead *et al.* (1989) found stimulated the uptake of 2-deoxy-D-glucose in rat adipocytes. This is also consistent with the concentration of 1.0 μM used by Lawrence *et al.* (1990b). Haystead *et al.* (1989) found that okadaic acid stimulated the uptake of 2-deoxy-D-glucose but with a 5 min lag. When Lawrence looked more closely at this they found that okadaic acid stimulated the transport rate by only about 50 % of the insulin stimulated rate. This is fairly similar to the 40 % stimulation shown in figure 3.8.

The same okadaic acid concentration range had a similar effect in 3T3-L1 adipocytes. Here, however, the maximal stimulation in the rate of 3-O-methyl-D-glucose uptake with 0.5 to 1.0 μM okadaic acid alone was only 35 % of the insulin stimulated transport rate, a little less than the rate for rat adipocytes. In both basal and insulin stimulated rat adipocytes GLUT4 is the dominant transporter isoform at the cell surface. In the plasma membrane of basal 3T3-L1 adipocytes there is much more GLUT1 than GLUT4 so that in these cells more of the 3-O-methyl-D-glucose uptake occurs via GLUT1 than in rat adipocytes. Thus if okadaic acid has a greater effect on GLUT4 than GLUT1 then the effect of the inhibitor will be less in 3T3-L1 adipocytes.

When ATB-BMPA was used to detect GLUT1 and GLUT4 in the plasma membrane then the small okadaic acid induced increase in the transport rate was found to be associated with a small increase in the concentration of transporters at the cell surface. In both rat and 3T3-L1 adipocytes the increased rate of uptake following okadaic acid stimulation could be accounted for by the increase in cell surface transporters if the intrinsic activities of GLUT1 and GLUT4 were more like those in insulin stimulated cells rather than basal ones. This finding is in agreement with that of Corvera *et al.* (1991) who also found that the submaximal stimulation of transport by okadaic acid was associated with only a small increase in cell surface GLUT4. They also reported that the intrinsic activity of GLUT4 following okadaic acid treatment was lower than would be expected for GLUT4 in insulin stimulated adipocytes. This difference may partially be explained by the observed decrease in the concentration of plasma membrane GLUT1 in rat adipocytes, figure 3.9.

Okadaic acid was found to have an inhibitory effect on the insulin stimulated uptake of 3-O-methyl-D-glucose transport (Lawrence *et al.*, 1990b; Corvera *et al.*, 1991). Since the stimulatory effects of okadaic acid and insulin are not additive this suggests that the stimulatory pathways of insulin and okadaic acid share at least one common component. The inhibition of insulin stimulation by okadaic acid was greater in the rat adipocytes than in the 3T3-L1 adipocytes. In rat adipocytes the rate of uptake

following insulin stimulation in the presence of 0.5 μM okadaic acid was only 30-40 % of the rate with insulin alone. This is similar to the inhibition of 2-deoxy-D-glucose uptake obtained by both Lawrence *et al.* (1990b) and Corvera *et al.* (1991). In the 3T3-L1 adipocytes the inhibitory effect of okadaic acid on insulin stimulated transport was much less than in the rat adipocytes. Here the transport rate following insulin stimulation in the presence of 1.0 μM okadaic acid was only a little less than for insulin stimulation alone. The effect of okadaic acid on insulin stimulation was similar whether the adipocytes were pretreated with insulin or okadaic acid before the addition of either okadaic acid or insulin respectively although pretreatment with okadaic acid generally had the greater inhibitory effect.

When the effect of okadaic acid on the insulin stimulated translocation of GLUT1 and GLUT4 to the cell surface was studied then it was found that there was a lower concentration of both transporters isoforms at the plasma membrane with okadaic acid and insulin than with insulin alone. This is consistent with the inhibitory effect of okadaic acid on the insulin stimulated transport rate. Thus it appears that the major effect of okadaic acid on transport is to modulate translocation rather than to simply reduce the intrinsic activity of the transporters already at the cell surface. Insulin has been shown by Lawrence *et al.* (1990b) to reduce the phosphorylation of GLUT4. Okadaic acid increases the level of GLUT4 phosphorylation, as expected from a phosphatase inhibitor. They suggested that GLUT4 phosphorylation acts as a signal for the internalisation of the transporter. The results presented here support the idea that the major effect of okadaic acid is to alter transporter translocation. A more recent study by Reusch *et al.* (1993) on GLUT4 phosphorylation and its effect on activity suggested that in plasma membrane vesicles the phosphorylated GLUT4 was 35 % less active than the dephosphorylated transporter. In order to test if okadaic acid was also causing a decrease in the intrinsic activity of the transporters the actual transport rate in okadaic acid stimulated rat adipocytes was compared with the potential rate of transport from the same number of transporters in insulin stimulated adipocytes. In

doing this the assumption was made that GLUT4 has an ≈ 3-fold higher transport capacity than GLUT1, as has been shown in 3T3-L1 adipocytes (Palfreyman et *al.*, 1992) and in *Xenopus* oocytes expressing rat transporters (Nishmura et *al.*, 1993). If this assumption is valid for rat adipocytes then the transport and photolabelling results given in figures 3.9a and b suggest that the transport rate in okadaic acid treated cells is between about 80 and 85 % of what would expected for the same number of transporters in insulin stimulated rat adipocytes. This therefore provides circumstantial evidence that okadaic acid and perhaps therefore phosphorylation does cause a decrease in the intrinsic activity of the transporters relative to insulin stimulation. However, because no measure was made of the degree of GLUT4 phosphorylation it is not possible to be certain whether this effect on the transport activity correlates with the phosphorylation of GLUT4 rather than with another conformational change.

The effect of okadaic acid on translocation was investigated by looking at the effect of okadaic acid on insulin reversal. Adipocytes which had been stimulated with insulin had this stimulation removed in either the presence or absence of okadaic acid. In the rat adipocytes (figure 3.10) the presence of okadaic acid did not prevent treatment with collagenase from causing the transport rate to decrease from the initial insulin stimulated rate. The rate decreased to a level similar to that for okadaic acid alone. The lack of sufficient time points in this experiment prevented the calculation of a $t_{½}$. In 3T3-L1 adipocytes (figure 3.13) okadaic acid also failed to prevent the insulin reversal treatment causing the transport rate to decrease. In figure 3.13a the transport rate after 30 min reversal in the presence of okadaic acid is higher than the rate for 30 min okadaic acid treatment of basal adipocytes. Several factors could contribute to this difference including the longer incubation period and possibly incomplete reversal. A time course for the reversal of the insulin stimulated transport rate in 3T3-L1 adipocytes in the presence and absence of okadaic acid is shown in figure 3.13b. The points were used to calculate the half-time for reversal in the presence or absence of okadaic acid using the equation $t_{1/2} = \ln 2/(K_{ex} + K_{en})$, K_{ex} and

K_{en} being calculated from % at surface $= (K_{ex} + K_{en}\exp(-t(K_{ex} + K_{en}))/(K_{ex} + K_{en})$ since a change in the transport rate is governed by the translocation of transporters to and from the cell surface. The calculated half time for the reversal of insulin stimulation in the absence of okadaic acid was ≈ 4.4 min and ≈ 6.5 min in the presence of okadaic acid. The $t_{½}$ for insulin reversal in the absence of okadaic acid is similar to that obtained by Yang *et al.* (1992a). The presence of okadaic acid increases the $t_{½}$ of reversal. This slower half time of reversal could be due to a decrease in the rate of transporter exocytosis or a decrease in the rate of endocytosis. Altering either of these parameters would result in an okadaic acid induced decrease in the reversal half time. If okadaic acid regulated translocation at both of these steps then it could inhibit the insulin stimulated increase in the transport rate by inhibiting the insulin induced increase in exocytosis and increase the basal transport rate by decreasing endocytosis.

The ability of okadaic acid to alter the rate of translocation is also suggested by the recycling of ATB-BMPA photolabelled transporters from the plasma membrane. Three conditions were compared; continued insulin stimulation, the reversal of insulin stimulation and reversal in the presence of okadaic acid. After 30 min the condition with the highest concentration of labelled transporter in the plasma membrane was that of reversal in the presence of okadaic acid. As figures 3.13a and b show that the reversal of insulin stimulated transport in the presence of okadaic acid results in a decrease in the insulin stimulated transport rate, the result of the transporter recycling must be taken as an indication of a low rate of transporter endocytosis and exocytosis when compared with insulin stimulation. Thus the plasma membrane pool of labelled transporters is diluted more slowly in the okadaic acid treated adipocytes than in the insulin treated cells. Unfortunately the translocation of GLUT4 from the plasma membrane was not complete for the reversal of insulin stimulation in the absence of okadaic acid. This suggests that the cells may have been damaged during the UV irradiation so this result can only be taken as a indication of the okadaic acid effect and is not entirely reliable.

Taken together these experiments indicate that okadaic acid has two separate effects on glucose transport in adipocytes affecting phosphorylation at two different sites. The first effect is at the level of the transporter itself. Okadaic acid either causes an increase the degree of GLUT4 phosphorylation or prevents the insulin induced dephosphorylation of GLUT4. This results in a small drop in the intrinsic activity of GLUT4. The second effect is at the level of the translocation mechanism. Here okadaic acid prevents the insulin stimulated increase in the rate of exocytosis and lowers basal endocytosis rate. Such effects are in agreement with the findings of Reusch *et al.* (1993) who reported that the phosphorylation of GLUT4 decreased its intrinsic activity but did not alter the distribution of insulin stimulated translocation of GLUT4 when phosphorylated by parathyroid hormone treatment. Since, therefore, the phosphorylation of GLUT4 does not appear to alter its distribution the effect of okadaic acid on GLUT4 translocation must be at another step in the mechanism. Cormont *et al.* (1993) have observed that both insulin and okadaic acid cause the cycling of GLUT4 and rab4. They have proposed that rab4 may be a component in the GLUT4 translocation mechanism of both insulin and okadaic acid. Insulin treatment also induces the phosphorylation of Rab4 (Cormont *et al.*, 1994).

Okadaic acid, at the concentrations of $\approx$ 1.0 μM required to have an effect in whole cells, will inhibit both PP1 and PP2A. There are however reports that insulin regulates these two phosphatases differently. The activated insulin receptor has been shown to phosphorylate protein phosphatase-2A at Tyr^{307}. Phosphorylation at this site deactivates the phosphatase (Chen *et al.*, 1992). Insulin has the opposite effect on protein phosphatase-1. Insulin, via the C terminus of the insulin receptor, has been shown to activate PP1 (Begum *et al.*, 1993b). Therefore if both of these phosphatases are involved in the insulin signalling pathway for stimulating glucose transport then okadaic acid could be having an insulin like effect on PP2A while inhibiting the effect of insulin on PP1. Hence okadaic acid could partially stimulate transport on its own while inhibiting insulin stimulated transport.

4.3 The effect of tyrosine kinase inhibitors on transport in adipocytes

Tyrosine kinase inhibitors, mostly based on tyrphostins, have been shown to inhibit the epidermal growth factor tyrosine kinase. Ten such tyrosine kinase inhibitors were provided by the Wellcome Research Laboratories and were used to investigate the involvement of tyrosine kinases in the insulin signalling pathway for the stimulation of glucose transport. Rat adipocytes were incubated with each of the ten inhibitors at a concentration of 0.68 μM before stimulating the adipocytes with insulin in the continued presence of the inhibitor. This concentration was chosen as it is double the average published IC_{50} for the inhibition of the epidermal growth factor receptor kinase by the ten inhibitors (table 3.2). It was expected that at this concentration at least some of the inhibitors would inhibit the insulin receptor tyrosine kinase (IRTK) and so prevent the insulin stimulated increase in the rate of 3-O-methyl-D-glucose uptake. At 0.68 μM not one of the inhibitors inhibited insulin stimulated 3-O-methyl-D-glucose uptake. Indeed in the presence of some of the inhibitors the transport rate was slightly but not significantly higher than with insulin alone. At the ≈ 1000-fold higher concentration of 0.5 mM all the inhibitors had some inhibitory effect on the insulin stimulated transport rate and several completely abolished transport, a result not obtained with the 0.1 % DMSO or ethanol in which the inhibitors were dissolved. The tyrosine kinase inhibitor 453C89, α-cyano-3,4-dihydroxythiocinnamide, had no significant effect at a concentration of 0.68 μM but virtually abolished insulin stimulated transport at 0.5 mM. This inhibitor was used for the further experiments.

The effect of 5 to 500 μM 453C89 on insulin stimulated 3-O-methyl-D-glucose uptake is the same in both rat and 3T3-L1 adipocytes (figures 3.15 and 3.17). At the lowest concentration of 5 μM 435C89 had a slight stimulatory effect on the insulin stimulated rate of uptake in both rat and 3T3-L1 adipocytes. In rat adipocytes the insulin stimulated rate in the presence of 500 μM 453C89 was less than the basal transport rate. In the 3T3-L1 adipocytes, however, the rate of insulin stimulated 3-O-methyl-D-glucose uptake in the presence of 500 μM 453C89 was not quite as low as the basal

rate. This may be a reflection of the higher proportion of surface GLUT1 relative to GLUT4 in the 3T3-L1 adipocytes and suggests that 453C89 has a greater effect on GLUT4 than on GLUT1.

Several experiments were carried out which suggested that the inhibition of insulin stimulated transport by 453C89 was unlikely to be due to the inhibition of the insulin receptor tyrosine kinase. A time course for the inhibition 3-*O*-methyl-D-glucose uptake in insulin stimulated rat adipocytes by 0.5 mM 453C89 showed total inhibition within one minute. Such a rapid inhibition suggests that 453C89 is not acting at the insulin receptor tyrosine kinase and is unlikely to be affecting the translocation of transporters. A lack of an effect by 453C89 on the translocation mechanism is further suggested by the significant inhibition of transport by 500 μM 453C89 in insulin stimulated 3T3-L1 adipocytes at 18 °C. The internalisation of transporters is temperature sensitive and is significantly inhibited at 18 °C (Clark *et al.*, 1991). As 453C89 still inhibits insulin stimulated transport at 18 °C, inhibition is unlikely to be due to a rapid translocation of transporters from the cell surface.

Further support for the idea that 453C89 acts at the level of the transporter rather than at the insulin receptor tyrosine kinase was provided by the observation that when 0.5 mM 453C89 and 3-*O*-methyl-D-glucose were simultaneously added to insulin stimulated 3T3-L1 adipocytes then the rate of transport is only 60 % of the insulin stimulated rate. This inhibition occurred within the 10 sec of the transport assay with both the inhibitor and the labelled sugar present at the same time.

In an attempt to determine if 453C89 could inhibit insulin stimulated glucose transport at the level of a tyrosine kinase 3T3-L1 adipocytes were incubated with a low concentration of the inhibitor for an extended period of time before stimulating the adipocytes with insulin and assaying transport. At 5 μM, a concentration high enough to inhibit the epidermal growth factor receptor tyrosine kinase (Yaish *et al.*, 1988) but which does not inhibit insulin stimulated transport after a short period of incubation,

453C89 did not inhibit insulin stimulated 3-O-methyl-D-glucose transport even after several hours incubation. This again suggests that 453C89 has not inhibited any tyrosine kinase involved in the insulin signalling pathway for the stimulation of glucose uptake.

The absence of inhibition of the insulin receptor tyrosine kinase by these tyrosine kinase inhibitors has been reported by others. Young *et al.* (1993) have found that in rat adipocytes both 690C88 and 453C89 inhibit both the basal and insulin stimulated rates of fatty acid synthesis from glucose. Neither inhibitor, however, significantly reduced the magnitude of the insulin effect. 453C89 was also found to inhibit aldehyde dehydrogenase, suggesting that this, and other inhibitors are not specific for tyrosine kinases (Young *et al.*, 1993). Alber *et al.* (1992) have reported that genistein (76W79) inhibits insulin stimulated glucose oxidation but does not inhibit insulin receptor autophosphorylation or the activity of the insulin receptor tyrosine kinase. Smith *et al.* (1993) have also shown that while genistein does not inhibit the insulin induced redistribution of GLUT4 to the plasma membrane it does inhibit both basal and insulin stimulated 3-O-methyl-D-glucose uptake.

The results of others and those reported here suggest that the inhibitory effect of 453C89, as with genistein, occurs at the level of the transporter itself and that it does not inhibit the insulin receptor tyrosine kinase. There are two possible mechanisms whereby 453C89 could inhibit transport. One is competitive inhibition with the inhibitor competing with the 3-O-methyl-D-glucose for the sugar binding site of the transporter. The second is non competitive inhibition with perhaps the inhibitor inducing a conformational change in the transporter that greatly reduces its activity. If 453C89 were simply competing with the sugar then 0.5 mM 453C89 would be expected to produce a similar level of inhibition of the uptake of 50 μM 3-O-methyl-D-glucose transport whether the cells were pretreated with the inhibitor or both the sugar and inhibitor were added together. Since the degree of inhibition was less when sugar and inhibitor were added together than when the sugar was added after a pre-

treatment with the inhibitor then non competitive inhibition seems more likely than competitive inhibition.

The difference between the degree of inhibition by 500 μM 453C89 in rat and 3T3-L1 adipocytes suggests that the inhibitor preferentially inhibits GLUT4, the higher proportion of GLUT1 in the 3T3-L1 adipocytes lessening the degree of inhibition. Such a difference between GLUT1 and GLUT4 might be less likely if the inhibitor was simply blocking transport. Thus it seems likely that 453C89 is inhibiting transport perhaps by inducing a conformational change reducing the intrinsic activity of the transporters. Furthermore the greater inhibitory effect appears to be on GLUT4 rather than on GLUT1. Such a conclusion is supported by the findings of Smith *et al.* (1993) who reported that while genistein did not alter the translocation of GLUT4 in rat adipocytes it did decrease the intrinsic activity of GLUT4 by inducing a conformational change at the C terminus. They were able to demonstrate that while insulin caused an increase in the level of immunocytochemical labelling at the C terminus of GLUT4, genistein induced a conformational change which decreased C-terminal labelling without affecting labelling at the N terminus. Thus they concluded that conformational changes at the C terminus of GLUT4 alter its intrinsic activity and that this results in a reduced rate of 3-*O*-methyl-D-glucose uptake.

In summary, the tyrosine kinase inhibitor 453C89, α-cyano-3,4-dihydroxythiocinnamide, does not appear to inhibit any tyrosine kinase involved in the insulin induced translocation of GLUT4 and indeed does not appear to be a specific tyrosine kinase inhibitor. It does, however, inhibit the uptake of 3-*O*-methyl-D-glucose at the level of the transporter itself with a preference for GLUT4. The inhibitory effect is possibly the result of a conformational change in the transporter which alters its intrinsic activity.

4.4 The targeting of transfected GLUT4 in fibroblasts

The facilitative glucose transporter GLUT1 occurs in many cell types and tissues including both insulin sensitive and insensitive cells. Much of the GLUT1 is expressed at the cell surface. GLUT4 expression is limited to the insulin sensitive adipose and muscle tissue. These cells express both GLUT1 and GLUT4. A greater proportion of the total GLUT1 is at the cell surface of basal adipocytes than GLUT4. However, following insulin stimulation a greater proportion of GLUT4 is translocated to the cell surface. The aim of these experiments was to determine if the differential distribution of GLUT1 and GLUT4 within adipocytes is a property of the GLUT4 protein itself or whether it is conferred on it by the insulin sensitivity of the cell in which it is expressed. In order to determine whether GLUT4 is intrinsically a plasma membrane protein or an intracellular protein it was expressed in insulin insensitive cells which do not normally express GLUT4.

It is not only in insulin sensitive cells that transporters are sequestered in intracellular pools. GLUT1 has been shown to be internally sequestered in many cells. These include BHK cells (Widnell *et al.*, 1990) and murine fibroblasts (Haspel *et al.*, 1986). The redistribution of GLUT1 to the cell surface has been shown to occur in these cells in response to stresses such as heat shock and glucose starvation. Yang *et al.* (1992b) have reported that in 3T3-L1 fibroblasts over 75 % of the GLUT1 can be sequestered to intracellular stores.

Attempts to transfect 3T3-L1 fibroblasts with the plasmid pRC-CMV-hGLUT4 and express GLUT4 proved not to be very successful as the level of expression, although detectable, was too low and the transfection was not reliable. There are two potential reasons for that this. One reason may be associated with the calcium phosphate precipitation method which may not have been reliable or may not have induced a high enough level of transfection. A second reason may be that the plasmid, pRC-CMV-hGLUT4, was designed specifically for transfection into COS-7 fibroblasts.

When COS-7 fibroblasts, an insulin insensitive cell line, were transfected with pRC-CMV-hGLUT4 by the DEAE-dextran method the level of transfection and expression was much higher. When the plasma membrane and low density microsomal fractions of the COS-7 fibroblasts were immunoblotted, figure 3.22, transfected GLUT4 was detected in both fractions. Most of the transfected GLUT4 appeared as a broad band in the plasma membrane fraction. A similar experiment by Schürmann *et al.* (1992b) also showed that the subcellular fraction of COS-7 with the greatest proportion of the total GLUT4 was the plasma membrane fraction. They also had a much broader GLUT4 band in COS-7 cells than in 3T3-L1 adipocytes which they suggested was due to heterogeneous glycosylation.

To better quantify the proportion of the total GLUT4 at the cell surface of both COS-7 and CHO fibroblasts the cells were photolabelled with ATB-BMPA. In order to determine the suitability of ATB-BMPA for the labelling of GLUT1 and GLUT4 in these cell lines transporters at the surface of COS-7 and CHO fibroblasts transfected with GLUT4 were photolabelled in either the presence or absence of glucose. A single glucose displaceable peak was obtained following either immunoprecipitation with GLUT1 or GLUT4 which confirmed that the label was still sufficiently specific and therefore suitable for quantifying the levels of GLUT4 and GLUT1 in these cells.

Surface and total photolabelling of transporters in nontransfected COS-7 fibroblasts and fibroblasts expressing GLUT4 was used to determine the percentage of the transporters at the cell surface. In both transfected and nontransfected cells the proportion of total GLUT1 at the cell surface was 55-60 %, a similar proportion to that reported by Schürmann *et al.* (1992b) who found ≈ 55 % of the GLUT1 at the surface of nontransfected cells as detected by counting Western blots. They also found ≈ 45 % of the transfected GLUT4 at the cell surface. Using ATB-BMPA, however, the photolabelling of fibroblasts transfected with GLUT4 appeared to indicate that 140 % of the total GLUT4 was at the cell surface! While such a value is obviously not possible it does suggest that most of the GLUT4 was at the surface of these cells. Such

a high calculated percentage of GLUT4 at the cell surface could be simply due to different levels of transfection and expression of the GLUT4 between the dishes of cells used for surface and total transporter photolabelling. An alternative explanation is that the digitonin treatment, used to permeabilize the fibroblasts and allow both the surface and intracellular pools of transporters to be photolabelled, resulted in the loss of a large proportion of the labelled GLUT4 from these dishes. This would give the appearance of a high proportion of the total GLUT4 at the cell surface. There was a loss of protein following the digitonin treatment of the CHO fibroblasts. The digitonin treated CHO fibroblasts had only 85 % of the protein of the intact cells. If the same protein loss occurred in the COS-7 fibroblasts then in addition to lowering the percentage of GLUT4 at the cell surface there would also be likely to be a lower percentage of GLUT1 at the cell surface.

In order to ensure the same level of GLUT4 expression between the different dishes of fibroblasts used for the photolabelling of surface and total transporter pools, CHO fibroblasts stably transfected with GLUT4 were used. In order to adjust for the loss of photolabelled transporters from the digitonin treated dishes of fibroblasts used to determine the total cellular transporter pool the results of a protein assay was used. In the nontransfected CHO fibroblasts only 40 % of the GLUT1 was at the cell surface. This percentage was a little lower in the cells expressing GLUT4. The total amount of GLUT1 in the cells expressing GLUT4 was also lower than in the nontransfected fibroblasts. This suggests that the expression of GLUT1 had been down regulated in response to the expression of GLUT4. Thus it appears that these fibroblasts may regulate GLUT1 expression according to their metabolic requirements, as suggested by Sargeant and Pâquet (1993).

The photolabelling of transporters in insulin insensitive CHO fibroblasts stably transfected with GLUT4 showed that about two thirds of the total GLUT4 was at the surface of these cells with the remaining third sequestered within the cells. This is a higher proportion of the GLUT4 in the plasma membrane than the 55 % at the cell

surface of the COS-7 fibroblasts of Schürmann *et al.* (1992b) and is much higher than the less than 20 % at the cell surface of the CHO fibroblasts of Piper *et al.* (1993a) and Asano *et al.* (1992b). When Hudson *et al.* (1993) expressed GLUT4 in the neuroendocrine cell line PC12 they found that GLUT4 was localised in the large density core vesicles with very little being detected at the plasma membrane. GLUT4 has also been expressed in *Xenopus* oocytes by Thomas *et al.* (1993) who found that over 70 % of the GLUT4 was located in intracellular membranes. These differences in GLUT4 localisation between cell types could be due to differences in N-glycosylation. Asano *et al.* (1993) have shown that non N-glycosylated GLUT1 is targeted to the cell interior rather than the cell surface. Alternatively the differences could be due to the different ways that different cell types have of sorting proteins or to the method used to transfect and express GLUT4 in the different cells.

There are several reasons why the surface labelling of GLUT4 might be so high in the CHO fibroblasts. One is the low level of GLUT4 and native GLUT1 expression. The GLUT1 peak area in the non transfected CHO fibroblasts is about 5-fold larger than that of the fibroblasts transfected with GLUT4. The GLUT4 peak area in the transfected cells in more than 5-fold smaller than the GLUT1 peak in these cells. Thus the relatively high proportion of GLUT4 at the cell surface may be necessary to compensate for the lower GLUT1 levels. Alternatively, as suggested for the COS-7 fibroblasts, the digitonin treatment may result in a significant loss of labelled GLUT4 from the dishes used to calculate the total transporter pool. If this were the case then the use of digitonin to determine the total transporter pool must be carefully tested on a particular cell line before it is used.

While it is difficult to confirm the essentially intracellular localisation of GLUT4 in these experiments they do suggest that the apparent localisation of GLUT4 may be affected by the method used for expressing GLUT4 in cells and the method used to detect its location. The results do show that the subcellular distribution of GLUT1 and GLUT4 is different even within non insulin sensitive cell lines.

4.5 Glucose transporter peptides and the targeting of GLUT4

GLUT4 and GLUT1 are differentially sorted and have a distinct distribution between intracellular membranes and the cell surface of insulin sensitive adipocytes. A large proportion of GLUT1 is in the plasma membrane (James *et al.*, 1993). GLUT4 is selectively excluded from the surface of unstimulated cells and is instead sequestered in a specific GLUT4 vesicle population within the tubulo-vesicular elements. The differential sorting of GLUT4 is believed to be intrinsic to the GLUT4 protein itself. Several groups have tried to identify specific regions within GLUT4 that are responsible for the isoform specific distribution of transporters. This was done by making GLUT1/GLUT4 chimeras and expressing them in fibroblasts including CHO and COS-7 fibroblasts. This has resulted in the implicating of three different regions of GLUT4 in its specific sorting. These are the GLUT4 N terminus (Piper *et al.*, 1992) a domain around helices 7 and 8 (Asano *et al.*, 1992b) and the C terminus (Czech *et al.*, 1993; Verhey *et al.*, 1993).

An alternative approach to determine which regions of GLUT4 are involved in its sorting and targeting was taken using peptides corresponding to different regions of the glucose transporters. The advantage of this approach is that the targeting of GLUT4 is investigated in 3T3-L1 adipocytes, an insulin sensitive cell line which expresses both GLUT1 and GLUT4. Furthermore it does not involve the construction and expression of transporter chimeras. Both the construct and the level of expression could affect the distribution. Very few regions of either GLUT1 or GLUT4 penetrate far beyond the phospholipid head groups of the membrane because the inter helical loops are too short. The regions that are exposed to the cytoplasm include the N- and C-terminal regions and the loop between helices 6 and 7. The peptides used in this study came from sequences within the N and C terminus of GLUT4 and the C terminus of GLUT1. A peptide with a sequence from within the first extracellular exofacial loop of GLUT2 was also included so that the specific effect of a peptide could be distinguished from a

non-specific effect resulting merely from the addition of a peptide. The sequences of all the peptides used in these experiments are given in table 2.1.

The effect of the peptides on the rate of uptake of 2-deoxy-D-glucose peptides in streptolysin-O permeabilized 3T3-L1 adipocytes was first tested, figures 3.29 to 3.31. The peptides were added to basal 3T3-L1 adipocytes and to insulin stimulated adipocytes either at the same time as the insulin or 15 minutes before the cells were stimulated with insulin in the presence of the peptide. The only one of the three peptides that consistently caused a significant difference in the transport rate relative to the rate either in the absence of peptide or in the presence of the GLUT2 loop peptide was the GLUT4 N-terminal peptide. In insulin stimulated, insulin stimulated after pre-treatment with the peptide and basal streptolysin-O permeabilized 3T3-L1 adipocytes the N-terminal peptide caused an increase in the rate of 2-deoxy-D-glucose uptake. There was a 2-fold increase in the basal rate, a 10 % increase in the insulin stimulated rate when added with insulin and a 30 % increase in insulin stimulated transport following a 15 min pre-treatment with the peptide. It is interesting to note that the N-terminal region of GLUT4 is 14 residues longer than that of GLUT1 and the N-terminal peptide sequence is from within this region.

In order to confirm that the N-terminal peptide was increasing the transport rate by altering transporter translocation, the transporters were photolabelled with ATB-BMPA. Streptolysin-O permeabilized 3T3-L1 adipocytes were stimulated with insulin in the presence of the GLUT4 N-terminal peptide. They were then photolabelled with ATB-BMPA and the plasma membrane purified. The cells simulated with insulin in the presence of the peptide were found to have a significantly higher concentration of GLUT4 at the plasma membrane compared to those stimulated with insulin alone. The level of cell surface GLUT1 was also increased in the presence of the peptide but to a lesser extent. However, due to the greater error in the GLUT1 measurement this difference was not significant. The influence of the N-terminal peptide on the distribution of GLUT1 as well as GLUT4 may be, as suggested by

Calderhead *et al.* (1990), an indication of poor sorting of the two isoforms in 3T3-L1 adipocytes which express much higher levels of GLUT1 than do primary adipocytes.

The results with the peptides do indicate an important role for the N-terminal region of GLUT4 in its translocation. The peptide induced increase in the concentration of GLUT4 in the plasma membrane could be due either to an increase in endocytosis or a decrease in exocytosis. In an attempt to resolve these alternatives the GLUT4 N-terminal peptide was added to 3T3-L1 adipocytes that had been stimulated with insulin prior to being permeabilized with streptolysin-O, figure 3.33. After 40 min the transport rate in the presence of the N-terminal peptide and insulin was ≈ 50 % higher than the rate in the presence of insulin alone. Such an increase suggests that the peptide is preventing GLUT4 from leaving the plasma membrane. An equivalent effect was not observed when the recycling of photolabelled GLUT1 and GLUT4 was followed. The level of photolabelled GLUT4 and GLUT1 remaining in the plasma membrane was the same whether the transporters were recycled in either the presence or absence of the GLUT4 N-terminal peptide. However, since after 40 min of recycling in the presence of insulin alone there was still 80 % of the labelled GLUT4 in the plasma membrane rather than the expected 40 to 50 %, this result probably demonstrates the effect of cell damage following UV irradiated and streptolysin-O permeabilization rather than the effect of the peptide.

An alternative approach to studying the effect of the GLUT4 N-terminal peptide on transporter recycling was to photolabel all the transporters in permeabilized basal cells. In basal adipocytes most of the GLUT4 would be in the intracellular pool and insulin stimulation and recycling would follow the departure of the labelled transporters from the low density microsomal fraction which is easier to purify than the plasma membrane fraction. Unfortunately this did not give a clear result as the immunoprecipitated GLUT4 gel peak was much broader than for simple cell surface photolabelling. However the preliminary experiment does show that after 40 min with insulin alone ≈ 55 % of the photolabelled GLUT4 was in the low density microsome

fraction while in the presence of insulin and the GLUT4 N-terminal peptide ≈ 51 % of the GLUT4 remained in the low density microsomal fraction. Such a difference in the presence of the peptide could be due either to a rate of exocytosis higher than that for insulin alone or, more likely in the light of the earlier observations, due to a decreased rate of endocytosis. It certainly suggests that the GLUT4 N-terminal peptide does not inhibit the departure of GLUT4 from the low density microsomal pool. This method of following the recycling of glucose transporters has the advantage of labelling a larger proportion of the transporters in one location and it is easier to obtain a purified low density microsome fraction than a pure plasma membrane fraction. The broad indistinct peak following SDS-PAGE is presumably due to the non-specific labelling of proteins by ATB-BMPA within the permeabilized 3T3-L1 adipocytes. This makes the results unreliable.

Overall these results show that there is a role for the N-terminal region of GLUT4 in the translocation of this protein. They also suggest that it may be involved in the sequestration of GLUT4 from the plasma membrane. Presumably the peptide, at a 500-fold higher concentration, competes with the N terminus of GLUT4 for the endocytosis machinery thus causing GLUT4 to build up in the plasma membrane. This conclusion agrees with the findings of James' group who transfected CHO fibroblasts with chimeras of GLUT1 and GLUT4. They found that when the GLUT4 N-terminal sequence PSGFQQI, residues 2-8 (contained within the N-terminal peptide), was incorporated into the N terminus of either GLUT1 or the transferrin receptor then both of these proteins adopted a GLUT4-like distribution. This substitution, however, had no effect on the rate of recycling of these proteins to the plasma membrane (Piper *et al.* 1992, 1993a; Garippa *et al.*, 1994). When the N terminus of GLUT4 was replaced with that of GLUT1 then a higher proportion of the chimera was at the cell surface compared to the wild type GLUT4 (Piper *et al.*, 1992, 1993a). Further mutational analysis of the N-terminal region led to the proposal that Phe^5 is an important part of the intracellular sequestration motif as substitution at this site causes

GLUT4 to accumulate in the plasma membrane (Piper *et al.*, 1993a). A similar phenylalanine/tyrosine based internalisation motif is found within other internalized proteins such as surface glycoproteins (Ktistakis *et al.*, 1990) and the mannose-6-phosphate/IGF II receptor (Jadot *et al.*, 1992). Garippa *et al.* (1994) demonstrated that the GLUT4 N-terminal motif is responsible only for the internalisation of GLUT4 and not for the retention of the transporter in the intracellular pool. This is also suggested by figure 3.34. Another sequence may therefore be required to maintain the intracellular localisation of GLUT4 in basal adipocytes.

The N terminus of GLUT4 is not the only region that has been implicated in the localisation of GLUT4. Asano *et al.* (1992b) have found evidence for the involvement of a domain between transmembrane helix 7 and the N-terminal half of the loop between helix 7 and 8 rather than the N terminus. Several groups have also implicated the C-terminal region (Czech *et al.*, 1993; Verhey *et al.*, 1993). This suggests that more than one region may be involved in GLUT4 targeting with perhaps the N terminus acting as a recognition sequence for internalisation and the C terminal motif retaining the transporter within the intracellular pool. Czech *et al.* (1993) identified within the GLUT4 cytoplasmic C-terminal region a dileucine motif at residues 489-490 which is involved in the targeting and sorting of GLUT4 and is similar to sequences involved in the targeting and sorting of other plasma membrane proteins.

The results obtained from the peptides and permeabilized 3T3-L1 adipocytes do support the idea that a phenylalanine based motif in the N terminus of GLUT4 is involved in the intracellular sequestration of the protein in an insulin sensitive cell line which expresses GLUT4. The lack of effect of the GLUT4 C-terminal peptide on transporter translocation in permeabilized 3T3-L1 adipocytes does not rule out a role for this region as a whole but does suggest that the last 14 residues of the transporter are not involved. As the dileucine motif is not within these last 14 residues the C-terminal peptide would not be expected to have an effect if this motif in addition to the N-terminal region of GLUT4 is involved in the sorting of GLUT4.

4.6 Rab proteins and insulin stimulated transport in adipocytes

Rab proteins are members of the large family of small GTP binding proteins. They have been shown to be involved in the regulation of membrane trafficking. One specific member of the rab family, rab4, has been shown to be associated with early endosomes and other vesicles that are involved in the recycling of the transferrin receptor in a number of cells types including CHO, HeLa, MDCK and NRK cell lines (van der Sluijs *et al.*, 1991). It was suggested that rab4 might be involved in the regulation of the receptor recycling pathway.

In order to probe adipocytes for the presence of rab4 an anti-rab4 antiserum was raised against a peptide whose sequence came from the middle of the protein (Zahraoui *et al.*, 1989). This serum was used to probe Western blots of membrane fractions from both rat and 3T3-L1 adipocytes in order to try and detect rab4 in these cells. No protein with the expected molecular weight of 23 to 25 kDa was detected in either the plasma membrane or low density microsome fractions of either rat or 3T3-L1 adipocytes. However, there was a strong band at the higher Mr of ≈ 150,000. This band appeared to be stronger in the plasma membrane fraction than in the low density microsomes. Densitometry of the ≈ 150 kDa band in both the plasma membrane and the low density microsomal fractions did not appear to show a difference in band intensity following insulin stimulation.

The cytoplasm was then probed with the antiserum. The protein in the supernatant remaining after the removal of the low density microsomal fraction was precipitated using chloroform/methanol and Western blotted. This fraction gave a different pattern of bands. The ≈ 150 kDa band was not detected in this subcellular fraction. Instead an ≈ 25 kDa band was detected. This band was of about the correct molecular weight to be rab4. The detection of rab4 in the cytosol is in agreement with the findings of van der Sluijs *et al.* (1991) who, in addition to detecting rab4 in endosomes, also detected the protein in the cytosol although at a four-fold lower concentration.

The identification of the higher Mr band is unclear. It could simply be due to the antiserum cross reacting with a different protein. A similar high molecular weight band was also detected in low density microsomes using an antibody against a small G-protein by Cormont *et al.* (1991). Alternatively this ≈ 150 kDa band could represent rab4 in very close association with another protein or proteins forming a complex. Such a complex could contain part of the machinery of membrane trafficking such as a guanine nucleotide exchange factor. If this band did prove to be a complex containing rab4 then it could be part of the mechanism of rab4 regulated translocation of vesicles from intracellular membranes to the plasma membrane with rab4 either being free and inactive in the cytosol or a part of the 150 kDa complex.

Such a sequence with rab4 cycling between being free in the cytosol and membrane bound has been partially described by Cormont *et al.* (1993). They detected rab4 in rat adipocytes. In basal adipocytes most of the protein was detected in the low and high density microsome fractions. Only a faint signal was detected in the cytosol and plasma membrane fraction of basal adipocytes. Both insulin and okadaic acid were shown to induce the redistribution of rab4 from the microsomal fraction to the cytosol. This change in the distribution of rab4 was also associated with the translocation of GLUT4 to the plasma membrane. They were also able to immunoprecipitate GLUT4 vesicles containing rab4. They reported that rab4 in the microsomal fraction was rapidly degraded even in the presence of protease inhibitors. The instability of rab4 could explain why free rab4 was not detected in the membrane fractions of the rat adipocytes in figure 3.37 even though it was detected in the cytosol. The ≈ 25 kDa band on this blot was stronger in the lane containing the supernatant of the insulin stimulated cells than the basal cells. The propensity of membrane associated rab4 to degrade may provide an alternative explanation to a strong complex for the inability to detect the ≈ 25 kDa band in the membrane fractions.

Rab3 is another small G-protein that has been shown to be associated with vesicles. In endocrine and neuronal cells it is associated with synaptic vesicles (Mollard *et al.*,

1990). Rab3d, a rab3 isotype, has been detected in mouse adipocytes and has been shown to increase during the differentiation of 3T3-L1 fibroblasts into adipocytes (Baldini *et al.*, 1992). The potential role of rab3d in the insulin stimulation of glucose transport in 3T3-L1 adipocytes was therefore investigated. Within rab proteins are effector domains through which rab may interact with effector proteins and the GTPase activating protein, GAP (Bourne *et al.*, 1991). Peptides from the effector domain of rab3a can in themselves activate rab3a regulated processes and have been shown to stimulate exocytosis in pancreatic acini (Padfield *et al.*, 1992) and mast cells (Oberhauser *et al.*, 1992). When the equivalent peptide from the effector domain of rab3d (amino acids 52-67) was added to permeabilized 3T3-L1 adipocytes no significant effect on either basal or insulin stimulated glucose transport was observed.

The effect of rab3d on the subcellular localisation of GLUT4 was also tested in CHO fibroblasts stably transfected with both GLUT4 and either wild type rab3d or mutant rab3d lacking either residues 62-67 or 62-68, part of the effector domain used in the peptides. There was no significant effect on the proportion of the total GLUT4 at the plasma membrane of the CHO fibroblasts transfected with either the wild type or a mutant rab3d. However, in the cells expressing the wild type rab3d there was a slight increase in the proportion of GLUT4 at the cell surface while in the cells expressing the deletion mutant 62-7 there was a slight decrease in the surface GLUT4. A much bigger effect was seen in the distribution of GLUT1. In the CHO fibroblasts expressing the wild type rab3d and GLUT4 there was a 2-fold increase in the level of GLUT1 at the cell surface. In cells expressing the mutant rab3d and GLUT4 the proportion of GLUT1 at the surface was similar to that of the nontransfected CHO cells. Providing that the CHO fibroblasts contain the necessary translocation machinery for rab3d to interact with then these results suggest that rab3d is not involved in the regulation of cell surface GLUT4. However, the result may be affected by digitonin treatment, as described in section 4.4. Whether rab3d is involved in the regulation of GLUT1 at the cell surface is less clear. The CHO fibroblasts transfected with either GLUT4 or

GLUT4 and rab3d expressed lower levels of GLUT1. The expression of GLUT4 was not the same in all the four cell lines either as the cells expressing rab3d expressed higher levels of GLUT4 than the cell line expressing GLUT4 alone. Thus it is possible that the differences in GLUT1 may merely be the result of different levels of GLUT4 expression rather than a direct effect of rab3d on GLUT1. The results do, however suggest a role for rab3d in the translocation of GLUT1 to the cell surface in CHO fibroblasts.

The absence of a significant effect on the distribution of GLUT4 or the transport rate with rab3d in CHO fibroblasts or the effector peptide in permeabilized 3T3-L1 adipocytes respectively is in agreement with the findings of Guerre-Millo *et al.* (1993) who were unable to detect rab3d in GLUT4 immunoprecipitated vesicles.

In summary, rab4 can be detected in the cytosol of adipocytes and may be involved in the translocation of GLUT4 in adipocytes. Rab3d does not appear to have a role in the translocation of GLUT4 although it may be involved in the redistribution of GLUT1 to the plasma membrane.

4.7 GTPγS and insulin stimulation in 3T3-L1 adipocytes

G-proteins are activated by the exchange of GDP for GTP. The proteins then remain active until the GTP is hydrolysed. One way to study the involvement of G-proteins in the insulin signalling pathway for the stimulation of glucose transport is to add the hydrolysis-resistant GTP analogue GTPγS to adipocytes. Because the GTPγS cannot be hydrolysed, once the G-protein has exchanged its GDP for GTPγS it remain active.

Baldini *et al.* (1991) looked at the effect of GTPγS on the subcellular localisation of GLUT4 in α-toxin permeabilized rat adipocytes. They found that 0.2 mM GTPγS induced an insulin-like translocation of GLUT4 to the plasma membrane.

When 0.2 mM GTPγS was added to basal 3T3-L1 adipocytes permeabilized with streptolysin-O it caused a rise in the rate of 2-deoxy-D-glucose uptake to a rate which was ≈ 60 % of the insulin stimulated rate. The GTPγS induced rise in 2-deoxy-D-glucose uptake was not additive with the insulin stimulated increase in transport. Indeed GTPγS may have a slight inhibitory effect on the insulin stimulated transport rate. The ≈ 3.5-fold increase in 2-deoxy-D-glucose uptake following insulin stimulation of the streptolysin-O permeabilized 3T3-L1 adipocytes and the increase in the basal transport rate in the presence of 0.2 mM GTPγS are similar to those of Suzuki *et al.* (1992) who measured 3-O-methyl-D-glucose uptake in electroporated rat adipocytes.

The effect of 0.2 mM GTPγS on the distribution of glucose transporters, as detected by ATB-BMPA photolabelling, was more pronounced than its effect on transport. In basal streptolysin-O permeabilized 3T3-L1 adipocytes GTPγS caused an increase in cell surface GLUT1 which was equivalent to that induced by insulin. The effect of GTPγS on the distribution of GLUT4 was greater. The concentration of cell surface GLUT4 in the adipocytes incubated with GTPγS was 2.5-fold higher concentration than the concentration of GLUT4 in the plasma membrane of insulin stimulated cells. This suggests that in the 3T3-L1 adipocytes exposed to 0.2 mM GTPγS virtually the entire GLUT4 pool was photolabelled and purified with the plasma membrane. Taken

together, the transport and photolabelling results suggest that while GTPγS increases the level of cell surface GLUT4 by either stimulating exocytosis and or inhibiting endocytosis GTPγS also lowers the intrinsic activity of GLUT4. Experiments in which the recycling of photolabelled GLUT4 was followed in the presence of either insulin or GTPγS, although unreliable, did indicate that GTPγS may inhibit endocytosis which would result in a large increase in level of GLUT4 in the plasma membrane.

Both Baldini *et al.* (1991) in rat adipocytes and Robinson *et al.* (1992) in 3T3-L1 adipocytes found that GTPγS caused the translocation of GLUT4 to the cell surface. However the amount of cell surface GLUT4 which they observed was similar to that obtained with insulin. This difference in the proportion of GLUT4 at the cell surface following treatment with GTPγS could be due to a difference in the method used to determine the distribution of GLUT4. Baldini *et al.* (1991) used α-toxin permeabilized rat adipocytes and detected the distribution of GLUT4 by Western blotting the subcellular fractions. Robinson *et al.* (1992) measured the level of GLUT4 at the plasma membrane of streptolysin-O 3T3-L1 adipocytes by immunolabelling plasma membrane lawns. In this study ATB-BMPA photolabelling and immunoprecipitation from purified plasma membrane was used to quantify the level of cell surface GLUT4. ATB-BMPA photolabelling is normally an accurate way of quantifying the level of transporters in the plasma membrane because it is impermeant and so only labels the cell surface transporters. Here, however, permeabilized 3T3-L1 adipocytes were photolabelled and so the entire pool of transporters was labelled, both surface and intracellular transporters. Thus the determination of the proportion of the transporters at the cell surface requires an effective purification of the photolabelled transporters in the plasma membrane from those in the low density microsomes by subcellular fractionation. The contamination of the plasma membrane fraction with microsomal transporters would reduce the difference between the basal and insulin stimulated levels of transporters at the plasma membrane. However, the level of GLUT4 in the plasma membrane following incubation with GTPγS, even allowing for

contamination of the plasma membrane fraction with labelled transporters from the microsomal fraction, was still about 2-fold higher than the insulin stimulated level and was higher than expected from the transport results. Thus an additional explanation of the high labelling results is required.

One explanation could be related to the ability of ATB-BMPA to photolabel glucose transporters in partially occluded vesicles (Satoh *et al.*, 1993). While such transporters can be photolabelled they cannot transport glucose. Thus while they would be detected by photolabelling they would have no effect on the rate of uptake of 2-deoxy-D-glucose. If these partially occluded transporters at the plasma membrane of 3T3-L1 adipocytes were lost from the plasma membrane while making the plasma membrane lawns by sonication but were retained with the plasma membrane by the subcellular fractionation procedure used here then this would account for the higher levels of GLUT4 at the cell surface. If a large proportion of the transporters were in such vesicles then this could also explain why the rate of transport which was lower than that expected from the photolabelling results.

It is possible that GTPγS may result in a large proportion of GLUT4 in partially occluded vesicles at the cell surface. In a cell-free system GTPγS was shown to inhibit transport between successive Golgi cisternae by preventing vesicles which had budded from the donor compartment from fusing with the acceptor compartment thus causing the vesicles to accumulate (Melançon *et al.*, 1987). GTPγS has also been shown to prevent budding from the donor compartment in yeast cells. In these cells when sar1p, a small protein with GTPase activity, was preloaded with GTPγS vesicles were unable to bud from the endoplasmic reticulum. This inhibition was proposed as being either due to GTPγS preventing interaction with the transport machinery or, more likely, because GTP hydrolysis is required for vesicle budding (Barlowe *et al.*, 1993). GTPγS has been shown initially to stimulate vesicle fusion but to ultimately to inhibit vesicular trafficking (Rexach and Schekman, 1991). Such an effect might result in the accumulation of GLUT4 in the plasma membrane. GTPγS is believed to have this effect

by preventing the recycling between the acceptor and donor membranes of the components required for vesicular transport, such as the rab proteins. The recycling of rab requires the GTP bound to rab to be hydrolysed at the acceptor membrane so that the rab GDP can be recycled back to the donor membrane in association with GDI (GDP-dissociation inhibitor). This association occurs only when the rab is in the GDP bound form (Araki et *al.*, 1990). Rab proteins have being implicated in the movement of vesicles to and from the plasma membrane with rab4 involved in the translocation of vesicles to the plasma membrane of rat adipocytes (Cormont et *al.*, 1993) and rab5 implicated in the movement of vesicles from the plasma membrane (Ullrich et *al.*, 1994). Therefore GTPγS, by any of the above mechanisms, could result in an increase of partially occluded GLUT4 at the plasma membrane. If the partially occluded GLUT4 is in vesicles that are either unable to correctly fuse with or bud from the plasma membrane then they may be lost from the plasma membrane fraction during certain fraction procedures such as sonication.

An alternative mechanism whereby GTPγS may have an insulin-like effect is via a ras type G-protein involved in the insulin signalling pathway. The insulin receptor activates ras proteins via Sos (the product of the son of sevenless gene), a guanine-nucleotide dissociation stimulator protein. Sos itself is activated following its association with GRB2 (growth factor receptor-bound protein 2) when GRB2 is associated with the tyrosine phosphorylated IRS-1. GRB2 interacts with the SH2 domain of IRS-1 while Sos binds to the SH3 domain of GRB2 (Skolnik et *al.*, 1993). The IRS-1-GRB2-Sos complex then activates ras by exchanging GDP for GTP (Baltensperger et *al.*, 1993). The activated ras can then activate the effector proteins which include, either directly or indirectly the ERK or MAP kinases leading to a serine/threonine phosphorylation cascade (Thomas et *al.*, 1992). It has been suggested that ras proteins may be involved in the translocation of glucose transport proteins in 3T3-L1 adipocytes. When N-ras^{61K}, a activated mutant, was transfected into 3T3-L1 adipocytes then the transport rate was similar to the insulin stimulated rate in nontransfected adipocytes. In the

transfected cells insulin had no effect on the transport rate. In the adipocytes, transfection with N-ras^{61K} resulted in an ≈ 1.5-fold increase in the amount of GLUT1 in the plasma membrane. The transfected cells had a much reduced total amount of GLUT4 but virtually all the GLUT4 was detected in the plasma membrane. Insulin had no effect on the distribution of GLUT1 and GLUT4 in the transfected cells (Kozma *et al.*, 1993). The insulin/ras activated MAP kinases have been shown to phosphorylate rab4 and this event might regulate the translocation of GLUT4 (Cormont *et al.*, 1994).

The effect of N-ras^{61K} on the distribution of GLUT1 and GLUT4 is similar to that for GTPγS in the streptolysin-*O* permeabilized 3T3-L1 adipocytes. This suggests that ras proteins are indeed intermediates in the insulin signalling pathway and that GTPγS interacts with the pathway at this point. The two effects are not directly comparable, however, because of the low level of GLUT4 expression in the 3T3-L1 adipocytes expressing N-ras^{61K}. Another difference between the results is the effect on the transport rate, although these too are not comparable for the same reason. GTPγS, unlike N-ras^{61K}, did not stimulate transport to the same degree as insulin or to a level expected from the photolabelling data. GTPγS did not, however, inhibit the insulin stimulated rate of transport. This suggests therefore that either the ras-like effect of GTPγS is insufficient on its own to fully activate the insulin signalling pathway or that GTPγS is also having an inhibitory effect at other places in the pathway and translocation mechanism.

GTPγS, in addition to its effect on G-proteins, may have a more direct effect on GLUT4 itself. Baldini *et al.* (1991) reported that they were unable to detect all the GLUT4 in the presence of GTPγS. This, they suggested, was due to a GTPγS induced conformational change in GLUT4. This change may help to explain the lower percentage of GLUT4 at the cells surface as detected by Western blotting in their study compared to the present study using ATB-BMPA photolabelling and immunoprecipitation. Such a conformational change may cause a decrease in the transport capacity of GLUT4 in the presence of GTPγS.

This inhibitory effect of GTPγS on GLUT4 has been reported by others. When Schürmann *et al.* (1989; 1992a) added GTPγS and GTP to insulin stimulated vesicles they found a 50 % inhibition in the rate of transport, an effect that was lost in vesicles from basal adipocytes or when vesicles were partially purified from G-proteins. GTPγS has also been reported to bind to GLUT4 itself (Studelska *et al.*, 1993). It was suggested that GTPγS might act as a gate and lower the intrinsic activity of GLUT4 or maintain it at the basal level. GTP analogues have also been reported to lower the rate of uptake of 2-deoxy-D-glucose in *Xenopus* oocytes expressing GLUT1 (Wellner *et al.*, 1993), although this was suggested as being due to the inhibition of hexokinase activity which would also result in a decreased rate of uptake in the 3T3-L1 adipocytes. Thus GTPγS may be inhibiting the activity of GLUT4 and the binding of GTP to the transporter may therefore be a mechanism for lowering the intrinsic activity of transporters in basal adipocytes.

It is not possible to determine from these results the effect of GTPγS on the transport rate in insulin stimulated 3T3-L1 adipocytes. The rate of 2-deoxy-D-glucose uptake with adipocytes stimulated with insulin in the presence of GTPγS was similar to that of insulin alone and was higher than the rate in the presence of GTPγS alone. This could be the result of an insulin induced reversal in the inhibitory effect of GTPγS on transporter activity thus causing a rise in the intrinsic activity of the transporters. A second explanation could be due to a resumption in the translocation of transporters to and from the plasma membrane.

The results from both the rab proteins and GTPγS do suggest a role for G-proteins, although perhaps not rab3d, in the translocation of transporters to and from the plasma membrane of 3T3-L1 adipocytes. The effect of GTPγS on adipocytes could be a broad one. It may be stimulating and then inhibiting the translocation mechanism while at the same time activating the G-proteins involved in the insulin signalling pathway and lowering the intrinsic activity of the transporters themselves, maintaining this at basal levels.

4.8 Conclusions

The aim of this project was to investigate the action of insulin on glucose transport in adipocytes. It has, however, been difficult to draw specific conclusions from some of the results presented here because of the level of errors in the data. One reason why experiments were not repeated to a higher degree of statistical significance is that during the course of the experiments results were published in the same area.

The use of an ATB-BMPA displacement method enabled the resolution of the separate kinetic properties of the glucose transporters GLUT1 and GLUT4 in 3T3-L1 adipocytes. The half maximal displacement by 3-O-methyl-D-glucose occurred at 20 mM for GLUT1 and 7.0 mM for GLUT4. The calculated transport capacities (turnover number/K_m) were 0.36 x 10^4 $mM^{-1}{\cdot}min^{-1}$ for GLUT1 and 1.13 x 10^4 $mM^{-1}{\cdot}min^{-1}$ for GLUT4. The turnover numbers were, however, similar, 7.2 x 10^4 min^{-1} for GLUT1 and 7.9 x 10^4 min^{-1} for GLUT4. Thus the ≈ 3-fold higher transport capacity of GLUT4 at low glucose concentrations is mainly due to the higher K_m of GLUT1, an effect also observed in *Xenopus* oocytes expressing either GLUT1 or 4 (Nishimura *et al.*, 1993).

Okadaic acid, a phosphatase inhibitor, has the effect of increasing general levels of cellular phosphorylation. Adipocytes were treated with okadaic acid to investigate the potential role of phosphorylation in the insulin signalling pathway to the glucose transporter. It was found to increase both 3-O-methyl-D-glucose uptake and the level of cell surface GLUT4 photolabelling in unstimulated adipocytes. In insulin stimulated rat adipocytes okadaic acid reduced the transport rate and the level of cell surface transporter photolabelling. Okadaic acid appears to alter both the intrinsic activity and translocation of transporters. The broad effects of okadaic acid, however, make it difficult to be certain what the specific effects of okadaic acid are on insulin stimulated glucose transport. The tyrosine kinase inhibitor α-cyano-3,4-dihydroxythiocinnamide (453C89) was used to examine the role of tyrosine kinases in the insulin induced increase in glucose transport. The inhibitor appeared not to inhibit the insulin receptor

tyrosine kinase but to inhibit 3-*O*-methyl-D-glucose uptake, perhaps by reducing the intrinsic activity of GLUT4. These findings and those of others (Smith *et al.*, 1993; Young *et al.*, 1993) suggest that the tyrosine kinase inhibitors may not be specific and care should be taken in the interpretation of results.

By expressing GLUT4 in the insulin insensitive fibroblast cell lines COS-7 and CHO, GLUT1 and GLUT4 were shown to adopt a different distribution between the cell surface and the intracellular pools. This suggests that the subcellular distribution of GLUT4, rather than being imposed upon it by the cell in which it expressed, is intrinsic to the protein, as has also been shown by others (e.g. Schürmann *et al.*, 1992b; Piper *et al.*, 1993a). The addition of peptides corresponding to different regions of GLUT1 and GLUT4 to streptolysin-*O* permeabilized 3T3-L1 adipocytes implicated the N-terminal region of GLUT4 in transporter recognition. The addition of a peptide corresponding to the N terminus of GLUT4 increased the transport rate and the level of cell surface GLUT4. This suggests that the N terminus of GLUT4 may be involved in the sequestration of GLUT4 from the plasma membrane.

Both rab4 and rab3d have been implicated in the trafficking of GLUT4 containing vesicles. Rab4 was detected in the supernatant of rat adipocytes using an anti-rab4 antiserum. Rab4 has also been shown to recycle in response to insulin and to be associated with GLUT4 containing vesicles (Cormont *et al.*, 1993). The expression of Rab3d in CHO fibroblasts expressing GLUT4 appeared not to affect the subcellular distribution of GLUT4 but may have affected the distribution of GLUT1. The nonhydrolyzable GTP analogue, GTPγS, was found to cause a small increase in basal 2-deoxy-D-glucose uptake but had little effect on the insulin stimulated transport rate in streptolysin-*O* permeabilized 3T3-L1 adipocytes. It also appears to cause the accumulation of inactive GLUT4 at the cell surface. Thus G proteins may be involved in insulin signalling and glucose transporter translocation. However the wide ranging effects of GTPγS make a specific interpretation of the results difficult.

In summary, the results presented here demonstrate that the translocation of GLUT4 is the major mechanism whereby insulin increases the rate of glucose uptake in adipocytes and that the N terminus of GLUT4 may be involved in the targeting and recycling of this insulin responsive glucose transporter. The findings also suggest a role for phosphorylation events and G-proteins in the insulin signalling pathway and the translocation pathway. They also, however, highlight the danger of using compounds whose effects are not or may not be specific to investigate specific events.

5.0 References

Akiyama, T., Ishida, J., Nakagawa, S., Ogawara, H., Watanabe, S., Itoh, N., Shibuya, M. and Fukami, Y. (1987). Genistein, a specific inhibitor of tyrosine-specific protein kinases. *J. Biol. Chem.* **262**, 5592-5595

Alber, A., Smith, J. A., Randazzo, P. A., Rothenberg, P. L. and Jarett, L. (1992). Genistein differentially inhibits postreceptor effects of insulin in rat adipocytes without inhibiting the insulin receptor kinase. *J. Biol. Chem.* **267**, 3946-3951

Allard, W. J. and Lienhard, G. E. (1985). Monoclonal antibodies to the glucose transporter from human erythrocytes. *J. Biol. Chem.* **260**, 8668-8675

Araki, S., Kikuchi, A., Hata, Y., Isomura, M. and Takai, Y. (1990). Regulation of reversible binding of *smg* p25A, a ras p21-like GTP-binding protein, to synaptic plasma membranes and vesicles by its specific regulatory protein, GDP dissociation inhibitor. *J. Biol. Chem.* **265**, 13007-13015

Asano, T., Shibasaki, Y., Kasuga, M., Kanazawa, Y., Takaku, F., Akanuma, Y. and Oka, Y. (1988). Cloning of a rabbit brain glucose transporter cDNA and alteration of glucose transporter mRNA during tissue development. *Biochem. Biophys. Res. Commun.* **154**, 1204-1211

Asano, T., Shibasaki, Y., Ohno, S., Taira, H., Lin, J.-L., Kasuga, M., Kanazawa, Y., Akanuma, Y., Takaku, F. and Oka, Y. (1989). Rabbit brain glucose transporter responds to insulin when expressed in insulin-sensitive Chinese hamster ovary cells. *J. Biol. Chem.* **264**, 3416-3420

Asano, T., Katagiri, H., Takata, K., Lin, J.-L., Ishihara, H., Inukai, K., Tsukuda, K., Kikuchi, M., Hirano, H., Yazaki, Y. and Oka, Y. (1991). The role of *N*-glycosylation of GLUT1 for glucose transport activity. *J. Biol. Chem.* **266**, 24632-24636

Asano, T., Katagiri, H., Takata, K., Tsukuda, K., Lin, J.-L., Ishihara, H., Inukai, K., Hirano, H., Yazaki, Y. and Oka, Y. (1992a). Characterization of GLUT3 protein expressed in Chinese hamster ovary cells. *Biochem. J.* **288**, 189-193

Asano, T., Takata, K., Katagiri, H., Tsukuda, K., Lin, J.-L., Ishihara, H., Inukai, K., Hirano, H., Yazaki, Y. and Oka, Y. (1992b). Domains responsible for the differential targeting of glucose transporter isoforms. *J. Biol. Chem.* **267**, 19636-19641

Asano, T., Takata, K., Katagiri, H., Ishihara, H., Inukai, K., Anai, M., Hirano, H., Yazaki Y. and Oka, Y. (1993). The role of *N*-glycosylation in the targeting and stability of GLUT1 glucose transporter. *FEBS Lett.* **324**, 258-261

Axelrod, J. D. and Pilch, P. F. (1983). Unique cytochalasin B binding characteristics of the hepatic glucose carrier. *Biochemistry* **22**, 2222-2227

Backer, J. M., Myers Jr., M. G., Shoelson S. E., Chin, D. J., Sun, X. J., Miralpeix, M., Hu, P., Margolis, B., Skolnik, E. Y., Schlessinger, J. and White, M. F. (1992a). Phosphatidylinositol 3'-kinase is activated by association with IRS-1 during insulin stimulation. *EMBO J.* **11**, 3469-3479

Backer, J. M., Shoelson, S. E., Weiss, M. A., Hua, Q. X., Cheatham, R. B., Haring, E., Cahill, D. C. and White, M. F. (1992b). The insulin receptor juxtamembrane region contains two independent tyrosine/β-turn internalization signals. *J. Cell Biol.* **118**, 831-839

Baldini, G., Hohman, R., Charron, M. J. and Lodish, H. F. (1991). Insulin and nonhydrolyzable GTP analogs induce translocation of GLUT4 to the plasma membrane in α-toxin-permeabilized rat adipose cells. *J. Biol. Chem.* **266**, 4037-4040

Baldini, G., Hohl, T., Lin, H. Y. and Lodish, H. F. (1992). Cloning of a Rab3 isotype predominately expressed in adipocytes. *Proc. Natl. Acad. Sci. USA* **89**, 5049-5052

Baldwin, S. A. (1993). Mammalian passive glucose transporters: members of an ubiquitous family of active and passive transport proteins *Biochim. Biophys. Acta* **1154**, 17-49

Baltensperger, K., Kozma, L. M., Cherniack, A. D., Klarlund, J. K., Chawla, A., Banerjee, U. and Czech, M. P. (1993). Binding of the ras activator son of sevenless to insulin receptor substrate-1 signalling complexes. *Science* **260**, 1950-1952

Barlowe, C., d'Enfert, C. and Schekman, R. (1993). Purification and characterization of SAR1p, a small GTP-binding protein required for transport vesicle formation from the endoplasmic reticulum. *J. Biol. Chem.* **268**, 873-879

Barnett, J. E. G., Holman, G. D., Chalkley, R. A. and Munday, K. A. (1975). Evidence for two asymmetric conformational states in the human erythrocyte sugar-transport system. *Biochem. J.* **145**, 417-429

Begum, N., Sussman, K. E. and Draznin, B. (1991). High levels of cytosolic free calcium inhibit dephosphorylation of insulin receptor and glycogen synthase. *Cell Calcium* **12**, 423-430

Begum, N., Sussman, K. E. and Draznin, B. (1992). Calcium-induced inhibition of phosphoserine phosphatase in insulin target cells is mediated by the phosphorylation and activation of inhibitor 1. *J. Biol. Chem.* **267**, 5959-5963

Begum, N., Leitner, W., Reusch, J. E.-B., Sussman, K. E. and Draznin, B. (1993a). GLUT-4 phosphorylation and its intrinsic activity. *J. Biol. Chem.* **268**, 3352-3356

Begum, N., Olefsky, J. M. and Draznin, B. (1993b). Mechanism of impaired metabolic signaling by a truncated human insulin receptor. *J. Biol. Chem.* **268**, 7917-7922

Bell, G. I., Kayano, T., Buse, J. B., Burant, C. F., Takeda, J., Lin, D., Fukumoto, H. and Seino, S. (1990). Molecular biology of mammalian glucose transporters. *Diabetes Care* **13**, 198-208

Bennett, M. K. and Scheller, R. H. (1993). The molecular machinery for secretion is conserved from yeast to neurons. *Proc. Natl. Acad. Sci. USA* **90**, 2559-2563

Berra, E., Diaz-Meco, M. T., Dominguez, I., Municio, M. M., Sanz, L., Lozano, J., Chapkin, R. S. and Moscat, J. (1993). Protein kinase C ζ isoform is critical for mitogenic signal transduction. *Cell* **74**, 555-563

Bialojan, C. and Takai, A. (1988). Inhibitory effect of a marine-sponge toxin, okadaic acid, on protein phosphatases. *Biochem. J.* **256**, 283-290

Bianchini, L., Woodside, M., Sardet, C., Pouyssegur, J., Takai, A. and Grinstein, S. (1991). Okadaic acid, a phosphatase inhibitor, induces activation and phosphorylation of the Na^+/H^+ antiport. *J. Biol. Chem.* **266**, 15406-15413

Birnbaum, M. J., Haspel, H. C. and Rosen, O. M. (1986). Cloning and characterization of a cDNA encoding the rat brain glucose-transporter protein. *Proc. Natl. Acad. Sci. USA* **83**, 5784-5788

Birnbaum, M. J. (1989). Identification of a novel gene encoding an insulin-responsive glucose transporter protein. *Cell* **57**, 305-315

Birnbaum, M. J. (1992). The insulin-sensitive glucose transporter. *Int. Rev. Cytol.* **137A**, 239-297

Birnbaumer, L. (1990). G proteins in signal transduction. *Annu. Rev. Pharmacol. Toxicol.* **30**, 675-705

Blackmore, P. F. and Augert, G. (1989). Effect of hormones on cytosolic free calcium in adipocytes. *Cell Calcium* **10**, 561-568

Blackshear, P. J., Witters, L. A., Girard, P. R., Kuo, J. F. and Quamo, S. N. (1985). Growth factor-stimulated protein phosphorylation in 3T3-L1 cells. *J. Biol. Chem.* **260**, 13304-13315

Blackshear, P. J., Haupt, D. M., App, H. and Rapp, U. R. (1990). Insulin activates the raf-1 protein kinase. *J. Biol. Chem.* **265**, 12131-12134

Blok, J., Gibbs, E. M., Lienhard, G. E., Slot, J. W. and Geuze, H. J. (1988). Insulin-induced translocation of glucose transporters from post-Golgi compartments to the plasma membrane of 3T3-L1 adipocytes. *J. Cell Biol.* **106**, 69-76

Bourne, H. R., Sanders, D. A. and McCormick, F. (1991). The GTPase superfamily: conserved structure and molecular mechanism. *Nature* **349**, 117-127

Bradford, M. M. (1976). A rapid and sensitive method for the quantitation of microgram quantities of protein utilizing the principle of protein-dye binding. *Anal. Biochem.* **72**, 248-254

Brown, S. J., Gould, G. W., Davis, A., Baldwin, S. A., Lienhard, G. E. and Gibbs, E. M. (1988). Characterization of vesicles containing insulin-responsive intracellular glucose transporters isolated from 3T3-L1 adipocytes by an improved procedure. *Biochim. Biophys. Acta* **971**, 339-350

Burant, C. F., Takeda, J., Brot-Laroche, E., Bell, G. I. and Davidson, N. O. (1992). Fructose transporter in human spermatozoa and small intestine is GLUT5. *J. Biol. Chem.* **267**, 14523-14526

Cain, C. C., Trimble, W. S. and Lienhard, G. E. (1992). Members of the VAMP family of synaptic vesicle proteins are components of glucose transporter-containing vesicles from rat adipocytes. *J. Biol. Chem.* **267**, 11681-11684

Cairns, M. T., Alvarez, J., Panico, M., Gibbs, A. F., Morris, H. R., Chapman, D. and Baldwin, S. A. (1987). Investigation of the structure and function of the human erythrocyte glucose transporter by proteolytic dissection. *Biochim. Biophys. Acta* **905**, 295-310

Calderhead, D. M. and Lienhard, G. E. (1988). Labeling of glucose transporters at the cell surface in 3T3-L1 adipocytes. *J. Biol. Chem.* **263**, 12171-12174

Calderhead, D. M., Kitagawa, K., Tanner, L. I., Holman, G. D. and Lienhard, G. E. (1990). Insulin regulation of two glucose transporters in 3T3-L1 adipocytes. *J. Biol. Chem.* **265**, 13800-13808

Carruthers, A. (1986). ATP regulation of the human red cell sugar transporter. *J. Biol. Chem.* **261**, 11028-11037

Carruthers, A. (1990). Facilitated diffusion of glucose. *Physiol. Rev.* **70**, 1135-1176

Carruthers, A. and Helgerson, A. L. (1989). The human erythrocyte sugar transporter is also a nucleotide binding protein. *Biochemistry* **28**, 8337-8346

Charron, M. J., Brosius III, F. C., Alper, S. L. and Lodish, H. F. (1989). A glucose transport protein expressed predominately in insulin-responsive tissues. *Proc. Natl. Acad. Sci. USA* **86**, 2535-2539

Chen, J., Martin, B. L. and Brautigan, D. L. (1992). Regulation of protein serine-threonine phosphatase type-2A by tyrosine phosphorylation. *Science* **257**, 1261-1264

Chin, J. E., Dickens, M. Tavare, J. M. and Roth, R. A. (1993). Overexpression of protein kinase C isoenzymes α, βI, γ, and ε in cells overexpressing the insulin receptor. *J. Biol. Chem.* **268**, 6338-6347

Chin, J. J., Jung, E. K. Y., Chen, V. and Jung, C. Y. (1987). Structural basis of human erythrocyte glucose transporter function in proteoliposome vesicles: circular dichroism measurements. *Proc. Natl. Acad. Sci. USA* **84**, 4113-4116

Ciaraldi, T. P. and Maisel, A. (1989). Role of guanine nucleotide regulatory proteins in insulin stimulation of glucose transport in rat adipocytes. *Biochem. J.* **264**, 389-396

Clancy, B. M. and Czech, M. P. (1990). Hexose transport stimulation and membrane redistribution of the glucose transporter isoforms in response to cholera toxin, dibutyryl cyclic AMP and insulin in 3T3-L1 adipocytes. *J. Biol. Chem.* **265**, 12434-12443

Clark, A. E. and Holman, G. D. (1990). Exofacial photolabelling of the human erythrocyte glucose transporter with an azitrifluoroethylbenzoyl-substituted bismannose. *Biochem. J.* **269**, 615-622

Clark, A. E., Holman, G. D. and Kozka, I. J. (1991). Determination of the rates of appearance and loss of glucose transporters at the cell surface of rat adipose cells. *Biochem. J.* **278**, 235-241

Clarke, J. F., Young, P. W., Yonezawa, K., Kasuga, M. and Holman, G. D. (1994). Inhibition of the translocation of GLUT1 and GLUT4 in 3T3-L1 cells by the phosphatidylinositol 3-kinase inhibitor, wortmannin. *Biochem. J.* **300**, 631-635

Cleland, W. W. (1979). Statistical analysis of enzyme kinetic data. *Methods Enzymol.* **63**, 103-138

Cohen, P., Holmes, C. F. B. and Tsukitani, Y. (1990). Okadaic acid: a new probe for the study of cellular regulation. *Trends Biochem. Sci.* **15**, 98-102

Cope, D. L., Holman, G. D., Baldwin, S. A. and Wolstenholme, A. J. (1994). Domain assembly of the GLUT1 glucose transporter. *Biochem. J.* **300**, 291-294

Cormont, M., Tanti, J.-F., Grémeaux, T., Van Obberghen, E. and Le Marchand-Brustel, Y. (1991). Subcellular distribution of low molecular weight guanosine triphosphate-binding proteins in adipocytes: colocalization with the glucose transporter GLUT4. *Endocrinology* **129**, 3343-3350

Cormont, M., Tanti, J.-F., Zahraoui, A., Van Obberghen, E., Tavitian, A. and Le Marchand-Brustel, Y. (1993). Insulin and okadaic acid induce rab4 redistribution in adipocytes. *J. Biol. Chem.* **268**, 19491-19497

Cormont, M., Tanti, J.-F., Zahraoui, A., Van Obberghen, E. and Le Marchand-Brustel, Y. (1994). Rab4 is phosphorylated by the insulin-activated extracellular-signal-regulated kinase ERK1. *Eur. J. Biochem.* **219**, 1081-1085

Corvera, S., Jaspers, S. and Pasceri, M. (1991). Acute inhibition of insulin-stimulated glucose transport by the phosphatase inhibitor, okadaic acid. *J. Biol. Chem.* **266**, 9271-9275

Crespo, P., Xu, N., Simonds, W. F. and Gutkind, J. S. (1994). Ras-dependent activation of MAP kinase pathway mediated by G-protein βγ subunits. *Nature* **369**, 418-420

Cushman, S. W. and Wardzala, L. J. (1980). Potential mechanism of insulin action on glucose transport in the isolated rat adipose cell. *J. Biol. Chem.* **255**, 4758-4762

Czech, M. P., Chawla, A., Woon, C.-W., Buxton, J., Armoni, M., Tang, W., Joly, M., and Corvera, S. (1993). Exofacial-epitope-tagged glucose transporter chimeras reveal COOH-terminal sequences governing cellular localization. *J. Cell Biol.* **123**, 127-135

Davidson, N. O., Hausman, A. M. L., Ifkovits, C. A., Buse, J. B., Gould, G. W., Burant, C. F. and Bell, G. I. (1992). Human intestinal glucose transporter expression and localization of GLUT5. *Am. J. Physiol.* **262**, C795-800

Davies, A., Ciardelli, T. L., Lienhard, G. E., Boyle, J. M., Whetton, A. D., Baldwin, S. A. (1990). Site-specific antibodies as probes of the topology and function of the human erythrocyte glucose transporter. *Biochem. J.* **266**, 799-808

Davis, H. W. and McDonald, J. M. (1990). Insulin receptor function is inhibited by guanosine 5'[γ-thio]triphosphate (GTP[S]). *Biochem. J.* **270**, 401-407

de Herreros, A. G. and Birnbaum, M. J. (1989). The acquisition of increased insulin-responsive hexose transport in 3T3-L1 adipocytes correlates with expression of a novel transporter gene. *J. Biol. Chem.* **264**, 19994-19999

Denton, R. M. (1986). Early events in insulin actions. *Adv. Cyclic Nucleotide Protein Phosphorylation Research* **20**, 293-341

Desbois, C., Capeau, J., Hainault, I., Wicek, D., Reynet, C., Veissière, M., Caron, M., Picard, J., Guerre-Millo, M. and Cherqui, G. (1992). Differential role of insulin receptor autophosphorylation sites 1162 and 1163 in the long-term insulin stimulation of glucose transport, glycogenesis and protein synthesis. *J. Biol. Chem.* **267**, 13488-13497

Devés, R. and Krupka, R. M. (1984). The relation ship between substrate dissociation constants derived from transport experiments and from the equilibrium binding assays. *Biochim. Biophys. Acta* **769**, 455-460

Ebina, Y., Ellis, L., Jarnagin, K., Edery, M., Graf, L., Clauser, E., Ou, J., Masiarz, F., Kan, Y. W., Goldfine, I. D., Roth, R. A. and Rutter, W. J. (1985). The human insulin receptor cDNA: the structural basis for hormone-activated transmembrane signalling. *Cell* **40**, 747-758

Elliott, K. R. F. and Craik, J. D. (1983). Sugar transport across the hepatocyte plasma membrane. *Biochem. Soc. Trans.* **10**, 12-13

Ellis, L., Clauser, E., Morgan, D. O., Edery, M., Roth, R. A. and Rutter, W. J. (1986). Replacement of insulin receptor tyrosine residues 1162 and 1163 compromises insulin-stimulated kinase activity and uptake of 2-deoxyglucose. *Cell* **45**, 721-732

Ezaki, O. and Kono, T. (1982). Effects of temperature of basal and insulin-stimulated glucose transport activities in fat cells. *J. Biol. Chem.* **257**, 14306-14310

Farese, R. V., Davis, J. S., Barnes, D. E., Standaert, M. L., Babischkin, J. S., Hock, R., Rosic, N. K. and Pollet, R. J. (1985). The *de novo* phospholipid effect of insulin is associated with increases in diacylglycerol, but not inositol phosphates or cytosolic Ca^{2+}. *Biochem. J.* **231**, 269-278

Fingar, D. C., Hausdorff, S. F., Blenis, J. and Birnbaum, M. J. (1993). Dissociation of pp70 ribosomal protein S6 kinase from insulin-stimulated glucose transport in 3T3-L1 adipocytes. *J. Biol. Chem.* **268**, 3005-3008

Fingar, D. C. and Birnbaum, M. J. (1994a). Characterization of the mitogen-activated protein kinase/90-kilodalton ribosomal protein S6 kinase signaling pathway in 3T3-L1 adipocytes and its role in insulin-stimulated glucose transport. *Endocrinology* **134**, 728-735

Fingar, D. C. and Birnbaum, M. J. (1994b). A role for raf-1 in the divergent signaling pathways mediating insulin-stimulated glucose transport. *J. Biol. Chem.* **269**, 10127-10132

Fischbarg, J., Cheung, M., Czegledy, F., Li, J., Iserovich, P., Kuang, K., Hubbard, J., Garner, M., Rosen, O. M., Golde, D. W. and Vera, J. C. (1993). Evidence that facilitative glucose transporters may fold as β-barrels. *Proc. Natl. Acad. Sci. USA* **90**, 11658-11662

Flier, J. S., Mueckler, M., McCall, A. L. and Lodish, H. F. (1987a). Distribution of glucose transporter messenger RNA transcripts in tissues of rat and man. *J. Clin. Invest.* **79**, 657-661

Flier, J. S., Mueckler, M. M., Usher, P. and Lodish, H. F. (1987b). Elevated levels of glucose transport and transporter messenger RNA are induced by *ras* or *src* oncogenes. *Science* **235**, 1492-1495

Froehner, S. C., Davies, A., Baldwin, S. A. and Lienhard, G. E. (1988). The blood-nerve barrier is rich in glucose transporter. *J. Neurocytol.* **17**, 173-178

Frost, S. C. and Lane, M. D. (1985). Evidence for the involvement of vicinal sulfhydryl groups in insulin-activated hexose transport by 3T3-L1 adipocytes. *J. Biol. Chem.* **260**, 2646-2652

Fukumoto, H., Seino, S., Imura, H., Seino, Y., Eddy, R. L., Fukushima, Y., Byers, M. G., Shows, T. B. and Bell, G. I. (1988). Sequence, tissue distribution and chromosomal localization of mRNA encoding a human glucose transporter-like protein. *Proc. Natl. Acad. Sci. USA* **85**, 5434-5438

Fukumoto, H., Kayano, T., Buse, J. B., Edwards, Y., Pilch, P. F., Bell, G. I. and Seino, S. (1989). Cloning and characterization of the major insulin-responsive glucose transporter expressed in human skeletal muscle and other insulin-responsive tissues. *J. Biol. Chem.* **264**, 7776-7779

Garippa, R. J., Judge, T. W., James, D. E. and McGraw, T. E. (1994). The amino terminus of GLUT4 functions as an internalization motif but not an intracellular retention signal when substituted for the transferrin receptor cytoplasmic domain. *J. Cell Biol.* **124**, 705-715

Gazit, A., Yaish, P., Gilon, C. and Levitzki, A. (1989). Tyrphostins I: synthesis and biological activity of protein tyrosine kinase inhibitors. *J. Med. Chem.* **32**, 2344-2352

Geck, P. (1971). Properties of a carrier model for the transport of sugars by human erythrocytes. *Biochim. Biophys. Acta* **241**, 462-472

Gibbs, E. M., Allard, W. J. and Lienhard, G. E. (1986). The glucose transporter in 3T3-L1 adipocytes is phosphorylated in response to phorbol ester but not in response to insulin. *J. Biol. Chem.* **261**, 16597-16603

Gibbs, E. M., Calderhead, D. M., Holman, G. D. and Gould, G. W. (1991). Phorbol ester only partially mimics the effects of insulin on glucose transport and glucose-transporter distribution in 3T3-L1 adipocytes. *Biochem. J.* **275**, 145-150

Gilman, A. G. (1987). G proteins: transducers of receptor-generated signals. *Annu. Rev. Biochem.* **56**, 615-649

Gluzman, Y. (1981). SV40-transformed simian cells support the replication of early SV40 mutants. *Cell* **23**, 175-182

Goldstein, B. J. and Dudley, A. L. (1990). The rat insulin receptor: primary structure and conservation of tissue-specific alternative messenger RNA splicing. *Mol. Endocrinol.* **4**, 235-244

Gould, G. W. and Holman, G. D (1993). The glucose transporter family: structure, function and tissue-specific expression. *Biochem. J.* **295**, 329-341

Gould, G. W. and Lienhard, G. E. (1989). Expression of a functional glucose transporter in *Xenopus* oocytes. *Biochemistry* **28**, 9447-9452

Gould, G. W., Thomas, H. M., Jess, T. J. and Bell, G. I. (1991). Expression of human glucose transporters in *Xenopus* oocytes: Kinetic characterization and substrate specificities of the erythrocyte, liver, and brain isoforms. *Biochemistry* **30**, 5139-5145

Gould, G. W., Merrall, N. W., Martin, S., Jess, T. J., Campbell, I. W., Calderhead, D. M., Gibbs, E. M., Holman, G. D. and Plevin, R. J. (1994). Growth factor-induced stimulation of hexose transport in 3T3-L1 adipocytes: evidence that insulin-induced translocation of GLUT4 is independent of activation of MAP kinase. *Cell. Signal.* **6**, 313-320

Green, H. and Kehinde, O. (1974). Sublines of mouse 3T3 cells that accumulate lipid. *Cell* **1**, 113-114

Green, H. and Meuth, H. (1974). An established preadipose cell line and its differentiation in culture. *Cell* **3**, 127-133

Guerre-Millo, M., Baldini, G., Lodish, H. F. and Cushman, S. W. (1993). Subcellular distribution of rab3d in rat adipose cell. *Diabetes* **42**, 167A

Hall, A. (1990). The cellular functions of small GTP-binding proteins. *Science* **249**, 635-640

Haney, P. M., Slot, J. W., Piper, R. C., James, D. E. and Mueckler, M. (1991). Intracellular targeting of the insulin-regulatable glucose transporter (GLUT4). is isoform specific and independent of cell type. *J. Cell Biol.* **114**, 689-699

Hashiramoto, M., Kadowaki, T., Clark, A. E., Muraoka, A., Momomura, K., Sakura, H., Tobe, K., Akanuma, Y., Yazaki, Y., Holman, G. D. and Kasuga, M. (1992). Site-directed mutagenesis of GLUT1 in helix 7 residue 282 results in perturbation of exofacial ligand binding. *J. Biol. Chem.* **267**, 17502-17507

Haspel, H. C., Wilk, E. W., Birnbaum, M. J., Cushman, S. W. and Rosen, O. M. (1986). Glucose deprivation and hexose transporter polypeptides of murine fibroblasts. *J. Biol. Chem.* **261**, 6778-6789

Haystead, T. A. J., Sim, A. T. R., Carling, D., Honnor, R. C., Tsukitani, Y., Cohen, P. and Hardie, D. G. (1989). Effects of the tumour promoter okadaic acid on intracellular protein phosphorylation and metabolism. *Nature* **337**, 78-81

Haystead, T. A. J., Weiel, J. E. Litchfield, D. W., Tsukitani, Y., Fischer, E. H. and Krebs, E. G. (1990). Okadaic acid mimics the action of insulin in stimulating protein kinase activity in isolated adipocytes. *J. Biol. Chem.* **265**, 16571-16580

Hedeskov, C. J. (1980). Mechanism of glucose-induced insulin secretion *Physiol. Rev.* **60** 442-509

Hellwig, B. and Joost, H. G. (1991). Differentiation of erythrocyte- (GLUT1)., liver- (GLUT2)., and adipocyte-type (GLUT4). glucose transporters by binding of the inhibitory ligands cytochalasin B, forskolin, dipyridamole, and isobutylmethyxanthine. *Mol. Pharmacol.* **40**, 383-389

Hiraki, Y., Rosen, O. M. and Birnbaum, M. J. (1988). Growth factors rapidly induce expression of the glucose transporter gene. *J. Biol. Chem.* **263**, 13655-13662

Hodgson, P. A., Osguthorpe, D. J. and Holman, G. D. (1992). Molecular modelling of the facilitative sugar transporter. 11th Annual Molecular Graphics Society Meeting, Abstract

Hoffman, J. M., Standaert, M. L., Nair, G. P. and Farese, R. V. (1991). Differential effects of pertussis toxin on insulin-stimulated phosphatidylcholine hydrolysis and glycerolipid synthesis de novo. Studies in BC3H-1 myocytes and rat adipocytes. *Biochemistry* **30**, 3315-3322

Holman, G. D., Busza, A. L., Pierce, E. J. and Rees, W. D. (1981). Evidence for negative cooperativity in human erythrocyte sugar transport. *Biochim. Biophys. Acta* **649**, 503-514

Holman, G. D., Kozka, I. J., Clark, A. E., Flower, C. J., Saltis, J., Habberfield, A. D., Simpson, I. A. and Cushman, S. W. (1990). Cell surface labeling of glucose transporter isoform GLUT4 by bis-mannose photolabel. *J. Biol. Chem.* **265**, 18172-18179

Honnor, R. C., Naghshineh, S., Cushman, S. W., Wolff, J., Simpson, I. A. and Londos, C. (1992). Cholera and pertussis toxins modify regulation of glucose transport activity in rat adipose cells: evidence for mediation of a cAMP-independent process by G-proteins. *Cell. Signal.* **4**, 87-98

Huang, F. L., Yoshida, Y., Cunha-Melo, J. R., Beaven, M. A. and Huang, K.-P. (1989). Differential down-regulation of protein kinase C isozymes. *J. Biol. Chem.* **264**, 4238-4243

Hudson, A. W., Ruiz, M. L. and Birnbaum, M. J. (1992). Isoform-specific subcellular targeting of glucose transporters in mouse fibroblasts. *J. Cell Biol.* **116**, 785-797

Hudson, A. W., Fingar, D. C., Seidner, G. A., Griffiths, G., Burke, B. and Birnbaum, M. J. (1993). Targeting of the "insulin-responsive" glucose transporter (GLUT4). to the regulated secretory pathway in PC12 cells. *J. Cell Biol.* **122**, 579-588

Huppertz, C., Schürmann, A. and Joost, H. G. (1993). Abundance and subcellular distribution of GTP-binding proteins in 3T3-L1 cells before and after differentiation to the insulin-sensitive phenotype. *Eur. J. Biochem.* **215**, 611-617

Inoue, G., Kuzuya, H., Hayashi, T., Okamoto, M., Yoshimasa, Y., Kosaki, A., Kono, S., Okamoto, M., Maeda, I., Kubota, M. and Imura, H. (1993). Effects of ML-9 on insulin stimulation of glucose transport in 3T3-L1 adipocytes. *J. Biol. Chem.* **268**, 5272-5278

Ishihara, H., Asano, T., Katagiri, H., Lin, J.-L., Tsukuda, K., Shibasaki, Y., Yazaki, Y. and Oka, Y. (1991). The glucose transport activity of GLUT1 is markedly decreased by substitution of a single amino acid with a different charge at residue 415. *Biochem. Biophys. Res. Commun.* **176**, 922-930

Isshiki, K., Imoto, M., Sawa, T., Umezawa, K., Takeuchi, T., Umezawa, H., Tsuchida, T., Yoshioka, T. and Tatsuta, K. (1987). Inhibition of tyrosine protein kinase by synthetic erbstatin analogs. *J. Antibiot.* **40**, 1209-1210

Jadot, M., Canfield, W. M., Gregory, W. and Kornfeld, S. (1992). Characterization of the signal for rapid internalization of the bovine mannose 6-phosphate/insulin-like growth-II receptor. *J. Biol. Chem.* **267**, 11069-11077

James, D. E., Brown, R., Navarro, J. and Pilch, P. F. (1988). Insulin-regulatable tissues express a unique insulin-sensitive glucose transport protein. *Nature* **333**, 183-185

James, D. E., Strube, M. and Mueckler, M. (1989a). Molecular cloning and characterization of an insulin-regulatable glucose transporter. *Nature* **338**, 83-87

James, D. E., Hiken, J. and Lawrence Jr., J. C. (1989b). Isoproterenol stimulates phosphorylation of the insulin-regulatable glucose transporter in rat adipocytes. *Proc. Natl. Acad. Sci. USA* **86**, 8368-8372

James, D. E., Piper, R. C. and Slot, J. W. (1993). Targeting of mammalian glucose transporters. *J. Cell Sci.* **104**, 607-612

Jo, H., Radding, W., Anantharamaiah, G. M. and McDonald, J. M. (1993). An insulin receptor peptide (1135-1156). stimulates guanosine 5'-[γ-thio]triphosphate binding to the 67 kDa G-protein associated with the insulin receptor. *Biochem. J.* **294**, 19-24

Johnson, K. F. and Kornfeld, S. (1992). The cytoplasmic tail of the mannose 6-phosphate/insulin-like growth factor-II receptor has two signals for lysosomal enzyme sorting in the Golgi. *J. Cell Biol.* **119**, 249-257

Joost, H. G., Weber, T. M., Cushman, S. W. and Simpson, I. A. (1986). Insulin-stimulated glucose transport in rat adipose cells. *J. Biol. Chem.* **261**, 10033-10036

Jordan, N. J. and Holman, G. D. (1992). Photolabelling of the liver-type glucose-transporter isoform GLUT2 with an azitrifluoroethylbenzoyl-substituted bis-D-mannose. *Biochem. J.* **286**, 649-656

Jullien, D., Tanti, J.-F., Heydrick, S. J., Gautier, N., Grémeaux, T., Van Obberghen, E. and Le Marchand-Brustel, Y. (1993). Differential effects of okadaic acid on insulin-stimulated glucose and amino acid uptake and phosphatidylinositol 3-kinase activity. *J. Biol. Chem.* **268**, 15246-15251

Kaestner, K. H., Christy, R. J., McLenithan, J. C., Braiterman, L. T., Cornelius, P., Pekala, P. H. and Lane, M. D. (1989). Sequence, tissue distribution and differential expression of mRNA for a putative insulin-responsive glucose transporter in mouse 3T3-L1 adipocytes. *Proc. Natl. Acad. Sci. USA* **86**, 3150-3154

Kaestner, K. H., Flores-Riveros, J. R., McLenithan, J. C., Janicot, M. and Lane, M. D. (1991). Transcriptional repression of the mouse insulin-responsive glucose transporter (GLUT4) gene by cAMP. *Proc. Natl. Acad. Sci. USA* **88**, 1933-1937

Karnieli, E., Zarnowski, M. J., Hissin, P. J., Simpson, I. A., Salans, L. B. and Cushman, S. W. (1981). Insulin-stimulated translocation of glucose transport systems in the isolated rat adipose cell. *J. Biol. Chem.* **256**, 4772-4777

Kasahara, M. and Hinkle, P. C. (1977). Reconstitution and purification of the D-glucose transporter from human erythrocytes. *J. Biol. Chem.* **252**, 7384-7390

Katagiri, H., Asano, T., Shibasaki, Y., Lin, J.-L., Tsukuda, K., Ishihara, H., Akanuma, Y., Takaku, F. and Oka, Y. (1991). Substitution of leucine for tryptophan 412 does not abolish cytochalasin B labeling but markedly decreases the intrinsic activity of GLUT1 glucose transporter. *J. Biol. Chem.* **266**, 7769-7773

Katagiri, H., Asano, T., Ishihara, H., Lin, J.-L., Inukai, K., Shanahan, M. F., Tsukuda, K., Kikuchi, M., Yazaki, Y., and Oka, Y. (1993). Role of tryptophan-388 of GLUT1 glucose transporter in glucose-transport activity and photoaffinity-labelling with forskolin. *Biochem. J.* **291**, 861-867

Kayano, T., Fukumoto, H., Eddy, R. L., Fan, Y.-S., Byers, M. G., Shows, T. B., and Bell, G. I. (1988). Evidence for a family of human glucose transporter-like proteins. *J. Biol. Chem.* **263**, 15245-15248

Kayano, T., Burant, C. F., Fukumoto, H., Gould, G. W., Fan, Y.-S., Eddy, R. L., Byers, M. G., Shows, T. B., Seino, S. and Bell, G. I. (1990). Human facilitative glucose transporters. *J. Biol. Chem.* **265**, 13276-13282

Kelada, A. S. M., Macaulay, S. L. and Proietto, J. (1992). Cyclic AMP acutely stimulates translocation of the major insulin-regulatable glucose transporter GLUT4. *J. Biol. Chem.* **267**, 7021-7025

Keller, K., Strube, M. and Mueckler, M. (1989). Functional expression of the human HepG2 and rat adipocyte glucose transporters in *Xenopus* oocytes. *J. Biol. Chem.* **264**, 18884-18889

Kellerer, M., Obermaier-Kusser, B., Pröfrock, A., Schleicher, E., Seffer, E., Mushack, J., Ermel, B. and Häring, H.-U. (1991). Insulin activates GTP binding to a 40 kDa protein in fat cells. *Biochem. J.* **276**, 103-108

Kelly, K. L. and Ruderman, N. B. (1993). Insulin-stimulated phosphatidylinositol 3-kinase. *J. Biol. Chem.* **268**, 4391-4398

Kenna, J. G. Major, G. N. and Williams, R. S. (1985). Methods for reducing non-specific antibody binding in enzyme-linked immunosorbent assays. *J. Immunol. Methods* **85**,409-419

Kingston, R. E. (1992). in Current Protocols in Molecular Biology (Janssen, K., ed.), 9.1-9.9, Greene Publishing Associates, Inc., New York

Kirsch, D., Obermaier, B. and Häring, H. U. (1985). Phorbolesters enhance basal D-glucose transport but inhibit insulin stimulation of D-glucose transport and insulin binding in isolated rat adipocytes. *Biochem. Biophys. Res. Comm.* **128**, 824-832

Klarlund, J. K., Khalaf, N., Kozma, L. and Czech, M. P. (1993). Activation of protein kinases by insulin and non-hydrolyzable GTP analogs in permeabilized 3T3-L1 adipocytes. *J. Biol. Chem.* **268**, 7646-7649

Klein, H. H., Matthaei, S., Drenkhan, M., Ries, W. and Scriba, P. C. (1991). The relationship between insulin binding, insulin activation of insulin-receptor tyrosine kinase and insulin stimulation of glucose uptake in isolated rat adipocytes. *Biochem. J.* **274**, 787-792

Kohanski, R. A. (1993a). Insulin receptor autophosphorylation. I. Autophosphorylation kinetics of the native receptor and its cytoplasmic kinase domain. *Biochemistry* **32**, 5766-5772

Kohanski, R. A. (1993b). Insulin receptor autophosphorylation. II. Determination of autophosphorylation sites by chemical sequence analysis and identification of the juxtamembrane sites. *Biochemistry* **32**, 5773-5780

Kono, T., Suzuki, K., Dansey, L. E., Robinson, F. W. and Blevins, T. L. (1981). Energy-dependent and protein synthesis-independent recycling of the insulin-sensitive glucose transport mechanism in fat cells. *J. Biol. Chem.* **256**, 6400-6407

Kozka, I. J., Clark, A. E. and Holman, G. D. (1991). Chronic treatment with insulin selectively down-regulates cell-surface GLUT4 glucose transporters in 3T3-L1 adipocytes. *J. Biol. Chem.* **266**, 11726-11731

Kozka, I. J. and Holman, G. D. (1993). Metformin blocks downregulation of cell surface GLUT4 caused by chronic insulin treatment of rat adipocytes. *Diabetes* **42**,1159-1165

Kozma, L., Baltensperger, K., Klarlund, J., Porras, A., Santos, E. and Czech, M. P. (1993). The ras signalling pathway mimics insulin action on glucose transporter translocation. *Proc. Natl. Acad. Sci. USA* **90**, 4460-4464

Ktistakis, N. T., Thomas, D. and Roth, M. G. (1990). Characteristics of the tyrosine recognition signal for internalization of transmembrane surface glycoproteins. *J. Cell Biol.* **111**, 1393-1407

Laemmli, U. K. (1970). Cleavage of structural proteins during the assembly of the head of bacteriophage T4. *Nature* **227**, 680-685

Lawrence Jr., J. C., Hiken, J. F. and James, D. E. (1990a). Phosphorylation of the glucose transporter in rat adipocytes. *J. Biol. Chem.* **265**, 2324-2332

Lawrence Jr., J. C., Hiken, J. F. and James, D. E. (1990b). Stimulation of glucose transport and glucose transporter phosphorylation by okadaic acid in rat adipocytes. *J. Biol. Chem.* **265**, 19768-19776

Lebwohl, D. E., Nunez, I., Chan, M. and Rosen, O. M. (1991). Expression of inducible membrane-anchored insulin receptor kinase enhances deoxyglucose uptake. *J. Biol. Chem.* **266**, 386-390

Lee, J., O'Hare, T., Pilch, P. F. and Shoelson, S. E. (1993). Insulin receptor autophosphorylation occurs asymmetrically. *J. Biol. Chem.* **268**, 4092-4098

Leevers, S. J., Paterson, H. F. and Marshall, C. J. (1994). Requirement for ras in raf activation is overcome by targeting raf to the plasma membrane. *Nature* **369**, 411-414

Levine, R. and Goldstein, M. S. (1955). On the mechanism of action of insulin. *Recent Prog. Horm. Res.* **11**, 343-380

Lewis, R. E., Wu, G. P., MacDonald, R. G. and Czech, M. P. (1990). Insulin-sensitive phosphorylation of serine 1293/1294 on the human insulin receptor by a tightly associated serine kinase. *J. Biol. Chem.* **265**, 947-954

Lin, J.-L., Asano, T., Katagiri, H., Tsukuda, K., Ishihara, H., Inukai, K., Yazaki, Y. and Oka, Y. (1992). Deletion of C-terminal 12 amino acids of GLUT1 protein does not abolish the transport activity. *Biochem. Biophys. Res. Commun.* **184**, 865-870

Liu, F-T, Zinnecker, M., Hamaoka, T. and Katz, D. H. (1979). New procedures for preparation and isolation of conjugates of proteins and a synthetic copolymer of D-amino acids and immunochemical characterization of such conjugates. *Biochemistry* **18**, 690-697

Lowe, A. G. and Walmsley, A. R. (1986). The kinetics of glucose transport in human red blood cells. *Biochim. Biophys. Acta* **857**, 146-154

Lowe, A. G. and Walmsley, A. R. (1987). A single half-turnover of the glucose carrier of the human erythrocyte. *Biochim. Biophys. Acta* **903**, 547-550

Luttrell, L. M., Hewlett, E. L., Romero, G. and Rogol, A. D. (1988). Pertussis toxin treatment attenuates some effects of insulin in BC3H-1 murine myocytes. *J. Biol. Chem.* **263**, 6134-6141

Matschinsky, F. M. (1990). Glucokinase as glucose sensor and metabolic signal generator in pancreatic β -cells and hepatocytes. *Diabetes* **39**, 647-652

McClain, D. A., Maegawa, H., Lee, J., Dull, T. J., Ulrich, A. and Olefsky, J. M. (1987). A mutant insulin receptor with defective tyrosine kinase displays no biologic activity and does not undergo endocytosis. *J. Biol. Chem.* **262**, 14663-14671

Maegawa, H., McClain, D. A., Freidenberg, G., Olefsky, J. M., Napier, M., Lipari, T., Dull, T. J., Lee J. and Ullrich, A. (1988). Properties of a human insulin receptor with COOH-terminal truncation. *J. Biol. Chem.* **263**, 8912-8917

Melançon, P., Glick, B. S., Malhotra, V., Weidman, P. J., Serafini, T., Gleason, M. L., Orci, L. and Rothman, J. E. (1987). Involvement of GTP-binding "G" proteins in transport through the Golgi stack. *Cell* **51**, 1053-1062

Merrall, N. W., Wakelam, M. J. O., Plevin, R. and Gould, G. W. (1993). Insulin and platelet-derived growth factor acutely stimulate glucose transport in 3T3-L1 fibroblasts independently of protein kinase C. *Biochim. Biophys. Acta* **1177**, 191-198

Mizel, S. B. and Wilson, L. (1972). Inhibition of the transport of several hexoses in mammalian cells by cytochalasin B. *J. Biol. Chem.* **247**, 4102-4105

Mollard, G. F. V., Mignery, G. A., Baumert, M., Perin, M. S., Hanson, T. J., Burger, P. M., Jahn, R. and Südhof, T. C. (1990). rab3 is a small GTP-binding protein exclusively localised to synaptic vesicles. *Proc. Natl. Acad. Sci. USA* **87**, 1988-1992

Mori, H., Hashiramoto, M., Clark, A. E., Yang, J., Muraoka, A., Tamori, Y., Kasuga, M. and Holman, G. D. (1994). Substitution of tyrosine 293 of GLUT1 locks the transporter into an outward facing conformation. *J. Biol. Chem.* **269**, 11578-11583

Mueckler, M., Caruso, C., Baldwin, S. A., Panico, M., Blench, I., Morris, H. R., Allard, W. J., Lienhard, G. E. and Lodish, H. F. (1985). Sequence and structure of a human glucose transporter. *Science* **229**, 941-945

Nakanishi, H., Brewer, K. A. and Exton, J. H. (1993). Activation of the ζ isozyme of protein kinase C by phosphatidylinositol 3,4,5-triphosphate. *J. Biol. Chem.* **268**, 13-16

Narahara, H. T. and Özand, P. (1963). Studies of tissue permeability. *J. Biol. Chem.* **238**, 40-49

Nishimura, H., Saltis, J., Habberfield, A. D., Garty, N. B., Greenberg, A. S., Cushman, S. W., Londos, C. and Simpson, I. A. (1991). Phosphorylation state of the GLUT4 isoform of the glucose transporter in subfractions of the rat adipose cell: Effects of insulin, adenosine and isoproterenol. *Proc. Natl. Acad. Sci. USA* **88**, 11500-11504

Nishimura, H., Pallardo, F. V., Seidner, G. A., Vannucci, S., Simpson, I. A. and Birnbaum, M. J. (1993). Kinetics of GLUT1 and GLUT4 glucose transporters expressed in *Xenopus* oocytes. *J. Biol. Chem.* **268**, 8514-8520

Nishizuka, Y. (1988). The molecular heterogeneity of protein kinase C and its implications for cellular regulation. *Nature* **334**, 661-665

Nishizuka, Y. (1992). Intracellular signaling by hydrolysis of phospholipids and activation of protein kinase C. *Science* **258**, 607-614

Oberhauser, A. F., Monck, J. R., Balch, W. E. and Fernandez, J. M. (1992). Exocytotic fusion is activated by rab3a peptides. *Nature* **360**, 270-273

Ockleford, C. D., Hsi, B.-L., Wakely, J., Badley, R. A., Whyte, A. and Faulk, W. P. (1981). Propidium iodide as a nuclear marker in immunofluorescence. II. Use with tissue and cytoskeleton studies. *J. Immunol. Methods* **43**, 261-267

Oka, Y., Asano, T., Shibasaki, Y., Lin, J.-L., Tsukuda, K., Katagiri, H., Akanuma, Y. and Takaku, F. (1990). C-terminal truncated glucose transporter is locked into an inward-facing form without transport activity. *Nature*, **345**, 550-553

Olefsky, J. M. (1978). Mechanisms of the ability of insulin to activate the glucose-transport system in rat adipocytes. *Biochem. J.* **172**, 137-145

Onoda, T., Iinuma, H., Sasaki, Y., Hamada, M., Isshiki, K., Naganawa, H., Takeuchi, T., Tatsuta, T. and Umezawa, K. (1989). Isolation of a novel tyrosine kinase inhibitor lavendustin A, from *Streptomyces griseolavendus*. *J. Nat. Prod.* **52**, 1252-1257

Padfield, P. J., Balch, W. E. and Jamieson, J. D. (1992). A synthetic peptide of the rab3a effector domain stimulates amylase release from permeabilized pancreatic acini. *Proc. Natl. Acad. Sci. USA* **89**, 1656-1660

Palfreyman, R. W., Clark, A. E., Denton, R. M., Holman, G. D. and Kozka, I. J. (1992). Kinetic resolution of the separate GLUT1 and GLUT4 glucose transport activities in 3T3-L1 cells. *Biochem. J.* **284**, 275-281

Piper, R. C., Hess, L. J. and James, D. E. (1991). Differential sorting of two glucose transporters expressed in insulin-sensitive cells. *Am. J. Physiol.* **260**, C570-C580

Piper, R. C., Tai, C., Slot, J. W., Hahn, C. S., Rice, C. M., Huang, H. and James, D. E. (1992). The efficient intracellular sequestration of the insulin-regulatable glucose transporter (GLUT4). is conferred by the NH_2 terminus. *J. Cell Biol.* **117**, 729-743

Piper, R. C., Tai, C., Kulesza, P., Pang, S., Warnock, D., Baenziger, J., Slot, J. W., Geuze, H. J., Puri, C. and James, D. E. (1993a). GLUT-4 NH_2 terminus contains a phenylalanine-based targeting motif that regulates intracellular sequestration. *J. Cell Biol.* **121**, 1221-1232

Piper, R. C., James, D. E., Slot, J. W., Puri, C. and Lawrence Jr., J. C. (1993b). GLUT4 phosphorylation and inhibition of glucose transport by dibutyryl cAMP. *J. Biol. Chem.* **268**, 16557-16563

Porras, A., Nebreda, A. R., Benito, M. and Santos, E. (1992). Activation of ras by insulin in 3T3 L1 cells does not involve GTPase-activating protein phosphorylation. *J. Biol. Chem.* **267**, 21124-21131

Prentki, M. and Matschinsky, F. M. (1987). Ca^{2+}, cAMP and phospholipid-derived messengers in coupling mechanisms of insulin secretion. *Physiol. Rev.* **67**, 1185-1248

Puck, T. T., Cieciura, S. J. and Robinson, A. (1958). Genetics of somatic mammalian cells. III. Long-term cultivation of euploid cells from human and animal subjects. *J. Exptl. Med.* **108**, 945-956

Ray, L. B. and Sturgill, T. W. (1987). Rapid stimulation by insulin of a serine/threonine kinase in 3T3-L1 adipocytes that phosphorylates microtubule-associated protein 2 *in vitro*. *Proc. Natl. Acad. Sci. USA* **84**, 1502-1506

Record, R. D., Smith, R. M. and Jarett, L. (1993). Insulin induces an unmasking of the carboxyl terminus of G_i proteins in rat adipocytes. *Exp. Cell Res.* **206**, 36-42

Rees, W. D. and Holman, G. D. (1981). Hydrogen bonding requirements for the insulin-sensitive sugar transport system of rat adipocytes. *Biochim. Biophys. Acta* **646**, 251-260

Reusch, J. E.-B., Begum, N., Sussman, K. E. and Draznin, B. (1991). Regulation of GLUT-4 phosphorylation by intracellular calcium in adipocytes. *Endocrinology* **129**, 3269-3273

Reusch, J. E.-B., Sussman, K. E. and Draznin, B. (1993). Inverse relationship between GLUT-4 phosphorylation and its intrinsic activity. *J. Biol. Chem.* **268**, 3348-3351

Rexach, M. F. and Schekman, R. W. (1991). Distinct biochemical requirements for the budding, targeting and fusion of ER-derived transport vesicles. *J. Cell Biol.* **114**, 219-229

Rist, R. J., Jones, G. E. and Naftalin, R. J. (1990). Synergistic activation of 2-deoxy-D-glucose uptake in rat and murine peritoneal macrophages by human macrophage colony-stimulating factor-stimulating coupling between transport and hexokinase activity and phorbol-dependent stimulation of pentose phosphate-shunt activity. *Biochem. J.* **265**, 243-249

Robinson, L. J., Pang, S., Harris, D. S., Heuser, J. and James, D. E. (1992). Translocation of the glucose transporter (GLUT4). to the cell surface in permeabilized 3T3-L1 adipocytes: effects of ATP, insulin and GTPγS and location of GLUT4 to clathrin lattices. *J. Cell Biol.* **117**, 1181-1196

Rosen, O. M. (1987). After insulin binds. *Science* **237**, 1452-1458

Rothenberg, P. L., Lane, W. S., Karasik, A., Backer, J., White, M. and Kahn, C. R. (1991). Purification and partial sequence analysis of pp185, the major cellular substrate of the insulin receptor tyrosine kinase. *J. Biol. Chem.* **266**, 8302-8311

Rubin, C. S., Hirsch, A., Fung, C. and Rosen, O. M. (1978). Development of hormone receptors and hormonal responsiveness *in vitro*. *J. Biol. Chem.* **253**, 7570-7578

Sadowski, H. B., Wheeler, T. T. and Young, D. A. (1992). Gene expression during 3T3-L1 adipocyte differentiation. *J. Biol. Chem.* **266**, 4722-4731

Sargeant, R. J. and Pâquet, M. R. (1993). Effect of insulin on the rates of synthesis and degradation of GLUT1 and GLUT4 glucose transporters in 3T3-L1 adipocytes. *Biochem. J.* **290**, 913-919

Satoh, S., Nishimura, H., Clark, A. E., Kozka, I. J., Vannucci, S. J., Simpson, I. A., Quon, M. J., Cushman, S. W. and Holman, G. D. (1993). Use of bismannose photolabel to elucidate insulin-regulated GLUT4 subcellular trafficking kinetics in rat adipose cells. *J. Biol. Chem.* **268**, 17820-17829

Schumacher, R., Mosthaf, L., Schlessinger, J., Brandenburg, D. and Ullrich, A. (1991). Insulin and insulin-like growth factor-1 binding specificity is determined by distinct regions of their cognate receptors. *J. Biol. Chem.* **266**, 19288-19295

Schumacher, R., Soos, M. A., Schlessinger, J., Brandenburg, D., Siddle, K. and Ullrich, A. (1993). Signaling-competent receptor chimeras allow mapping of major insulin receptor binding domain determinants. *J. Biol. Chem.* **268**, 1087-1094

Schürmann, A., Rosenthal, W., Hinsch, K. D. and Joost, H. G. (1989). Differential sensitivity to guanine nucleotides of basal and insulin-stimulated glucose transporter activity reconstituted from adipocyte membrane fractions. *FEBS Lett.* **255**, 259-264

Schürmann, A., Rosenthal, W., Schultz, G. and Joost, H. G. (1992a). Characterization of GTP-binding proteins in Golgi-associated membrane vesicles from rat adipocytes. *Biochem. J.* **283**, 795-801

Schürmann, A., Monden, I., Joost, H. G. and Keller, K. (1992b). Subcellular distribution and activity of glucose transporter isoforms GLUT1 and GLUT4 transiently expressed in COS-7 cells. *Biochim. Biophys. Acta* **1131**, 245-252

Schürmann, A., Keller, K., Monden, I., Brown F. M., Wandel, S., Shanahan, M. F. and Joost, H. G. (1993). Glucose transport activity and photolabelling with 3-[^{125}I]iodo-4-azidophenethylamido-7-*O*-succinyldeacetyl (IAPS).-forskolin of two mutants at tryptophan-388 and -412 of the glucose transporter GLUT1: association of the binding domains of forskolin and glucose. *Biochem. J.* **290**, 497-501

Shepherd, P. R., Gould, G. W., Colville, C. A., McCoid, S. C., Gibbs, E. M. and Kahn, B. B. (1992). Distribution of GLUT3 glucose transporter protein in human tissues. *Biochem. Biophys. Res. Commun.* **188**, 149-154

Shibasaki, Y., Asano, T., Lin, J.-L., Tsukuda, K., Katagiri, H., Ishihara, H., Yazaki, Y. and Oka, Y. (1992). Two glucose transporter isoforms are sorted differentially and are expressed in distinct cellular compartments. *Biochem. J.* **281**, 829-834

Shibata, H., Robinson, F. W., Soderling, T. R. and Kono, T. (1991). Effects of okadaic acid on insulin-sensitive cAMP phosphodiesterase in rat adipocytes. *J. Biol. Chem.* **266**, 17948-17953

Shiraishi, T., Owada, M. K., Tatsuka, M., Yamashita, T., Watanabe, K. and Kakunaga, T. (1989). Specific inhibitors of tyrosine-specific protein kinases: properties of 4-hydroxycinnamamide derivatives *in Vitro*. *Cancer Res.* **49**, 2374-2378

Shoelson, S. E., White, M. F. and Kahn, C. R. (1988). Tryptic activation of the insulin receptor. *J. Biol. Chem.* **263**, 4852-4860

Shoelson, S. E., Chatterjee, S., Chaudhuri, M. and White, M. F. (1992). YMXM motifs of IRS-1 define substrate specificity of the insulin receptor kinase. *Proc. Natl. Acad. Sci. USA* **89**, 2027-2031

Shoelson, S. E., Lee, J., Lynch, C. S., Backer, J. M. and Pilch, P. F. (1993). Bpa^{B25} insulins. *J. Biol. Chem.* **268**, 4085-4091

Shoyab, M. and Todaro, G. J. (1980). Specific high affinity cell membrane receptors for biologically active phorbol and ingenol esters. *Nature* **288**, 451-455

Simpson, I. A., Yver, P. R., Hissin, P. J., Wardzala, L. J., Karnieli, E., Salans, L. B. and Cushman, S. W. (1983). Insulin-stimulated translocation of glucose transporters in the isolated rat adipose cells: characterization of subcellular fractions. *Biochim. Biophys. Acta* **763**, 393-407

Skolnik, E. Y., Batzer, A., Li, N., Lee, C.-H., Lowenstein, E., Mohammadi, M., Margolis, B. and Schlessinger, J. (1993). The function of GRB2 in linking the insulin receptor to ras signaling pathways. *Science* **260**, 1953-1955

Smith, R. M., Tiesinga, J. J., Shah, N., Smith, J. A. and Jarett, L. (1993). Genistein inhibits insulin-stimulated glucose transport and decreases immunocytochemical labeling of GLUT4 carboxyl-terminus without affecting translocation of GLUT4 in isolated rat adipocytes: additional evidence of GLUT4 activation by insulin. *Arch. Biochem. Biophys.* **300**, 238-246

Soldati, T., Shapiro, A. D., Svejstrup, A. B. D. and Pfeffer, S. R. (1994). Membrane targeting of the small GTPase rab9 is accompanied by nucleotide exchange. *Nature* **369**, 76-78

Söllner, T., Whiteheart, S. E., Brunner, M., Erdjument-Bromage, H., Geromanos, S., Tempst, P. and Rothman, J. E. (1993). SNAP receptors implicated in vesicle targeting and fusion. *Nature* **362**, 318-324

Studelska, D. R., Hanpeter, D. E. and James, D. E. (1993). The insulin-regulatable glucose transporter (GLUT4). binds GTP. *FASEB J.* **7**, A850

Sun, X. J., Rothenberg, P., Kahn, C. R., Backer, J. M., Araki, E., Wilden, P. A., Cahill, D. A., Goldstein, B. J. and White, M. F. (1991). Structure of the insulin receptor substrate IRS-1 defines a unique signal transduction protein. *Nature* **352**, 73-77

Suzuki, K. and Kono, T. (1980). Evidence that insulin causes translocation of glucose transport activity to the plasma membrane from an intracellular storage site. *Proc. Natl. Acad. Sci. USA* **77**, 2542-2545

Suzuki, Y., Shibata, H., Inoue, S. and Kojima, I. (1992). Stimulation of glucose transport by guanine nucleotides in permeabilized rat adipocytes. *Biochem. Biophys. Res. Commun.* **189**, 572-580

Takata, K., Kasahara, T., Kasahara, M., Ezaki, O. and Hirano, H. (1990). Erythrocyte/HepG2-type glucose transporter is concentrated in cells of blood-tissue barriers. *Biochem. Biophys. Res. Commun.* **173**, 67-73

Tamori, Y., Hashiramoto, M., Clark, A. E., Mori, H., Muraoka, A., Kadowaki, T., Holman, G. D. and Kasuga, M. (1994). Substitution at Pro^{385} of GLUT1 perturbs the glucose transport function by reducing conformational flexibility. *J. Biol. Chem.* **269**, 2982-2986

Tavaré, J. M. and Denton, R. M. (1988). Studies on the autophosphorylation of the insulin receptor from human placenta. *Biochem. J.* **252**, 607-615

Tavaré, J. M. and Siddle, K. (1993). Mutational analysis of insulin receptor function: consensus and controversy. *Biochim. Biophys. Acta* **1178**, 21-39

Taylor, L. P. and Holman, G. D. (1981). Symmetrical kinetic parameters for 3-*O*-methyl-D-glucose transport in adipocytes in the presence and in the absence of insulin. *Biochim. Biophys. Acta* **642**, 325-335

Thomas, H. M., Takeda, J. and Gould, G. W. (1993). Differential targeting of glucose transporter isoforms heterologously expressed in *Xenopus* oocytes. *Biochem. J.* **290**, 707-715

Thomas, S. M., DeMarco, M., D'Arcangelo, G., Halegoua, S. and Brugge, J. S. (1992). Ras is essential for nerve growth factor- and phorbol ester-induced tyrosine phosphorylation of MAP kinases. *Cell* **68**, 1031-1040

Thorens, B., Sarkar, H. K., Kaback, H. R. and Lodish, H. F. (1988). Cloning and functional expression in bacteria of a novel glucose transporter present in liver, intestine, kidney and β-pancreatic islet cells. *Cell* **55**, 281-290

Thorens, B., Cheng, Z.-Q., Brown, D. and Lodish, H. F. (1990). Liver glucose transporter: a basolateral protein in hepatocytes and insulin and kidney cells. *Am. J. Physiol.* **259**, C279-C285

Tordjman, K. M., Leingang, K. A., James, D. E. and Mueckler, M. M. (1989). Differential regulation of two distinct glucose transporter species expressed in 3T3-L1 adipocytes: Effect of chronic insulin and tolbutamide treatment. *Proc. Natl. Acad. Sci. USA* **86**, 7761-7765

Tordjman, K. M., Leingang, K. A. and Mueckler, M. (1990). Differential regulation of the HepG2 and adipocyte/muscle glucose transporters in 3T3-L1 adipocytes. *Biochem. J.* **271**, 201-207

Tornqvist, H. E., Pierce, M. W., Frackelton, A. R., Nemenoff, R. A. and Avruch, J. (1987). Identification of insulin receptor tyrosine residues autophosphorylated *in Vitro*. *J. Biol. Chem.* **262**, 10212-10219

Treadway, J. L., Morrison, B. D., Soos, M. A., Siddle, K., Olefsky, J., Ullrich, A., McClain, D. A. and Pessin, J. E. (1991). Transdominant inhibition of tyrosine kinase activity in mutant insulin/insulin-like growth factor I hybrid receptors. *Proc. Natl. Acad. Sci. USA* **88**, 214-218

Ullrich, A., Bell, J. R., Chen, E. Y., Herrera, R., Petruzzelli, L. M., Dull, T. J., Gray, A., Coussens, L., Liao, Y.-C., Tsubokawa, M., Mason, A., Seeburg, P. H., Grunfeld, C., Rosen, O. M. and Ramachandran, J. (1985). Human insulin receptor and its relationship to the tyrosine kinase family of oncogenes. *Nature* **313**, 756-761

Ullrich, A. and Schlessinger, J. (1990). Signal transduction by receptors with tyrosine kinase activity. *Cell* **61**, 203-212

Ullrich, O., Horiuchi, H., Bucci, C. Zerial, M. (1994). Membrane association of rab5 mediated by GDP-dissociation inhibitor and accompanied by GDP/GTP exchange. *Nature* **368**, 157-160

Umezawa, K., Hori, T., Tajima, H., Imoto, M., Isshiki, K. and Takeuchi, T. (1990). Inhibition of epidermal growth factor-induced DNA synthesis by tyrosine kinase inhibitors. *FEBS Lett.* **260**, 198-200

van der Sluijs, P., Hull, M., Zahraoui, A., Tavitian, A., Goud, B. and Mellman, I. (1991). The small GTP-binding protein rab4 is associated with early endosomes. *Proc. Natl. Acad. Sci. USA* **88**, 6313-6317

van der Sluijs, P., Hull, M., Webster, P., Mâle, P., Goud, B. and Mellman, I. (1992). The small GTP-binding protein rab4 controls an early sorting event on the endocytic pathway. *Cell* **70**, 729-740

van Putten, J. P. M. and Krans, H. M. J. (1985). Glucose as a regulator of insulin-sensitive hexose uptake in 3T3 adipocytes. *J. Biol. Chem.* **260**, 7996-8001

Vannucci, S. J., Nishimura, H., Satoh, S., Cushman, S. W., Holman, G. D. and Simpson, I. A. (1992). Cell surface accessibility of GLUT4 glucose transporters in insulin-stimulated rat adipose cells. *Biochem. J.* **288**, 325-330

Verhey, K. J., Hausdorff, S. F. and Birnbaum, M. J. (1993). Identification of the carboxy terminus as important for the isoform-specific subcellular targeting of glucose transporter proteins. *J. Cell Biol.* **123**, 137-147

Waddell, I. D., Scott, H., Grant, A. and Burchell, A. (1991). Identification and characterization of a hepatic microsomal glucose transport protein. *Biochem. J.* **275**, 363-367

Waddell, I. D., Zomerschoe, A. G., Voice, M. W. and Burchell, A. (1992). Cloning and expression of a hepatic microsomal glucose transport protein. *Biochem. J.* **286**, 173-177

Walmsley, A. R. (1988). The dynamics of the glucose transporter. *Trends Biochem. Sci.* **13**, 226-231

Wang, J.-F., Falke, J. J. and Chan, S. I. (1986). A proton NMR study of the mechanism of the erythrocyte glucose transporter. *Proc. Natl. Acad. Sci. USA* **83**, 3277-3281

Wardzala, L. J., Cushman, S. W. and Salans, L. B. (1978). Mechanism of insulin action on glucose transport in the isolated rat adipose cell. *J. Biol. Chem.* **253**, 8002-8005

Ways, D. K., Cook, P. P., Webster, C. and Parker, P. J. (1992). Effect of phorbol esters on protein kinase C-ζ. *J. Biol. Chem.* **267**, 4799-4805

Weber, M. J., Evans, P. K., Johnson, M. A., McNair, T. F., Nakamura, K. D. and Salter, D. W. (1984). Transport of potassium, amino acids and glucose in cells transformed by Rous sarcoma virus. *Fed. Proc. Fed. Am. Soc. Exp. Biol.* **43**, 107-112

Weiland, M., Schürmann, A., Schmidt, W. E. and Joost, H. G. (1990). Development of the hormone-sensitive glucose transport activity in differentiating 3T3-L1 murine fibroblasts. *Biochem. J.* **270**, 331-336

Weiler-Guettler, H., Zinke, H., Moeckel, B., Frey, A. and Gassen, H. G. (1989). Complementary DNA cloning and sequence analysis of the glucose transporter from porcine blood-brain barrier. *Biol. Chem. Hoppe Seyler* **370**, 467-474

Wellner, M., Mueckler, M. M. and Keller, K. (1993). GTP analogs suppress uptake but not transport of D-glucose analogs in GLUT1 glucose transporter-expressing *Xenopus* oocytes. *FEBS Lett.* **327**, 95-98

Wessel, D. and Flügge, U. I. (1984). A method for the quantitative recovery of protein in dilute solution in the presence of detergents and lipids. *Anal. Biochem.* **138**, 141-143

Wheeler, T. J. and Hinkle, P. C. (1981). Kinetic properties of the reconstituted glucose transporter from human erythrocytes. *J. Biol. Chem.* **256**, 8907-8914

White, M. F., Maron, R. and Kahn, C. R. (1985). Insulin rapidly stimulates tyrosine phosphorylation of a Mr-185,000 protein in intact cells. *Nature* **318**, 183-186

White, M. F. and Kahn, C. R. (1994). The insulin signalling system. *J. Biol. Chem.* **269**, 1-4

Widdas, W. F. (1952). Inability of diffusion to account for the placental glucose transfer in the sheep and consideration of the kinetics of a possible carrier transfer. *J. Physiol.(Lond.).* **118**, 23-39

Widnell, C. C., Baldwin, S. A., Davis, A., Martin, S. and Pasternak, C. A. (1990). Cellular stress induces a redistribution of the glucose transporter. *FASEB J.* **4**, 1634-1637

Wilden, P.A., Siddle, K., Haring, E., Backer, J. M., White, M. F. and Kahn, C. R. (1992a). The role of insulin receptor kinase domain autophosphorylation in receptor-mediated activities. *J. Biol. Chem.* **267**, 13719-13727

Wilden, P.A., Kahn, C. R., Siddle, K. and White, M. F. (1992b). Insulin receptor kinase domain autophosphorylation regulates receptor enzymatic function. *J. Biol. Chem.* **267**, 16660-16668

Yaish, P., Gazit, A., Gilon, C. and Levitzki, A. (1988). Blocking of EGF-dependent cell proliferation by EGF receptor kinase inhibitors. *Science* **242**, 933-935

Yang, J., Clark, A. E., Harrison, R., Kozka, I. J. and Holman, G. D. (1992a). Trafficking of glucose transporters in 3T3-L1 cells. *Biochem. J.* **281**, 809-817

Yang, J., Clark, A. E., Kozka, I. J., Cushman, S. W. and Holman, G. D. (1992b). Development of an intracellular pool of glucose transporters in 3T3-L1 cells. *J. Biol. Chem.* **267**, 10393-10399

Yang, J. and Holman, G. D. (1993). Comparison of GLUT4 and GLUT1 subcellular trafficking in basal and insulin-stimulated 3T3-L1 cells. *J. Biol. Chem.* **268**, 4600-4603

Yano, H., Seino, Y., Inagaki, N., Hinokio, Y., Yamamoto, T., Yasuda, K., Masuda, K., Someya, Y. and Imura, H. (1991). Tissue distribution and species difference of the brain type glucose transporter (GLUT3). *Biochem. Biophys. Res. Commun.* **174**, 470-477

Yano, Y., Sumida, Y., Benzing, C. F., Robinson, F. W. and Kono, T. (1993). Primary sites of actions of staurosporine and H-7 in the cascade of insulin action to glucose-transport in rat adipocytes. *Biochim. Biophys. Acta* **1176**, 327-332

Yoneda, T., Lyall, R. M., Alsina, M. M., Persons, P. E., Spada, A. P., Levitzki, A., Zilberstein, A. and Mundy, G. R. (1991). The antiproliferative effects of tyrosine kinase inhibitors tyrphostins on a human squamous cell carcinoma *in Vitro* and in nude mice. *Cancer Res.* **51**, 4430-4435

Young, S. W., Poole, R. C., Hudson, A. T., Halestrap, A. P., Denton, R. M. and Tavaré, J. M. (1993). Effects of tyrosine kinase inhibitors on protein kinase-independent systems. *FEBS Lett.* **316**, 278-282

Zahraoui, A., Touchot, N., Chardin, P. and Tavitian, A. (1989). The human *Rab* genes encode a family of GTP-binding proteins related to yeast YPT1 and SEC4 products involved in secretion. *J. Biol. Chem.* **264**, 12394-12401

Zorzano, A., Wilkinson, W., Kotliar, N., Thoidis, G., Wadzinkski, B. E., Ruoho, A. E. and Pilch, P. F. (1989). Insulin-regulated glucose uptake in rat adipocytes is mediated by two transporter isoforms present in at least two vesicle populations. *J. Biol. Chem.* **264**, 12358-12363

Biochem. J. (1992) **284**, 275–281 (Printed in Great Britain)

Kinetic resolution of the separate GLUT1 and GLUT4 glucose transport activities in 3T3-L1 cells

Robin W. PALFREYMAN,* Avril E. CLARK,* Richard M. DENTON,† Geoffrey D. HOLMAN* and Izabela J. KOZKA*

*Department of Biochemistry, University of Bath, Claverton Down, Bath BA2 7AY, U.K., and †Department of Biochemistry, University of Bristol, University Walk, Bristol BS8 1TD, U.K.

A bis-mannose-photolabel-displacement method has been developed for resolving the separate kinetic properties of the glucose transporters GLUT1 and GLUT4, which are both present in 3T3-L1 cells. We have quantified the cell-surface transporter abundance ($B_{max.}$) for the two isoforms by displacing radiolabelled 2-*N*-[4-(1-azi-2,2,2-trifluoroethyl)benzoyl]-1,3-bis-(D-mannos-4-yloxy)-2-propylamine (ATB-BMPA) by non-labelled ATB-BMPA. In cells acutely treated with insulin, the GLUT1 $B_{max.}$ was 0.19 μM and the GLUT4 $B_{max.}$ was 0.17 μM. In cells which were chronically treated with insulin, the GLUT1 $B_{max.}$ was increased by ~ 4-fold to 0.7 μM, whereas the GLUT4 was decreased by ~ 50% ($B_{max.}$ = 0.1 μM). However, this large increase in total concentrations of cell-surface transporters (the sum of GLUT1 and GLUT4 concentrations) was not reflected in a large increase in 3-*O*-methyl-D-glucose transport, suggesting that GLUT1 makes a smaller contribution to transport than does GLUT4. In acutely insulin-treated cells at 37 °C, the apparent kinetic parameters for 3-*O*-methyl-D-glucose transport were $V_{max.}^{app.}$ = 0.52 mM·s^{-1} and $K_m^{app.}$ = 12.3 mM. In chronically insulin-treated cells the $V_{max.}^{app.}$ = 1.24 mM·s^{-1} and $K_m^{app.}$ = 23.0 mM. We have measured the displacement of ATB-BMPA by different concentrations of 3-*O*-methyl-D-glucose to resolve the separate affinity constants of GLUT1 and GLUT4 for this transported ligand. In acute- and chronic-insulin-treated cells the GLUT1 K_m for 3-*O*-methyl-D-glucose was ~ 20 mM, and the GLUT4 K_m for 3-*O*-methyl-D-glucose was ~ 7 mM. An analysis of these data and the 3-*O*-methyl-D-glucose transport rates was carried out to calculate transport capacity (TK values) for the two isoforms at 37 °C. In acute- and chronic-insulin-treated cells the TK values were 0.36×10^4 mM^{-1}·min^{-1} for GLUT1 and 1.13×10^4 mM^{-1}·min^{-1} for GLUT4. Thus GLUT1 has an ~ 3-fold lower transport capacity than GLUT4 at low concentrations of transported sugar. The lower GLUT1 transport capacity was shown to be mainly due to the high K_m of GLUT1. The calculated turnover numbers were 7.2×10^4 min^{-1} for GLUT1 and 7.9×10^4 min^{-1} for GLUT4.

INTRODUCTION

Five major mammalian glucose transporter isoforms appear to show some markedly specific tissue distributions. It has been suggested [1–3] that the abundance of a distinct isoform in a particular tissue is related to its transport kinetic properties and therefore its function in that tissue. Cultured cells have been shown to contain high concentrations of the GLUT1 isoform. Cell transformation with oncogenes [4,5], growth factors [6,7], cytokines [8,9] and starvation [10–12] have been shown to increase markedly the concentration of this transporter, with a consequent increase in glucose transport activity. It has been proposed that GLUT2 has a high K_m for D-glucose so that it can function to export rapidly a large range of glucose concentrations from a liver which is undergoing rapid glycogenolysis [13]. The GLUT3 isoform has been detected in many cell and tissue types, including brain and foetal muscle [14]. The GLUT4 isoform has a relatively low K_m, and the translocation of this isoform to the cell surface of adipose cells and muscle [15–19] is stimulated by insulin. The GLUT5 isoform is found in intestinal enterocytes and kidney [20]. Tissue specialized metabolic requirements and kinetic demands for glucose can thus be regulated by expression of tissue-specific transporter isoforms which have distinct transport kinetic properties.

Cultured 3T3-L1 cells also contain high levels of the GLUT1 isoform, but can be differentiated in a regime involving insulin, dexamethasone and isobutylmethylxanthine treatment to give high levels of the acutely insulin-sensitive isoform GLUT4. Calderhead *et al.* [21] and Kozka *et al.* [12] have shown that the acute insulin treatment increases the cell-surface availability of both GLUT4 and GLUT1, so that both are present at the surface in equal amounts. Tordjman *et al.* [22] and Kozka *et al.* [12] have shown, however, that a 24 h chronic insulin treatment increases GLUT1 by 4–5-fold. We have shown [12], by cell-surface labelling, that GLUT4 is down-regulated by 50%. Thus there is a marked change in the isoform type (the GLUT1:GLUT4 ratio increases to 10:1) and a large change in the total concentration of transporter, but these changes are associated with an only ~ 40% increase in transport activity, as measured by the uptake of 2-deoxy-D-glucose at tracer concentrations. These findings suggest that GLUT4 and GLUT1 make unequal contributions to the transport rate. To analyse this possibility further, a method for resolving the separate parameters of GLUT1 and GLUT4 kinetic contributions to transport activity is thus required.

Further analysis of the kinetic differences between the GLUT1 and GLUT4 isoforms that are present in 3T3-L1 cells has necessitated the use of the non-metabolized analogue 3-*O*-methyl-D-glucose in transport kinetic measurements. Because transport measurements alone cannot be easily used to calculate K_m and $V_{max.}$ for each transporter (four parameters), we have determined the separate affinities of the two isoforms for 3-*O*-methyl-D-glucose by measuring the displacement of the bis-mannose photolabel 2-*N*-[4-(1-azi-2,2,2-trifluoroethyl)benzoyl]-1,3-bis-(D-mannos-4-yloxy)-2-propylamine (ATB-BMPA) by a range of concentrations of 3-*O*-methyl-D-glucose. By measuring the binding of the photolabel at a range of ATB-BMPA concentrations,

Abbreviations used: ATB-BMPA, 2-*N*-[4-(1-azi-2,2,2-trifluoroethyl)benzoyl]-1,3-bis-(D-mannos-4-yloxy)-2-propylamine; DMEM, Dulbecco's modified Eagle's medium; $C_{12}E_9$, nona(ethylene glycol) dodecyl ether.

we have determined the concentrations of GLUT1 and GLUT4 at the cell surface. We show how the use of data on transporter concentration and affinity for 3-*O*-methyl-D-glucose can be used to simplify the analysis of transport data to resolve just two parameters (the TK values for GLUT1 and GLUT4). Since the TK is the turnover number divided by K_m (or $V_{max.}/K_m$ divided by transporter concentration), we have used this parameter to calculate the transporter turnover number for each isoform. The TK is formally equivalent to an association constant [23,24]. The TK thus represents the maximum permeability (or transport capacity) of each transporter. A low transporter capacity (TK) is thus due to a low association with substrate because of either a low turnover or a low affinity. We have also examined the issue of photolabelling efficiency.

MATERIALS AND METHODS

Materials

ATB-BMPA and ATB-[2-^{3}H]BMPA (sp. radioactivity ~ 10 Ci/mmol) were prepared as described previously [25,26]. 3-*O*-Methyl-D-[U-^{14}C]glucose was from Amersham International. Dulbecco's modified Eagle's medium (DMEM) was from Flow Laboratories. Foetal-bovine serum was from Gibco. Monocomponent pig insulin was a gift from Dr. Ronald Chance, Eli Lilly Corp. Dexamethasone, isobutylmethylxanthine, phloretin, 3-*O*-methyl-D-glucose and Protein A–Sepharose were from Sigma. $C_{12}E_9$ [nona(ethylene glycol) dodecyl ether] was from Boehringer.

Cell culture

3T3-L1 fibroblasts were obtained from American Type Culture Collection and were cultured in DMEM and differentiated to adipocytes by treatment with insulin, dexamethasone and isobutylmethylxanthine as described previously [12,21,27]. Before use in 3-*O*-methyl-D-glucose transport assays or in cell-surface labelling experiments, the cells were subjected to a standard washing procedure. Cells were washed with phosphate-buffered saline (154 mM-NaCl, 12.5 mM-sodium phosphate, pH 7.4) and were then incubated for 2 h in serum-free medium containing 25 mM-D-glucose. This was followed by three washes in Krebs–Ringer–Hepes (KRH) buffer (136 mM-NaCl, 4.7 mM-KCl, 1.25 mM-$CaCl_2$, 1.25 mM-$MgSO_4$, 10 mM-Hepes, pH 7.4). Cells were then maintained at 37 °C with or without 100 nM pig monocomponent insulin for 30 min in 1 ml of KRH buffer. In chronic-insulin treatment, fully differentiated cells were incubated for 24 h in DMEM with 25 mM-glucose and 500 nM insulin.

3-*O*-Methyl-D-glucose transport assays

3T3-L1 cell monolayers in 35 mm-diam. dishes, treated as described above, were equilibrated with 0–40 mM-3-*O*-methyl-D-glucose in 0.5 ml of KRH buffer for 30 min at 37 °C. The cells were then incubated with 0.5 ml of KRH containing the equilibrium concentrations of 3-*O*-methyl-D-glucose and 0.3 μCi of 3-*O*-methyl-D-[U-^{14}C]glucose. At 10 s for insulin-treated cells and at 120–160 s for basal cells, 1 ml of ice-cold KRH containing 0.3 mM-phloretin was added to arrest transport. The dishes were rapidly washed three times in the stopping solution. The cell-associated radioactivity was then extracted and counted. The radioactivity associated with the cells at zero time was determined by adding stopping solution before the radioactive 3-*O*-methyl-D-glucose. The radioactivity associated with the cells at equilibrium was determined by incubating insulin-treated cells with 3-*O*-methyl-D-glucose for 15 min. The total cell volume per 35 mm dish was calculated from the equilibrated 3-*O*-methyl-D-glucose and was found to be 2.81 ± 0.43 μl/dish (from six experiments; two experiments acute-insulin, three experiments chronic-insulin, one experiment basal). Equilibrium exchange uptake rate constants (k) were then calculated from the equation $k = n(1-f)/t$, where t is the uptake time and f is the fractional filling [28,29]. In experiments used to estimate the half-maximal inhibition constant (K_i) for ATP-BMPA, the inhibitor was added with 50 μM-3-*O*-methyl-D-glucose as substrate. The extent of irreversible inhibition of transport produced by photoincorporation of ATB-BMPA was determined by irradiating cells in 35 mm dishes (for 1 min in a Rayonet photochemical reactor [12]) in the presence of 0.5–2 mM-ATB-BMPA in 500 μl of KRH. The dishes were then washed three times in KRH to remove non-incorporated ATB-BMPA and then assayed for residual transport of 50 μM-3-*O*-methyl-D-glucose as described above.

ATB-BMPA photolabelling

Differentiated cells in 35 mm dishes were washed in KRH buffer at 37 °C and were irradiated for 1 min in the presence of 100 μCi of ATB-[2-^{3}H]BMPA as described previously [12]. To determine the binding kinetic parameters, the specific radioactivity of the label was decreased by addition of non-radioactive ATB-BMPA at the concentrations indicated in the Figures. Bound ATB-BMPA (mol) was calculated from the d.p.m. recovered after immunoprecipitation and gel electrophoresis of the photolabelled GLUT1 or GLUT4. The free ATB-BMPA was assumed to be equal to the combined concentration of the non-radioactive and radioactive ligand, and was not corrected for the small amount of ATB-BMPA bound to the cells.

Immunoprecipitation and electrophoresis

The irradiated cells were washed three times in KRH buffer and solubilized in 1.5 ml of detergent buffer, containing 2% $C_{12}E_9$, 5 mM-sodium phosphate and 5 mM EDTA, pH 7.2, and with the proteinase inhibitors antipain, aprotinin, pepstatin and leupeptin, each at 1 μg/ml. After centrifugation at 20000 $g_{max.}$ for 20 min, the supernatants were subjected to sequential immunoprecipitation with 20 μl of Protein A–Sepharose coupled to 100 μl of either anti-GLUT1 or anti-GLUT4 antiserum. These antisera were raised against *C*-terminal peptides as described previously [23,26]. After incubation for 1.5–2 h at 0–4 °C and washing of the immunoprecipitates three times with 1.0% and once with 0.1% $C_{12}E_9$ detergent buffer, the labelled glucose transporters were released from the antibody complexes with electrophoresis sample buffer (10% SDS/6 M-urea/10% mercaptoethanol) and then subjected to electrophoresis on 10%-acrylamide gels. The radioactivity on the gel was measured by cutting and counting gel slices. The radioactivity in transporter peaks was corrected for a background which was based on the average radioactivity of the slices on either side of the peak [21]. We have determined that, after immunoprecipitation with anti-GLUT1 and anti-GLUT4 antibodies, the amount of photolabelled transporter remaining in the supernatants is < 20% of the unprecipitated total of labelled transporters.

RESULTS

3-*O*-Methyl-D-glucose transport

The exchange uptake of 3-*O*-methyl-D-glucose was studied. This transport protocol was equivalent to that used in the photolabel-displacement experiments described below. Thus the cells were pre-equilibrated with non-radioactive 3-*O*-methyl-D-glucose, and then the influx of radioactive 3-*O*-methyl-D-glucose was measured. When a single transporter isoform is present, the concentration of 3-*O*-methyl-D-glucose at which the rate constant is decreased by half is formally equivalent to the equilibrium binding constant between 3-*O*-methyl-D-glucose and the trans-

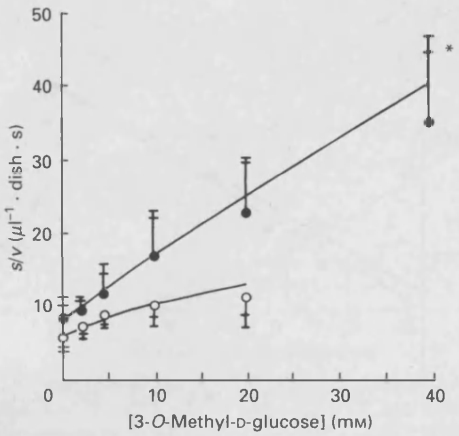

Fig. 1. Equilibrium exchange uptake of 3-*O*-methyl-D-glucose in 3T3-L1 cells

3T3-L1 cells in 35 mm dishes were either acutely treated with 100 nM-insulin for 30 min (●) or chronically treated with 500 nM-insulin for 24 h (○), and uptake of 3-*O*-methyl-D-glucose was determined as described in the Materials and methods section. s/v, the reciprocal of the uptake rate constant, was plotted against the 3-*O*-methyl-D-glucose concentration. The values shown were means from four experiments each with triplicate estimates of uptake rate constants. The inner S.E.M. bars were calculated with $n = 12$ (combining the replicate values), and the outer S.E.M. bars were calculated with $n = 4$ (by using the mean of the replicates from each independent experiment), except the value indicated by *, where the inner bar is the S.E.M. ($n = 4$) and the outer bar is the S.E.M. ($n = 12$). To convert the s/v values from $\mu l^{-1} \cdot$dish$\cdot$s into s, the plotted values were divided by the equilibrium intracellular volume of 2.81 μl/dish. The lines for both acute and chronic insulin treatments were derived from a single set of calculated TK values of 3.58×10^3 and 11.34×10^3 mM$^{-1} \cdot$min^{-1} for GLUT1 and GLUT4 respectively and by using the $B_{max.}$ and K_m values listed in row 5 of Table 1.

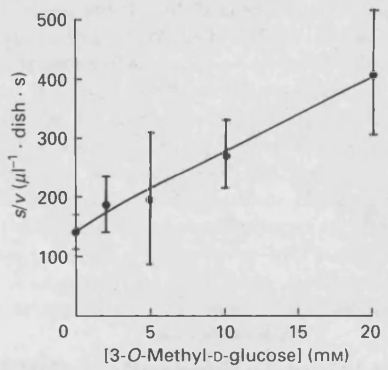

Fig. 2. Equilibrium exchange uptake of 3-*O*-methyl-D-glucose in basal 3T3-L1 cells

The uptake of 3-*O*-methyl-D-glucose into basal cells was determined as described in the Materials and methods section. s/v, the reciprocal of the uptake rate constant (●), was plotted against 3-*O*-methyl-D-glucose concentration, and the values are means ± S.E.M. ($n = 6$ from two experiments with triplicate estimates of the uptake rate constants). Additional experiments were carried out at 50 μM-3-*O*-methyl-D-glucose to estimate the range of variation of basal activity between experiments. In basal cells the s/v value was 144.9 ± 18.1 $\mu l^{-1} \cdot$dish$\cdot$s ($n = 11$, mean ± S.E.M. of 11 experiments each with triplicate estimates of the rate constants). In this series of experiments, acute insulin treatment decreased the s/v value 15-fold, to 9.57 ± 1.64 $\mu l^{-1} \cdot$dish$\cdot$s ($n = 11$, mean ± S.E.M. from 11 experiments each with triplicate estimates of the rate constant). To convert the s/v values from $\mu l^{-1} \cdot$dish$\cdot$s into s, the plotted values were divided by the equilibrium intracellular volume of 2.81 μl/dish. The line was derived from the TK, $B_{max.}$ and K_m values listed in row 6 of Table 1.

porter (the equilibrium exchange K_m). This has been shown to equal the concentration of 3-*O*-methyl-D-glucose that displaces the binding of tracer concentrations of another ligand such as cytochalasin B or ATB-BMPA [30].

When two isoforms are present, the relationship between the reciprocal of the exchange rate constant and the 3-*O*-methyl-D-glucose concentration may be curvilinear. The reciprocal plots shown in Fig. 1 are slightly curved, and this is likely to be due to the varying contributions of the two isoforms as the 3-*O*-methyl-D-glucose concentration is varied. The lines in Fig. 1 were therefore derived from the analysis of the separate GLUT1 and GLUT4 contributions to transport as described in the Discussion section. Fitting the data to the Michaelis–Menten equation, however, revealed an apparent K_m for 3-*O*-methyl-D-glucose of 12.3 ± 1.3 mM and $V_{max.} = 0.52 \pm 0.04$ mM$\cdot$s^{-1} in acute-insulin-treated cells (derived from the mean values of the rate constants from four experiments). These estimates are similar to those determined by Clancy *et al.* [31], who have also measured the kinetic parameters for 3-*O*-methyl-D-glucose transport in insulin-stimulated 3T3-L1 cells. They report values of $K_m = 10.9$ mM and $V_{max.} = 2.76$ pmol/min per 10^6 cells. Calculations using their estimate of cell volume of 5.6 μl/10^6 cells gave a $V_{max.}$ of 0.46 mM$\cdot$s^{-1}. However, we note that the cell volume in our experiments was ~ 2–3-fold smaller than that estimated by Clancy *et al.* [31].

In chronically-insulin treated cells we have found that the apparent K_m and $V_{max.}$ were increased to 23.0 ± 9.1 mM and 1.24 ± 0.40 mM$\cdot$s^{-1} respectively (determined from mean values of the rate constants obtained from four experiments). The large S.E.M. for these parameters is due to the curvilinearity of the kinetic plot, rather than the between-experiment variations in the kinetic parameters. The chronic-insulin treatment altered the GLUT1:GLUT4 ratio from 1:1 to 10:1 (see below). Thus the high apparent K_m for 3-*O*-methyl-D-glucose transport found in this condition is likely to reflect a high GLUT1 K_m for this substrate.

The apparent K_m and $V_{max.}$ for 3-*O*-methyl-D-glucose transport in basal cells obtained by fitting of the Michaelis–Menten equation were 11.5 ± 1.7 mM and 0.028 ± 0.003 mM$\cdot$s^{-1} respectively (determined from mean values of the rate constants obtained in two experiments) (Fig. 2).

We have also determined the K_i for the bis-mannose photolabel, ATB-BMPA, as an inhibitor of 3-*O*-methyl-D-glucose uptake (Fig. 3). We have used a 3-*O*-methyl-D-glucose substrate concentration of 50 μM, which is low in comparison with the affinity of either GLUT1 or GLUT4 for 3-*O*-methyl-D-glucose. Under these conditions the K_i can be calculated from the equation $v_0/v = 1 + I/K_i$, where v_0/v is the fractional inhibition and I is the inhibitor concentration [29]. The calculated K_i was 263 ± 30 μM in the acute-insulin treatment, which was not significantly different from the K_i determined in chronically insulin-treated cells, which gave $K_i = 200 \pm 53$ μM (one experiment).

We have examined the efficiency of irreversible inactivation of the transport rate owing to photoincorporation of ATB-BMPA. We have found that, after irradiation of 3T3-L1 cells in the presence of 0.5 mM-, 1 mM- and 2 mM-ATB-BMPA and removal of unbound ligand by washing, 2-deoxy-D-glucose transport was inhibited by 48%, 54% and 68% respectively compared with untreated samples. Since at these concentrations of ATB-BMPA 33%, 20% and 12% of the sites are unoccupied (assuming a K_d for ATB-BMPA of 250 μM), it can be calculated that, when all the sites are occupied, ~ 75% of the sites would have been irreversibly inactivated (results from two experiments).

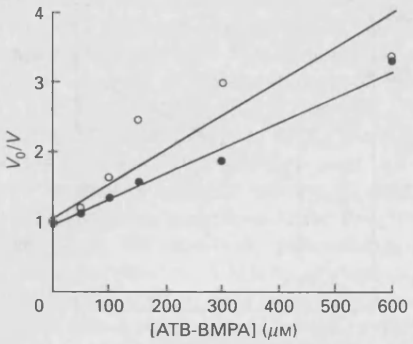

Fig. 3. Inhibition of 3-*O*-methyl-D-glucose uptake by ATB-BMPA

3T3-L1 cells in 35 mm dishes were either acutely (●) or chronically (○) treated with insulin, and the ratio of the rate constant for uptake of 50 μM-3-*O*-methyl-D-glucose in the absence and presence of ATB-BMPA (v_0/v) was plotted against the ATB-BMPA concentration (I). The results are from a single experiment with triplicate determinations of the rate constant. The line was derived by fitting the equation $v_0/v = 1 + I/K_i$ by using non-linear regression analysis weighted for relative error. This gave K_i values of 263 ± 30 μM (acute treatment) and 200 ± 53 μM (chronic treatment).

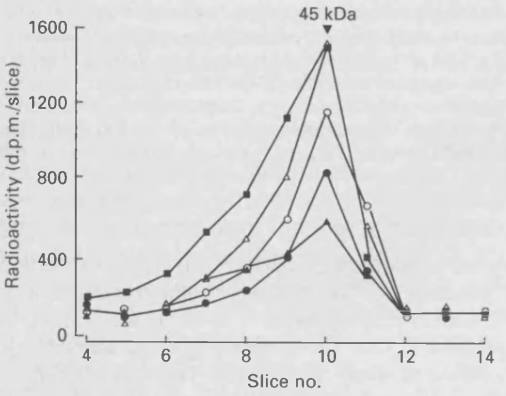

Fig. 4. Displacement of radiolabelled ATB-BMPA from GLUT4 by non-labelled ligand

3T3-L1 cells in 35 mm dishes were acutely treated with insulin and then photolabeled with 40 μM-ATB-[2-^{3}H]BMPA (100 μCi) either alone (■) or with additional non-labelled ATB-BMPA at 50 μM (△), 100 μM (○), 150 μM (●) or 300 μM (▲). GLUT4 was immunoprecipitated with anti-*C*-terminal-peptide antibody and subjected to electrophoresis. The radioactivity was measured by cutting and counting the gel slices. The data were used to calculate the concentration of ATB-BMPA bound. The position of the 45 kDa marker protein (ovalbumin) is shown

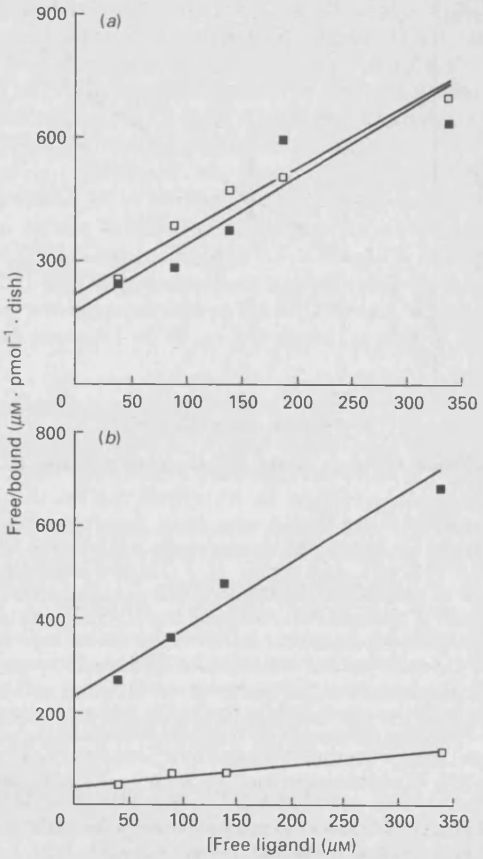

Fig. 5. Determination of the $B_{max.}$ values for ATB-BMPA binding to GLUT1 and GLUT4 glucose transporters in 3T3-L1 cells

3T3-L1 cells in 35 mm dishes were in (*a*) acutely treated with 100 nM-insulin for 30 min and in (*b*) chronically treated with 500 nM-insulin for 24 h and then described in the legend to Fig. 4, except that the data show the binding in immunoprecipitated GLUT4 (■) and GLUT1 (□). The results shown are from a single experiment. To convert the bound ATB-BMPA from pmol^{-1}·dish into μM, the values were divided by the equilibrium cell volume of 2.81 μl/dish. In acutely insulin-treated cells the GLUT1 $B_{max.}$ was 0.19 ± 0.03 μM and the GLUT4 $B_{max.}$ was 0.17 ± 0.03 μM (from three experiments). In chronically insulin-treated cells the GLUT1 $B_{max.}$ was 0.7 ± 0.07 μM, whereas the GLUT4 $B_{max.}$ was 0.099 ± 0.017 μM (from three experiments).

ATB-BMPA photolabelling

We have shown from results obtained by immunoprecipitating glucose transporters with antibodies against GLUT1 and GLUT4 *C*-terminal peptide that GLUT1 is the predominant isoform present in the cell membrane in the basal cells and that this is increased by ~ 3–5-fold after insulin treatment. Only low levels of GLUT4 were detected at the cell surface in the basal state, but an ~ 10–15-fold increase was observed after insulin treatment [12,21]. We have extended these observations here by measuring the binding of ATB-BMPA at a range of concentrations and calculated the K_d and apparent $B_{max.}$ for GLUT1 and GLUT4. Fig. 4 shows the displacement of ATB-[2-^{3}H]BMPA by a range of concentrations of non-labelled ATB-BMPA from GLUT4 in acutely insulin-treated cells. From these data the amount of ATB-BMPA bound was calculated, and these data were used to calculate $B_{max.}$ and K_d values by non-linear regression analysis of bound versus free ATB-BMPA concentration. Reciprocal plots are shown in Figs. 5(*a*) and 5(*b*). Fig. 5(*a*) shows that in acutely insulin-treated cells GLUT1 and GLUT4 have K_d values which were not significantly different and were ~ 150 μM. Thus binding of the photolabel at the high specific radioactivity of 10 Ci/mmol and low tracer concentrations of 40 μM (the present study) and 80 μM [12] is proportional to the number of GLUT1 and GLUT4 binding sites and is not dependent on an affinity difference between the two isoforms. We have previously shown that a chronic insulin treatment increases the tracer labelling of GLUT1 by 4–5-fold compared with the acute treatment. In Fig. 5(*b*) this is confirmed not to be due to an affinity change. The plots in Figs. 5(*a*) and 5(*b*) show bound ligand as pmol bound per 35 mm dish and are from one experiment. The $B_{max.}$ values were obtained from these data by dividing by the 3-*O*-methyl-D-glucose equilibrium space of 2.81 μl/dish, which gave transporter concentrations in μmol/l of intracellular water or μM. In acutely insulin-treated cells the GLUT1 $B_{max.}$ was 0.19 ± 0.03 μM and the GLUT4

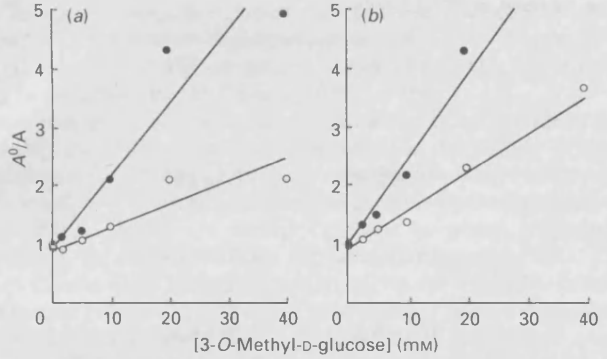

Fig. 6. Determination of the K_m values for 3-*O*-methyl-D-glucose displacement of ATB-BMPA from GLUT1 and GLUT4 glucose transporters in 3T3-L1 cells

3T3-L1 cells in 35 mm dishes were in (*a*) acutely treated with 100 nM-insulin for 30 min and in (*b*) chronically treated with 500 nM-insulin for 24 h and then photolabelled with 100 μCi of ATB-BMPA at the indicated concentrations of 3-*O*-methyl-D-glucose. Photolabelled GLUT1 (○) and GLUT4 (●) were then immunoprecipitated with anti-*C*-terminal-peptide antibodies and subjected to electrophoresis. Radioactivity was determined by cutting and counting gel slices. The ratio of the radioactivity associated with the peaks obtained in the absence (A^0) and presence (A) of competing ligand were then determined. The results shown are the mean values from three experiments (acute treatment) and two experiments (chronic treatment). The K_m values were obtained by fitting the equation $A^0/A = 1+s/K_m$ by using non-linear regression analysis weighted for relative error. In the acute treatment the GLUT1 K_m was 23.4 ± 7.6 mM and the GLUT4 K_m was 7.2 ± 2.0 mM. In the chronic treatment the GLUT1 K_m was 16.4 ± 2.9 mM and the GLUT4 K_m was 6.85 ± 1.5 mM.

$B_{max.}$ was 0.17 ± 0.03 μM (from three experiments). The GLUT1 $B_{max.}$ for ATB-BMPA in chronically insulin-treated cells was 0.70 ± 0.07 μM. The GLUT4 $B_{max.}$ in these cells was decreased to 0.099 ± 0.017 μM (from three experiments).

A similar photolabel-displacement methodology was used to measure the separate affinity constants of GLUT1 and GLUT4 for 3-*O*-methyl-D-glucose. Concentrations of 3-*O*-methyl-D-glucose of 0–20 mM were incubated with the photolabel in either acutely or chronically insulin-treated 3T3-L1 cells. Fig. 6(*a*) shows that in acutely insulin-treated cells the K_m for 3-*O*-methyl-D-glucose displacement was 23.4 ± 7.6 mM, which was ~ 3-fold higher than the GLUT4 K_m, which was 7.2 ± 2.0 mM (from three experiments). In chronically insulin-treated cells (Fig. 6*b*) the GLUT1 K_m for 3-*O*-methyl-D-glucose was 16.4 ± 2.9 mM and was ~ 3-fold higher than the GLUT4 K_m, which was 6.8 ± 1.5 mM (from two experiments). The results of the 3-*O*-methyl-D-glucose displacement were used in conjunction with the $B_{max.}$ values to calculate TK values for GLUT1 and GLUT4 as described in the Discussion section. Table 1 shows that the TK value for GLUT4 was ~ 3-fold higher than for GLUT1.

In the basal state, the GLUT1 and GLUT4 K_m values for 3-*O*-methyl-D-glucose and their K_d values for the photolabel could not be examined directly by using the ATB-BMPA displacement methodology, because the radioactive ATB-BMPA incorporated was very low and any displacement by ligand would decrease the recovered radiolabel even further. However, we have shown, in basal rat adipocytes and 3T3-L1 cells, that the ATB-BMPA concentration required for half-maximal inhibition of transport is not significantly different from that required for half-maximal inhibition of transport in insulin-treated cells [21,23]. In view of the limited applicability of the photolabel-displacement methodology to the basal state, we have determined GLUT1 and GLUT4 levels from the photolabelling of basal cells with tracer concentrations (80 μM) of ATB-BMPA. We have then calculated the concentrations of unoccupied sites ($x1$ and $x4$ in eqn. 4 in the Discussion section), using the assumption that the K_d for ATB-BMPA and the K_m for 3-*O*-methyl-D-glucose were the same as in the insulin-stimulated cells. This analysis method (Table 1) showed that the calculated GLUT1 and GLUT4 TK values in basal cells were ~ 2-fold lower than in the insulin-treated cells. Because the analysis of photolabelling and transport data in the basal state involved greater error and used more assumptions than the analysis of the data from insulin-stimulated cells, we place less reliance on the TK values calculated for the basal cells.

DISCUSSION

Determination of the intrinsic activity of GLUT1 and GLUT4

We have shown that 80% of the cell-surface transporter labelling is immunoprecipitated by GLUT1 and GLUT4 antibodies. Thus if other isoforms are present they are not very abundant and are not likely to significantly contribute to transport. As discussed by Calderhead *et al.* [21], uptake is thus given by the sum of two Michaelis–Menten equations representing the separate flux attributable to each of the isoforms:

$$v = \frac{V_{max.1}\cdot S/K_{m1}}{(1+S/K_{m1})} + \frac{V_{max.4}\cdot S/K_{m4}}{(1+S/K_{m4})} \quad (1)$$

where $V_{max.}$ and K_m are the equilibrium exchange transport parameters.

$V_{max.}$ values are dependent on the transporter concentrations and the catalytic rate constants. The $1/(1+S/K_m)$ or $K_m/(K_m+S)$ terms represent the fraction of unoccupied sites. Thus eqn. (1) can be written as follows:

$$v = \frac{TK1\cdot S\cdot[GLUT1]}{(1+S/K_{m1})} + \frac{TK4\cdot S\cdot[GLUT4]}{(1+S/K_{m4})} \quad (2)$$

where [GLUT1] and [GLUT4] are the transporter isoform concentrations and TK1 and TK4 are the association constants, which are equal to turnover number/K_m and thus represent the tendency of the substrate to associate with unoccupied sites.

Values for the GLUT1 and GLUT4 concentrations used for substitution into eqn. (2) were determined from ATB-BMPA binding data, which we have shown in the Results section gave values for K_d and $B_{max.}$. The terms in eqn. (2) representing the reciprocal of the fraction of unoccupied sites can be directly obtained from the displacement of the photolabel, where:

$$A^0/A = 1+S/K_m \quad (3)$$

where A^0/A values are the ratios of the radioactivity associated with the photolabelled transporters in the presence (A) and absence (A^0) of competing 3-*O*-methyl-D-glucose and used to calculate the TK values shown in rows 1–3 in Table 1. The K_m values of GLUT1 and GLUT4 can also be obtained from the 3-*O*-methyl-D-glucose displacement of the photolabel (eqn. 3). These K_m values can then be used in an alternative method to calculate the fraction of unoccupied sites (rows 4–6 in Table 1).

Multiplying the $B_{max.}$ values by the fraction of unoccupied sites (either A/A^0 or $1/(1+S/K_m)$ gave $x1$ and $x4$ (the concentrations of unoccupied sites). Values of TK1 and TK4 were then derived from eqn. (4) by least-squares regression, by the methods described by Cleland [32]:

$$v/S = TK1\cdot x1 + TK4\cdot x4 \quad (4)$$

Table 1 compares the results of analysis of TK values carried out by several different methods for calculating the concentration of unoccupied sites. The method appears to be quite robust and can handle the combined errors involved in using transport data

Table 1. Calculation of GLUT1 and GLUT4 TK values for 3-*O*-methyl-D-glucose transport in 3T3-L1 cells

	Analysis method	$10^{-3} \times$ TK1 ($mM^{-1} \cdot min^{-1}$)	$10^{-3} \times$ TK4 ($mM^{-1} \cdot min^{-1}$)
1. Acute insulin	Direct use of A^0/A values $B_{max.1} = 0.19\ \mu M$ $B_{max.4} = 0.17\ \mu M$	4.90±2.03	7.92±2.86
2. Chronic insulin	Direct use of A^0/A values $B_{max.1} = 0.70\ \mu M$ $B_{max.4} = 0.099\ \mu M$	3.82±2.20	8.60±18.4
3. Combined data from acute and chronic treatments	Direct use of A^0/A values $B_{max.}$ values as above	3.71±0.31	9.50±1.26
4. Combined data from acute and chronic treatments	Acute insulin $K_{m1} = 23.4$ mM $K_{m4} = 7.2$ mM Chronic insulin $K_{m1} = 16.4$ mM $K_{m4} = 6.85$ mM $B_{max.}$ values as above	3.73±0.26	10.92±1.11
5. Combined data from acute and chronic treatments	Using average K_m: $K_{m1} = 19.9$ mM $K_{m4} = 7.0$ mM $B_{max.}$ values as above	3.58±0.24	11.34±1.06
6. Basal	Using average K_m: $K_{m1} = 19.9$ mM $K_{m4} = 7.0$ mM $B_{max.1} = 0.055\ \mu M$ $B_{max.4} = 0.015\ \mu M$	1.20±0.36	5.73±2.02

and A/A^0 values directly. TK values were obtained which were similar to those obtained when the error in $x1$ and $x4$ was decreased by using $x1$ and $x4$ values which were calculated from the 3-*O*-methyl-D-glucose K_m values. Table 1 shows that the TK values for GLUT1 and GLUT4 were similar for both the acute-insulin and the chronic-insulin treatments. The GLUT1 TK was found to be 0.36×10^4 $mM^{-1} \cdot min^{-1}$, whereas the GLUT4 TK was ~ 3-fold higher (1.13×10^4 $mM^{-1} \cdot min^{-1}$). Multiplying these values by the GLUT1 and GLUT4 average K_m values of 20.0 and 7.0 mM respectively gave a GLUT1 turnover number, or catalytic rate constant, of 7.2×10^4 min^{-1} and a value for GLUT4 turnover number of 7.9×10^4 min^{-1}. Thus, at low concentrations of 3-*O*-methyl-D-glucose, GLUT1 makes a substantially smaller contribution to flux than does an equal concentration of the GLUT4 isoform. However, this is due to the low affinity of GLUT1 for this substrate, which decreases its association with the transporter.

The GLUT1 turnover calculated from this data on 3T3-L1 cells (7.2×10^4 min^{-1} at 37 °C) is of the same order as that calculated from GLUT1 in other systems, but at 20 °C. The GLUT1 turnover for 3-*O*-methyl-D-glucose at 20 °C has been determined in oocytes injected with GLUT1 mRNA [33,34]. Gould and Lienhard [33] estimated that their oocytes expressed 7 ng of GLUT1 per oocyte and calculated a turnover number of 1×10^4 min^{-1}. However, Keller *et al.* [34] have estimated that their system expressed 0.2 ng of GLUT1 per oocyte and calculated a 3-*O*-methyl-D-glucose turnover at 20 °C of 13.4×10^4 min^{-1}. Our own estimate of the rate constant for 50 μM-3-*O*-methyl-D-glucose uptake in erythrocytes at 20 °C was 15.2 min^{-1} [35], giving a calculated turnover of 4.3×10^4 min^{-1} (assuming a GLUT1 concentration of 7 μM and a 3-*O*-methyl-D-glucose exchange K_m of 20.0 mM). The GLUT4 turnover that we have calculated from the data obtained for 3-*O*-methyl-D-glucose transport in 3T3-L1 cells (7.9×10^4 min^{-1} at 37 °C) is very similar to that obtained in rat adipocytes, where the 3-*O*-methyl-D-glucose turnover at 37 °C was calculated by Simpson *et al.* [36] to be 5.6×10^4 min^{-1}. Our own estimate [37] of the 3-*O*-methyl-D-glucose exchange $V_{max.}$ was 50.4 $mM \cdot min^{-1}$ at 37 °C. Since the GLUT4 concentration was ~ 1.5 μM (calculated from [36]), the calculated turnover number is 3.4×10^4 min^{-1}.

In the basal state the calculated turnover numbers for GLUT1 and GLUT4 are ~ 2-fold lower than that found for insulin-stimulated 3T3-L1 cells. There are many inaccuracies in measuring transport and photolabelling in the basal state. However, the result is consistent with the ~ 1.5–2-fold suppression of transport activity in the basal state that we have shown in rat adipocytes [23,38].

Assumptions used in the analysis of GLUT1 and GLUT4 activity

In the analysis above, we have demonstrated that the ATB-BMPA displacement methodology can be used to provide information on the relative activities of the GLUT1 and GLUT4 transporters when these are present in the same cell population. The analysis assumes that the radioactivity recovered in the immunoprecipitates reflects the relative abundance of these isoforms, and we now examine this assumption.

We have attempted to determine whether all the sites which reversibly bind the photolabel irreversibly react with it when irradiated. We have shown from the transport inhibition observed at 0.5, 1 and 2 mM ligand that most of the sites bind label irreversibly when occupied. This would be consistent with observations made with human erythrocyte membranes, where close to 100% efficiency of the photochemical reaction was apparent with ATB-BMPA as the probe [26]. The high photochemical efficiency which is observed with the diazirine-substituted bis-hexose was much greater than that obtained with aryl azide-substituted compounds, where the estimated efficiency was only ~ 25% [39].

We have found that, after immunoprecipitation of both GLUT1 and GLUT4 from $C_{12}E_9$-solubilized cells, < 20% of the radioactivity running in the transporter region of the gel is left in

the immunoprecipitation supernatants. These findings are consistent with previous observations that the efficiencies of immunoprecipitation of GLUT1 and GLUT4 in human erythrocytes [26] and in rat adipocytes [23] are ~ 80%.

Another factor which is relevant to the use of ATB-BMPA to quantify the level of transporter isoforms is the affinity of the transporter for the ligand. In the present study we have observed that the K_i is ~ 250 μM in acutely and chronically insulin-treated cells. These results are similar to those in which transport inhibition by ATB-BMPA in erythrocytes showed a GLUT1 K_i ~ 250 μM [26]. Transport inhibition by ATB-BMPA in rat adipocytes (where GLUT4 is the predominant isoform) showed a GLUT4 K_i which was also ~ 250 μM [23]. A more direct way of examining the affinities of the two transporters for the ligand is to carry out photolabel-binding experiments at a range of concentrations. We have shown here that the affinity constants (in this case K_d) for ATB-BMPA binding to GLUT1 and GLUT4 are equal and are ~ 150 μM. The GLUT2 isoform in liver membranes also has a K_d for ATB-BMPA of ~ 200 μM (N. J. Jordan & G. D. Holman, unpublished work). Thus the binding of ATB-BMPA (a non-transported ligand) is approximately equal for all the mammalian isoforms tested (GLUT1, GLUT4 and GLUT2). However, these isoforms have different K_m values for transported substrates. The ability to bind a non-transported ligand at the outside site is kinetically a simpler reaction than that involved in binding and transporting a substrate. The apparent K_m for equilibrium sugar binding or exchange is dependent on rate constants for the membrane translocation step and the affinity constant at the inside site, and it is these parameters that may vary between different transporter isoforms.

These considerations suggest that the ATB-BMPA displacement methodology that we have used can be considered to give a good approximation of the transporter isoform concentrations at the cell-surface. We have shown that in acutely insulin-treated cells the GLUT1 concentration at the cell surface was 0.19 μM or 29.7 ng/35 mm dish, and the GLUT4 concentration was 0.17 μM or 27 ng/35 mm dish. This estimate of GLUT4 concentration compares reasonably well with the total cellular GLUT4 concentration as estimated by Western blotting. Calderhead *et al.* [21] found 50 ng/35 mm dish, and this is consistent with about half of GLUT4 being at the cells surface. However, the estimated cell surface GLUT1 appears to be a low proportion (~ $\frac{1}{5}$) of the total cellular GLUT1, which was determined by Western blotting to be 150 ng/35 mm dish [21].

We note that an under-estimate of the cell-surface glucose transporter concentration owing to factors such as low labelling or immunoprecipitation efficiency would lead us to over-estimate the transporter turnover numbers.

Regulation of the transport activities in 3T3-L1 cells

Large changes in cell-surface levels of glucose transporters occur in 3T3-L1 cells. We have determined that in basal cells the GLUT1:GLUT4 ratio was ~ 3:1. This was decreased by acute insulin treatment to 1:1, but increased to 10:1 owing to a prolonged chronic insulin treatment ([12]; the present work). It has been shown that in adipose cells translocation of GLUT4 glucose transporters from an intracellular pool [23,40–42] accounts for most of the observed acute insulin response. However, we have observed here that the intrinsic activities calculated from data obtained with insulin-stimulated cells cannot account entirely for the low transport rates observed in basal cells. This may be because the intrinsic activity of glucose transporters is slightly suppressed in the basal state, as suggested by Czech and co-workers [43,44] and by Zorzano *et al.* [45]. The analysis of intrinsic activity in the basal cells was not as accurate as that carried out with insulin-stimulated cells. However, GLUT1 and GLUT4 appear to have ~ 2-fold lower turnovers in basal cells. The suppression of GLUT1 activity may be slightly greater than suppression of GLUT4 activity.

The discrepancy between transport rate and photolabelling that we have observed here and elsewhere [21,38,46] suggest that the photolabel can combine with transporters that are at the surface but which do not participate fully in transport. We have suggested [46] that this suppression of transport activity may occur because transporters associate with trafficking proteins present as intermediates in the translocation process. An alternative possibility that has been suggested is that regulation of the activity of the GLUT1 isoform may be dependent on intracellular small molecules or inhibitory proteins which allosterically modify the transport catalysis rate [31,43,44,47]. This possible susceptibility of GLUT1 to allosteric control may account for the unusual kinetic properties of this isoform found in erythrocytes, where transport is kinetically asymmetric and shows accelerated exchange [28,47]. In contrast with these kinetic features of GLUT1 we have found [37] that in rat adipocytes, where GLUT4 is the predominant isoform and translocation is the predominant regulatory mechanism, the transport system is kinetically symmetric and does not show accelerated exchange.

Chronic insulin treatment greatly increases, by new protein synthesis, the total cellular content and the cell-surface concentration of GLUT1 [12,22], and we have suggested that this may be a response which compensates for the down-regulation of cell surface GLUT4 [12]. Consistent with this possibility is the observation that GLUT4 is down-regulated in 4–6 h, whereas GLUT1 rises steadily over 24 h. We have suggested [12] that the down-regulation of GLUT4 may be due to an impairment of the translocation mechanism, so that it may be of regulatory value to the cell to be able to produce, by new protein synthesis, an isoform which has different transport properties.

We are grateful to the M.R.C. and the British Diabetic Association for financial support.

REFERENCES

1. Pilch, P. F. (1990) Endocrinology (Baltimore) **126**, 3–5
2. Mueckler, M. (1990) Diabetes **39**, 6–10
3. Gould, G. W. & Bell, G. I. (1990) Trends Biochem. Sci. **15**, 18–22
4. Flier, J. S., Mueckler, M. M., Usher, P. & Lodish, H. F. (1987) Science **235**, 1492–1495
5. Birnbaum, M. J., Haspel, H. C. & Rosen, O. M. (1987) Science **235**, 1495–1498
6. Hiraki, Y., Rosen, O. M. & Birnbaum, M. J. (1988) J. Biol. Chem. **263**, 13655–13662
7. Rollins, B. J., Morrison, E. D., Usher, P. & Flier, J. S. (1988) J. Biol. Chem. **263**, 16523–16526
8. Cornelius, P., Marlowe, M., Lee, M. D. & Pekala, P. H. (1990) J. Biol. Chem. **265**, 20506–20516
9. Bird, T. A., Davies, A., Baldwin, S. A. & Saklatvala, J. (1990) J. Biol. Chem. **265**, 13578–13583
10. Haspel, H. C., Wilk, E. W., Birnbaum, M. J., Cushman, S. W. & Rosen, O. M. (1986) J. Biol. Chem. **261**, 6778–6789
11. Tordjman, K. M., Liengang, K. A. & Mueckler, M. (1990) Biochem. J. **271**, 201–207
12. Kozka, I. J., Clark, A. E. & Holman, G. D. (1991) J. Biol. Chem. **266**, 11726–11731
13. Thorens, B., Sarkar, H. K., Kaback, R. H. & Lodish, H. F. (1988) Cell **55**, 281–290
14. Kayano, T., Fukumoto, M., Eddy, R. L., Fan, Y.-S., Byers, M. G., Showa, T. G. & Bell, G. I. (1988) J. Biol. Chem. **263**, 15245–15248
15. James, D. E., Strube, M. I. & Mueckler, M. (1989) Nature (London) **338**, 83–87
16. Charron, M. J., Brosius, F. C., Alper, S. L. Lodish, H. F. (1989) Proc. Natl. Acad. Sci. U.S.A. **86**, 2535–2539
17. Kaestner, K. H., Christy, R. J., McLenithan, J. C., Braiterman, L. T., Cornelius, P., Pekela, P. H. & Lane, M. D. (1989) Proc. Natl. Acad. Sci. U.S.A. **86**, 3150–3154

18. Birnbaum, M. J. (1989) Cell **57**, 305–315
19. Fukumoto, H., Kayano, T., Buse, J. B., Edwards, Y., Pilch, P. F., Bell, G. I. & Seino, S. (1989) J. Biol. Chem. **264**, 7776–7779
20. Kayano, T., Burant, C. F., Fukumoto, H., Gould, G. W., Fan. Y.-S., Eddy, R. L., Byers, M. G., Shows, T. B., Seino, S. & Bell, G. I. (1990) J. Biol. Chem. **265**, 13276–13282
21. Calderhead, D. M., Kitagawa, W., Tanner, L. T., Holman, G. D. & Lienhard, G. E. (1990) J. Biol. Chem. **265**, 13800–13808
22. Tordjman, K. M., Leingang, K. A., James, D. E. & Mueckler, M. (1989) Proc. Natl. Acad. Sci. U.S.A. **86**, 7761–7765
23. Holman, G. D., Kozka, I. J., Clark, A. E., Flower, C. J., Saltis, J., Habberfield, A. D., Simpson, I. A. & Cushman, S. W. (1990) J. Biol. Chem. **265**, 18172–18179
24. Stein, W. D. (1986) Transport and Diffusion across Cell Membranes, pp. 356–357, Academic Press, London
25. Holman, G. D. & Midgley, P. J. W. (1985) Carbohydr. Res. **135**, 337–341
26. Clark, A. E. & Holman, G. D. (1990) Biochem. J. **269**, 615–622
27. Frost, S. C. & Lane, M. D. (1985) J. Biol. Chem. **260**, 2646–2652
28. Eilam, Y. & Stein, W. D. (1972) Biochim. Biophys. Acta **266**, 161–173
29. Rees, W. D. & Holman, G. D. (1982) Biochim. Biophys. Acta **642**, 251–260
30. Deves, R. & Krupka, R. M. (1984) Biochim. Biophys. Acta **769**, 455–460
31. Clancy, B. M., Harrison, S. A., Buxton, J. M. & Czech, M. P. (1991) J. Biol. Chem. **266**, 10122–10130
32. Cleland, W. W. (1979) Methods Enzymol. **63**, 103–138
33. Gould, G. W. & Lienhard, G. E. (1989) Biochemistry **28**, 9447–9452
34. Keller, K., Strube, M & Mueckler, M. (1989) J. Biol. Chem. **264**, 18884–18889
35. Holman, G. D., Busza, A. L., Pierce, E. J. & Rees, W. D. (1981) Biochim. Biophys. Acta **649**, 503–514
36. Simpson, I. A., Yver, D. R., Hissin, P. J., Wardzala, L. J., Karnieli, E., Salans, L. B. & Cushman, S. W. (1983) Biochim. Biophys. Acta **763**, 393–407
37. Taylor, L. P. & Holman, G. D. (1980) Biochim. Biophys. Acta **642**, 325–335
38. Clark, A. E., Holman, G. D. & Kozka, I. J. (1991) Biochem. J. **278**, 235–241
39. Holman, G. D., Parkar, B. A. & Midgley, P. J. W. (1986) Biochim. Biophys. Acta **855**, 115–126
40. Cushman, S. W. & Wardzala, L. T. (1990) J. Biol. Chem. **255**, 4758–4762
41. Suzuki, K. & Kono, T. (1980) Proc. Natl. Acad. Sci. U.S.A. **77**, 2542–2545
42. Slot, J. W., Gueze, H. J., Gigengack, S., Lienhard, G. E. & James, D. E. (1991) J. Cell Biol. **113**, 123–135
43. Clancy, B. M. & Czech, M. P. (1990) J. Biol. Chem. **265**, 12434–12443
44. Harrison, S. A., Buxton, J. M., Clancy, B. M. & Czech, M. P. (1990) J. Biol. Chem. **265**, 20106–20116
45. Zorzano, A., Wilkinson, W., Kotliar, N., Thoidis, G., Wadzinski, B. E., Ruoho, A. E. & Pilch, P. F. (1988) J. Biol. Chem. **264**, 12358–12363
46. Yang, J., Clark, A. E., Harrison, R., Kozka, I. J. & Holman, G. D. (1992) Biochem. J. **281**, 809–817
47. Carruthers, A. (1990) Physiol. Rev. **70**, 1135–1176

Received 3 September 1991/2 December 1991; accepted 13 December 1991